

# **ECE 538: 2D Material Electronics and Photonics**

## **Chapter 1: Graphene**

**Wenjuan Zhu**

**Associate Professor**

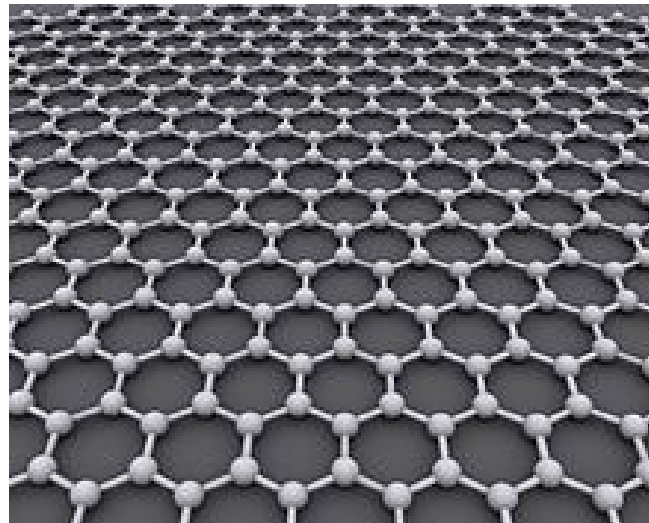
**Department of Electrical and Computer Engineering**  
**Office: MNTL 3258, Email: [wjzhu@Illinois.edu](mailto:wjzhu@Illinois.edu)**

# Outline

- 
- Introduction of graphene
  - Synthesis of graphene
  - Current transport and electronic devices
  - Optical properties and photonic devices
  - Bandgap engineering in graphene

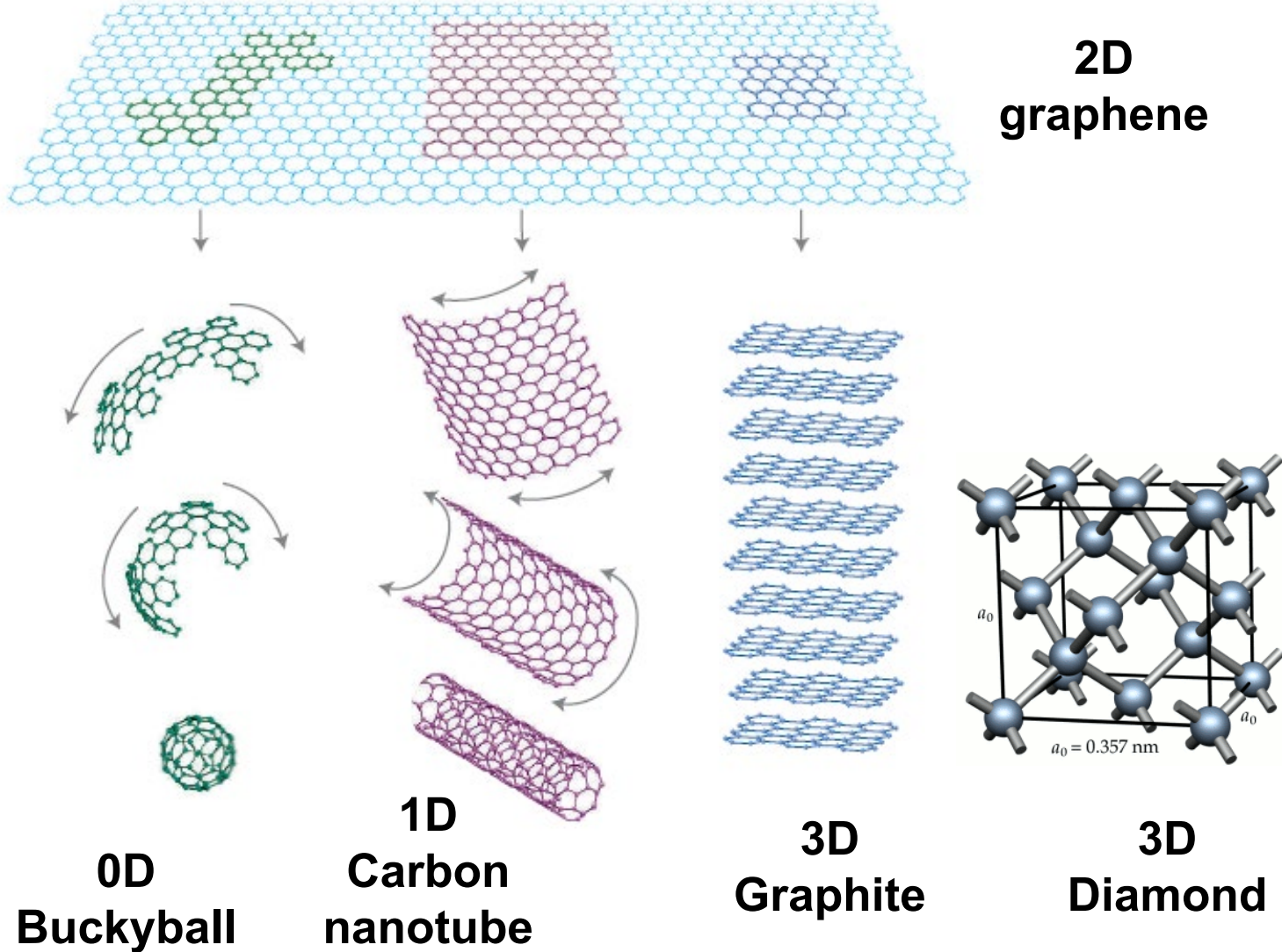
# What is graphene?

- Graphene is an allotrope of carbon consisting of a single layer of carbon atoms arranged in a hexagonal lattice.



- Graphene is a semi-metal with zero bandgap.

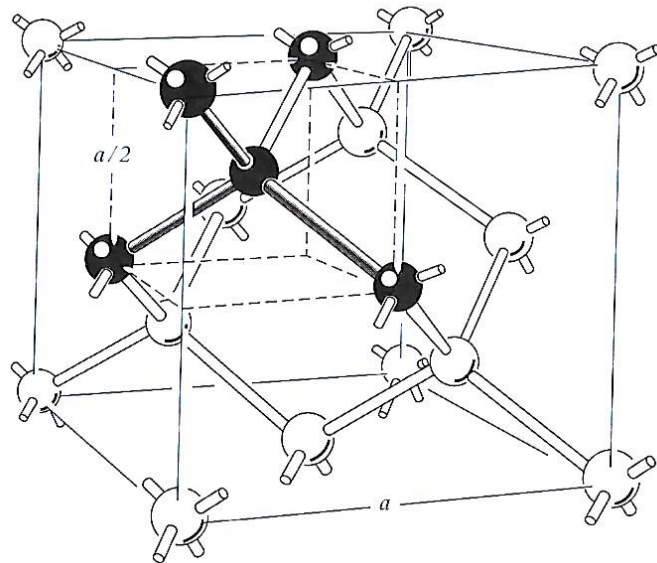
# Carbon Allotropes



A. Geim, and K. Novoselov, The rise of graphene, Nature Mater 6, 183 (2007)

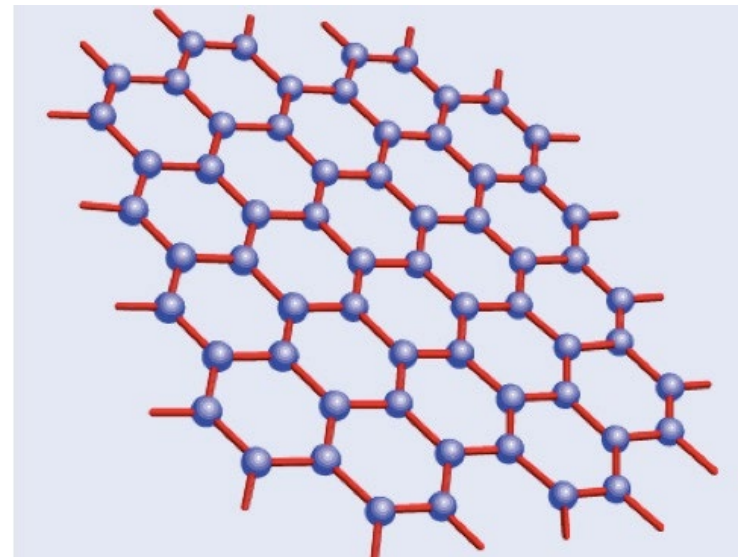
# Crystal structure

Silicon



3D, diamond lattice

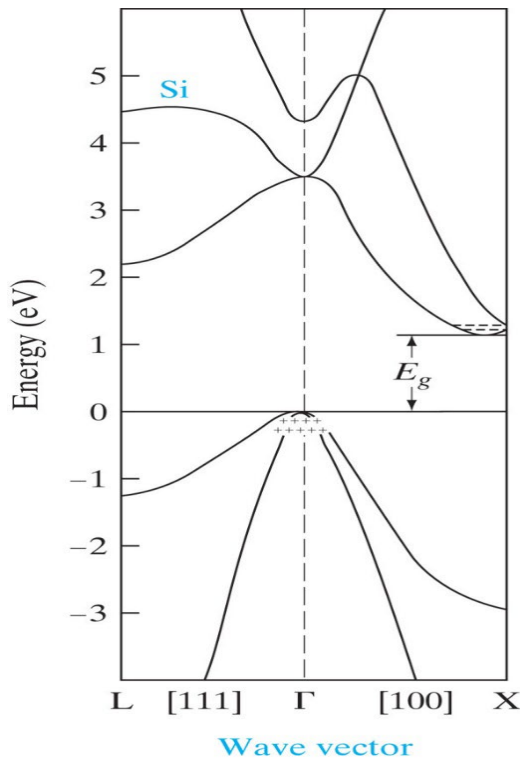
Graphene



2D, hexagonal lattice

# Energy band structure

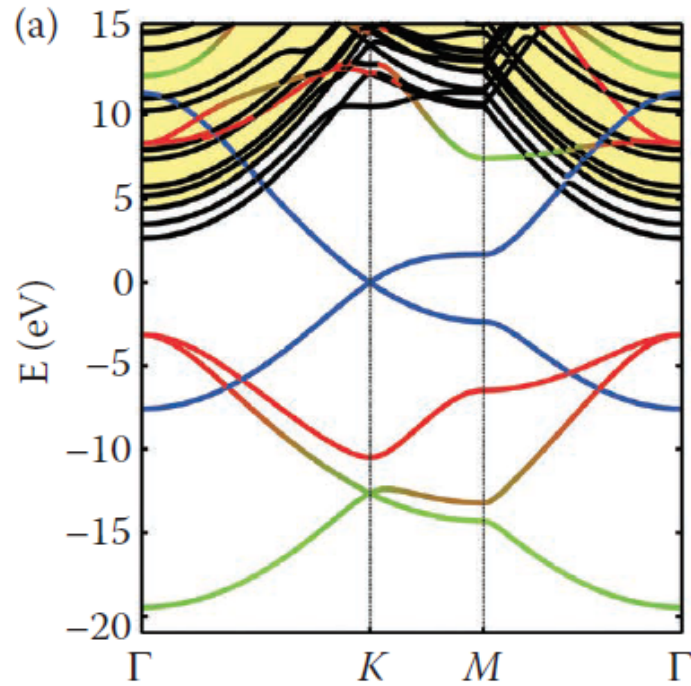
Silicon



Bandgap: 1.12 eV

Near band edge, the band shape is parabolic

Monolayer Graphene

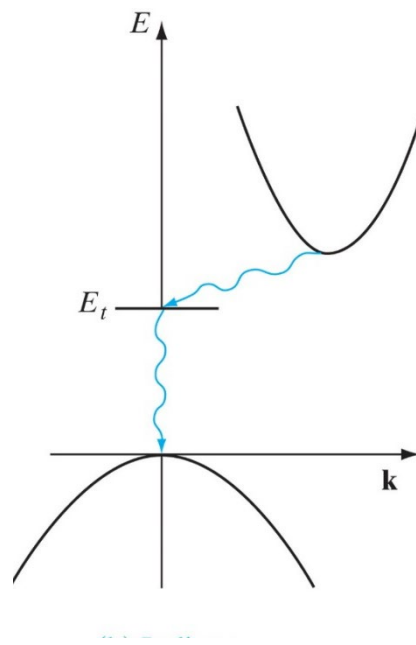


Bandgap: 0 eV

Near band edge, the band shape is linear

# Dispersion relationship

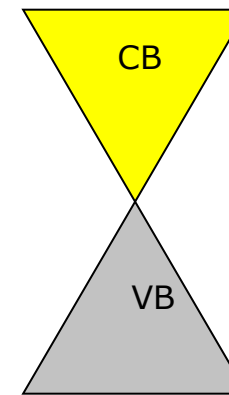
Silicon



- Parabolic dispersion

$$E = \hbar^2 k^2 / 2m^*$$

Monolayer graphene



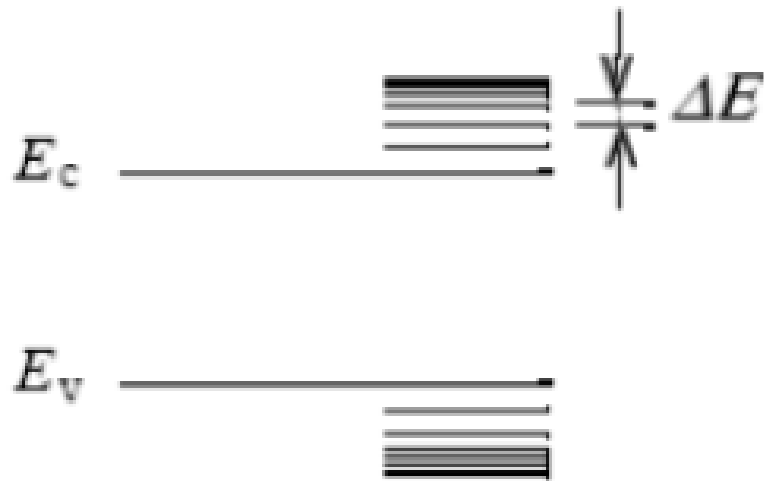
- Linear dispersion

$$E_{F-SL} = \hbar v_F k \quad \text{Massless}$$

Fermi velocity  $v_F \sim 10^6 m/s$

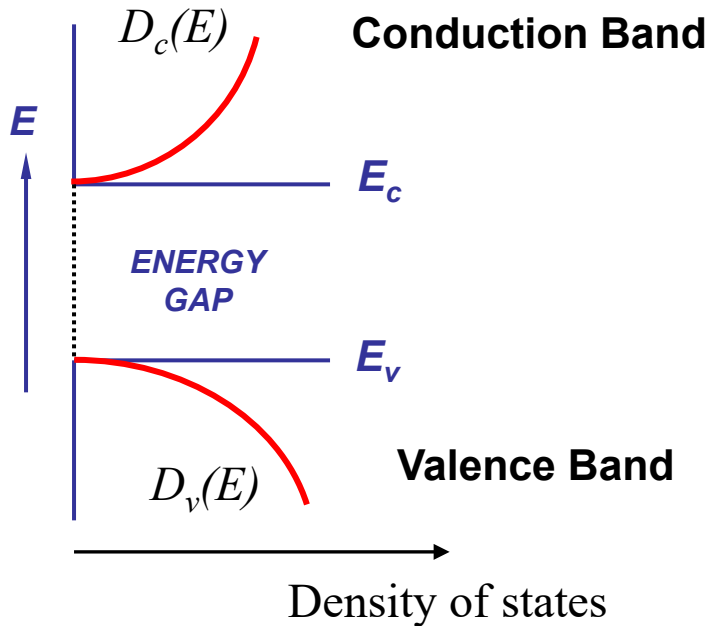
# Density of state concept

- Density of state  $D(E)$ : number of available state per unit volume per unit energy (unit:  $\text{cm}^{-3}\text{eV}^{-1}$ )
- $D(E)dE$ : number of available state per unit of volume lying in the energy range between  $E$  and  $E + dE$  (unit:  $\text{cm}^{-3}$ )

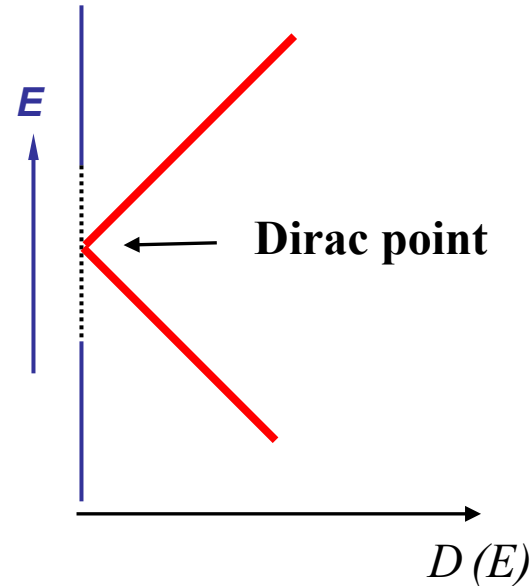


# Density of States

## Silicon



## Monolayer graphene



**Conduction band**  $D_c(E) = \frac{\sqrt{2}}{\pi^2} \left( \frac{m_n^*}{\hbar^2} \right)^{\frac{3}{2}} (E - E_c)^{1/2}$

**Valence band**  $D_v(E) = \frac{\sqrt{2}}{\pi^2} \left( \frac{m_p^*}{\hbar^2} \right)^{\frac{3}{2}} (E_v - E)^{1/2}$

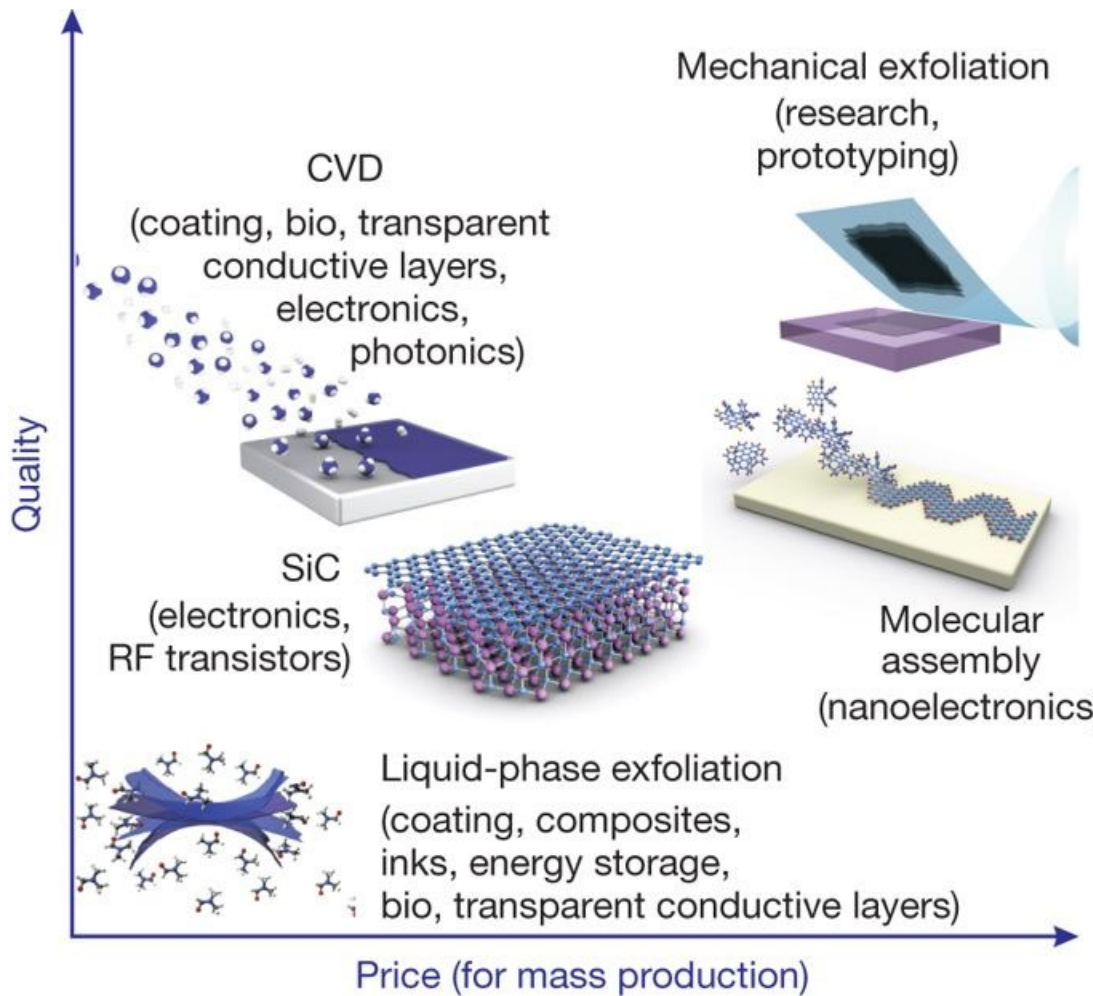
For both electron and holes:

$$D(E_F) = \frac{2|E - E_{Dirac}|}{\pi(\hbar v_F)}$$

# Outline

- Introduction of graphene
- Synthesis of graphene
  - Epitaxial graphene on SiC
  - CVD graphene on metal
- Current transport and electronic devices
- Optical properties and photonic devices
- Bandgap engineering in graphene

# Synthesis of graphene



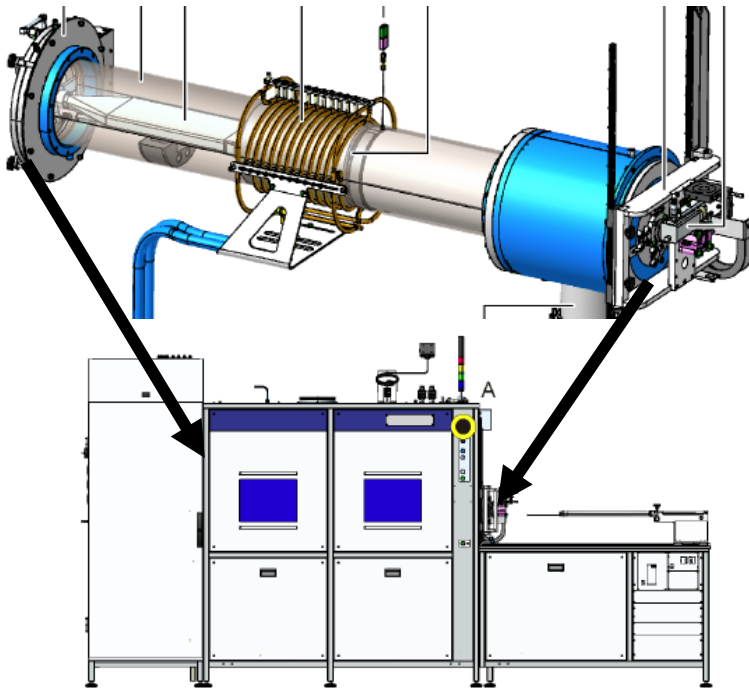
K. S. Novoselov, K. Kim, Nature, Vol. 490, p.192, 2012

# Synthesis graphene on SiC

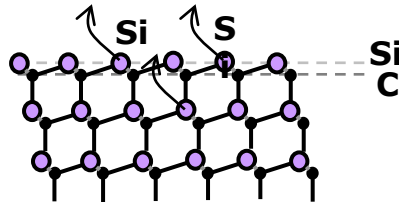
Home-built clustered UHV tool



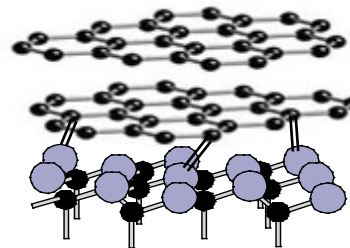
AIXTRON VP508



**SiC surface decomposition**

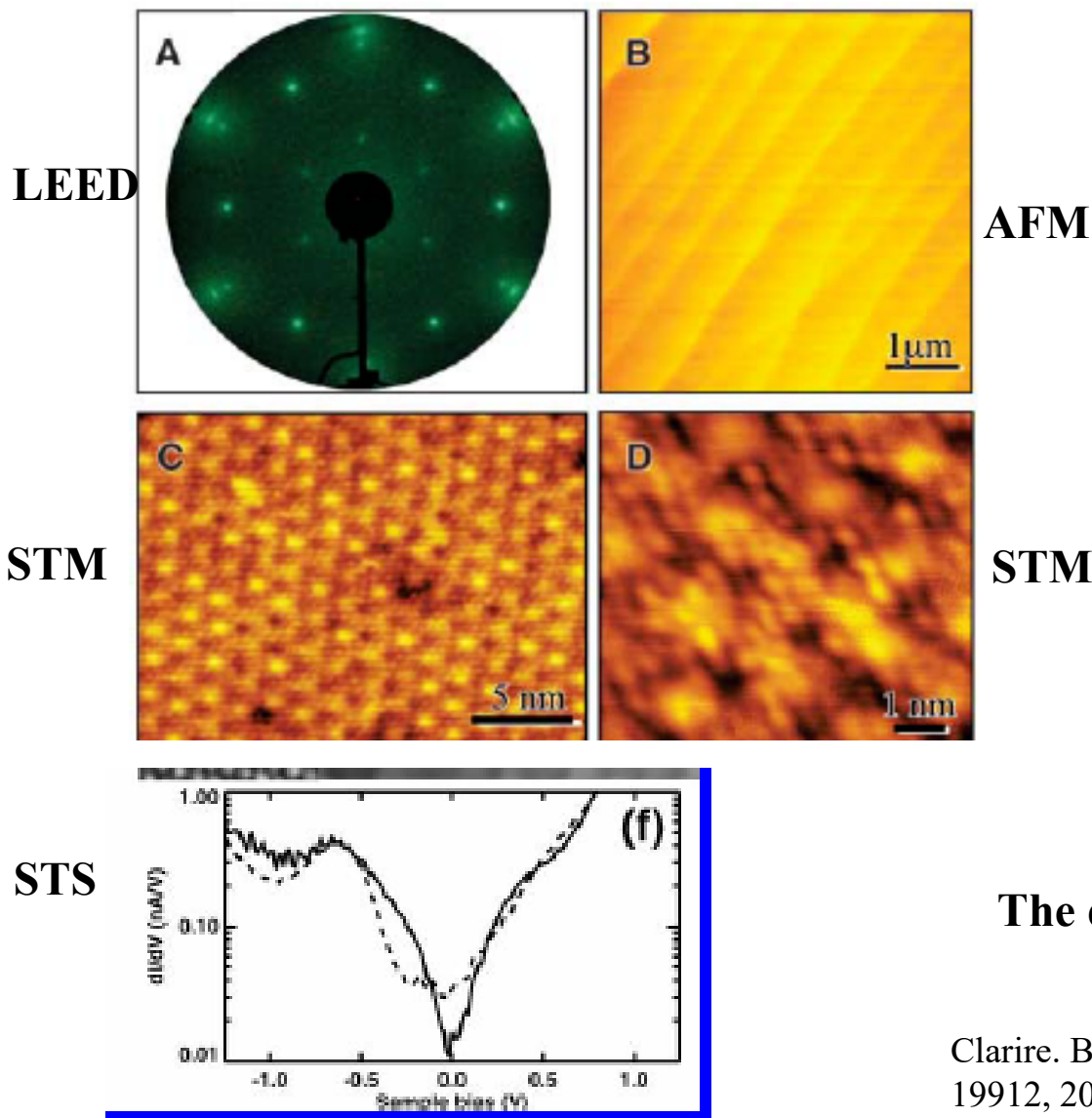


**Graphene formation**



**Graphene  
Buffer  
SiC**

# Graphene epitaxially grown on SiC



- Epitaxial graphite was grown on single-crystal silicon carbide by vacuum graphitization.
- Mobilities exceeding  $2.5 \times 10^4 \text{ cm}^2/\text{V}\cdot\text{s}$ .
- Charge carriers shows Dirac nature

The domain size is small: 30–200 nm

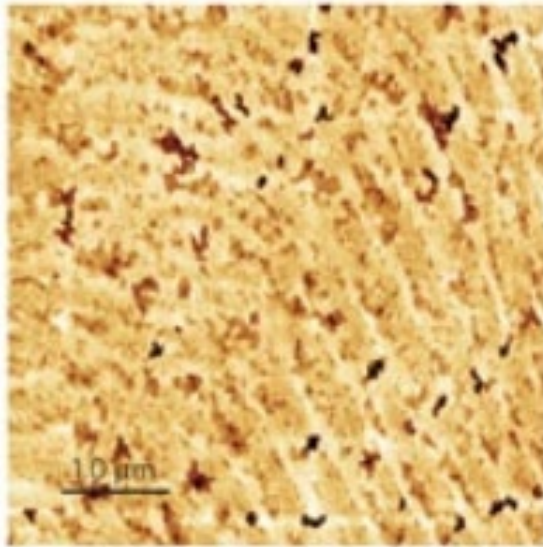
Clarire. Berger, Walt de Heer, et. al., J. Phys. Chem, B, 108, 19912, 2004; Nature 1191, 2006

# Graphitization in UHV versus in Ar

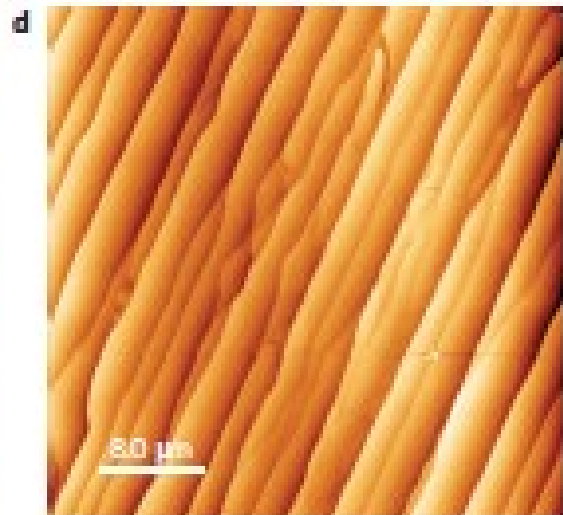
Before growth



After graphene growth,  
in UHV



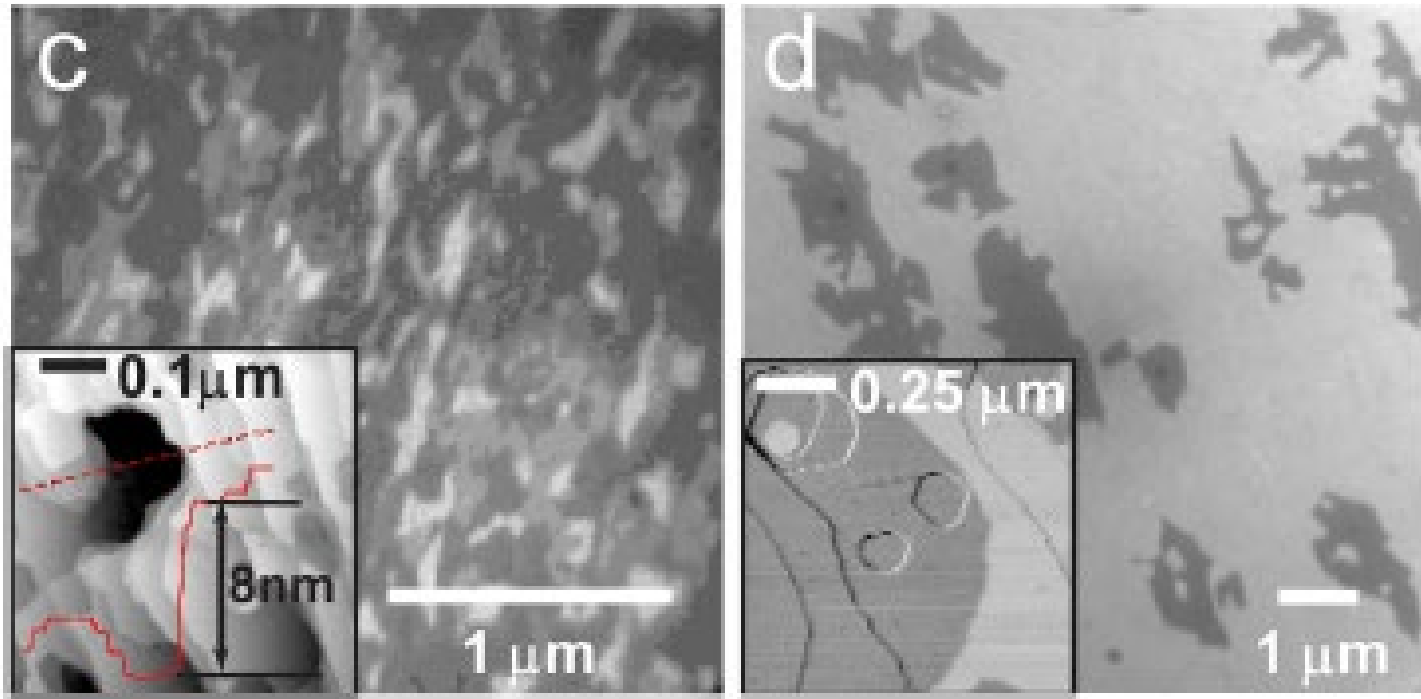
After graphene  
growth, in Ar



- Ar-mediated growth results in a better morphology compared to the UHV graphitization. Furthermore, the graphene domains obtained in an Ar environment were much larger in size.

K. Emtsev, T. Seyller, et.al., Nature Materials, 8, 203, 2009

# Graphitization with silicon background pressure



In the absence of disilane, the surface is very rough.  
Graphitization with disilane, the surface is much smoother.  
Larger domains with more uniform graphene were formed.

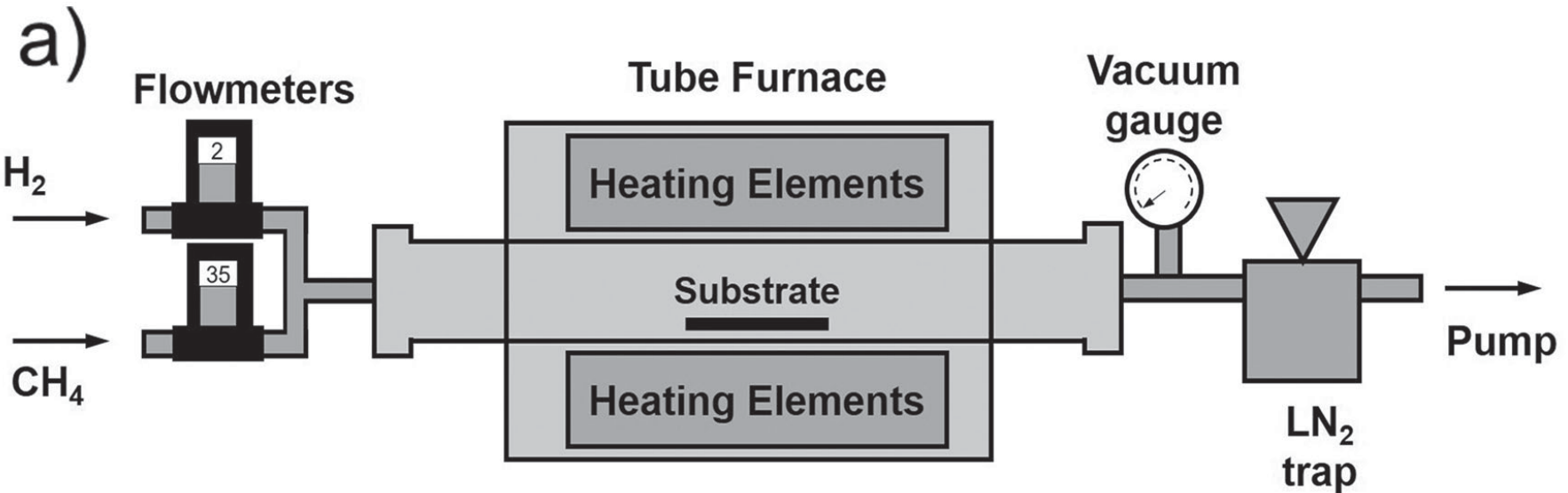
R. M. Tromp, and J. B. Hannon, PRL, 102, 106104 (2009)

# Outline

- Introduction of graphene
- Synthesis of graphene
  - Epitaxial graphene on SiC
  - CVD graphene on metal
- Current transport and electronic devices
- Optical properties and photonic devices
- Bandgap engineering in graphene



# Schematic of CVD system for graphene synthesis

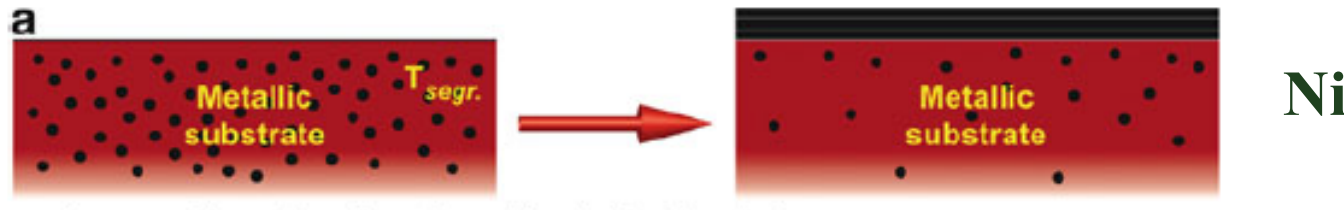


- Hydrocarbon gas, such as methane, is typically used at the carbon source.
- Copper or nickel is usually used as the substrate.

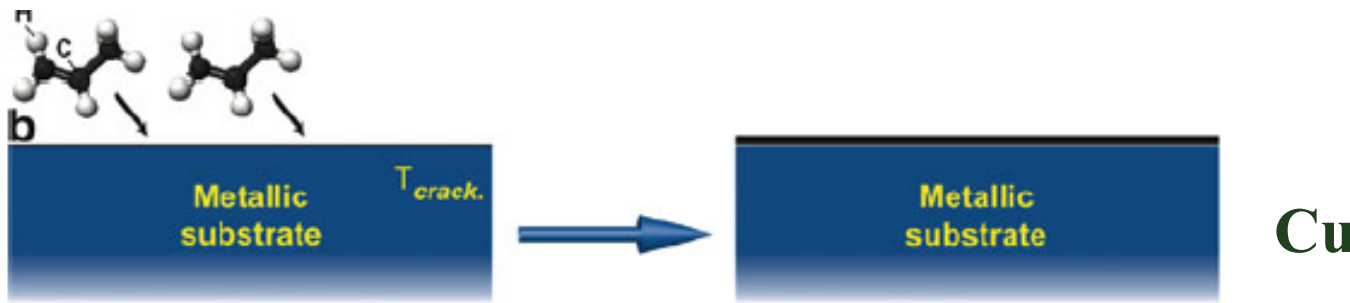
Xuesong Li , Rodney S. Ruoff, Synthesis of Graphene Films on Copper Foils by Chemical Vapor Deposition, Adv. Mater. 28, 6247,2016

# Synthesis of graphene on metal

Type 1: Segregation of carbon from the bulk of metal



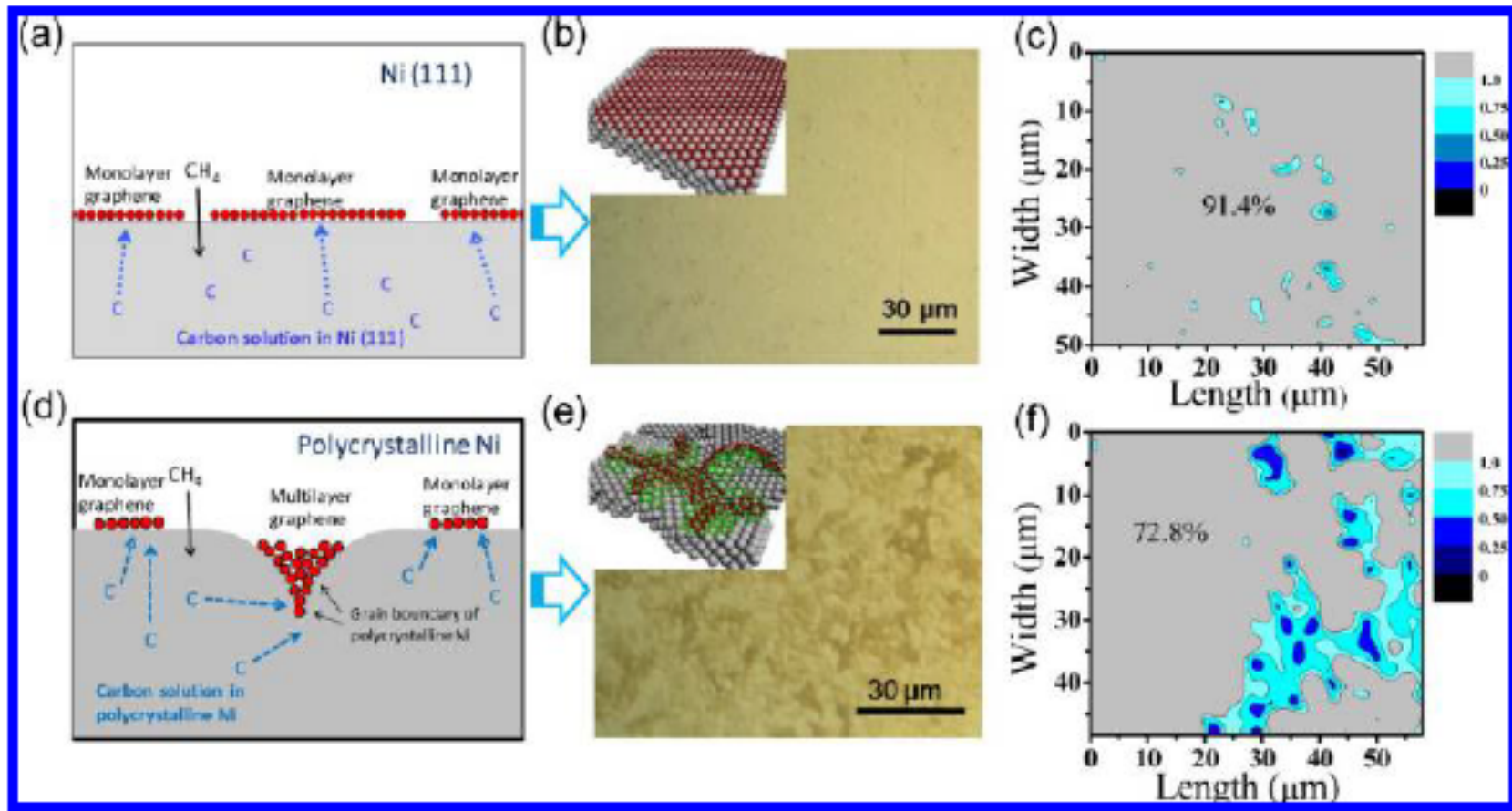
Type 2: Decomposition of hydrocarbons at the surface



- Two growth mechanisms have been observed for graphene growth on metals in a CVD process: i) a surface segregation/precipitation process of C to form graphitic carbon, and ii) by a surface adsorption process.

E. Voloshina, "Physics and Applications of Graphene" (book), 2011

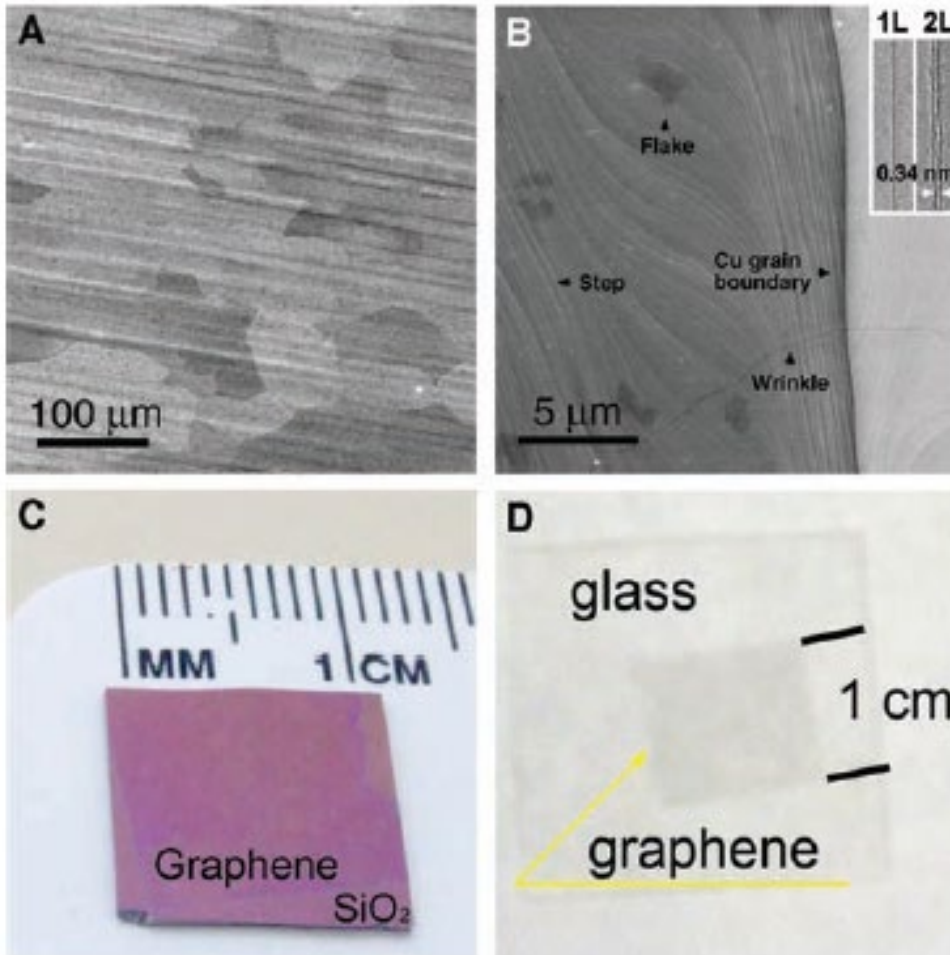
# Graphene growth on Ni



- Graphene films grown on Ni substrates are usually continuous with monolayer and few-layers regions.
- Most of the multilayer nucleation occurs at Ni grain boundaries which are defects in the polycrystalline Ni substrates.

Y. Zhang, Accounts of chemical research, Vol. 46, 2329, 2013

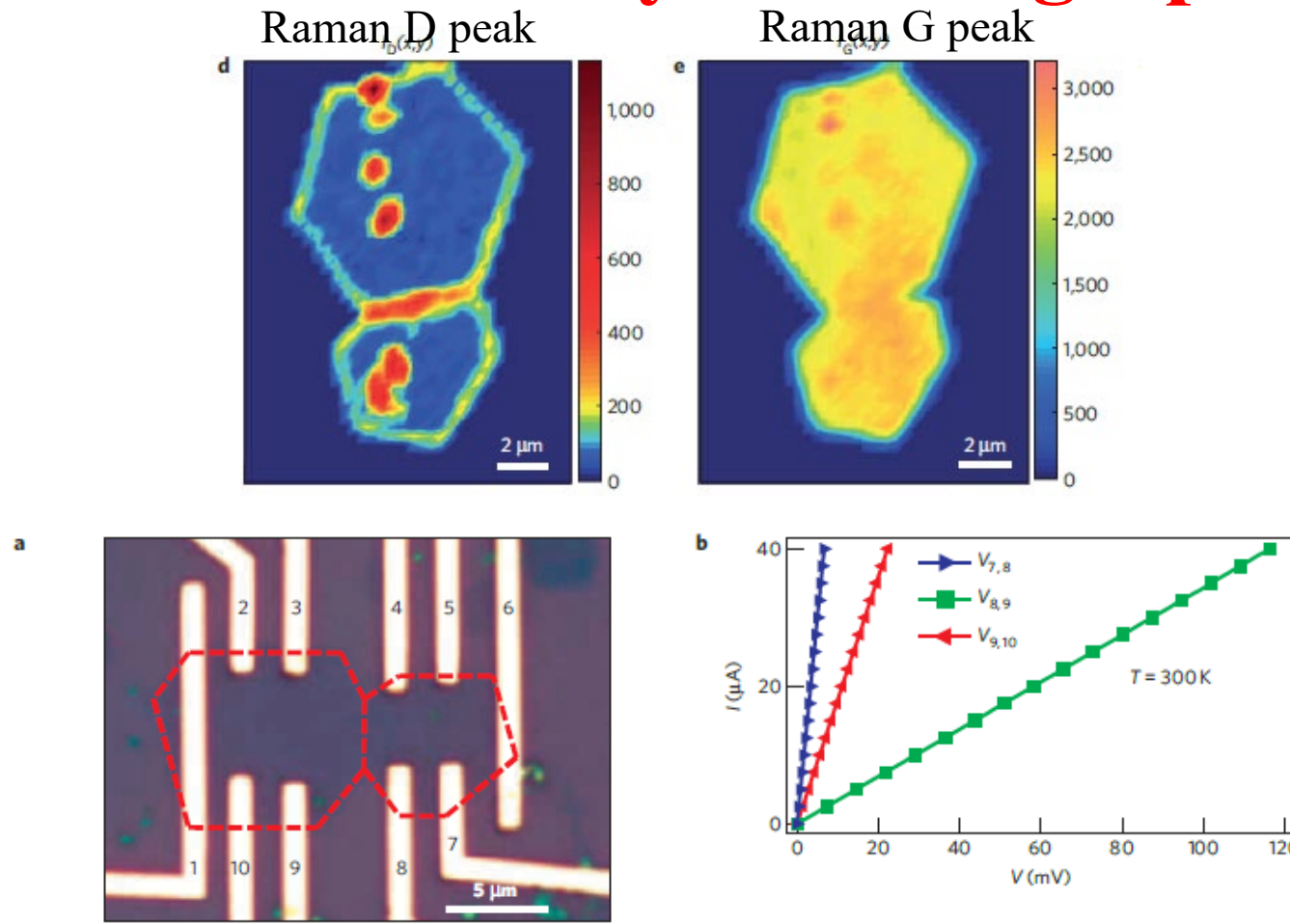
# CVD graphene on copper



- Large-area graphene films in the order of centimeters were grown on copper by chemical vapor deposition using methane.
- Carrier mobility of the CVD graphene is  $\sim 4050$   $\text{cm}^2/\text{V}\cdot\text{s}$ .
- The film is predominately monolayer graphene (>95%) with small fractions of bilayer (~3 to 4%).

X. Li, R. Ruoff, et.al., Science, 324, 1312, 2009

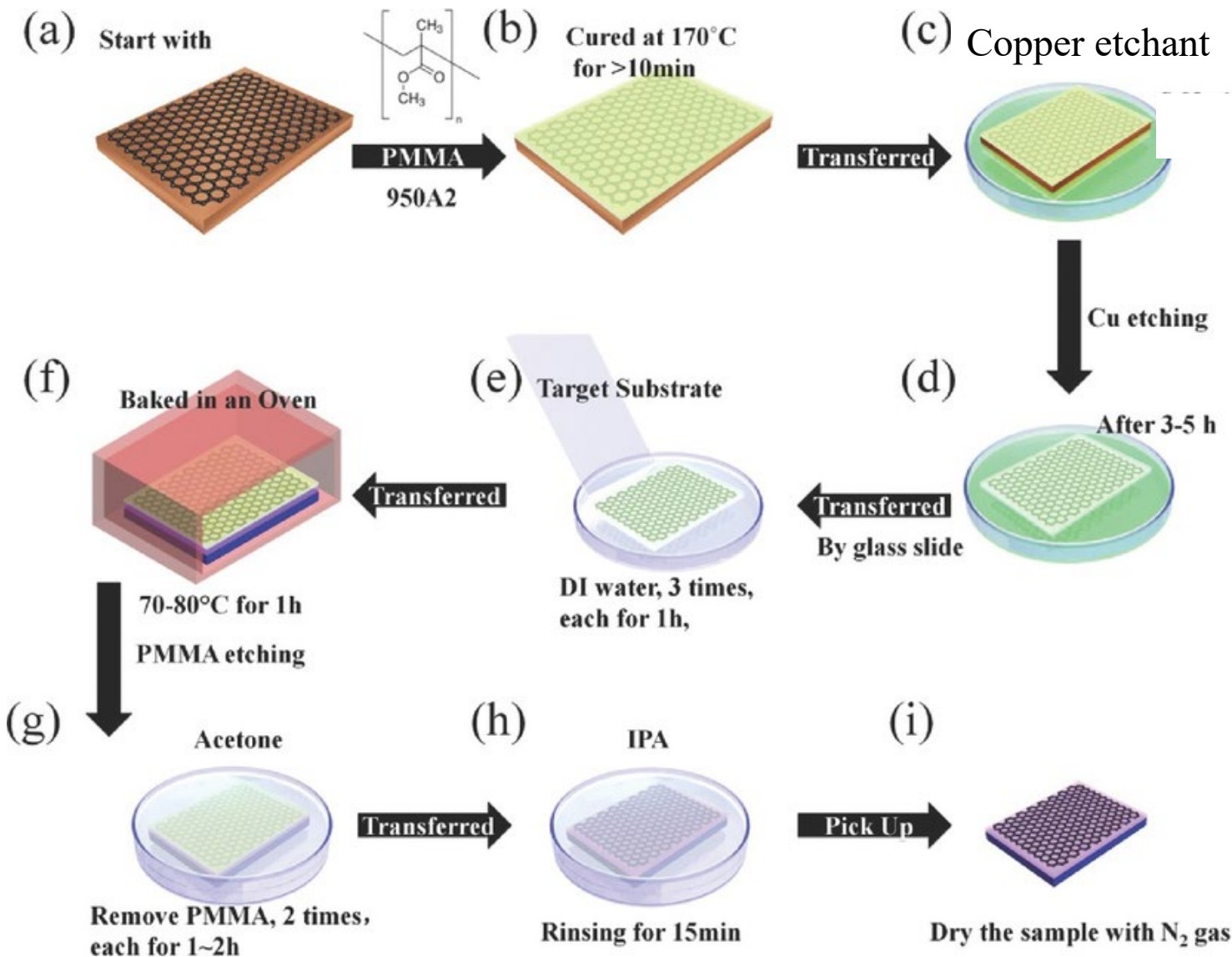
# Grain boundary in CVD graphene



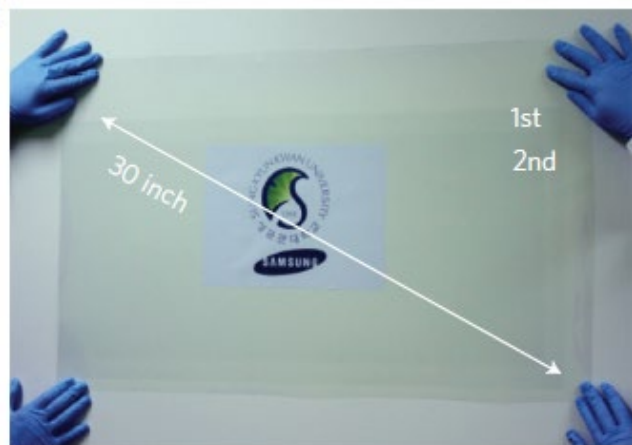
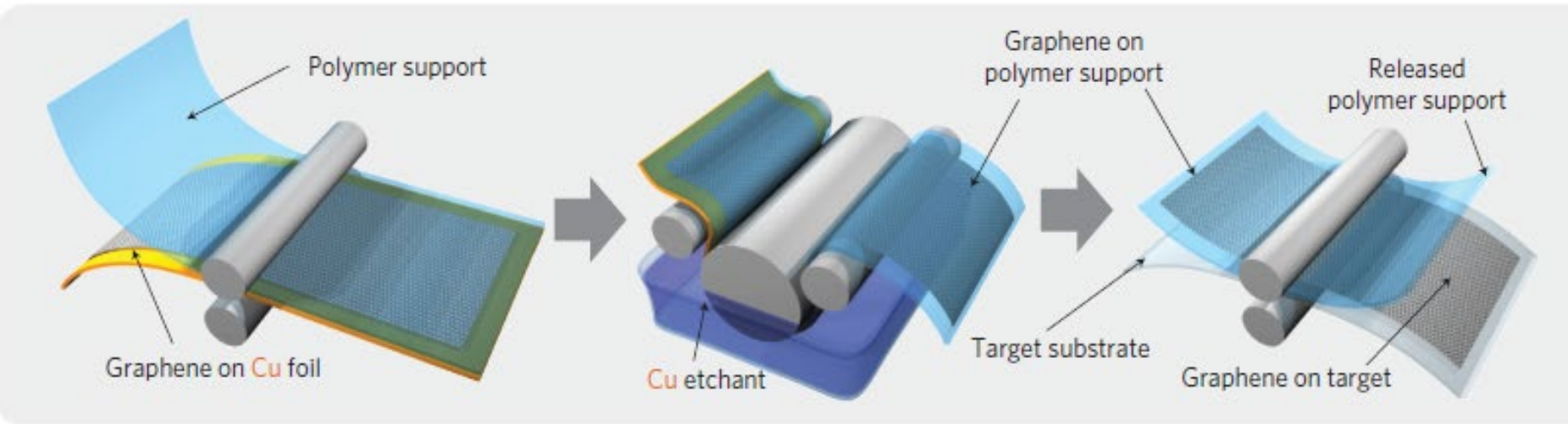
Grain boundaries in CVD graphene give a significant Raman ‘D’ peak (defect peak). Higher resistance was observed when the channel is crossing a grain boundary.

Q. Yu, Y. Chen, et.al., Nature Materials, 10, 443, 2011

# Transfer Graphene From Metal Substrate



# Roll-to-roll production of graphene



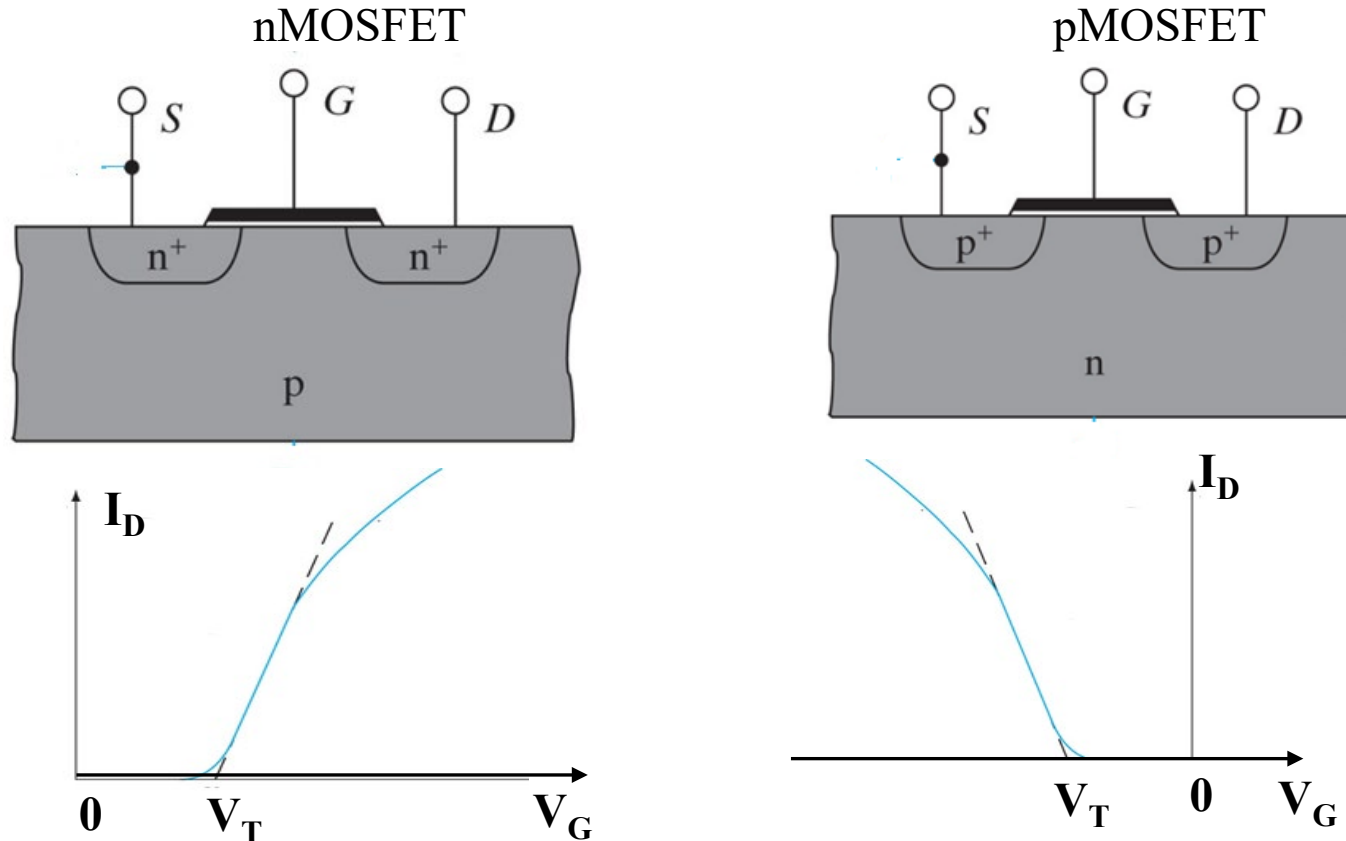
- Roll-to-roll production of monolayer 30-inch graphene films was grown by chemical vapour deposition onto flexible copper substrates.
- The films have sheet resistances as low as  $\sim 125 \Omega$  per square with 97.4% optical transmittance, which is promising for transparent electrodes.

S. Bae, S. Lijima, et.al., Nature Nanotechnology, 5, 574, 2010

# Outline

- Introduction of graphene
- Synthesis of graphene
- Current transport and electronic devices
  - Current transport
    - Dirac voltage
    - Carrier mobility
    - Minimum conductance
    - Current saturation and negative resistance
    - Quantum Hall Effect
  - Electronic devices
- Optical properties and photonic devices
- Bandgap engineering in graphene

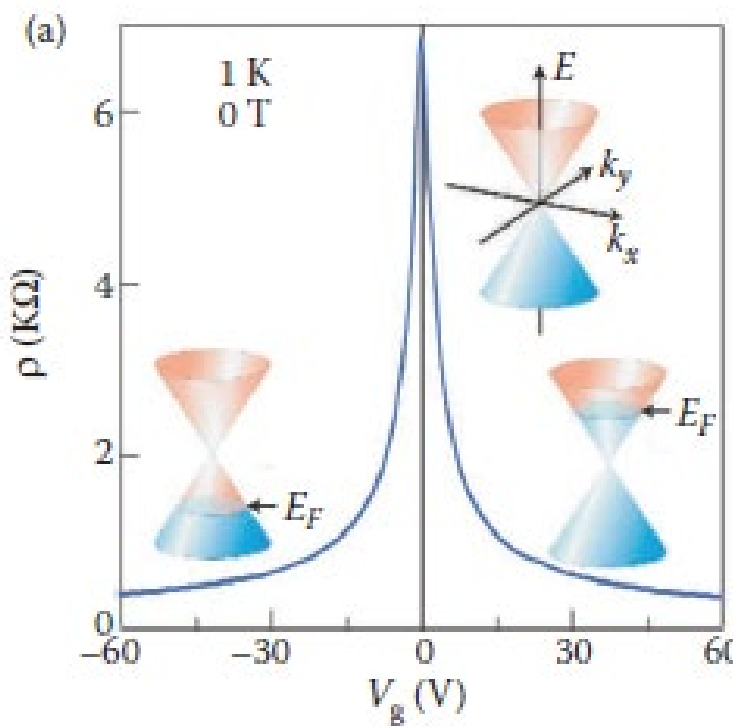
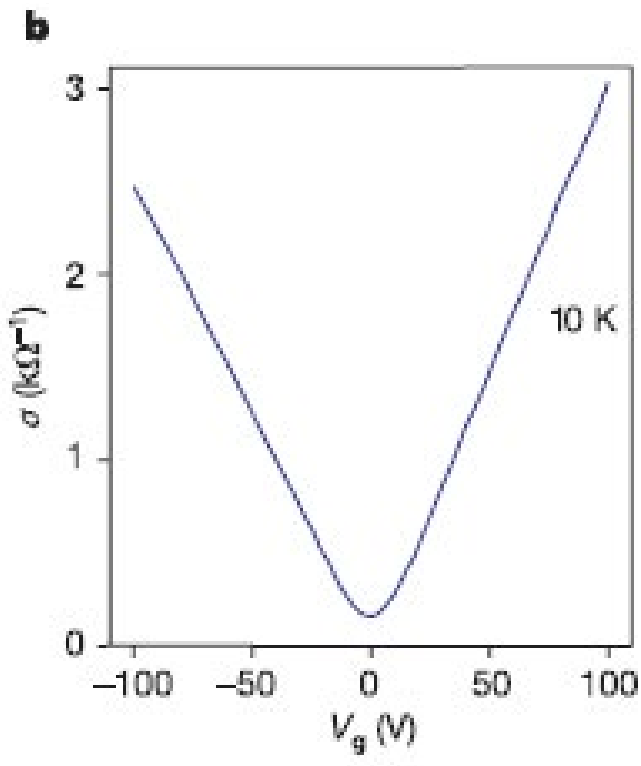
# Recap: Si transistors



- Silicon MOSFETs are unipolar transistors, which uses only one type of carriers for conduction from drain to source.

Threshold voltage  $V_T = \phi_{ms} - \frac{q_i}{c_i} - \frac{q_{dm}}{c_i} + 2\phi_F$

# Characteristics of graphene transistor



- Graphene transistor shows ambipolar transport.
- The channel conductance of graphene transistor reaches minimum (or resistance reaches maximum) at Dirac point, due to the reduced carrier density as Fermi level approaches the Dirac point of grapheme, at which the density of states vanishes.

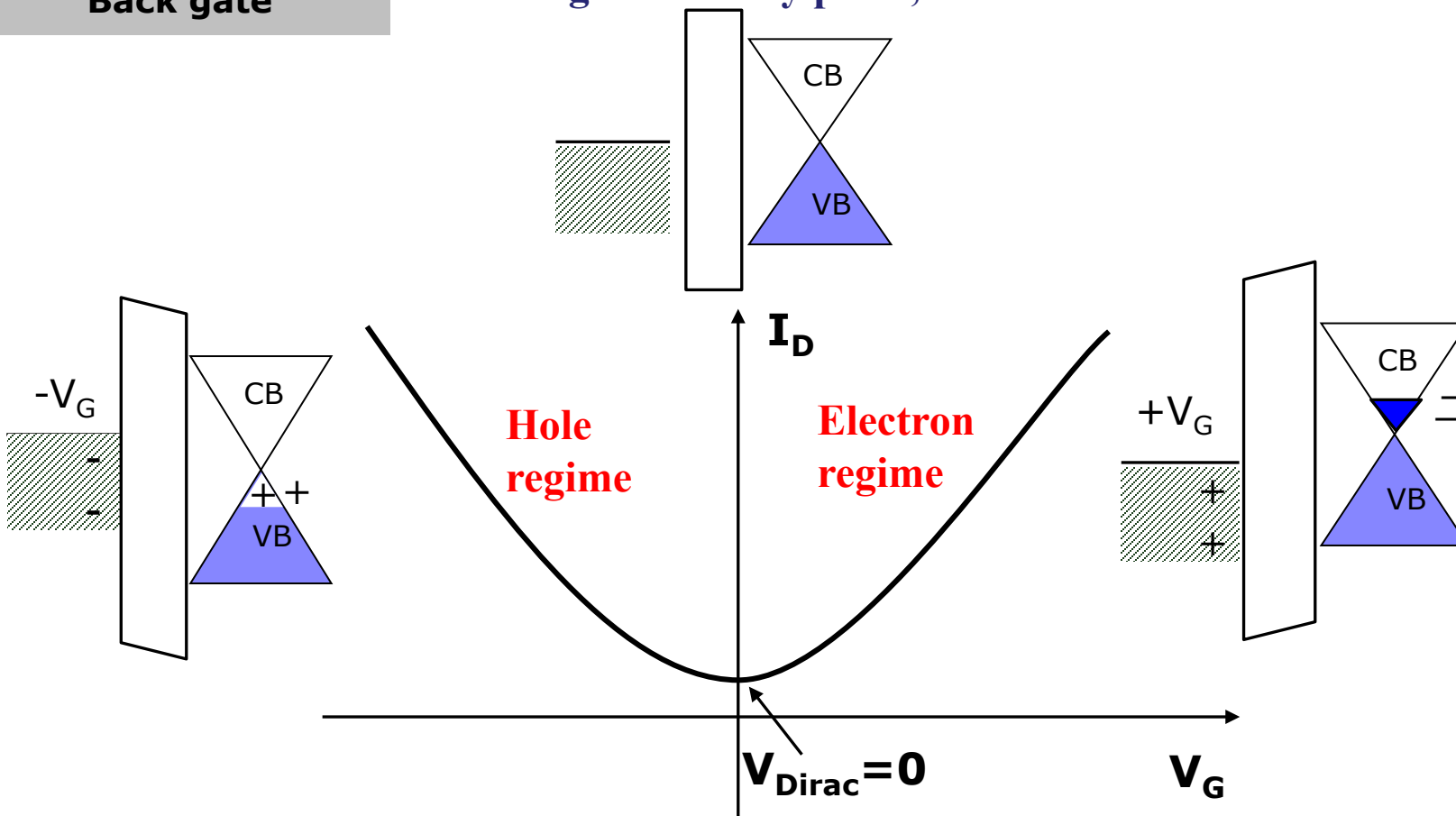
K. Novoselov, et.al., Nature, 197, 2005

A. Geim & K. Novoselov, Nature Materials Vol. 6, 183 (2007)

# Current transport in graphene: ideal case

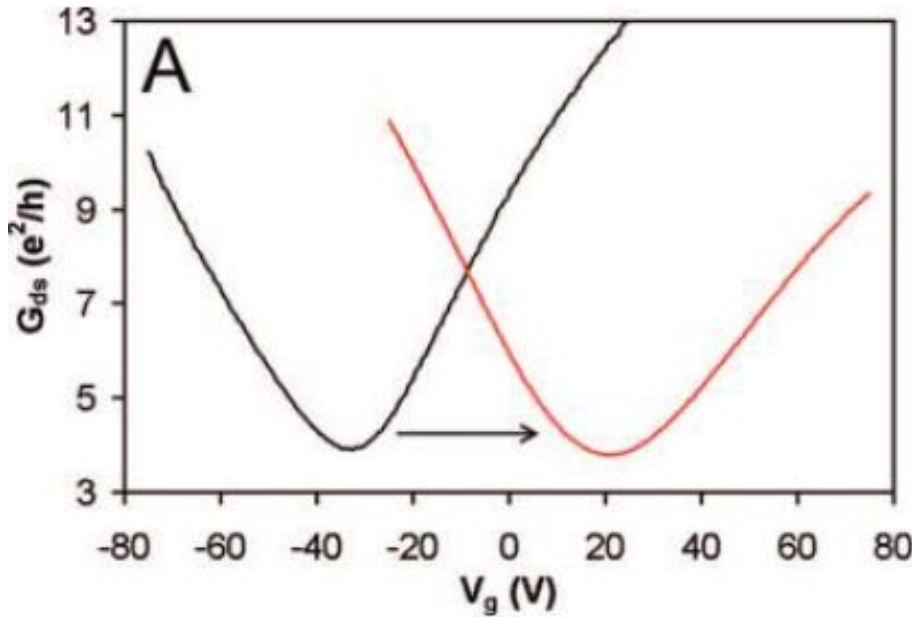


Assuming there is no charge impurities in the oxide, graphene has no doping, the work function of the metal is equal to the work function of graphene, then when gate voltage is zero, graphene is at charge neutrality point, i.e. reach minimum conductance.

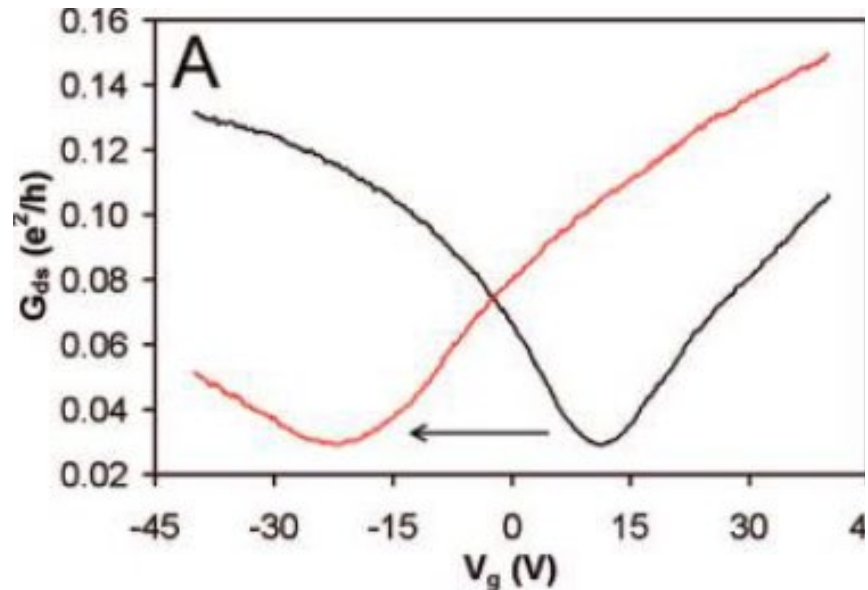


# Impact of doping in graphene on Dirac voltage

Diazonium doping  
(p-type doping)



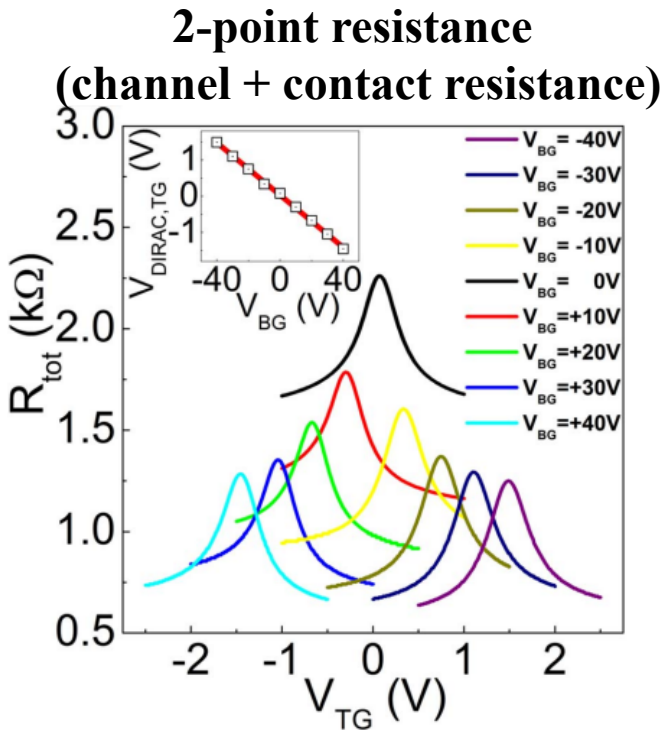
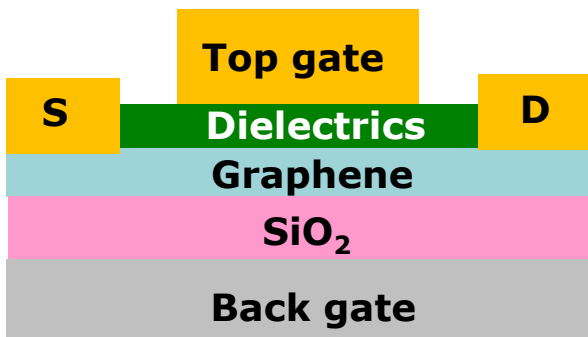
PEI doping  
(n-type doping)



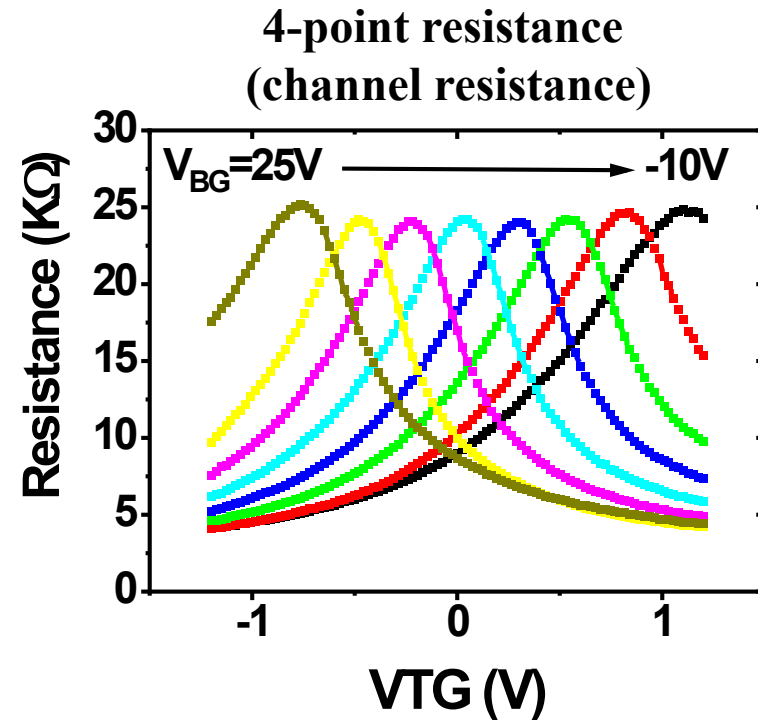
- P-type doping in graphene induces positive shift of Dirac voltage, while n-type doping leads to negative shift of Dirac voltage.

D. Farmer, et al., Nano Letters, Vol. 9, 1, 388, 2009

# Electrostatic doping in graphene



S. Kim, Appl. Phys. Lett. 94, 062107, 2009



W. Zhu, et.al., Nano Letters, 10, 3572, 2010

$$\Delta V_{\text{Dirac,TG}} \cdot C_{\text{TG}} = -\Delta V_{\text{BG}} \cdot C_{\text{BG}}$$

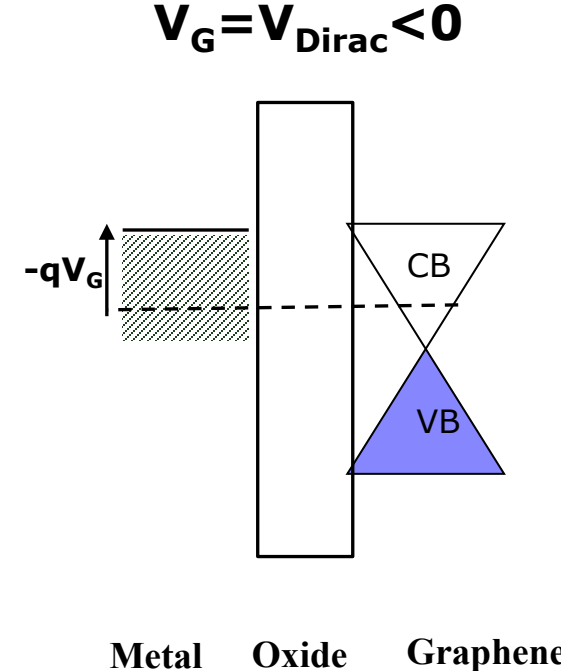
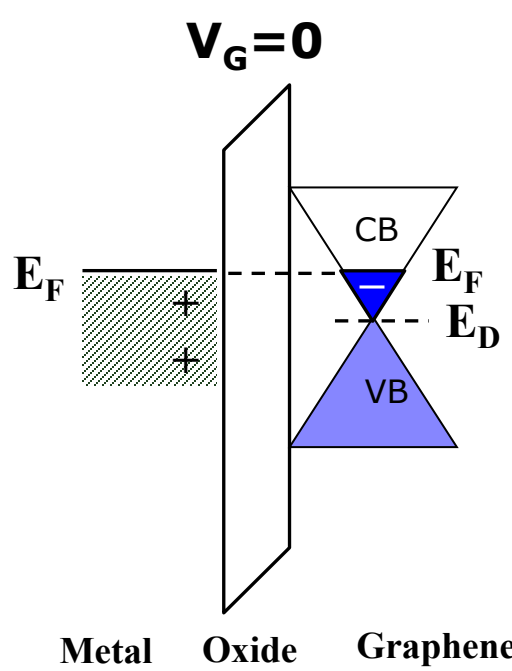
- Electrostatic doping in graphene can also shift the Dirac voltage. Negative back gate bias will induce holes in the graphene, which will lead to positive shift of Dirac voltage.

# Impact of doping in graphene on Dirac voltage

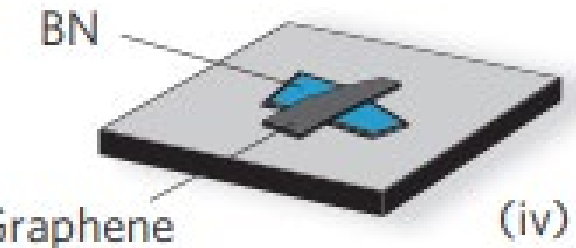
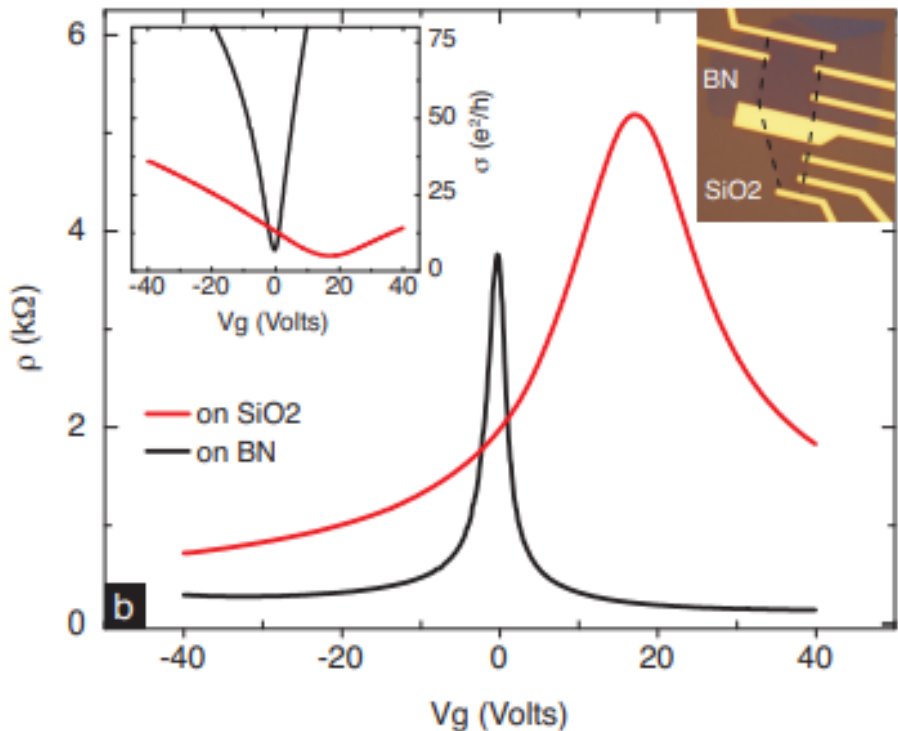
If graphene is doped, the Dirac voltage shift due to doping will be

$$\Delta V_{Dirac} \approx \frac{Q_{doping}}{C_{ox}}$$

Assuming there is no oxide charges and the  $\Phi_{ms}=0$



# Impact of oxide trap charges on graphene Dirac point



- On h-BN, graphene transistor exhibits a very narrow resistivity peak and a Dirac voltage close to zero.
- However, on  $\text{SiO}_2$  substrate, graphene transistor shows a Dirac voltage  $\sim 25$  V, and a broad resistivity peak, due to the charge impurities in the  $\text{SiO}_2$  substrate.

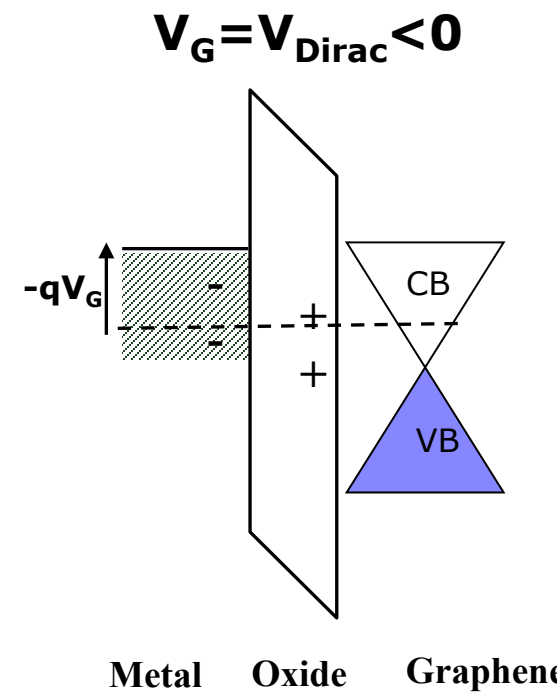
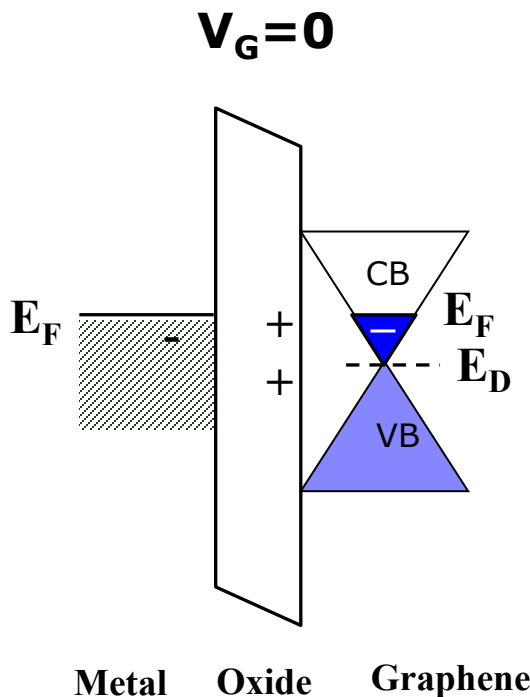
C. Dean, et al., Nature Nanotechnology, Vol. 5, 722, (2010)

# Impact of oxide trap charges on graphene Dirac point

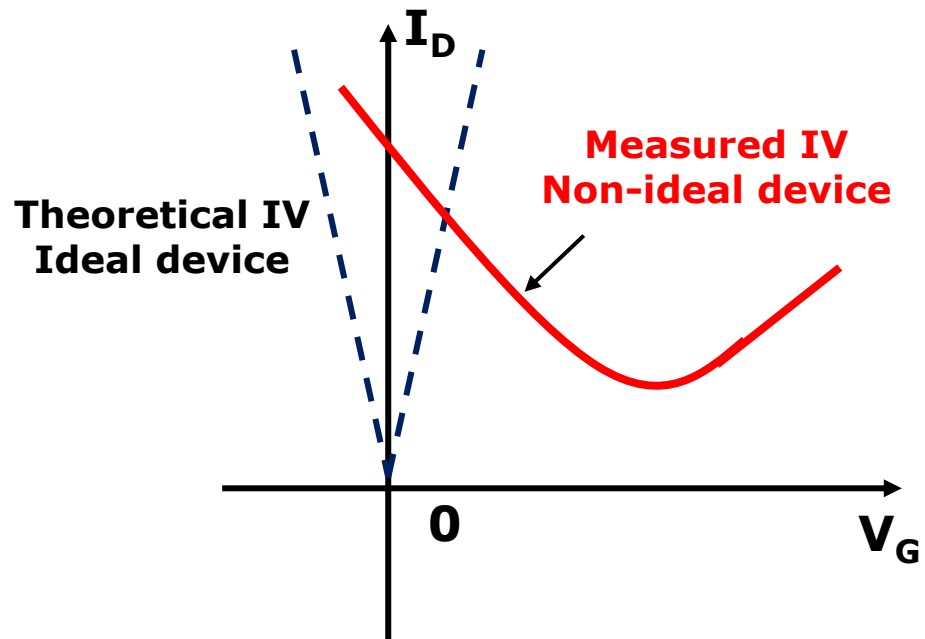
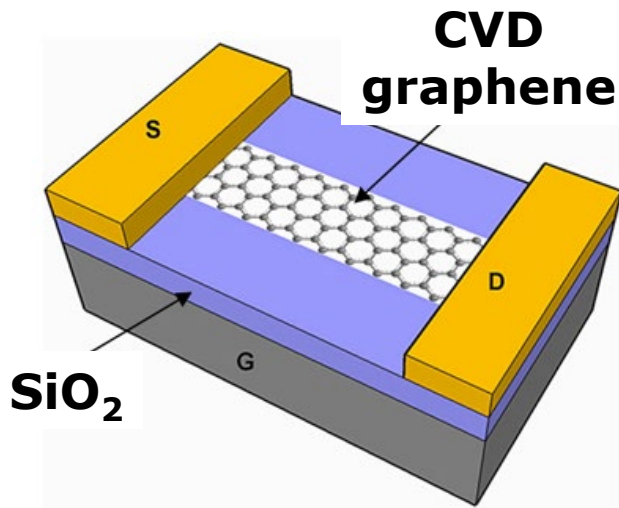
If there is charge impurities in the oxide,  $Q_{ox}$ , the Dirac voltage shift will be

$$\Delta V_{Dirac} = -\frac{Q_{ox}}{C_{ox}}$$

If there is a layer of positive charge in the oxide, then we have:

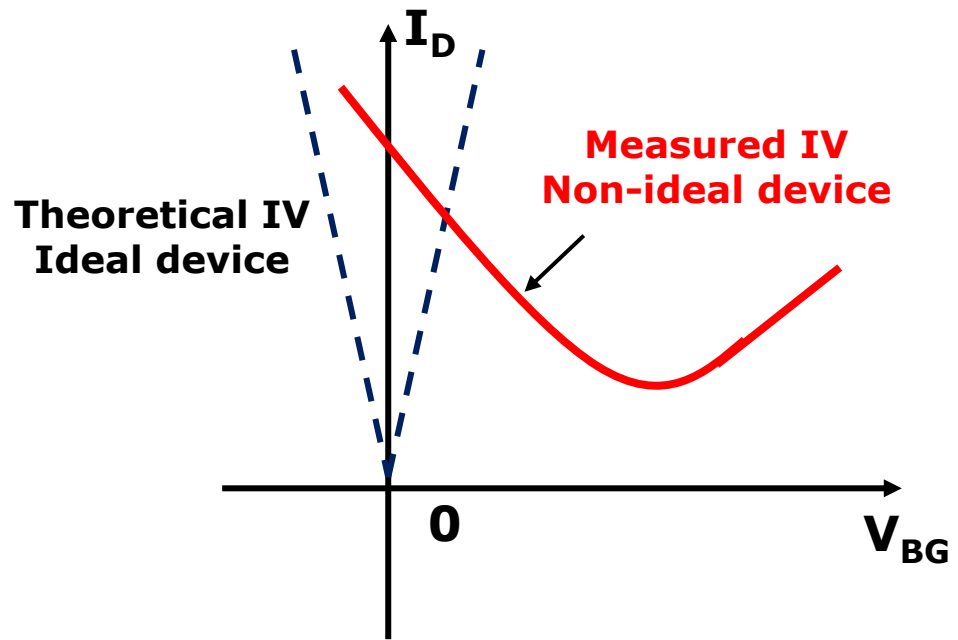


# Question



- If the Dirac voltage shift in the fabricated device is due to doping in graphene, is doping n-type or p-type?
- If the Dirac voltage shift in the fabricated device is due to oxide trap charge, is the trap charge positive or negative?

# Question



If a top gate is added on the graphene transistor, shall we apply positive or negative voltage on the top gate to bring the Dirac voltage to zero?

# Outline

- Introduction of graphene
- Synthesis of graphene
- Current transport and electronic devices
  - Current transport
    - Dirac voltage
    - Carrier mobility
    - Minimum conductance
    - Current saturation and negative resistance
    - Quantum Hall Effect
  - Electronic devices
- Optical properties and photonic devices
- Bandgap engineering in graphene



# Extraction of carrier density and mobility in graphene transistors

The mobility can be extracted from the slope of the  $I_D \sim V_G$  curves

From electron branch,  $V_G \gg V_{Dirac}$ , we can extract electron carrier density and mobility

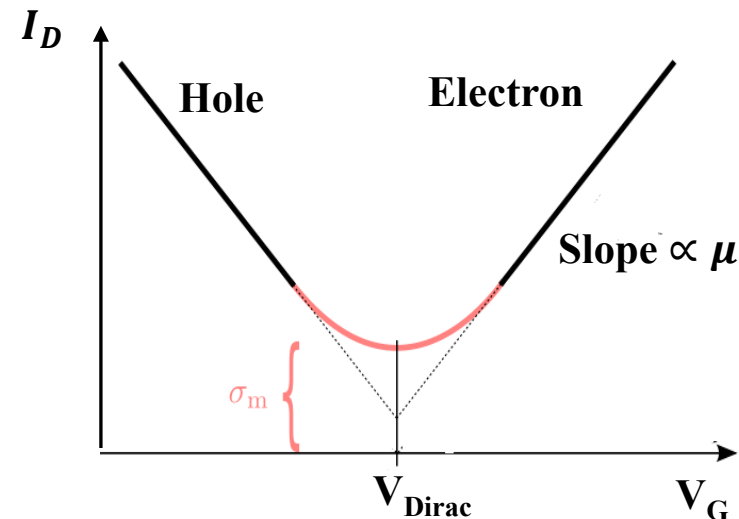
$$n = C_G(V_G - V_{Dirac})/q$$

$$\mu_n = \frac{\sigma_n}{qn} = \frac{L}{WV_D C_G} |\text{slope}|$$

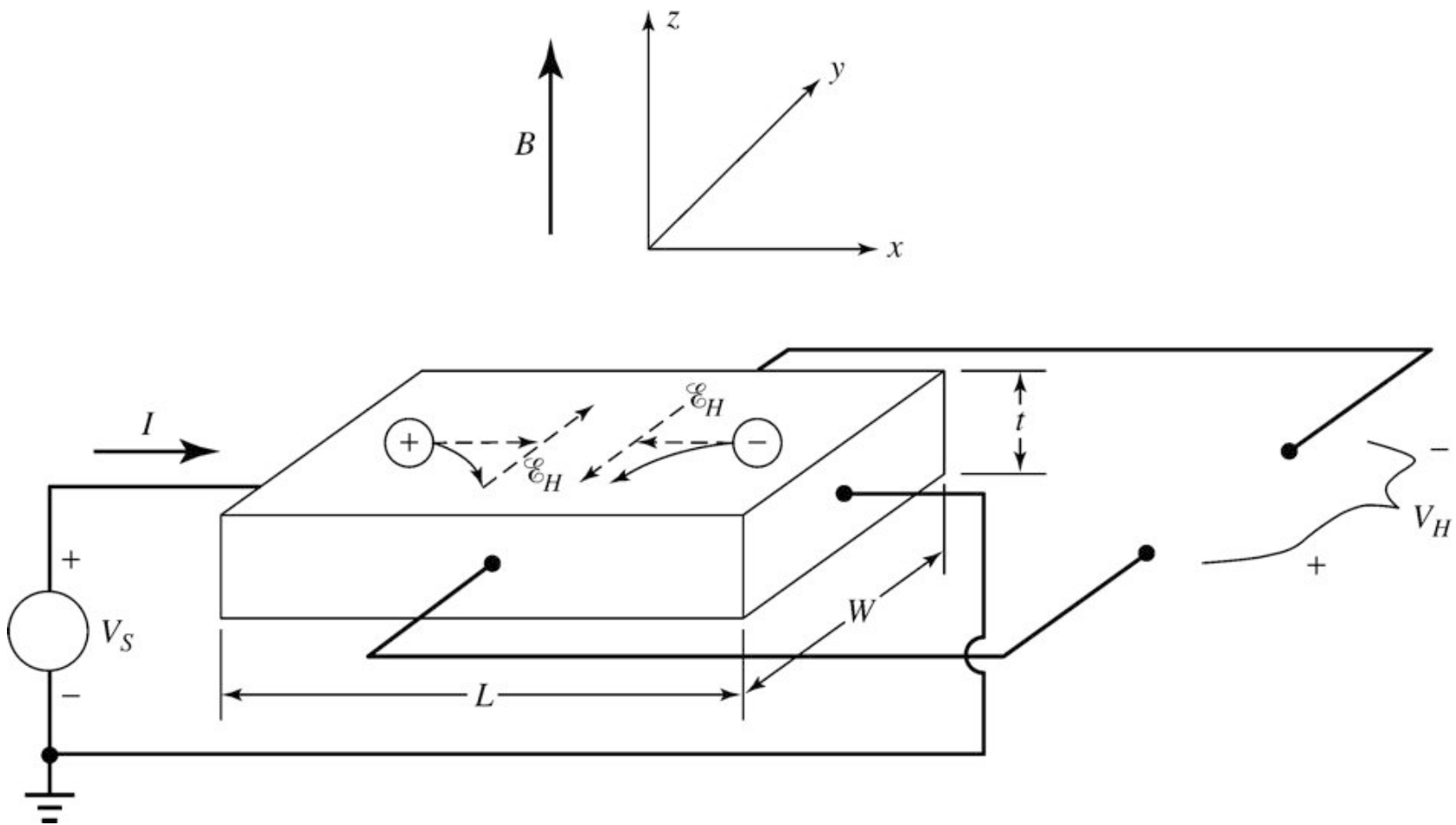
From hole branch,  $V_G \ll V_{Dirac}$ , we can extract hole carrier density and mobility

$$p = C_G(V_{Dirac} - V_G)/q$$

$$\mu_p = \frac{\sigma_p}{qp} = \frac{L}{WV_D C_G} |\text{slope}|$$



# Extract mobility from Hall measurement



# Physics of Hall Effect

The force on a particle with charge  $q$  and velocity  $v$  moving in a magnetic field  $\vec{B}$  is:

$$\vec{F} = qv \times \vec{B}$$

At steady state:  $qv_x B = q\mathcal{E}_H \quad \rightarrow \text{Hall voltage} \quad \mathcal{E}_H = v_x B = \frac{J_x}{qp} B$

**For p-type material:**

Hall resistivity:  $\rho_{xy} = \frac{\mathcal{E}_H}{J_x} = \frac{B}{qp} \quad \rightarrow \text{Hole density} \quad p = \frac{B}{q\rho_{xy}}$

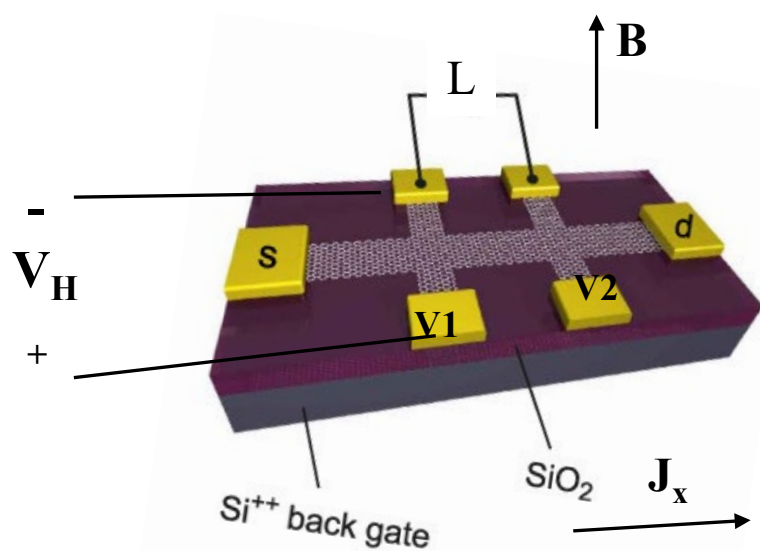
Channel resistivity:  $\rho_{xx} = \frac{\mathcal{E}_x}{J_x} = \frac{1}{\sigma_{xx}} = \frac{1}{qp\mu_h} \quad \rightarrow \text{Hole mobility} \quad \mu_h = \frac{1}{qp\rho_{xx}}$

**For n-type material:**

Hall resistivity:  $\rho_{xy} = -\frac{\mathcal{E}_H}{J_x} = \frac{B}{qn} \quad \text{Electron density} \quad n = \frac{B}{q\rho_{xy}}$

Channel resistivity:  $\rho_{xx} = \frac{\mathcal{E}_x}{J_x} = \frac{1}{\sigma_{xx}} = \frac{1}{qp\mu_h} \quad \text{Electron mobility} \quad \mu_h = \frac{1}{qn\rho_{xx}} \quad 38$

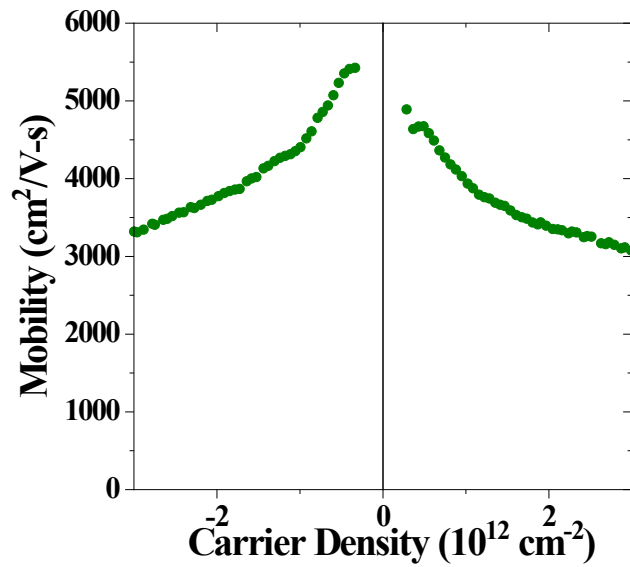
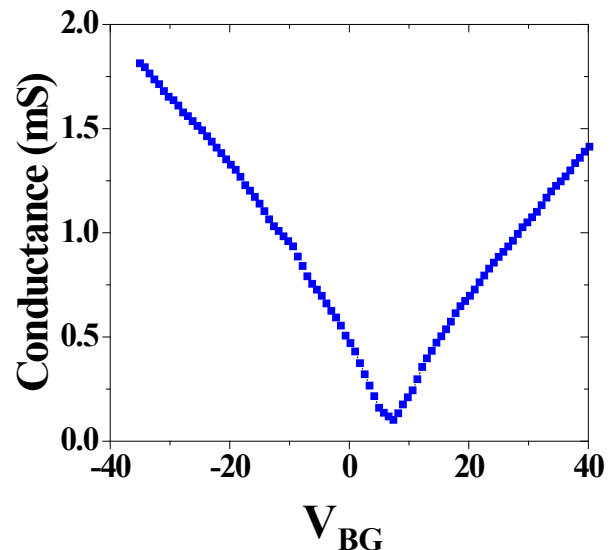
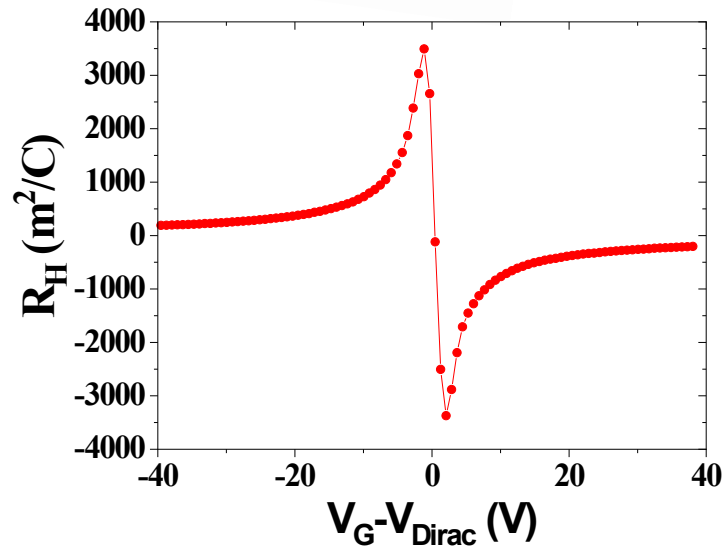
# Hall effect mobility in graphene (example)



$$R_H = \frac{\epsilon_H}{J_x B}$$

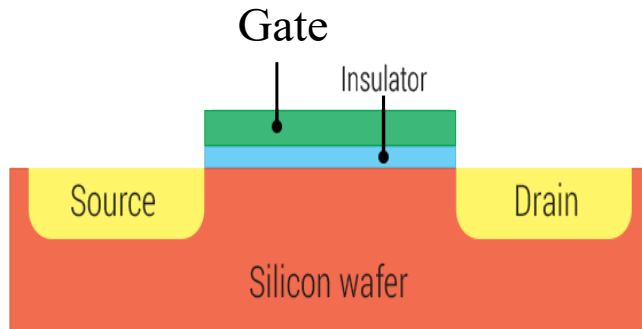
$$\rightarrow R_H = \frac{1}{qp}$$

$$R_H = \frac{-1}{qn}$$

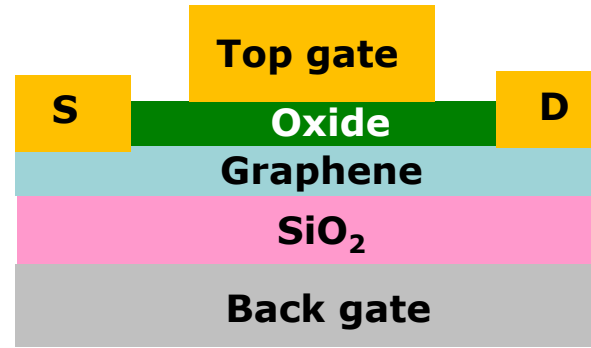


# Comparison of carrier mobility in silicon transistor and graphene transistor

Silicon transistor



Graphene transistor



## Intrinsic mobility:

Mobilities limited by silicon phonon at room temperature are:

Electron:  $1350 \text{ cm}^2/\text{V}\cdot\text{s}$

Hole:  $480 \text{ cm}^2/\text{V}\cdot\text{s}$

## Extrinsic Mobility:

Coulomb scattering

Surface roughness scattering

Phonon scattering from gate dielectrics

## Intrinsic mobility:

Mobilities limited by graphene phonon at room temperature:  $>2 \times 10^5 \text{ cm}^2/\text{V}\cdot\text{s}$

## Extrinsic Mobility:

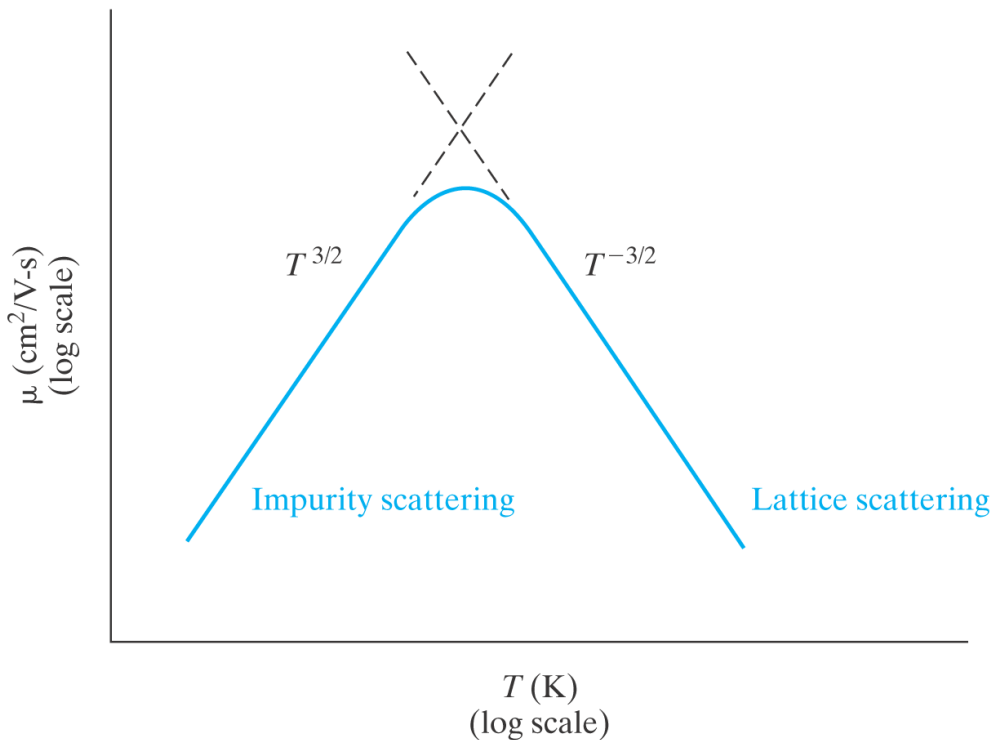
Phonon scattering from substrate and dielectrics

Coulomb scattering

Short-range scattering

Surface roughness scattering

# Recap: carrier mobility in silicon



**Mobility in silicon is limited by impurity scattering at low temperature and by silicon lattice scattering at high temperature.**

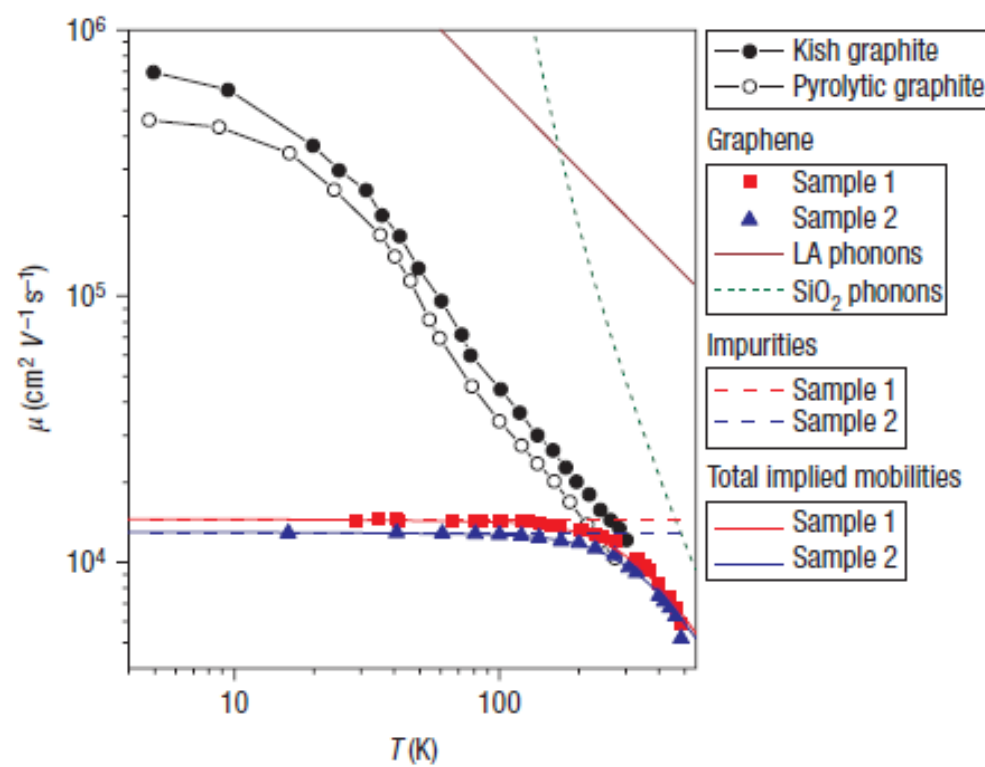
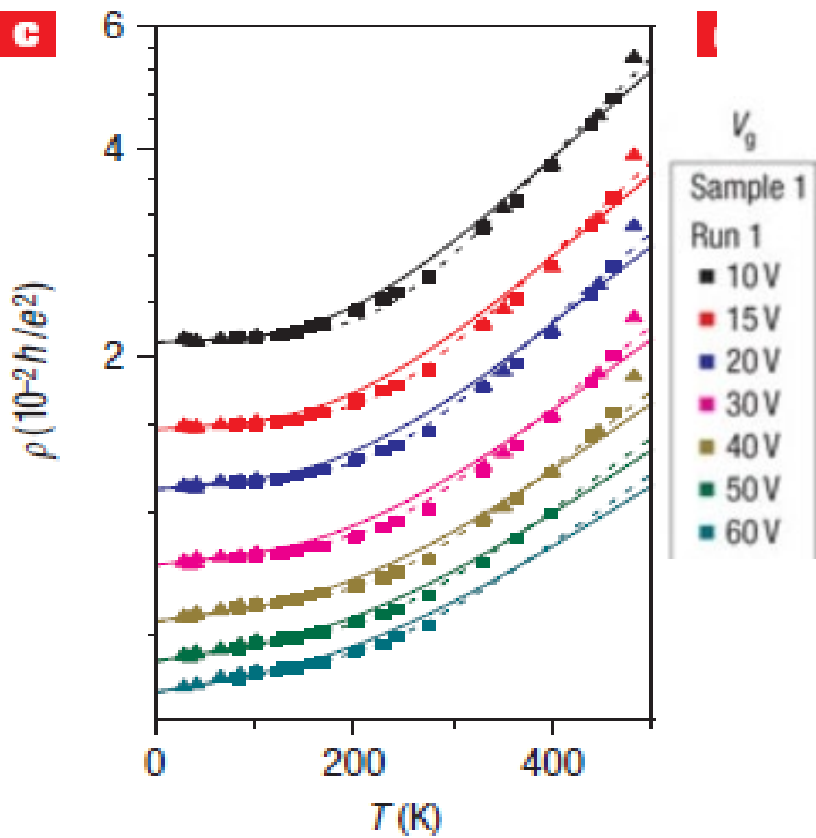
**Carrier mobility due to two or more scattering mechanisms is:**

$$\frac{1}{\mu} = \frac{1}{\mu_1} + \frac{1}{\mu_2} + \dots$$

**Matthiessen Rule:**

**The mechanism causing the lowest mobility value dominants.**

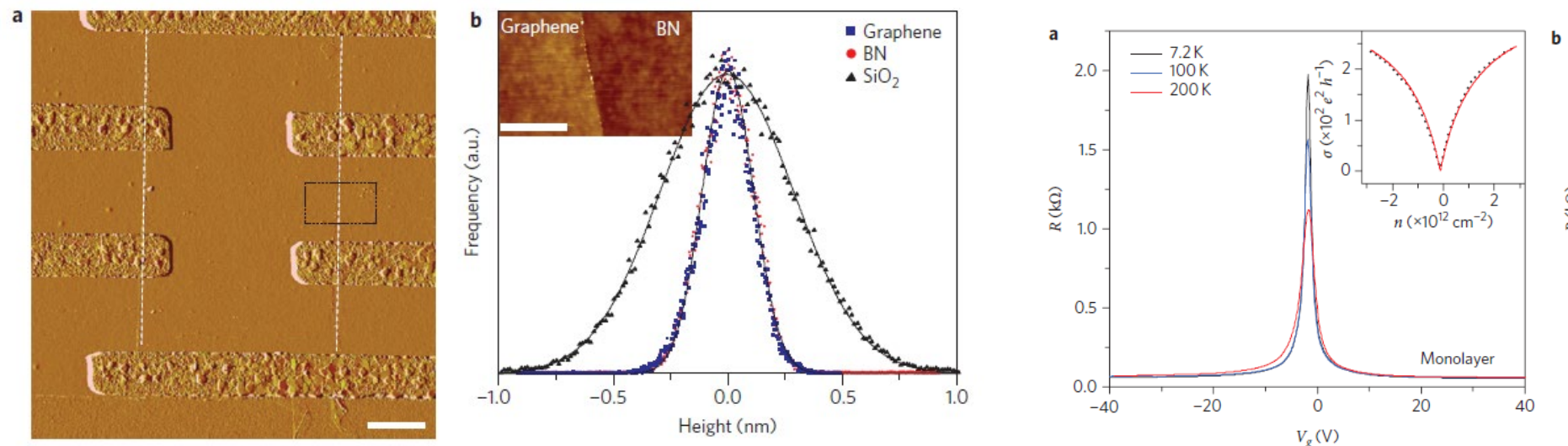
# Temperature dependence of mobility in graphene



- The temperature-dependent resistivity results reveal that extrinsic scattering by surface phonons at the SiO<sub>2</sub> is one of key factor that limits the mobility of graphene transistor on SiO<sub>2</sub>/Si substrates.

J. Chen, M. Fuhrer, et.al., Nature Nanotechnology, 3, 206, 2008

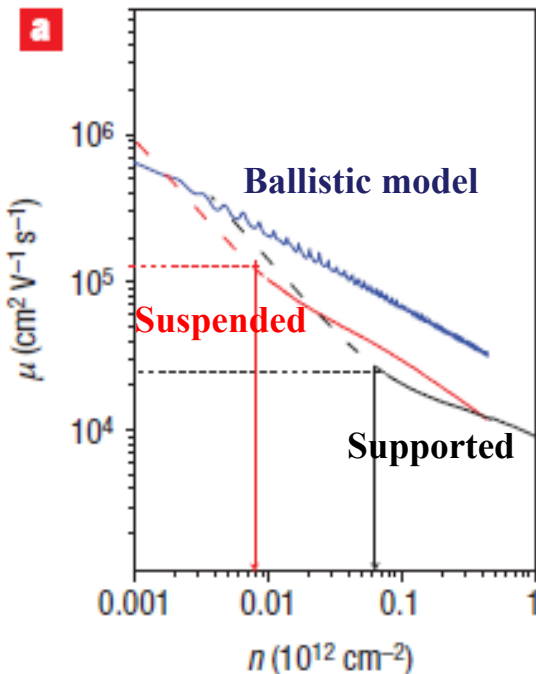
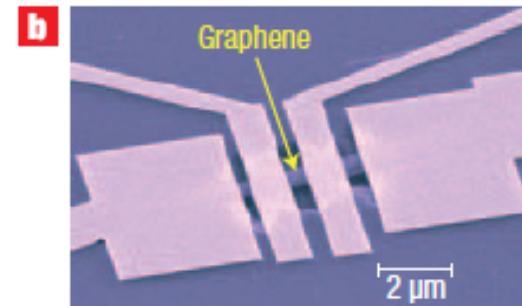
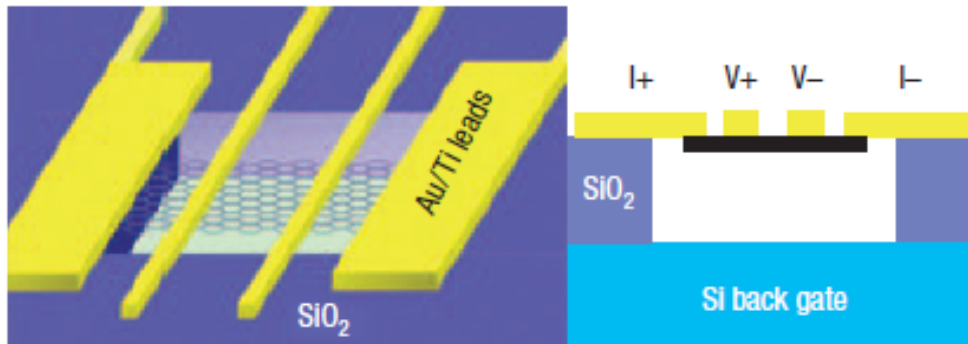
# Impact of substrate on mobility in graphene



- Hexagonal boron nitride (**h-BN**) has atomically smooth surface and large optical phonon energy and a large electrical bandgap, which are ideal as gate dielectric.
- Graphene devices on h-BN substrates have mobilities and carrier inhomogeneities that are almost an order of magnitude better than devices on SiO<sub>2</sub>. Hall mobility was 25,000 cm<sup>2</sup>/V-s at high carrier densities.

C. Dean, J. Hone, et.al., Nature Nanotechnology, 5, 722, 2010

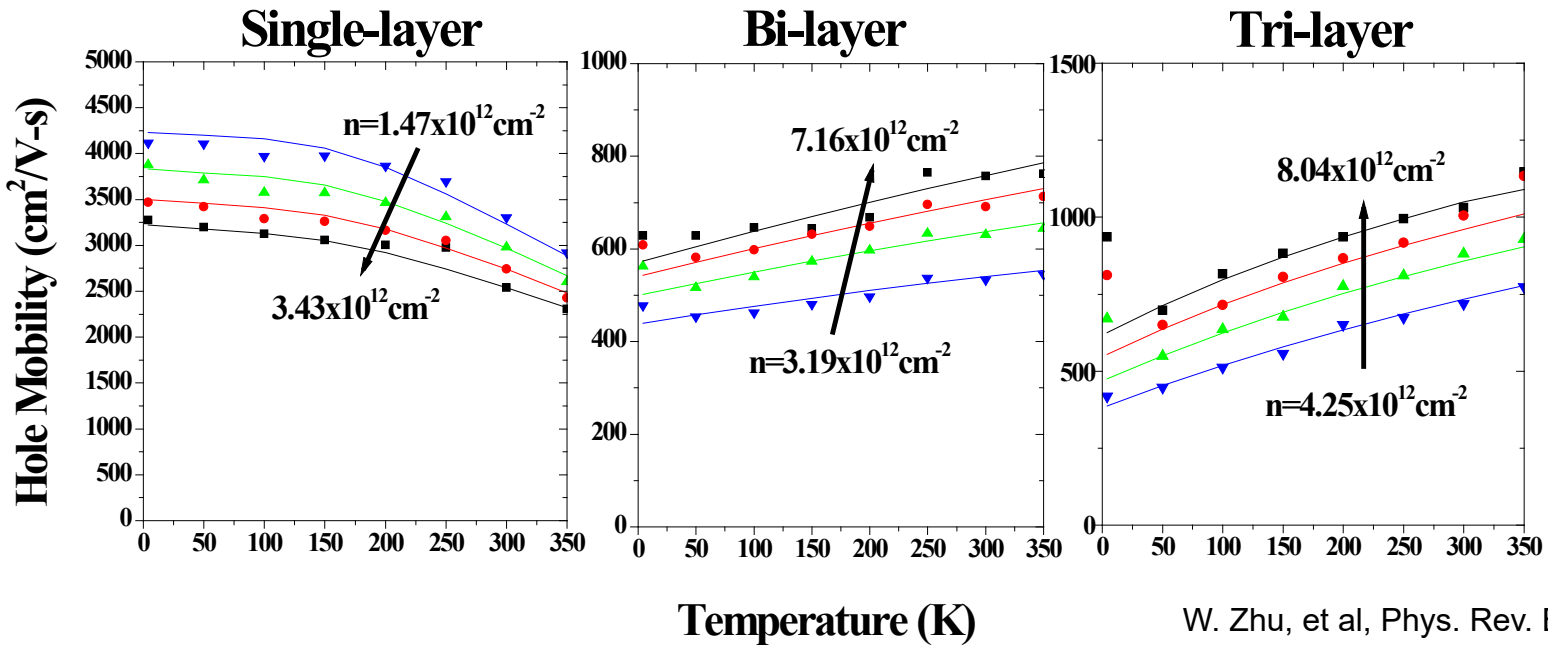
# Carrier mobility in suspended graphene



- Suspended graphene samples show low temperature mobility approaching  $200,000 \text{ cm}^2 \text{ V}^{-1} \text{ s}^{-1}$  for carrier densities below  $5 \times 10^9 \text{ cm}^{-2}$ .
- The maximum mobility of the suspended samples is significantly larger than that measured in the best non-suspended samples.

X. Du, et al., Nature Nanotechnology, Vol. 3, p.491, (2008)

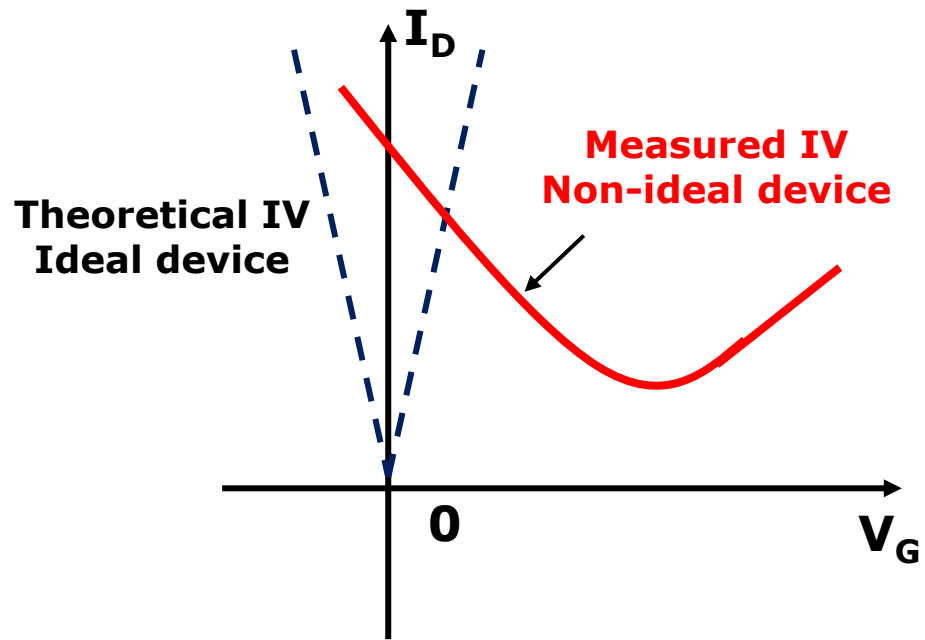
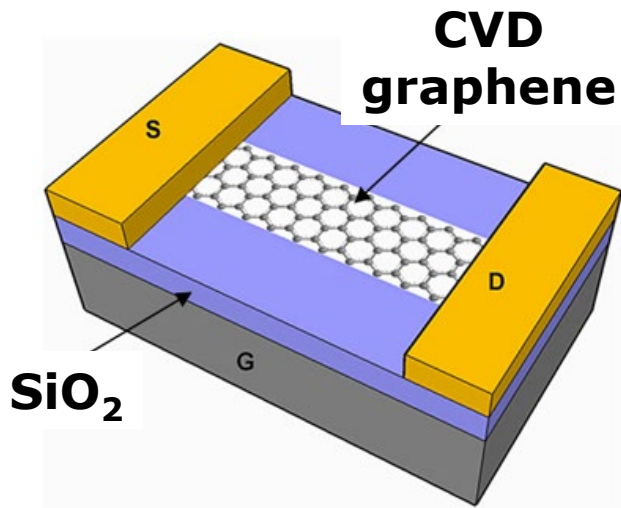
# Mobility in single-layer and multi-layer graphene



W. Zhu, et al, Phys. Rev. B, 2009

- Single-layer graphene:  $\mu \downarrow$  with increasing temperature, due to substrate optical phonon scattering:  $\tau_{ox}^{-1} \propto \sum_i \frac{c_i}{e^{\hbar\omega_i/\kappa_B T} - 1}$
- Bi- and tri-layer graphene:  $\mu \uparrow$  with increasing temperature, due to Coulomb scattering.  
Substrate phonon scattering is screened in bi- and tri-layer graphene.

# Question

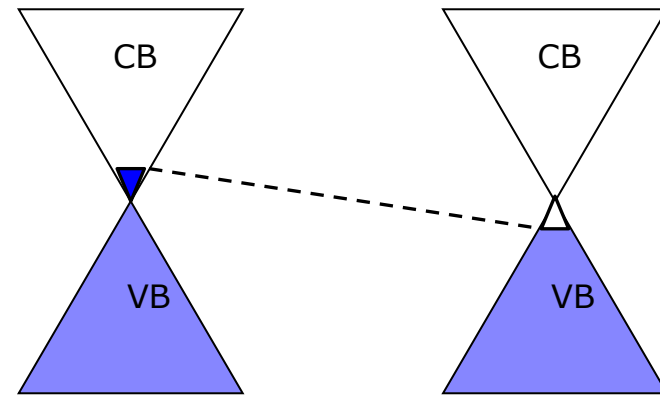
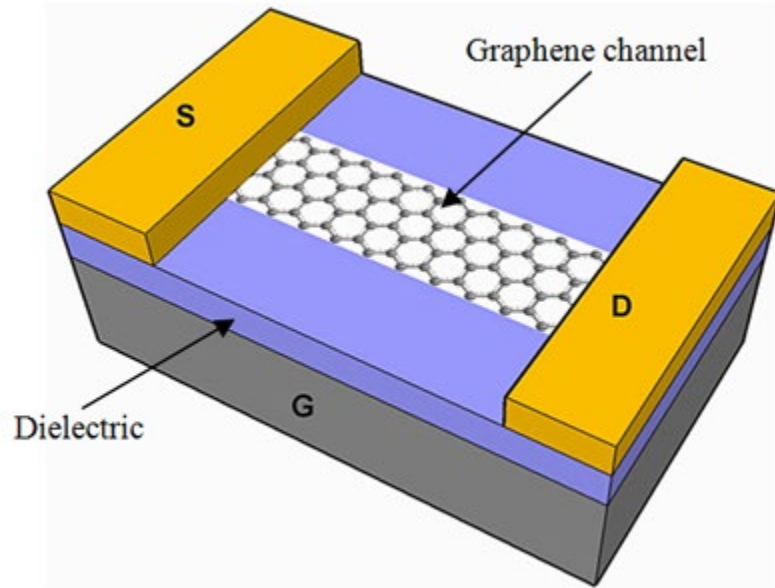


What are the possible approaches to increase the slope of the transfer curve in graphene transistor?

# Outline

- Introduction of graphene
  - Synthesis of graphene
  - Current transport and electronic devices
    - Current transport
      - Dirac voltage
      - Carrier mobility
    - • Minimum conductance
    - Current saturation and negative resistance
    - Quantum Hall Effect
  - Electronic devices
- Optical properties and photonic devices
  - Bandgap engineering in graphene

# Minimum conductance in graphene transistor

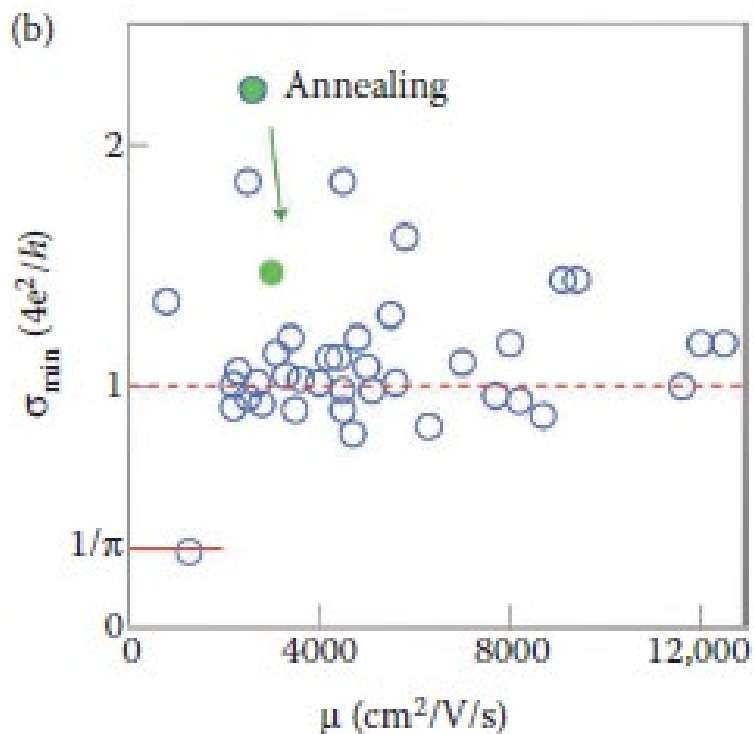


Assume there is no charge impurities and temperature is 0 K, the theoretical minimum conductance is:

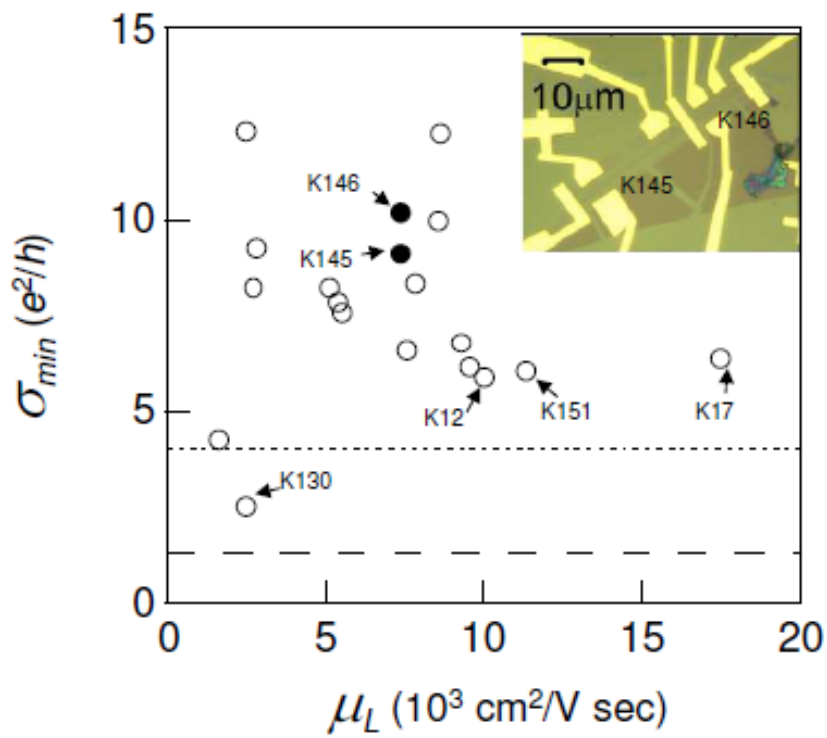
$$\sigma_{min} = \frac{4e^2}{\pi h}$$

M.I. Katsnelson, Eur. Phys. J. B 51, 157–160 (2006)  
M. Houssa, “2D materials for Nanoelectronics” CRC Press, 2016

# Realistic minimum conductance



A. Geim, Nature Materials, 6, 183, (2007)



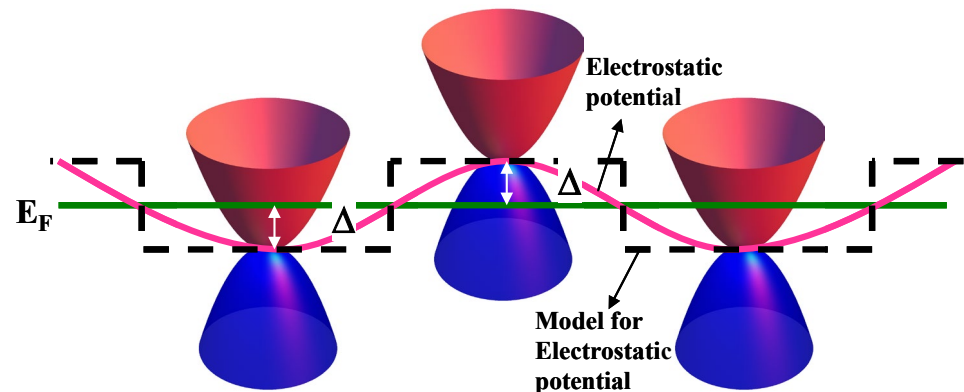
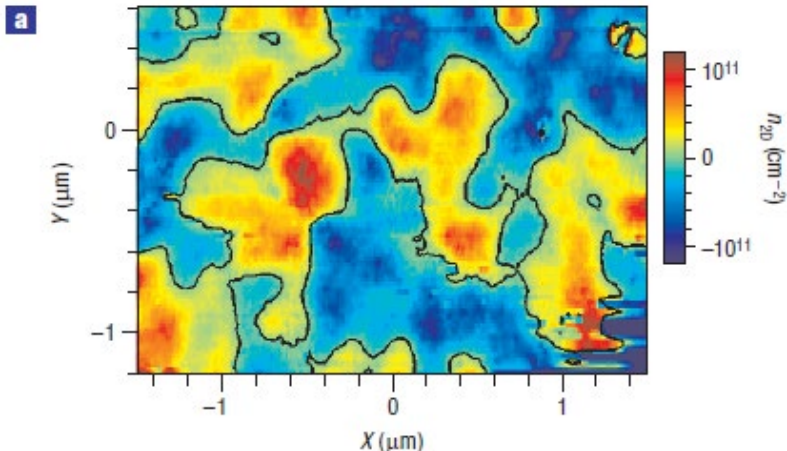
Y. Zhang, P. Kim, Nature, 2005, 201

Y. Tan, P. Kim, et.al., Physical Review Letters, 99. 246803, 2008

In real devices, the minimum conductance varies from sample to sample and is usually much larger than theoretical predicted values.

# Impact of charge impurity on minimum conductance

Map of the spatial density variations



The blue regions correspond to holes and the red regions correspond to electrons.

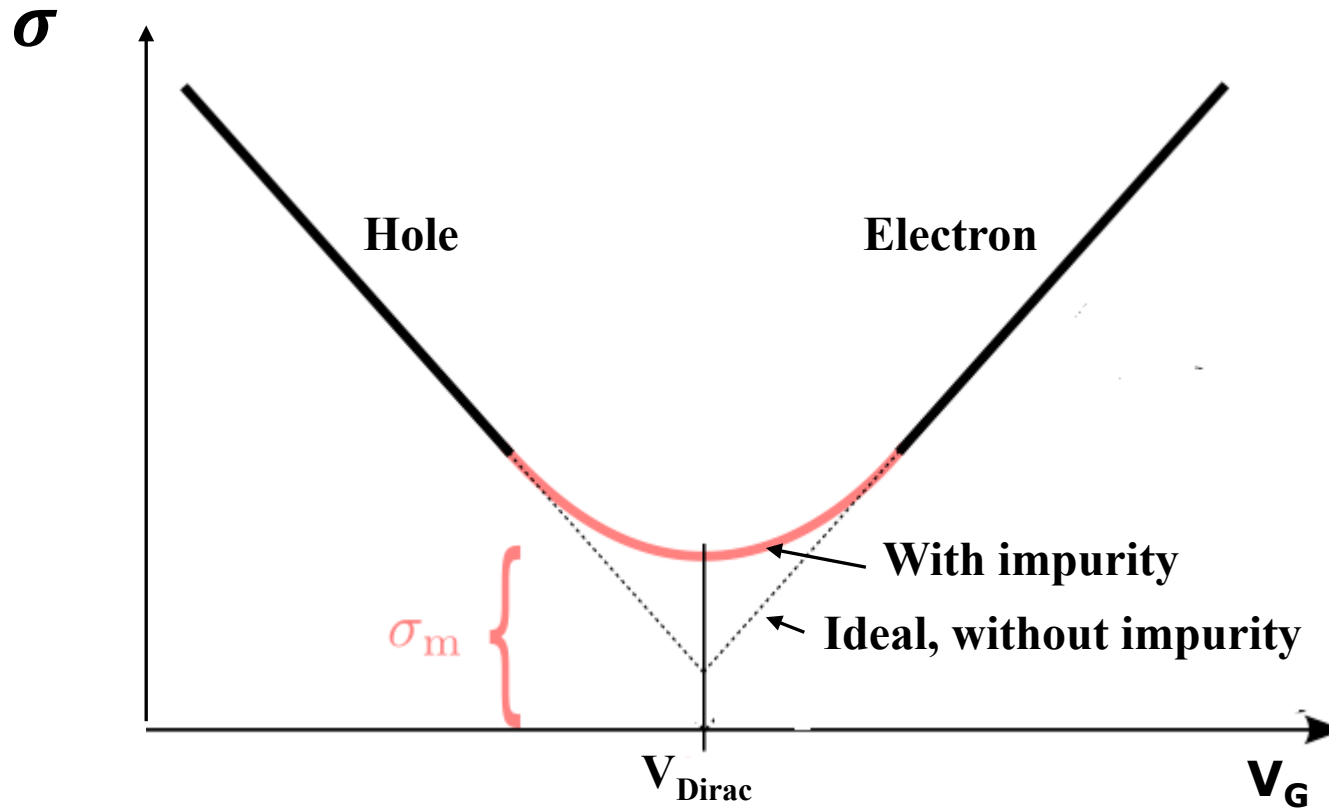
Total carrier density at the Dirac point is:

$$n_{dirac} = 2n_e = 2n_h = \int_{-\Delta}^{\infty} D(E + \Delta) \frac{1}{e^{E/k_B T} + 1} dE + \int_{\Delta}^{\infty} D(E - \Delta) \frac{1}{e^{E/k_B T} + 1} dE$$

W. Zhu, et al, Phys. Rev. B, 80, 235402 2009

J. Martin, A. Yacoby, et.al., Nature Physics, 4, 144, 2008

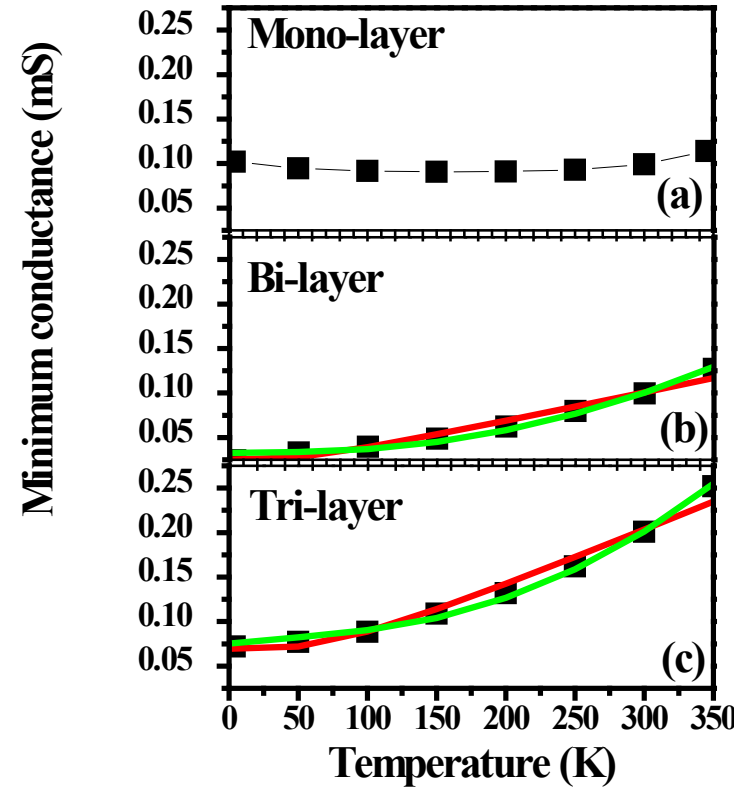
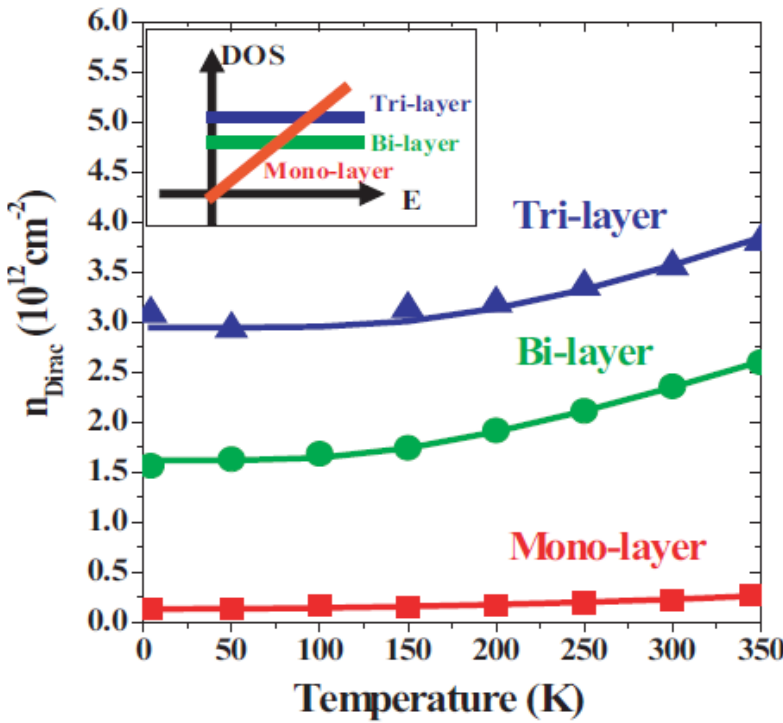
# Impact of charge impurities on minimum conductance



The conductance of graphene transistor can be written as:

$$\sigma \approx \mu \sqrt{(en_{Dirac})^2 + C_G^2(V_G - V_{Dirac})^2}$$

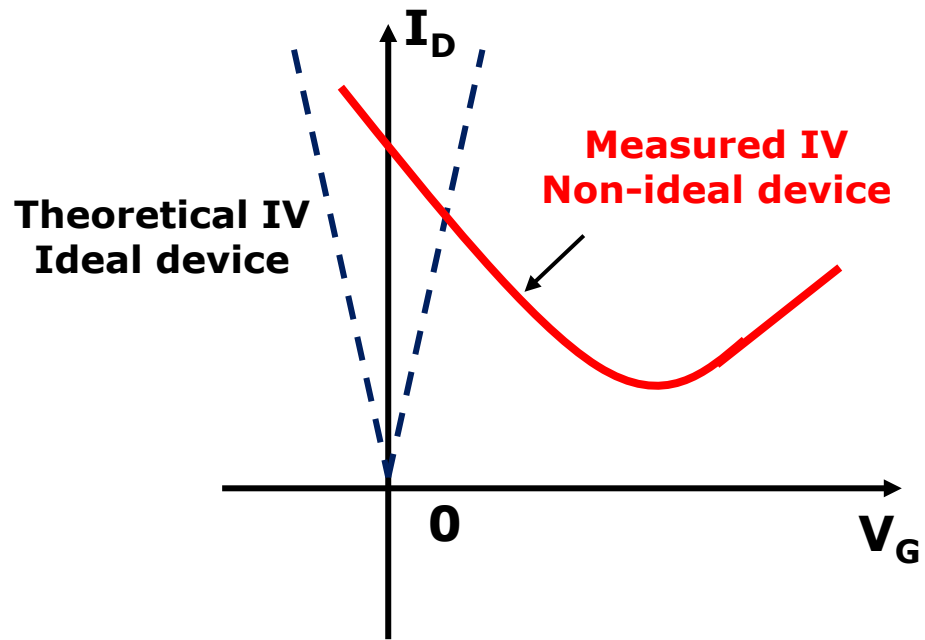
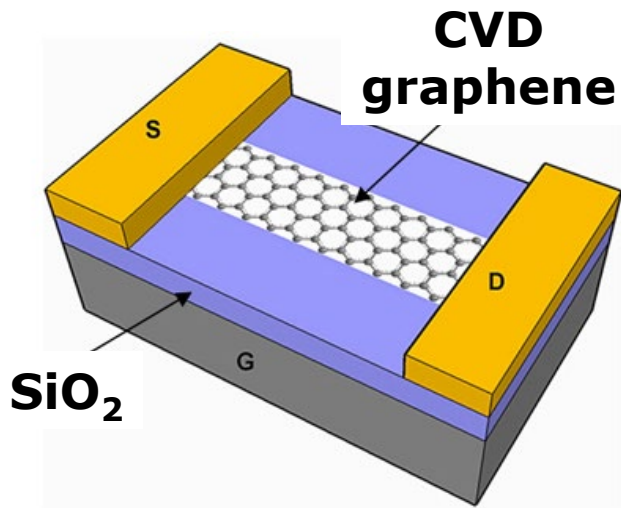
# Temperature dependence of minimum conductance



- Carrier density at Dirac point increases with temperature. Carrier density at the Dirac point increases with layer number, due to the increasing density-of-states near the Dirac point.
- For bilayer and trilayer graphene, minimum conductance increases with temperature, since both the carrier density and the mobility increase with temperature.
- For monolayer graphene, minimum conductance has very weak temperature dependence, since mobility decreases with temperature while carrier density increases with temperature.

W. Zhu, et al, Phys. Rev. B, 80, 235402 2009

# Question

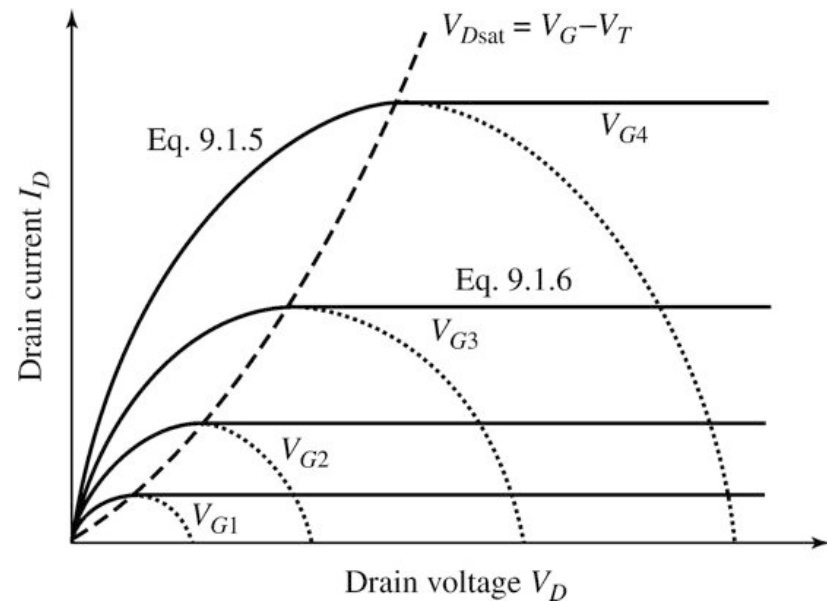
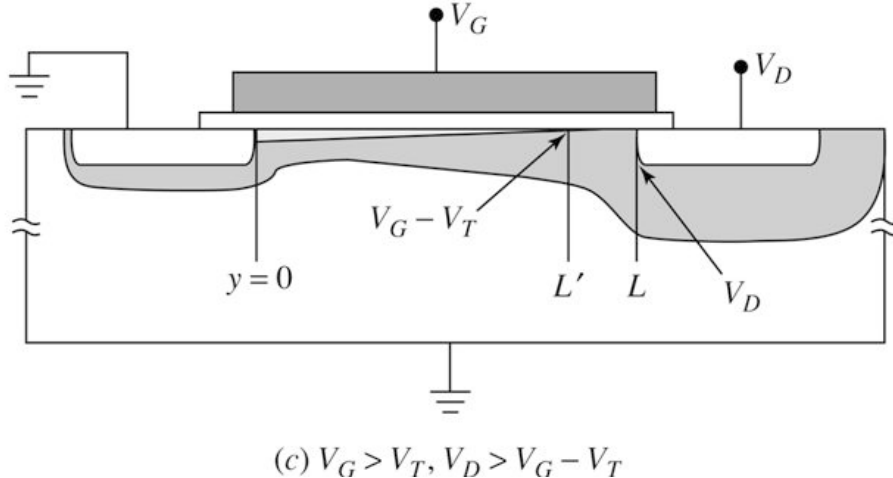


What are the possible approaches to reduce minimum conductivity of a graphene transistor?

# Outline

- Introduction of graphene
  - Synthesis of graphene
  - Current transport and electronic devices
    - Current transport
      - Dirac voltage
      - Carrier mobility
      - Minimum conductance
    - • Current saturation and negative resistance
    - Quantum Hall Effect
  - Electronic devices
- Optical properties and photonic devices
  - Bandgap engineering in graphene

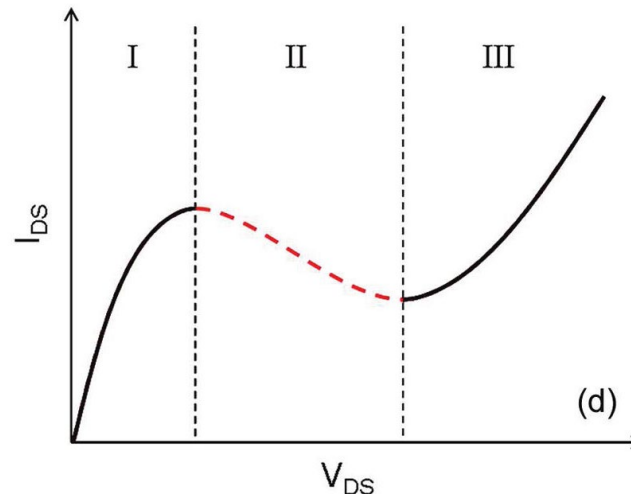
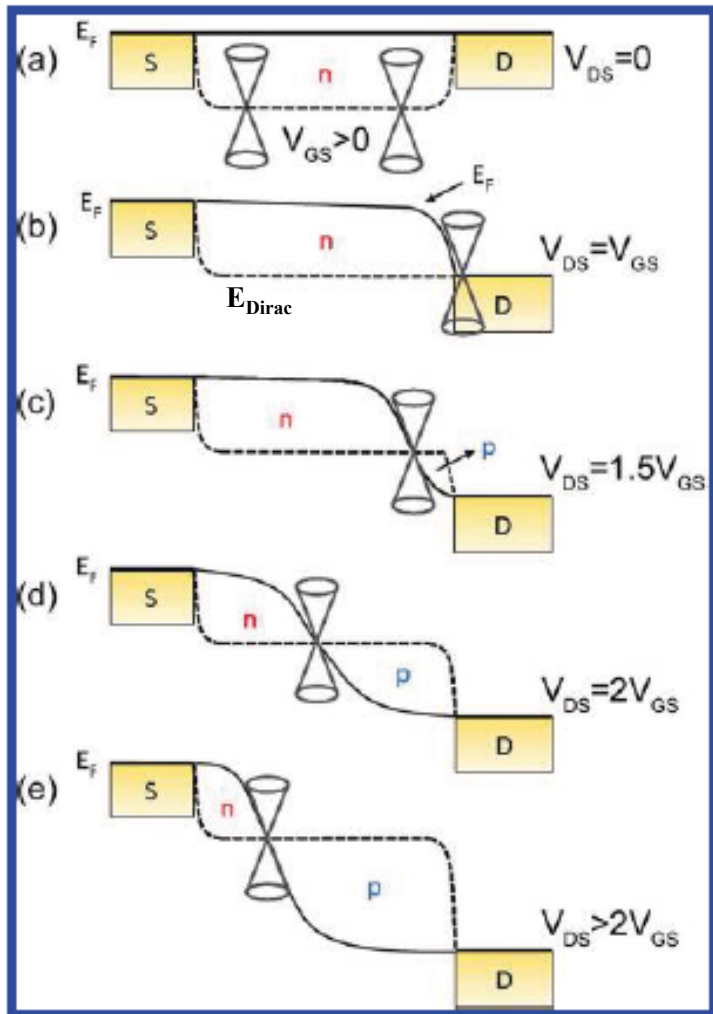
# Recap: Current saturation in silicon



When the mobile-electron density in the channel at  $y = L$  decrease to zero (a condition described as *pinch-off*), the current reaches saturation.

- When  $\frac{1}{2}V_D \ll V_G - V_T$ ,  $I_D$  increase linearly with  $V_D$ ;
- When  $\frac{1}{2}V_D$  is comparable with  $V_G - V_T$ , the slope decreases with  $V_D$ ;
- When  $V_D \geq V_G - V_T$ , the drain current remains constant

# Negative resistance in graphene



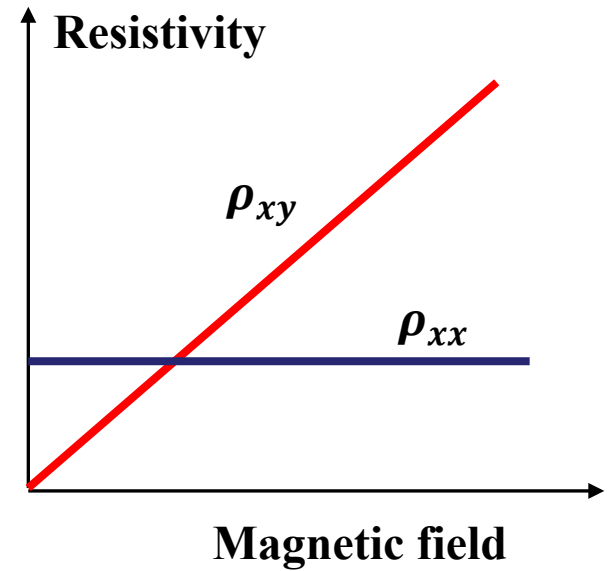
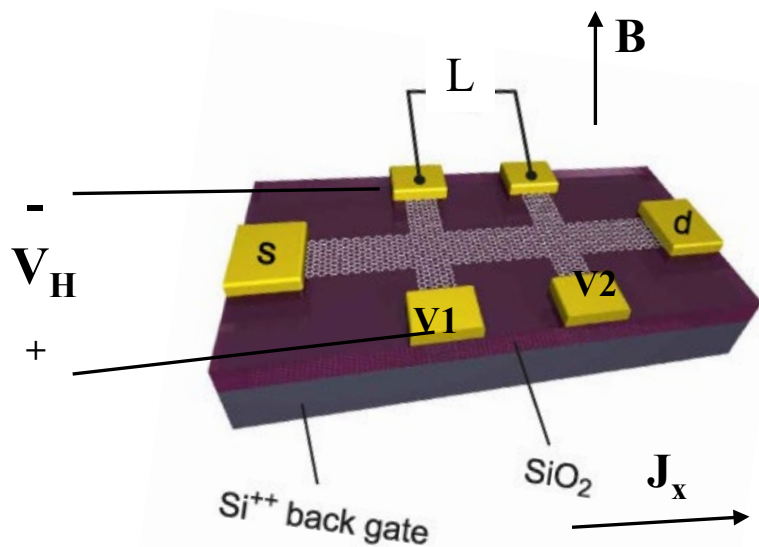
- When  $V_{GS} > 0$  and  $V_{DS}$  is small, the dominant carriers in the channel are electrons and the channel resistance is nearly constant.
- As  $V_{DS} = V_{GS}$ , the local Fermi energy at the drain coincides with the Dirac point.
- When  $V_{DS} > V_{GS}$ , the Dirac point moves further into the channel. Part of the electron dominated channel is replaced by a hole-dominated region with a lower carrier density, so the drain current reduces.
- When  $V_{DS} > 2V_{GS}$ , the Dirac point passes half way of the channel, the drain current will increase again.

Y. Wu., Y. Lin, et.al., ACS Nano, 6, 2610, 2012

# Outline

- Introduction of graphene
- Synthesis of graphene
- Current transport and electronic devices
  - Current transport
    - Dirac voltage
    - Minimum conductance
    - Carrier mobility
    - Current saturation and negative resistance
  - • Quantum Hall Effect
  - Electronic devices
- Optical properties and photonic devices
- Bandgap engineering in graphene

# Recap: Hall Effect



Hall resistivity:

$$\rho_{xy} = \frac{\mathcal{E}_H}{J_x} = \frac{B}{qn_p}$$

Electrons

$$\rho_{xy} = \frac{B}{qn_e}$$

Channel resistivity:

$$\rho_{xx} = \frac{\mathcal{E}_x}{J_x} = \frac{1}{qn_p \mu_h}$$

$$\rho_{xx} = \frac{1}{qn_e \mu_e}$$

# Quantum Hall effect

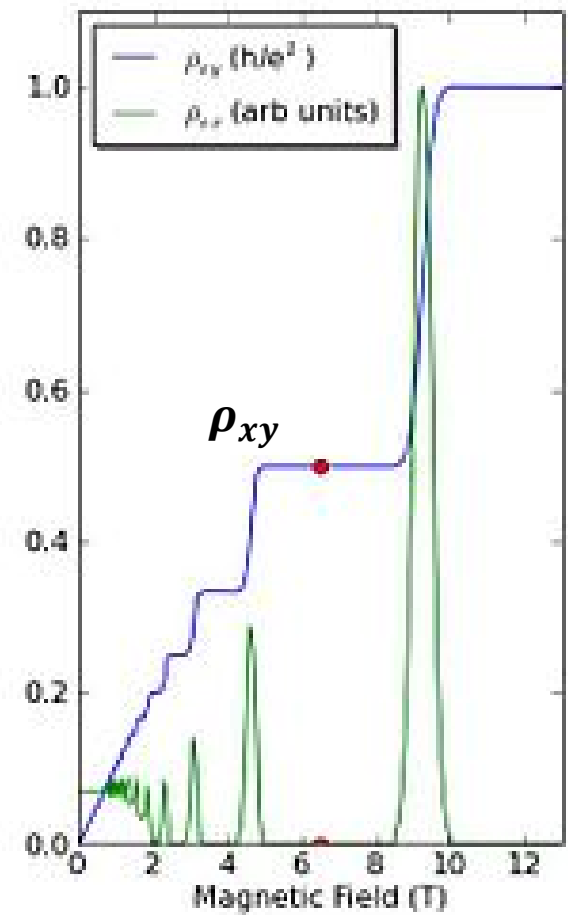
The quantum Hall effect: at strong magnetic fields, the Hall conductance takes on the quantized values:

$$G_{xy} = \frac{I_x}{V_H} = v \frac{e^2}{h}$$

$h$  is Planck's constant,  $e$  is elementary charge,  
 $v$  is called filling factor, which can take on  
either integer ( $v=1, 2, 3 \dots$ ) or fractional ( $v = \frac{1}{3}, \frac{2}{5} \dots$ ) values.

The plateau in the Hall resistance is accompanied by a vanishing longitudinal resistance.

Integer quantum Hall effect was discovered by Klitzing, Dorda, and Pepper in 1980 and the Nobel Prize was given in 1985.



# Cyclotron frequency

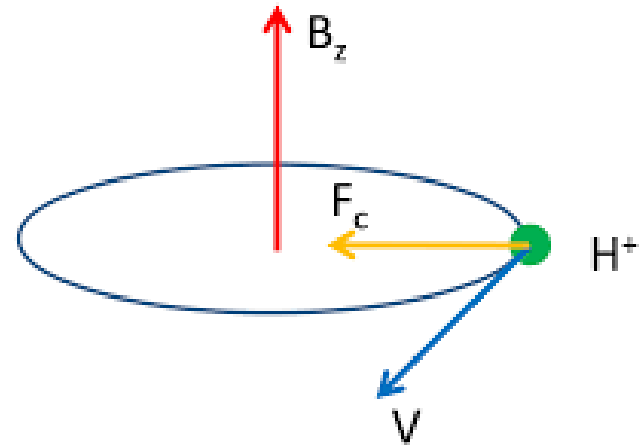
- When a charge particle is moving perpendicular to the direction of a uniform magnetic field  $B$ , the motion is circular.
- The centripetal force equals to magnetic Lorentz force

$$\frac{mv^2}{r} = qvB$$



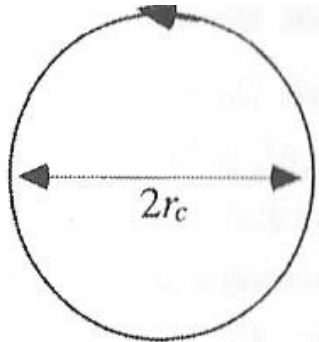
- Cyclotron frequency:

$$\omega_c = \frac{v}{r} = \frac{qB}{m}$$



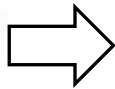
# Landau Quantization

A rough explanation:



An electron in a magnetic field goes around in a circular orbit. The circumference must be an integer number of the de Broglie wavelength:

$$2\pi r_c = nh/mv$$



The energy levels of these quantized orbitals take on discrete values.

More precisely:

Time-independent Schrödinger equation  $H\Psi = E\Psi$

Hamiltonian of a particle in Magnetic field (non-relativistic):

$$H = \frac{(\vec{p} + e\vec{A})^2}{2m}$$

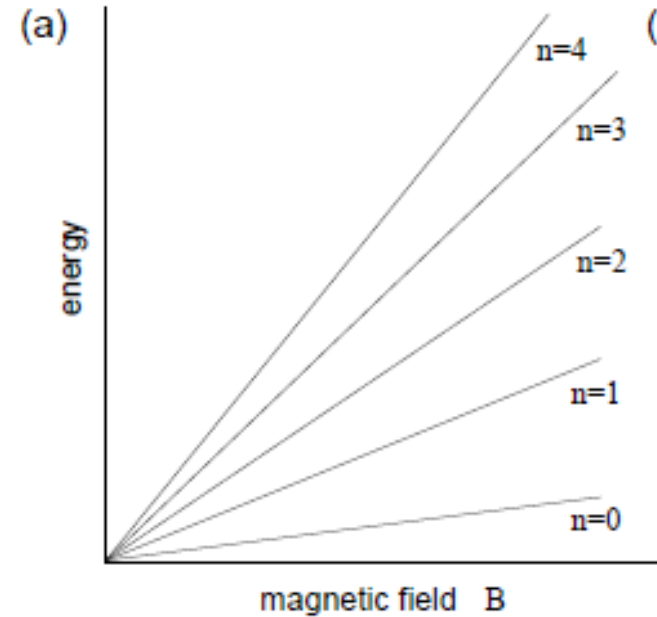
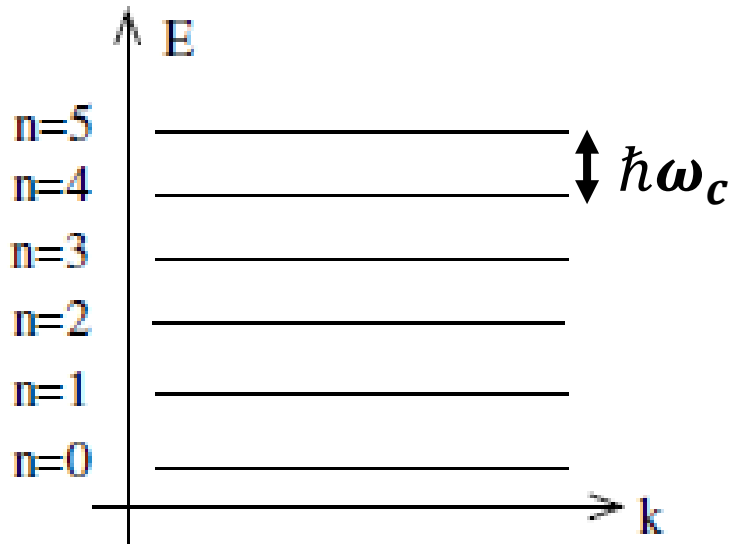
Where  $\vec{A}$  is the vector potential that generates the magnetic field  $\vec{B} = \nabla \times \vec{A}$

# Landau Levels (non-relativistic)

Solving the Schrödinger equation reveals that the energy levels of the 2D charged non-relativistic particle are discrete and labelled by the integer  $n$  (called Landau index):

$$E_n = \hbar\omega_c(n + 1/2)$$

Where  $\omega_c$  is the cyclotron frequency. These energy levels are known as Landau levels.



# Degeneracy of Landau levels

The magnetic field causing all the states in an energy range  $\hbar\omega_c$  to be concentrated into a single Landau level.

At zero magnetic field, the density of states of 2D electron gas (considering spin degeneracy) can be expressed as:

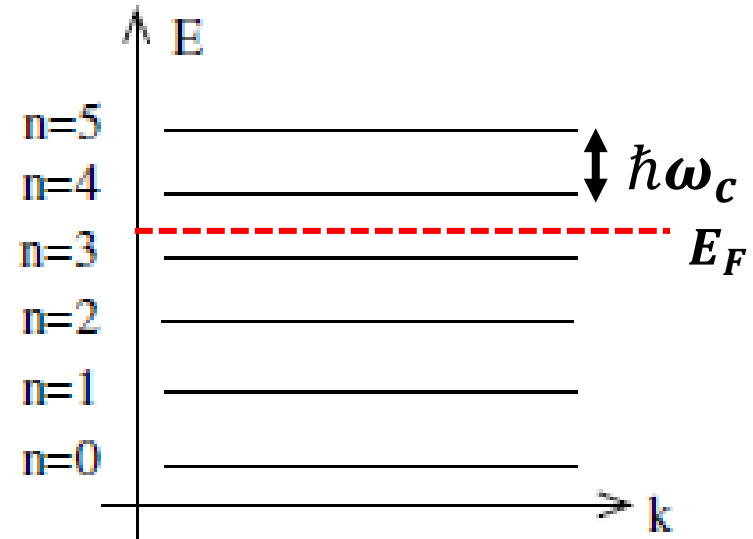
$$D(E) = m/\pi\hbar^2$$

At magnetic field B, the number of states in each Landau levels per unit area is

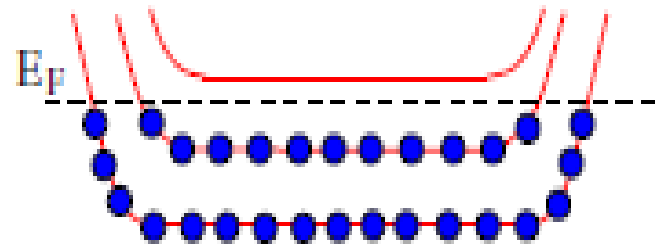
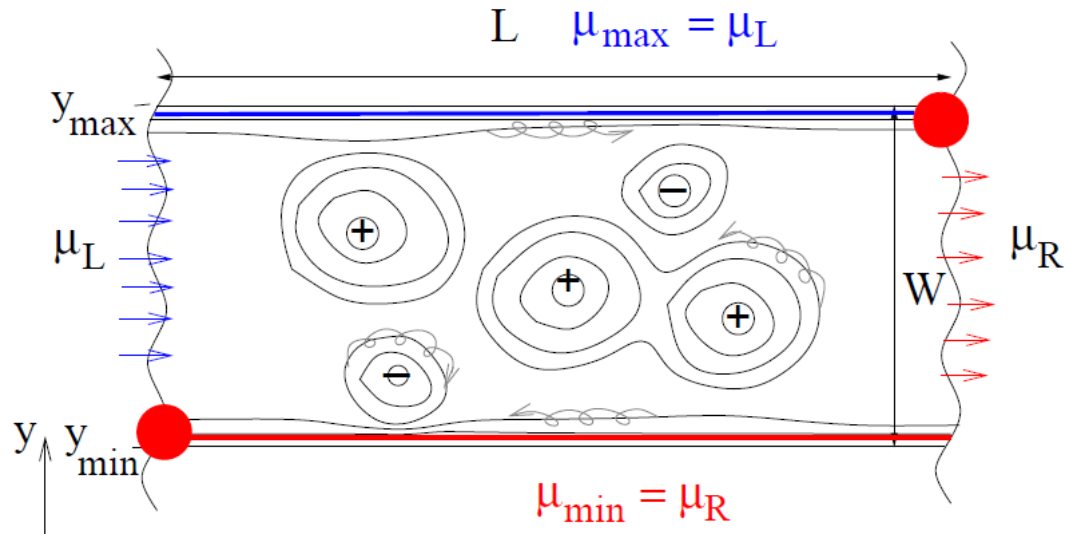
$$N_0 = \hbar\omega_c \times \frac{m}{\pi\hbar^2} = 2eB/h$$

The number of occupied Landau levels is

$$n = \frac{n_e}{N_0} = \frac{n_e h}{2eB}$$



# Hall conductivity and longitudinal resistance



- The chemical potential is constant along a sample edge, but there is a potential difference between the two edges.

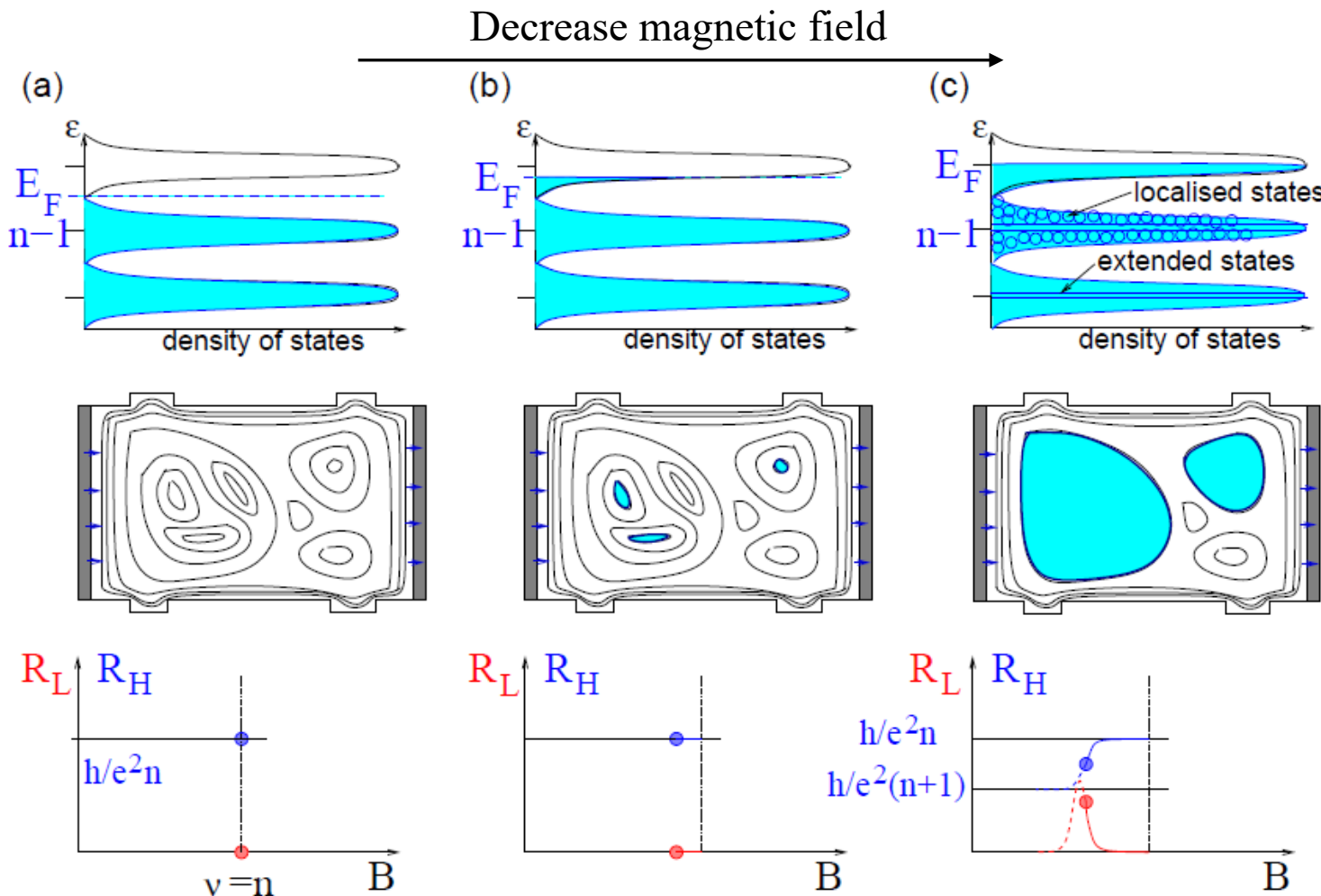
Therefore, the Hall conductivity is:

$$G_{xy} = \frac{I_x}{V_y} = \frac{e^2}{h} \nu$$

- Particles move in one direction on one side of the sample, and in the other direction on the other side of the sample.
- Backscattering processes are therefore strongly suppressed, which leads to vanishing longitudinal resistance.

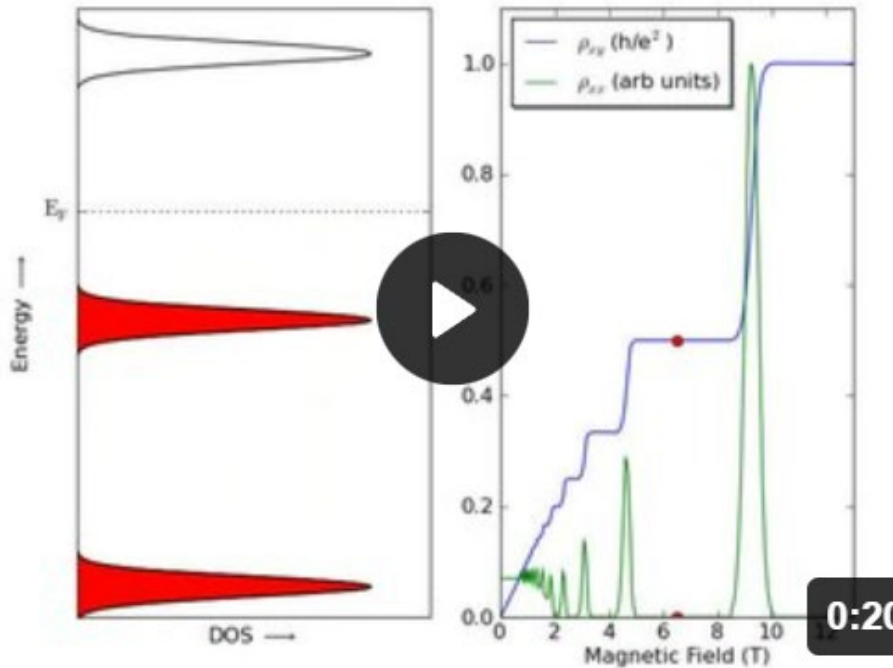
$$\rho_{xx} = 0$$

# Impurities and localized states



When magnetic field decreases, electrons start to populate the localized states in the  $n$ th LL, which do not affect the global transport. When one continues to increase magnetic field, electrons start to occupy the extended states. The longitudinal resistance is no longer zero due to backscattering and Hall resistance transits to the next plateau.

# Animation of quantum Hall effect



Animated graph showing filling of Landau levels as  $B$  changes and the corresponding position on a graph of hall coefficient and magnetic field|Illustrative only. The levels spread out with increasing field. Between the levels the quantum hall effect is seen.

# Quantum Hall Effect in Graphene

Non-relativistic particle  
(ex. e/h in silicon)

Relativistic particle  
(ex. e/h in monolayer graphene)

Dispersion relation:  $E = \hbar^2 k^2 / 2m^*$

$$E = \hbar k v_F$$

$$H = \frac{(\mathbf{p} + e\vec{A})^2}{2m}$$

$$\mathbf{H} = (\mathbf{p} + e\vec{A})v_F$$

(for one sublattice)

Landau level  $E_n = \hbar\omega_c(n + 1/2)$

$$E_n = \pm \sqrt{2e\hbar v_F^2 |n| B}$$

Hall conductivity  $G_{xy} = \frac{e^2}{h} \nu$

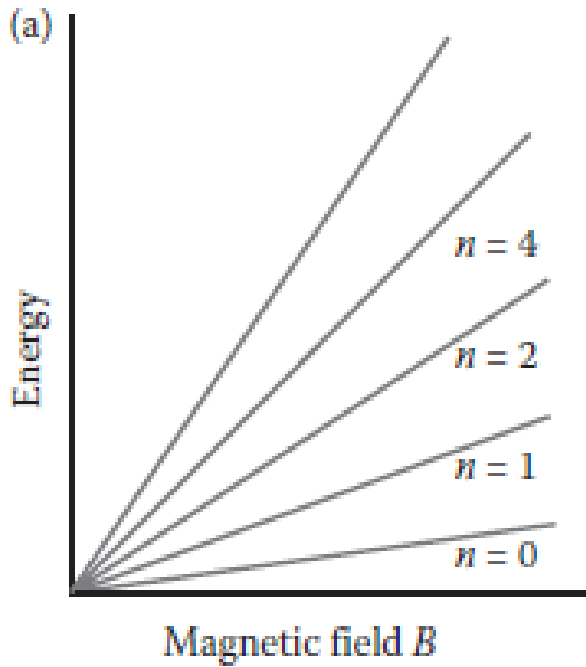
$$G_{xy} = \frac{e^2}{h} \nu$$

where  $\nu = 2n$ , if consider spin degeneracy

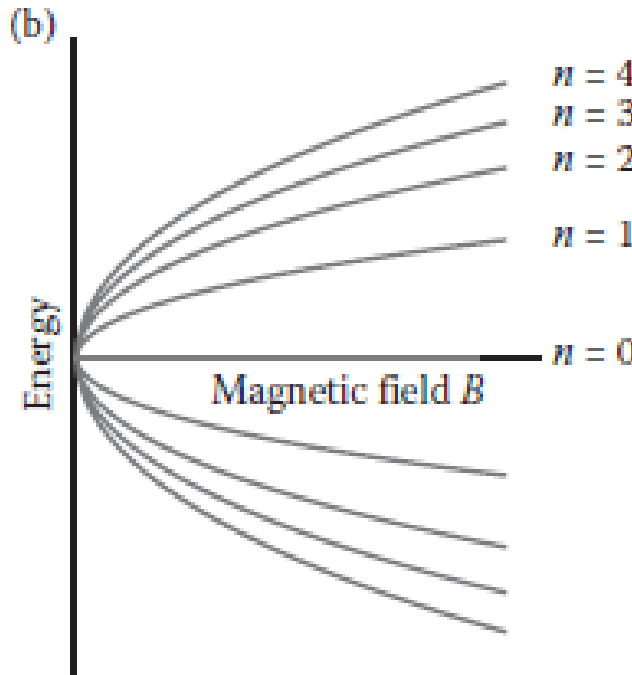
where  $\nu = \pm 4 \left( n + \frac{1}{2} \right)$   
Spin and sublattice degeneracy

# Landau level energy

Traditional bulk materials



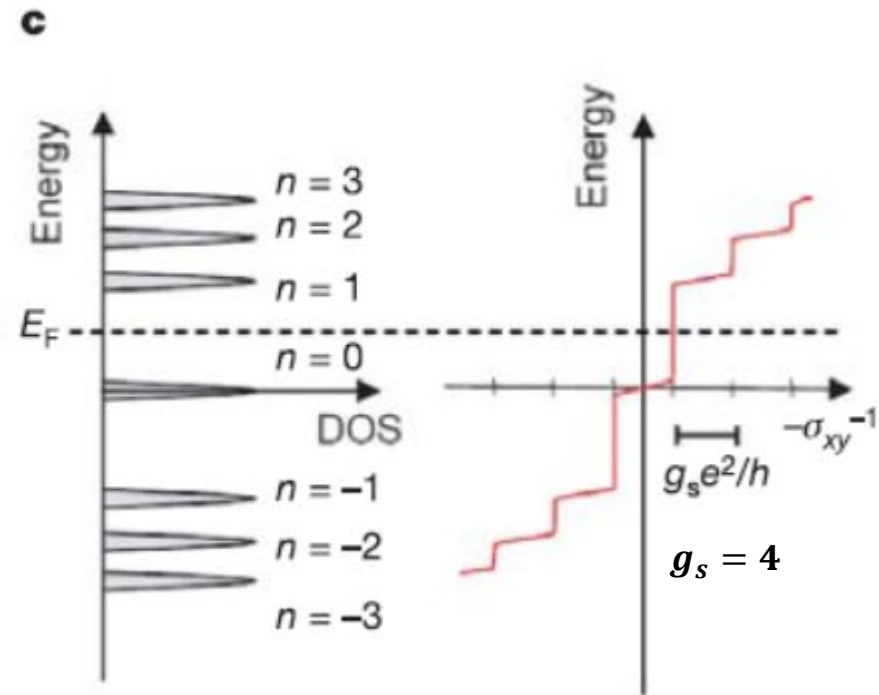
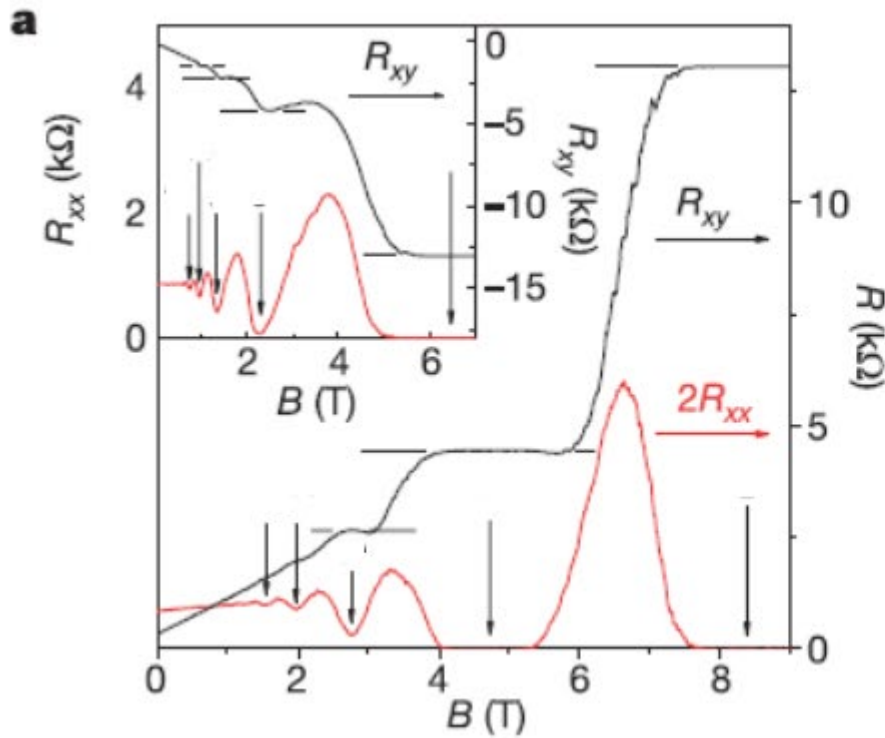
Monolayer graphene



- For bulk material with parabolic energy-momentum relation, landau level energy depends linearly on the magnetic field.  $E_n \propto B$ .
- For monolayer graphene,  $E_n \propto \sqrt{B}$

M. Houssa, “2D materials for Nanoelectronics” CRC Press, 2016

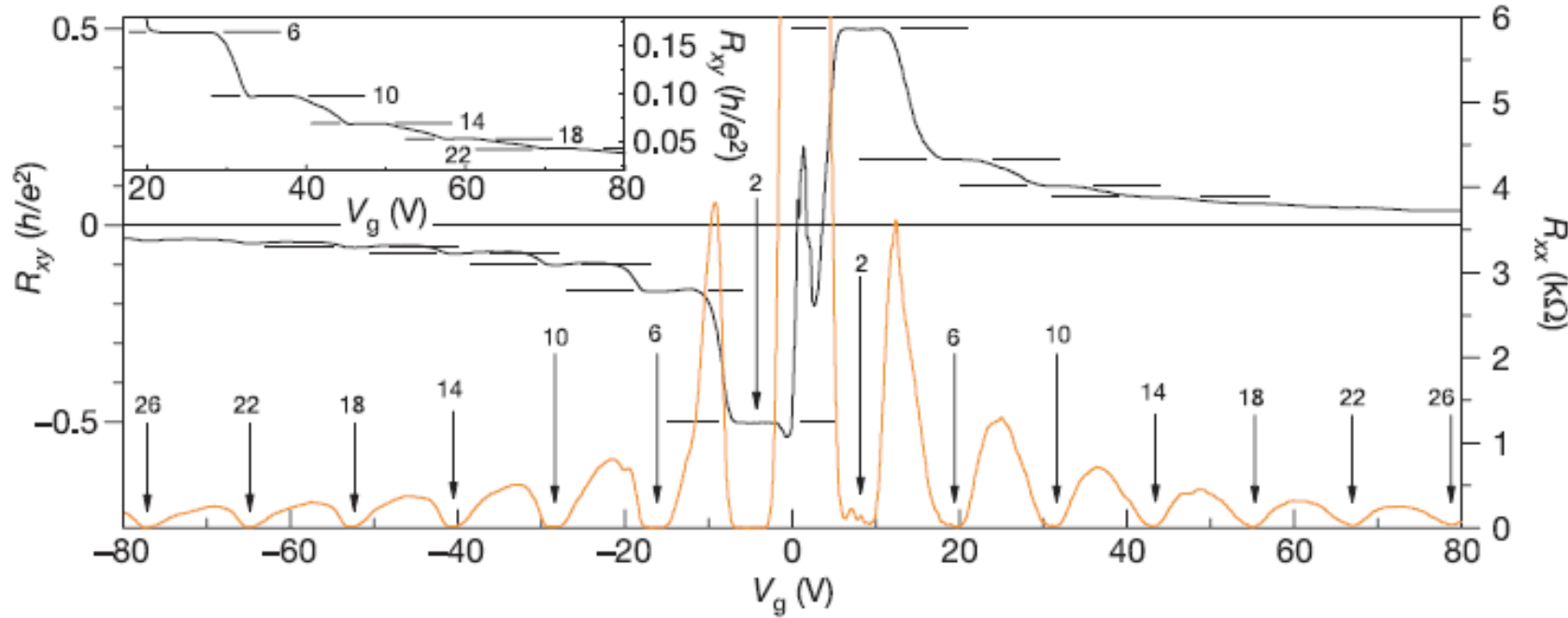
# Quantum Hall Effect in monolayer graphene



- At high magnetic field,  $R_{xy}(B)$  exhibits plateau and  $R_{xx}$  is vanishing, which are the hallmark of the quantum Hall effect.

Y. Zhang, P. Kim, Nature, 2005, 201

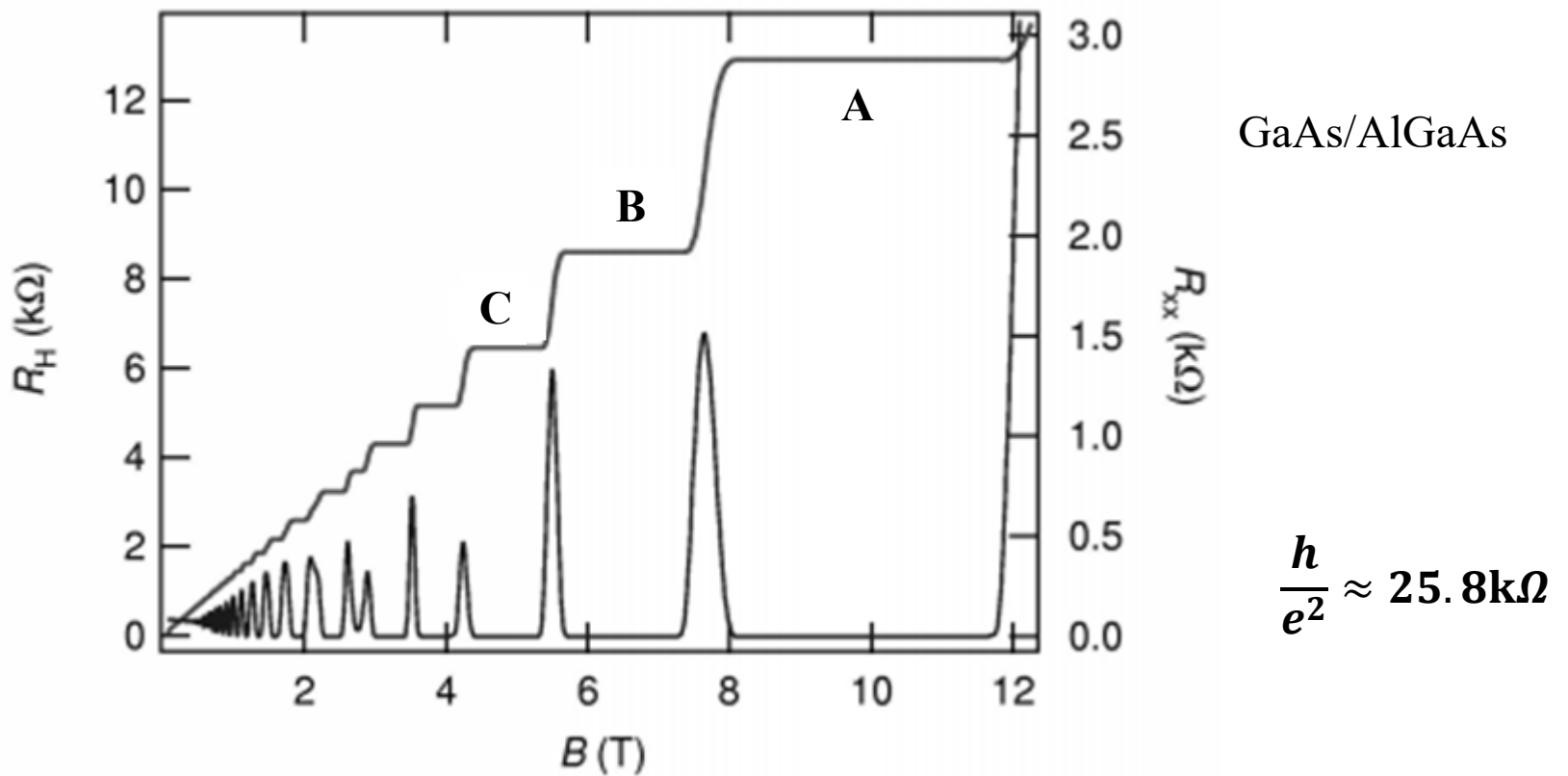
# Quantum Hall effect in monolayer graphene



- $\sigma_{xy}$  exhibits quantum Hall effect plateau when the Fermi level  $E_F$  (tuned by  $V_g$ ) falls between Landau-levels (LLs), and jumps by an amount of  $4 e^2/h$ , when  $E_F$  crosses a LL.

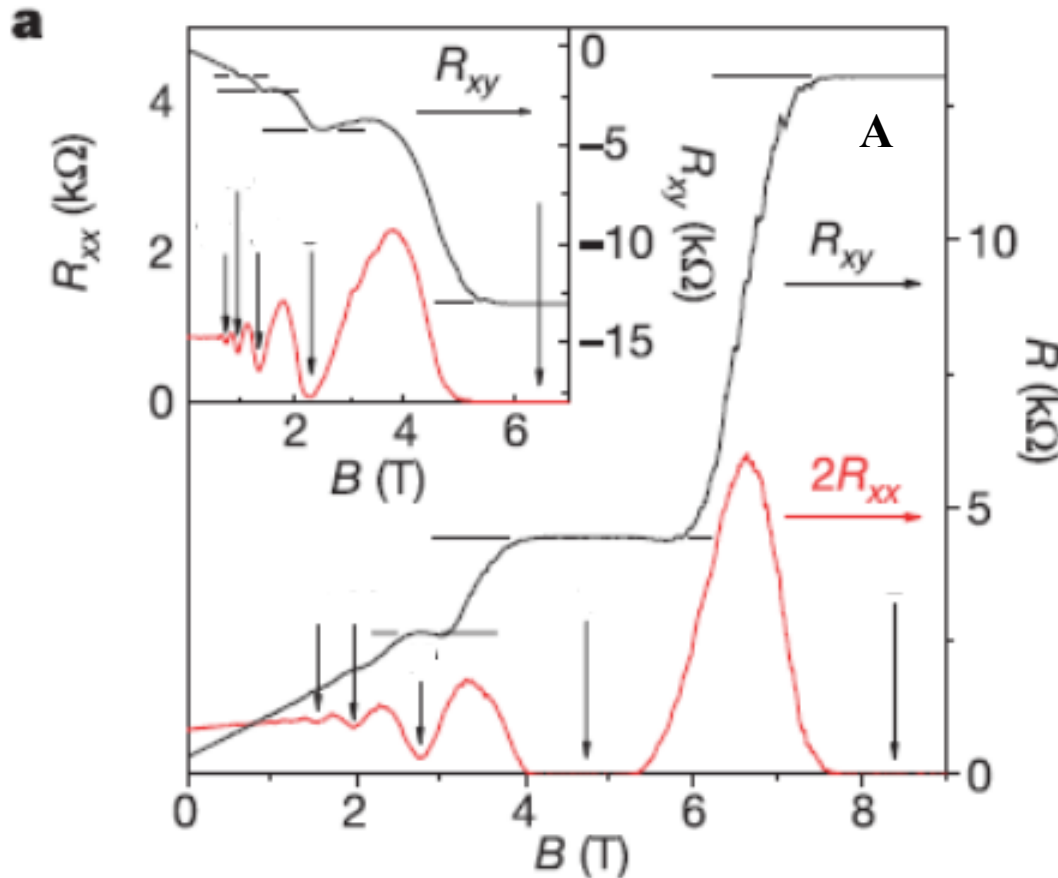
Y. Zhang, P. Kim, Nature, 2005, 201

# Question



What is the Landau filling factor  $\nu$  at position A, B,C?

# Question

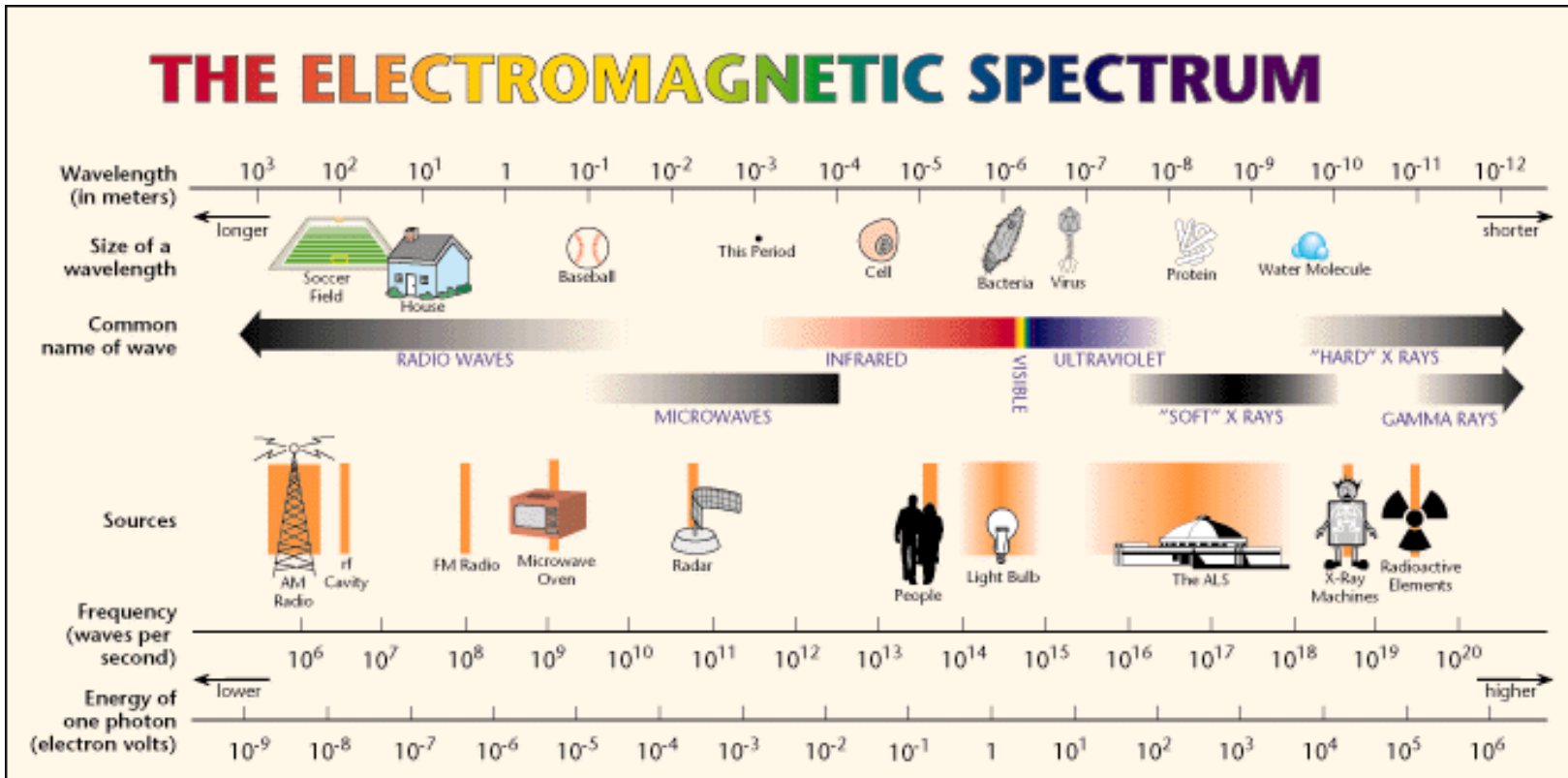


What is filling factor  $\nu$  and Landau index  $n$  at position A?

# Outline

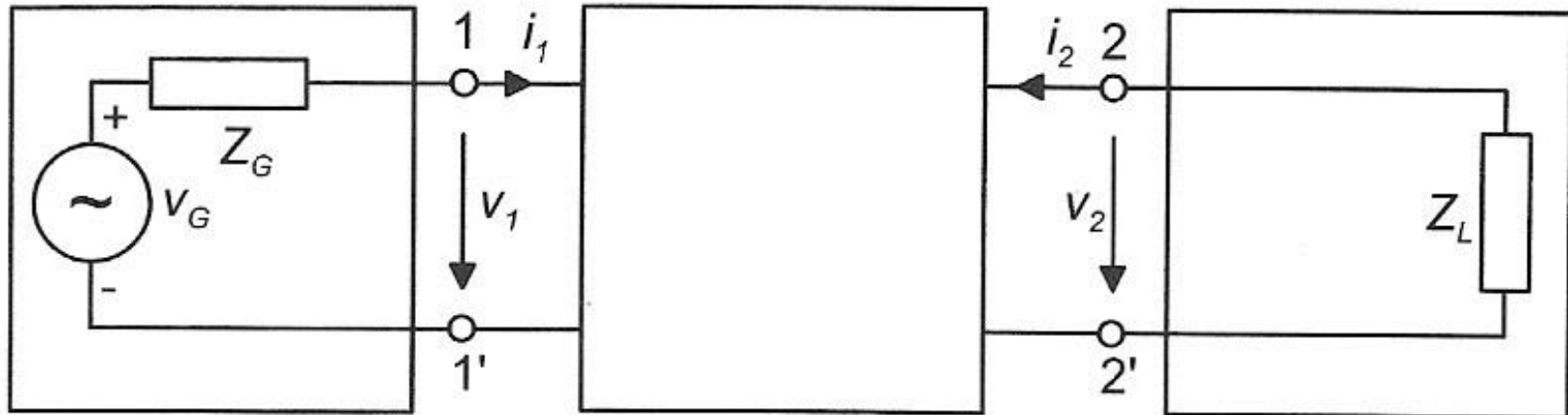
- Introduction of graphene
- Synthesis of graphene
- Current transport and electronic devices
  - Current transport
  - Electronic devices
- • Graphene RF devices
  - Graphene tunneling devices
  - Graphene varactor
  - Graphene memory
  - Graphene barrister
- Optical properties and photonic devices
- Bandgap engineering in graphene

# Radio Frequency (RF)



**Radio frequency:** a frequency or band of frequencies in the range  $10^4$  to  $10^{11}$  or  $10^{12}$  Hz, suitable for use in telecommunications.

# Two-port Networks



Signal source

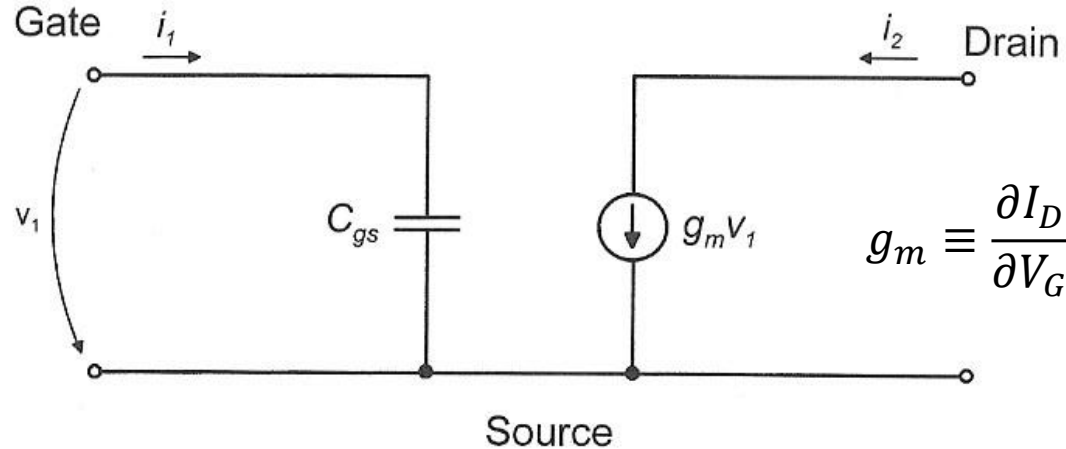
Two-port  
(active device)

Load

- Any active devices such as a RF transistor can be treated as a two-port network.
- The input of such a two-port network is connected to a signal source consist of a voltage source  $v_G$  and a source impedance  $Z_G$  and the output is connected to a load with load impedance  $Z_L$ .

# Cut-off frequency (1): intrinsic

- Cut-off frequency,  $f_T$ , is defined as the frequency at which the magnitude of current gain has dropped to unity.



$$g_m \equiv \frac{\partial I_D}{\partial V_G}$$

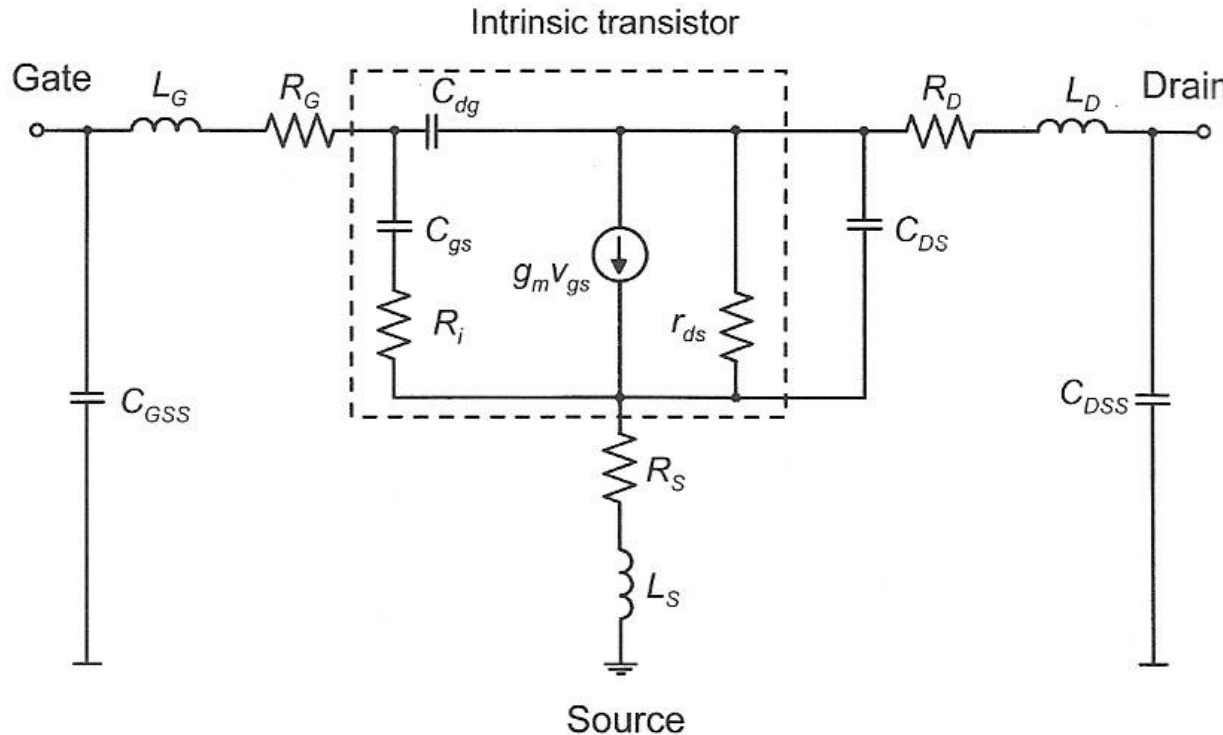
The magnitude of the current gain:

$$|h_{21}| = \left| \frac{i_2}{i_1} \right| = \left| \frac{g_m v_1}{j\omega C_{gs} v_1} \right| = \frac{g_m}{2\pi f C_{gs}}$$

→ When  $|h_{21}| = 1$ , the cut-off frequency is

$$f_T = \frac{g_m}{2\pi C_{gs}}$$

# Cut-off frequency (2): extrinsic



If consider the gate-to-drain capacitance  $C_{gd}$ , charging resistance for gate-source capacitance  $R_i$ , drain resistance  $r_{ds}$ , gate resistance  $R_G$ , and series resistances at source and drain  $R_s$  and  $R_D$ , the cut-off frequency can be written as:

$$f_T = \frac{g_m}{2\pi} \times \frac{1}{(C_{gs} + C_{gd})[1 + g_{ds}(R_s + R_D)] + C_{gd}g_m(R_s + R_D)}$$

# Maximum frequency of oscillation

- Maximum frequency of oscillation,  $f_{\max}$ , is defined as the frequency at which the unilateral power gain equals unity.
- The unilateral power gain,  $U$ , is defined as the power gain of a two-port network have no output-to-input feedback, but with input and output conjugately impedance-matched to signal source and load, respectively.

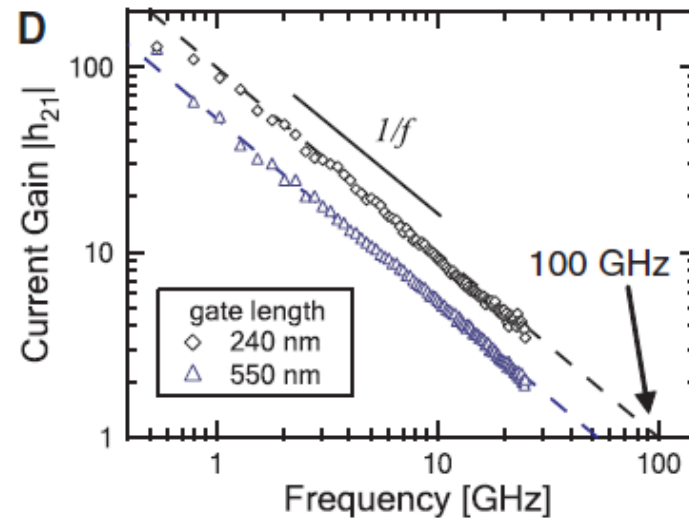
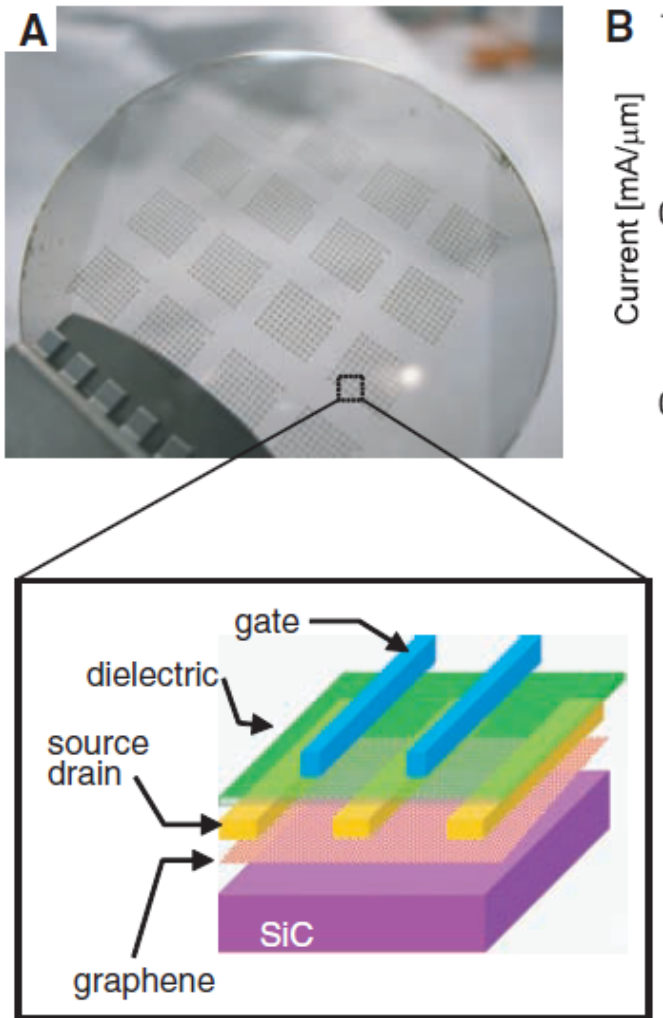
The intrinsic maximum oscillation frequency can be written as:

$$f_{\max} = \frac{g_m}{4\pi C_{gs}\sqrt{g_{ds}R_i}} \quad \text{where } g_{ds} \equiv \frac{\partial I_D}{\partial V_D}$$

The extrinsic maximum oscillation frequency can be written as:

$$f_{\max} = \frac{g_m}{4\pi C_{gs}\sqrt{g_{ds}(R_i + R_s + R_G) + g_m R_g (C_{gs} + C_{gd})}}$$

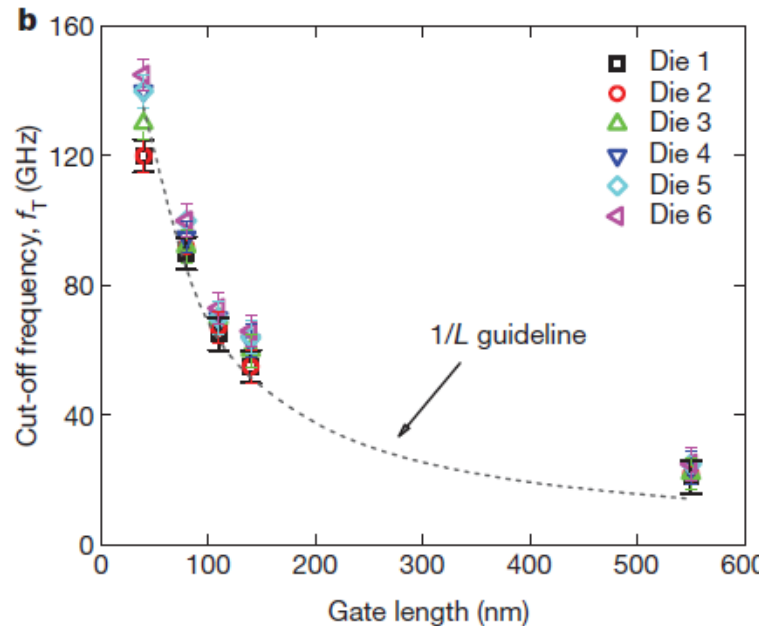
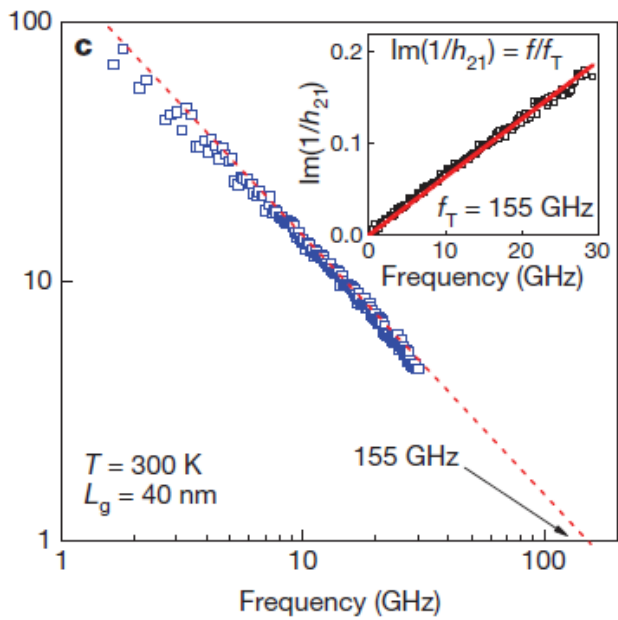
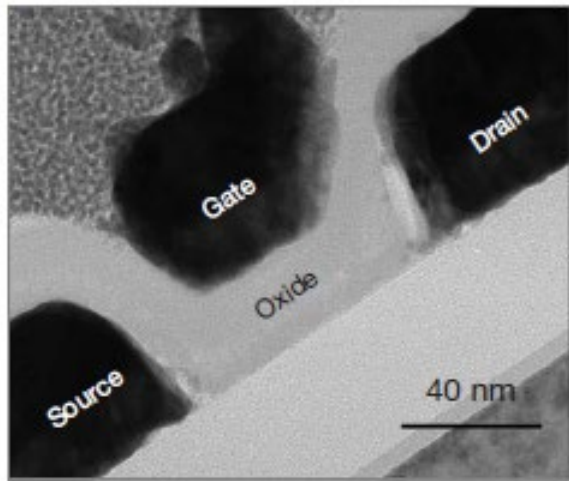
# Graphene RF transistor on SiC



- **100-GHz cutoff frequency was demonstrated on graphene grown on SiC.**

Y. Lin, Ph. Avouris, et.al., Science, 327, 662, 2010

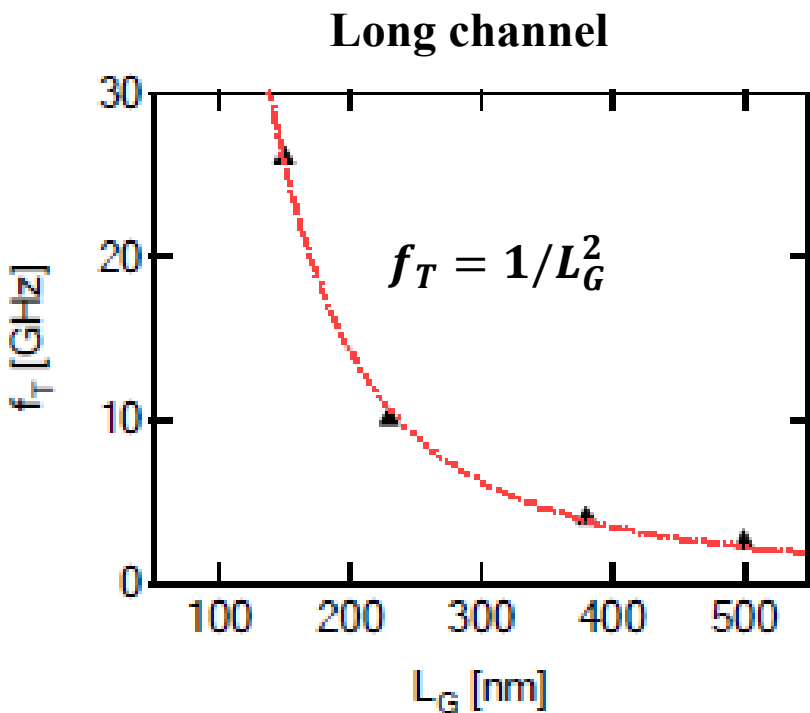
# Graphene RF device on diamond-like carbon (DLC)



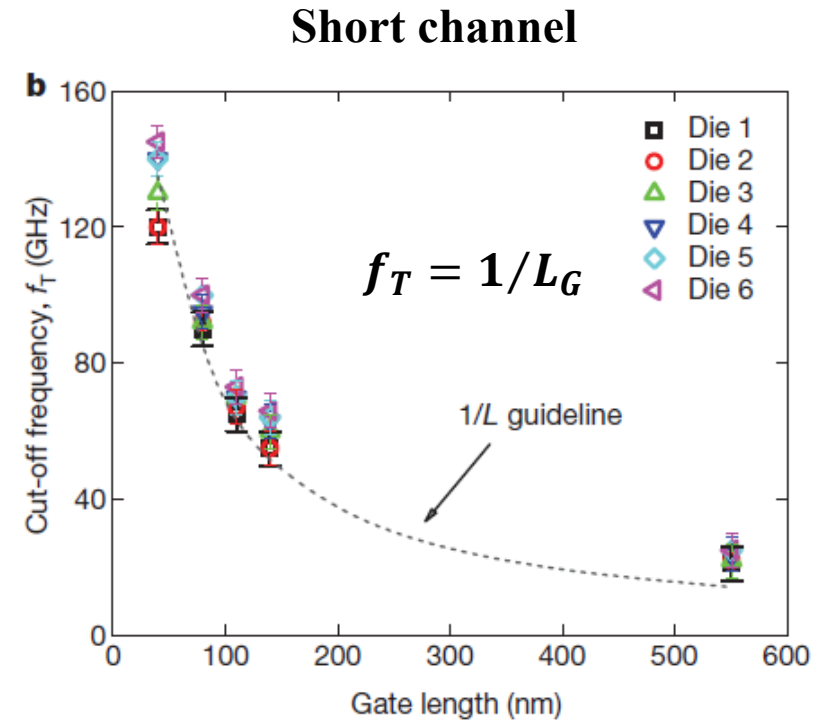
- The CVD graphene was grown on copper film and transferred to a wafer of diamond-like carbon.
- DLC film has a higher phonon energy ( $\sim 165 \text{ meV}$ ) and a lower surface trap density than  $\text{SiO}_2$ . (DLC is non-polar and chemically inert).
- Cut-off frequencies as high as 155 GHz have been obtained for the 40-nm transistors, and the cut-off frequency was found to scale as  $1/(gate\ length)$

Y. Wu, Ph. Avouris, et.al., Nature, 472, 74, 2011

# Channel length dependence of cut-off frequency in graphene RF devices



Y. Lin, IEDM 2009



Y. Wu, Nature 2011

# Channel length dependence of cut-off frequency

In MOSFET, the input capacitance  $C_{in} \approx (2/3)C_{ox}$

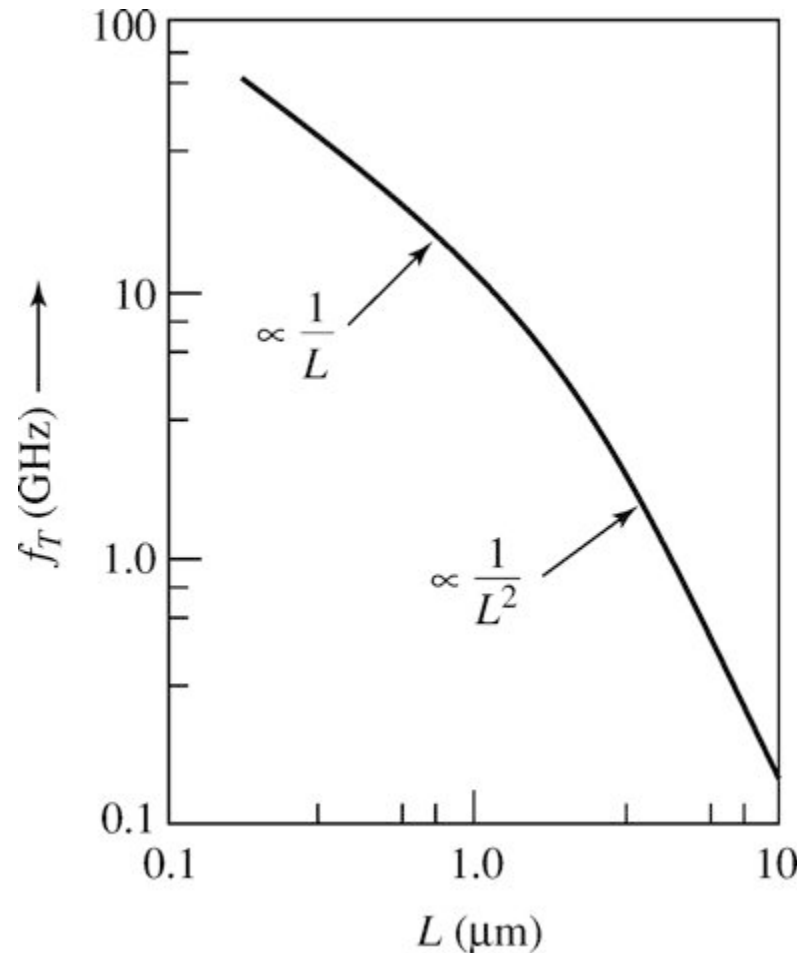
For a long channel MOSFET:

$$f_T = \frac{3\mu_n(V_G - V_T)}{4\pi L^2}$$

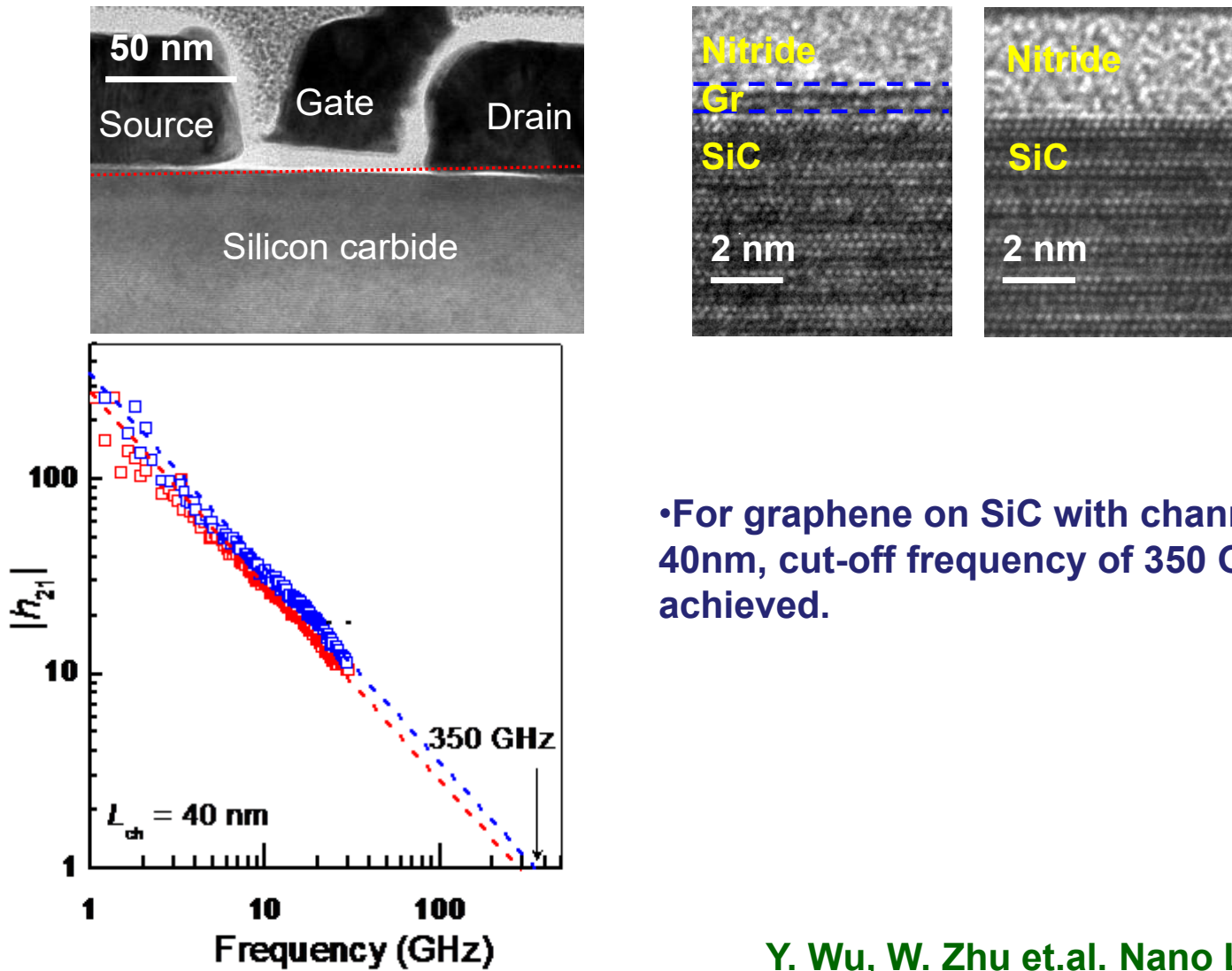
For a short channel MOSFET:

$$f_T = \frac{3v_{sat}(V_G - V_T)(V_G - V_T + 2\varepsilon_{sat}L)}{4\pi L(V_G - V_T + \varepsilon_{sat}L)^2}$$

When  $\varepsilon_{sat}L \ll (V_G - V_T)$ ,  $f_T = \frac{3v_{sat}}{4\pi L}$

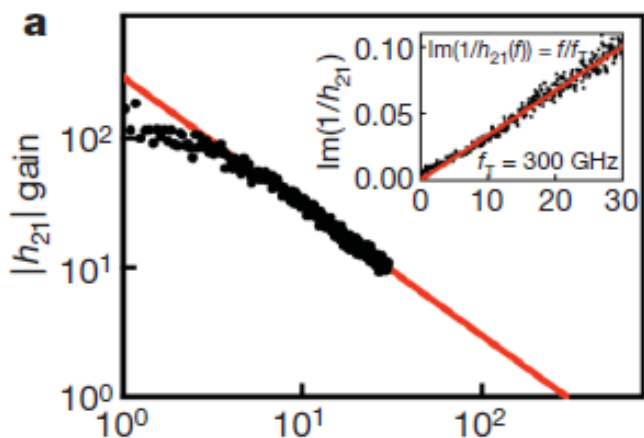
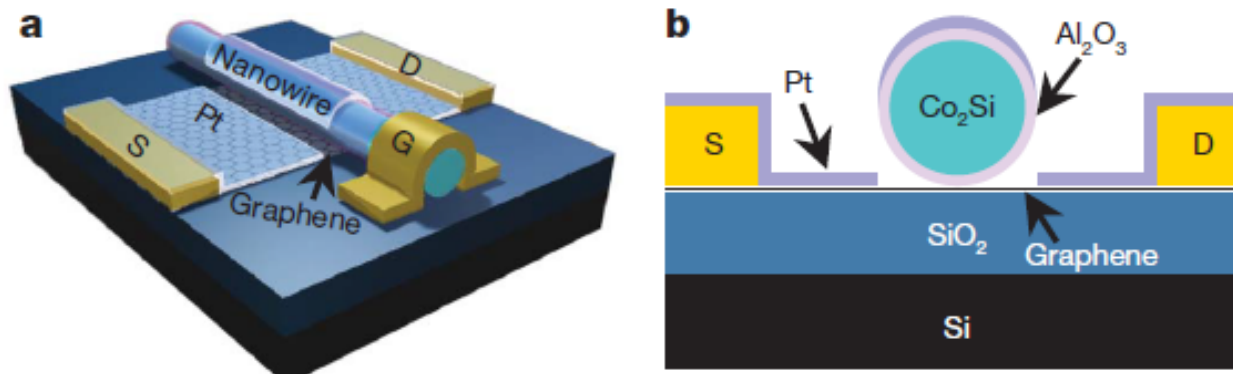


# Graphene RF device with short channels



Y. Wu, W. Zhu et.al. Nano Letters, 2012

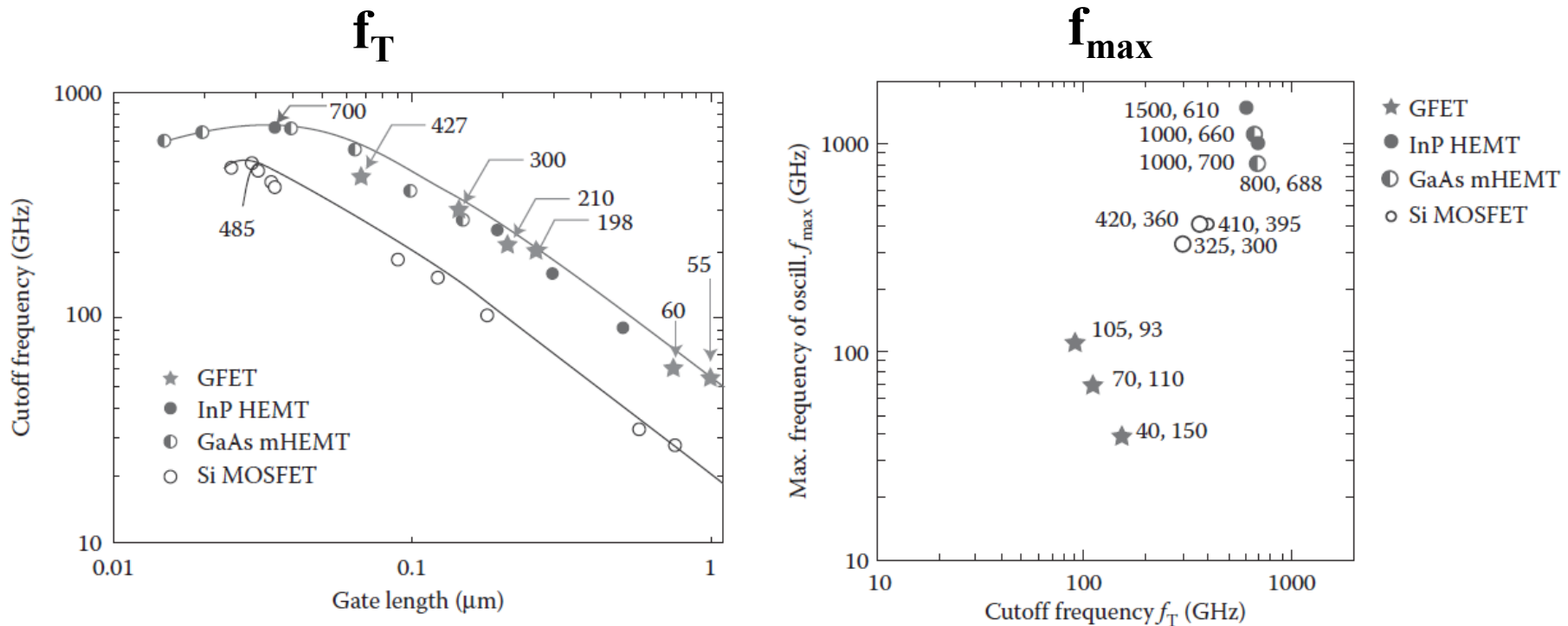
# Graphene RF device with nanowire gate



- A Co<sub>2</sub>Si–Al<sub>2</sub>O<sub>3</sub> core–shell nanowire is used as the gate, with the source and drain electrodes defined through a self-alignment process and the channel length defined by the nanowire diameter.
- Graphene transistors with a channel length as low as 140 nm have been fabricated with  $f_T=100\text{--}300 \text{ GHz}$ .

L. Liao, X. Duan, Nature, 467, 305, 2010

# State-of-the-art RF devices

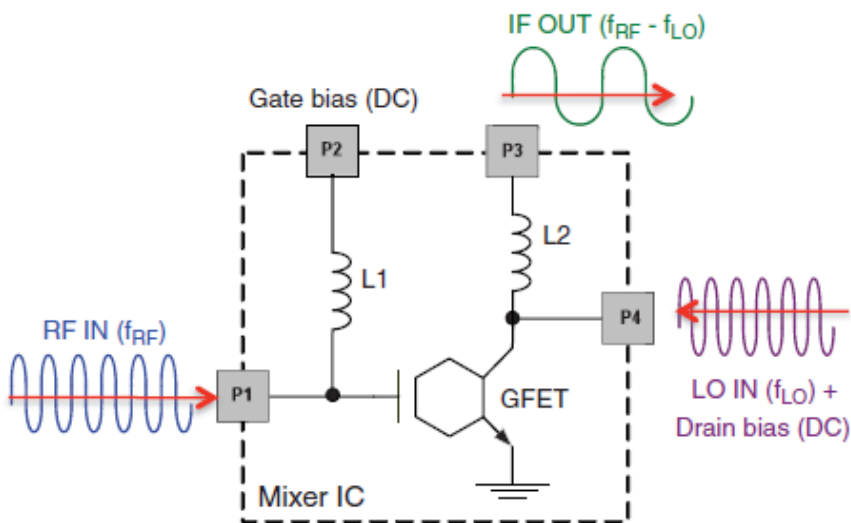


In terms of cut-off frequency  $f_T$ , graphene transistors compete well, outperform silicon MOSFETs and show similar cutoff frequencies as the best III-V devices. However, the  $f_{\max}$  in graphene transistors is much lower than that in III-V and silicon devices.

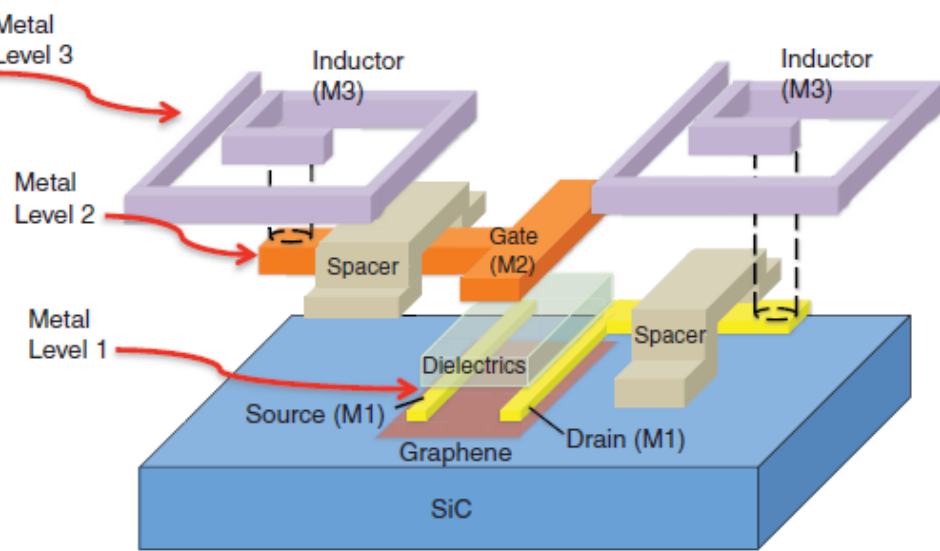
Max C. Lemme, "Graphene for RF Analogue Applications", in book "2D materials for Nanoelectronics"

# Graphene RF integrated circuits

A



B



- A wafer-scale graphene circuit was demonstrated in which all circuit components, including graphene field-effect transistor and inductors, were monolithically integrated on a single silicon carbide wafer.
- The integrated circuit operates as a broadband radio-frequency mixer at frequencies up to 10 gigahertz.

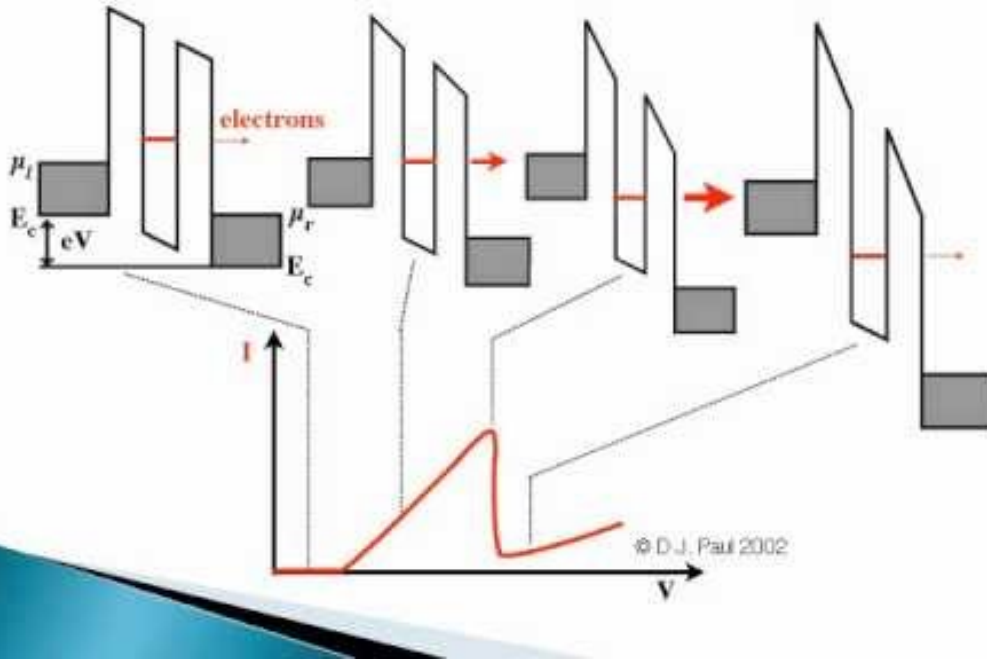
Y. Lin, K. Jenkins, et.al., Science, 332, 1294, 2011

# Outline

- Introduction of graphene
- Synthesis of graphene
- Current transport and electronic devices
  - Current transport
  - Electronic devices
    - Graphene RF devices
    - Graphene tunneling devices
    - Graphene varactor
    - Graphene memory
    - Graphene barrister
- Optical properties and photonic devices
- Bandgap engineering in graphene

# Resonant tunneling diode (RTD)

## Resonant Tunneling Diode



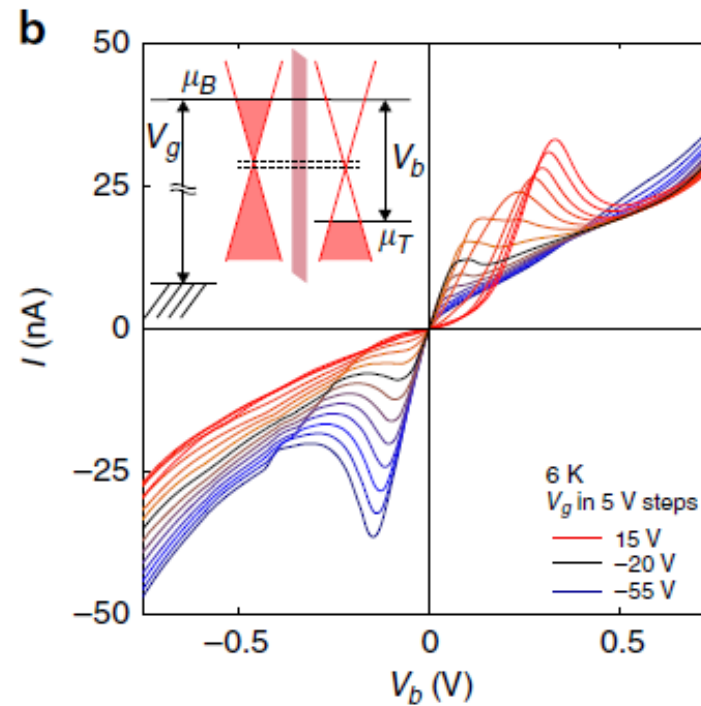
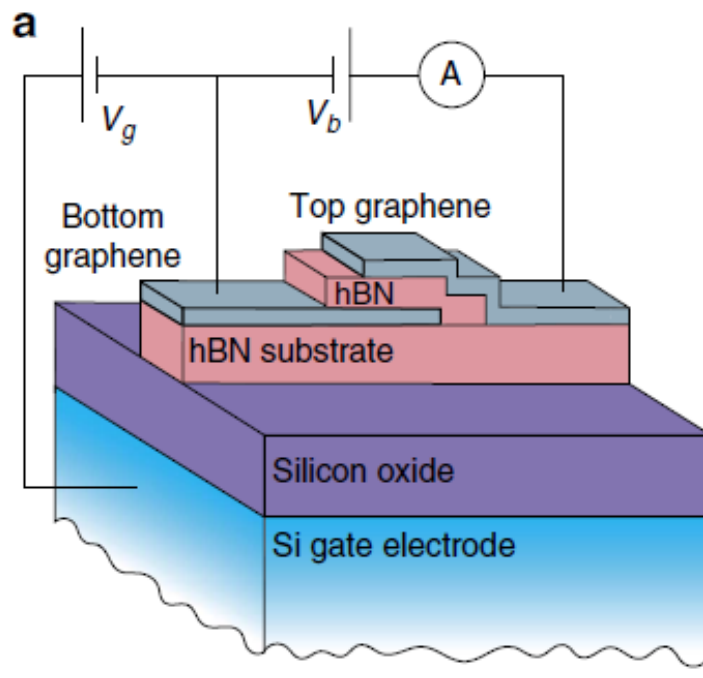
- The resonant tunneling diodes involve a device with two electrodes with two tunnel barriers between the electrodes.
- The quantum confinement leads to a set of discrete electron energy levels in the quantum well.
- Only when an electron from the electrode has an energy that corresponds to the allowed state in the quantum well can it quantum mechanically tunnel through the two barriers and quantum well, and reach the right electrode

NDR: negative differential resistance

PDR: positive differential resistance

D. Paul, Nanoelectronics, p285, 2003

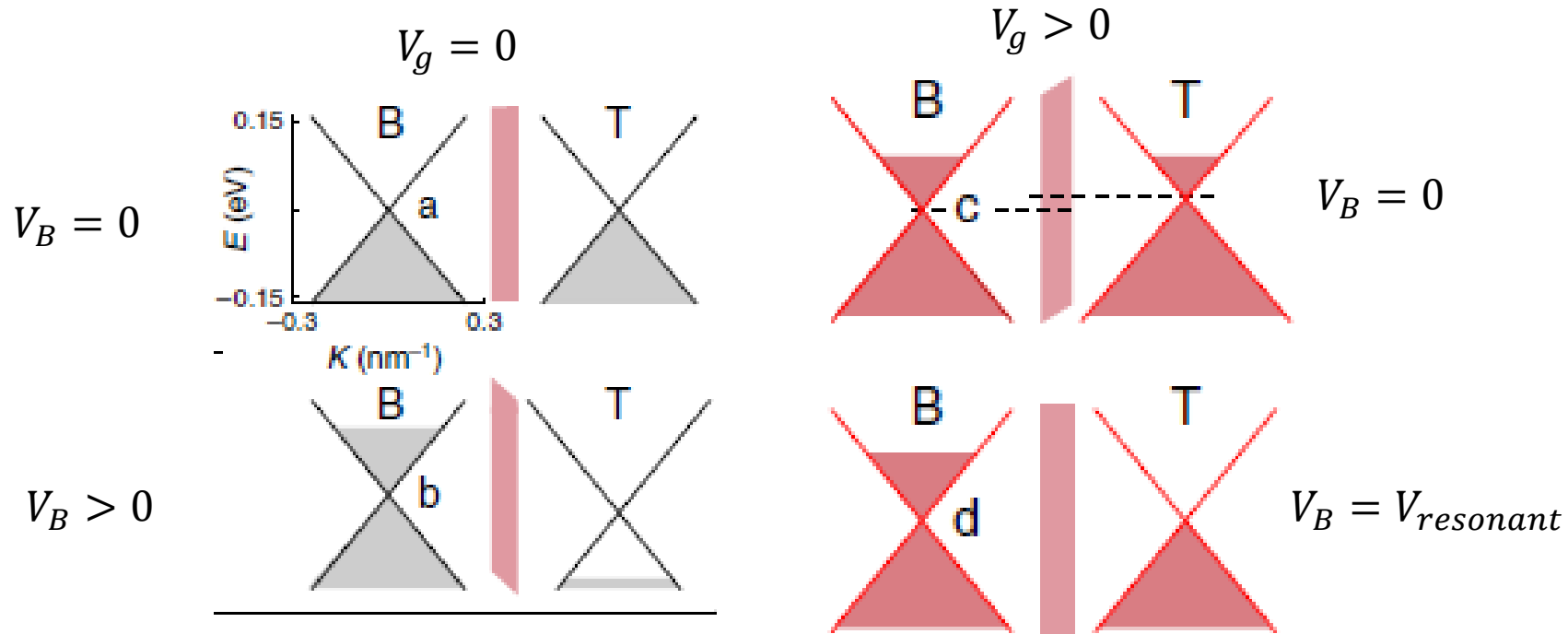
# Resonant tunneling device based on graphene



- Resonant tunneling was observed in graphene/BN/graphene heterostructure.
- The resonance occurs when the electronic spectra of the two electrodes are aligned.
- Negative differential conductance is gate voltage-tunable due to graphene's unique Dirac-like spectrum.

L. Britnell, Nature Communications 2817, 2013

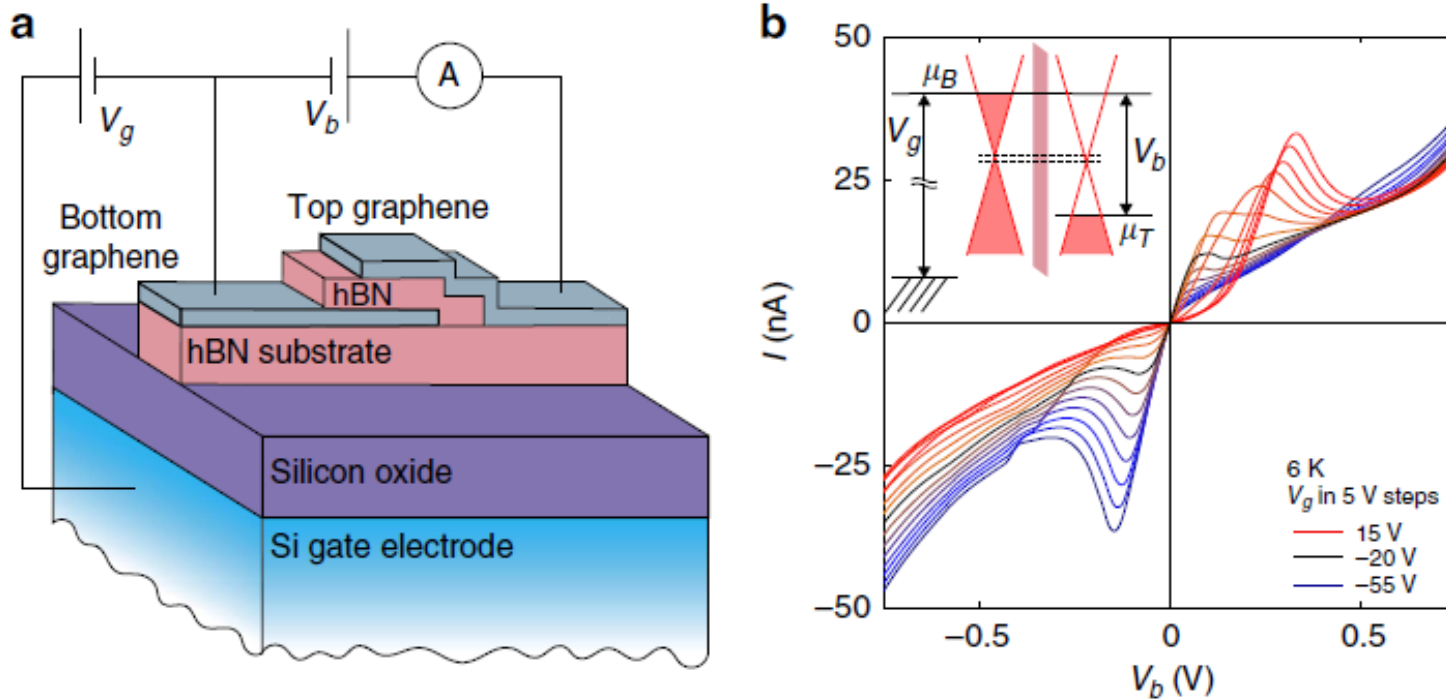
# Operating principle of graphene RTD



- If  $V_g = 0$ , when  $V_B = 0$ , the Fermi energy in each layer is at the Dirac point and the two Dirac points are at the same energy. If  $V_B > 0$ , electrons accumulate in the negatively biased electrode with an equal number of holes in the positive electrode. This charging of the two layers generates an electric field, which misaligns the two Dirac points. Therefore, in order for a carrier to tunnel from one electrode to the other, its in-plane wavevector must change. Such a change is forbidden.
- If  $V_g > 0$ , the Dirac point in bottom layer is lower than that in top layer. A positive  $V_B$  can bring the Dirac points of the two electrodes into alignment, thus allowing all carriers whose energies are between the now distinct chemical potentials of the two electrodes to tunnel resonantly.

L. Britnell, Nature Communications 2817, 2013

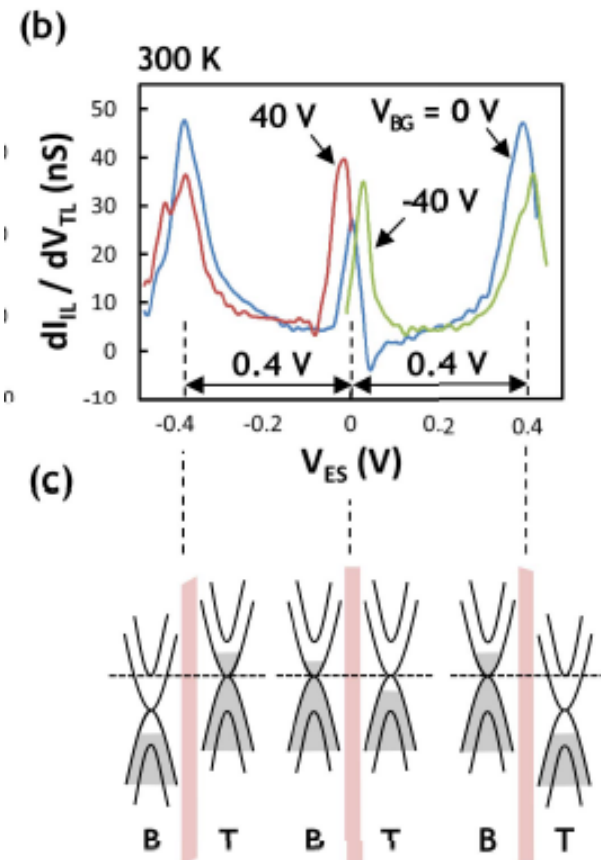
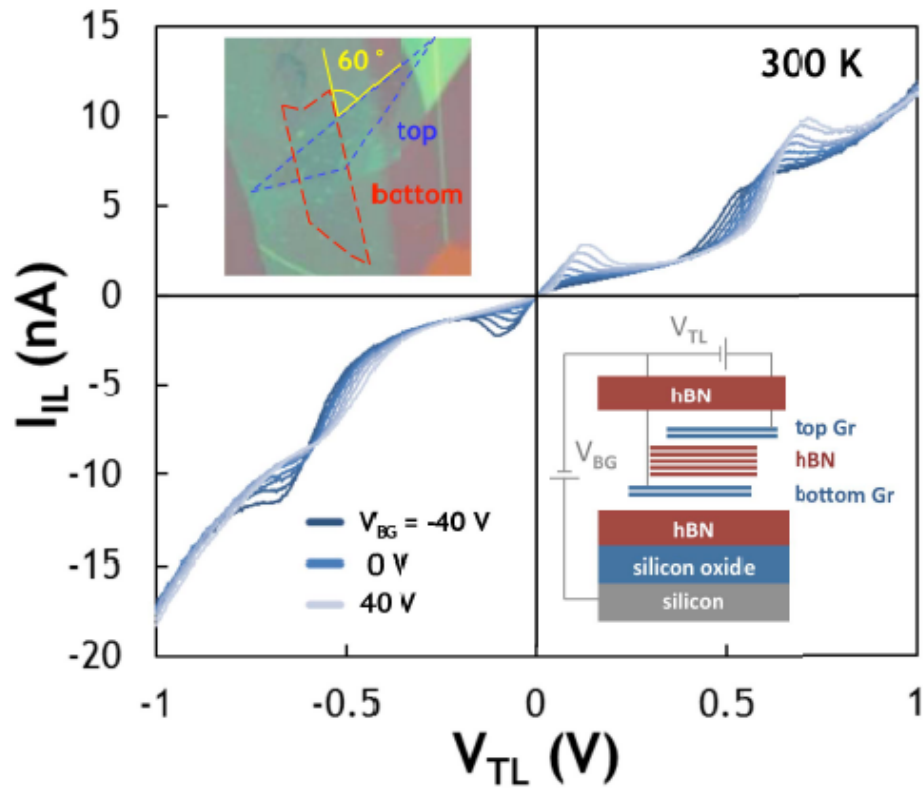
# Tuning peak voltage with gate bias



Higher gate voltage induces larger mismatch of Dirac point between top and bottom graphene layer, which means larger interlayer bias  $V_b$  is needed to realign the two Dirac cones, i.e. the peak voltage will be higher.

L. Britnell, Nature Communications 2817, 2013

# Tunneling FET based on bilayer graphene



- Vertical tunneling field-effect transistor using a stacked double bilayer graphene (BLG) and hexagonal boron nitride heterostructure was demonstrated.
- The device shows two tunneling resonances with negative differential resistance (NDR).

Sangwoo Kang, IEEE ELECTRON DEVICE LETTERS, 36, 405, 2015

# Outline

- Introduction of graphene
- Synthesis of graphene
- Current transport and electronic devices
  - Current transport
  - Electronic devices
    - Graphene RF devices
    - Graphene tunneling devices
    - Graphene varactor
    - Graphene memory
    - Graphene barrister
- Optical properties and photonic devices
- Bandgap engineering in graphene



# Quantum capacitance

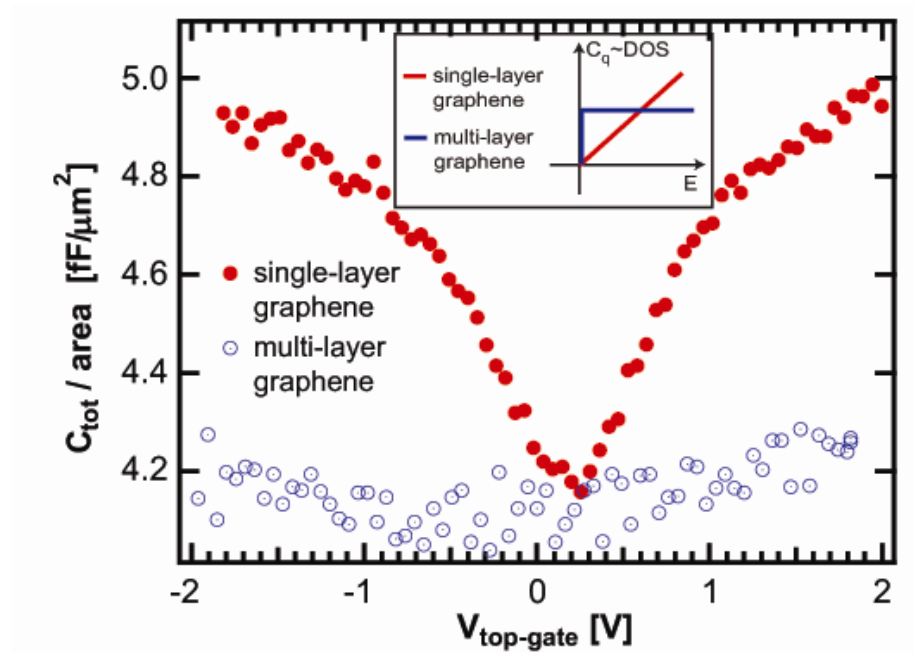
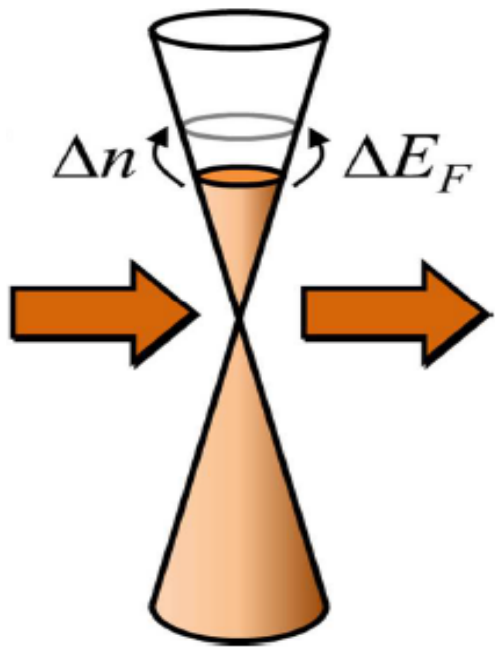
**Quantum capacitance is defined as the variation of electrical charge with respect to the variation of electrochemical potential**

$$C_q = \frac{dQ}{d\mu}$$

**Take a capacitor where one side is a metal with essentially-infinite density of states. The other side is the low density-of-states material, e.g. a 2DEG, with density of states DOS, the quantum capacitance is**

$$C_q = q^2 DOS$$

# Quantum capacitance of graphene

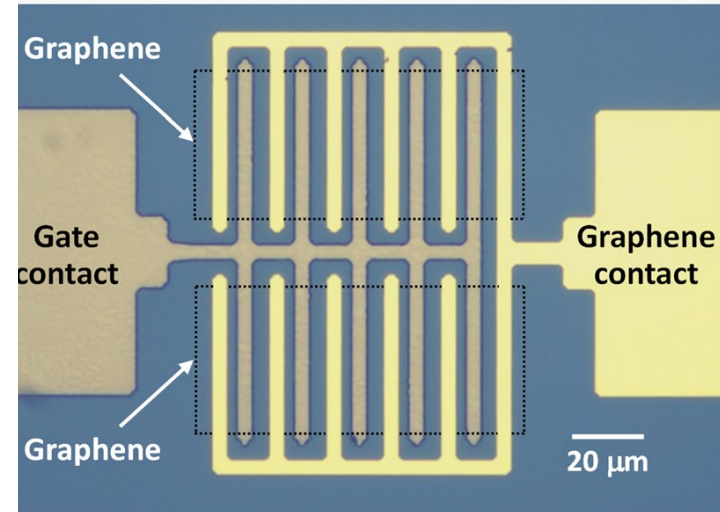
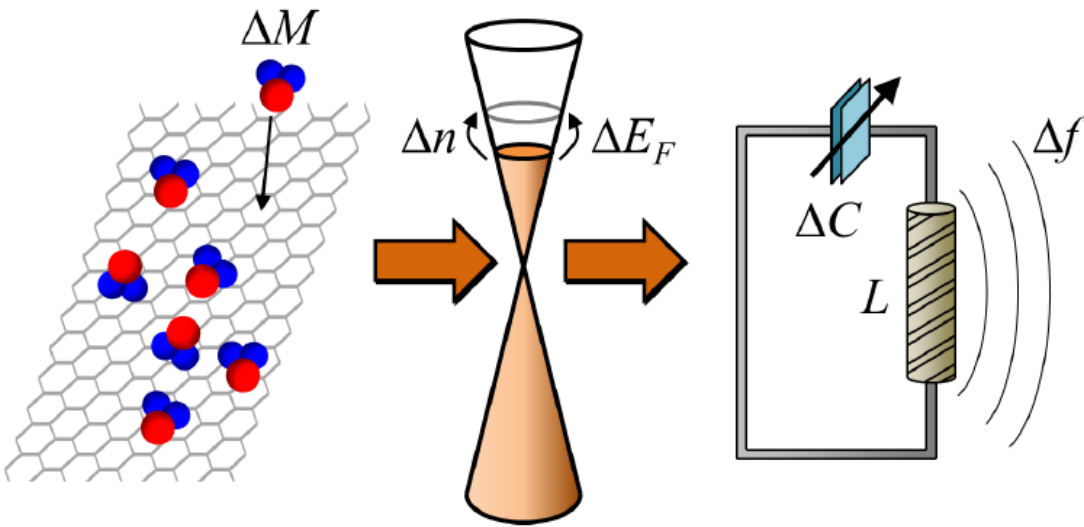


**Monolayer graphene:**  $C_Q = \frac{dQ}{dE_F/q} \approx q^2 DOS = \frac{2q^2}{\pi(\hbar v_F)^2} |E - E_{\text{Dirac}}|$

**Bilayer or multilayer graphene:**  $C_Q = \frac{dQ}{dE_F/q} \approx q^2 DOS = \frac{2q^2 m}{\pi \hbar^2}$

Z. Chen, IEEE IEDM, 2008

# Graphene variable capacitor (varactor)



- The low density of states in graphene makes it possible for the quantum capacitance to be of the same order of magnitude as the oxide capacitance.
- Density of states of monolayer graphene varies as a function of energy, means that the capacitance in a graphene capacitor can be tuned by varying the carrier concentration.
- High mobility and zero band gap in graphene also allow it to remain conductive throughout the entire tuning range, making graphene an idea material for varactor.
- Graphene varactors and on-chip inductor forms an  $LC$  oscillator circuit, which could serve as sensors with wireless readout capability.

M. A. Ebrish, S. J. Koester, Applied Physics Letters, 100, 143102, 2012  
D. A. Deen, S. J. Koester, IEEE Sensors Journal, 14, 1459, 2014

# Outline

- Introduction of graphene
- Synthesis of graphene
- Current transport and electronic devices
  - Current transport
  - Electronic devices
    - Graphene RF devices
    - Graphene tunneling devices
    - Graphene varactor
    - Graphene memory
    - Graphene barrister
- Optical properties and photonic devices
- Bandgap engineering in graphene



# Semiconductor memory

Semiconductor memory is a digital electronic data storage device, implemented with semiconductor devices.

Random-access memories is a form of computer memory that can be read and changed in any order.

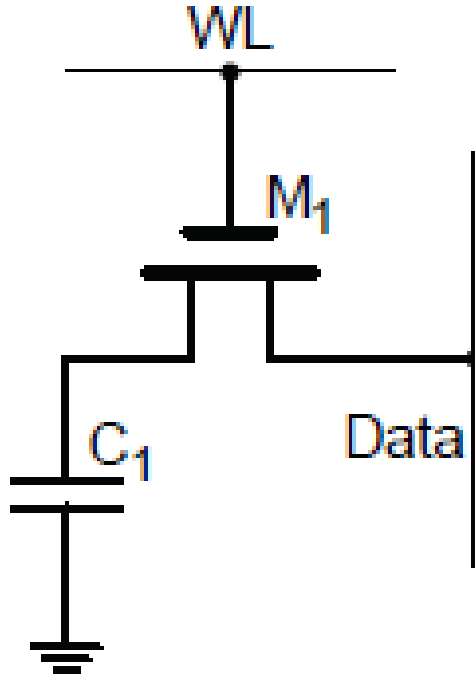
Volatile Memory

- └ DRAM (Dynamic RAM)
- └ SRAM (Static RAM)

Non-volatile Memory

- └ Flash memory
- └ RRAM (Resistive RAM)
- └ FRAM (Ferroelectric RAM)
- └ MRAM (Magnetic RAM)
- └ PCRAM (Phase change RAM)

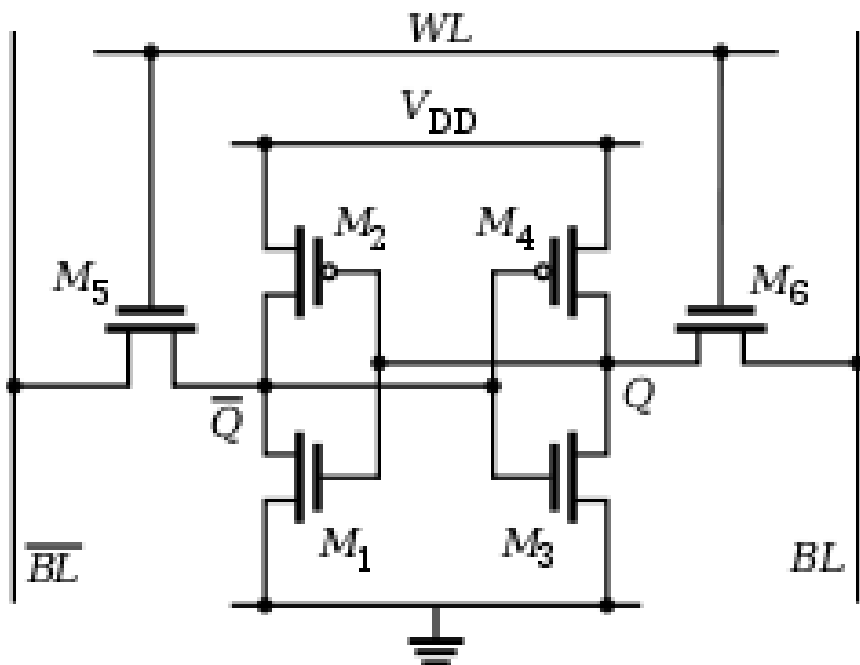
# DRAM



- DRAM memory cell typically consists of a capacitor and a transistor.
- The capacitor can either be charged or discharged; these two states are taken to represent the two values of a bit.
- The electric charge on the capacitors slowly leaks off. To prevent this, DRAM requires a periodically rewrite operation to restore the charges in the capacitor.
- Advantage: structural simplicity (high density)
- Disadvantage: consumes large amounts of power

# SRAM

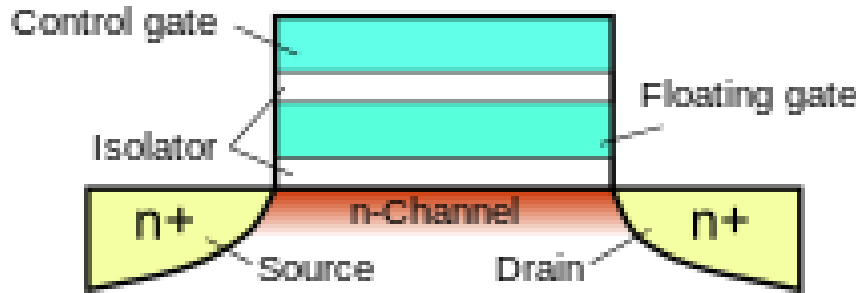
SRAM is a type of semiconductor random-access memory (RAM) that uses bistable latching circuitry (flip-flop) to store each bit.



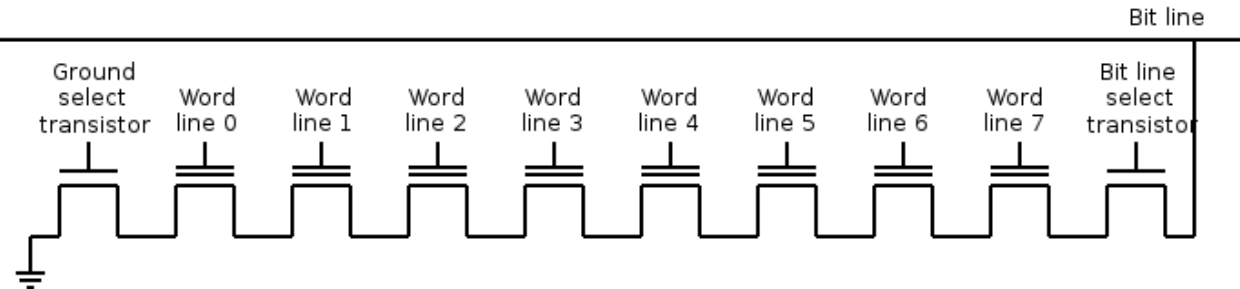
- **Write:** To write a state 0, we would set the bit lines (BL) to 0 and  $\overline{BL}$  to 1.
- **Read:** First precharge both bit lines BL and  $\overline{BL}$  to high (logic 1) voltage. Then assert the word line WL enables both the access transistors M<sub>5</sub> and M<sub>6</sub>. A sense amplifier will sense which line has the higher voltage and thus determine whether there was 1 or 0 stored.
- **Advantage:** a refresh circuit is not needed, Low idle power consumption
- **Disadvantage:** high price, low density

# Flash memory

Flash memory stores information in an array of memory cells made from floating-gate transistors.

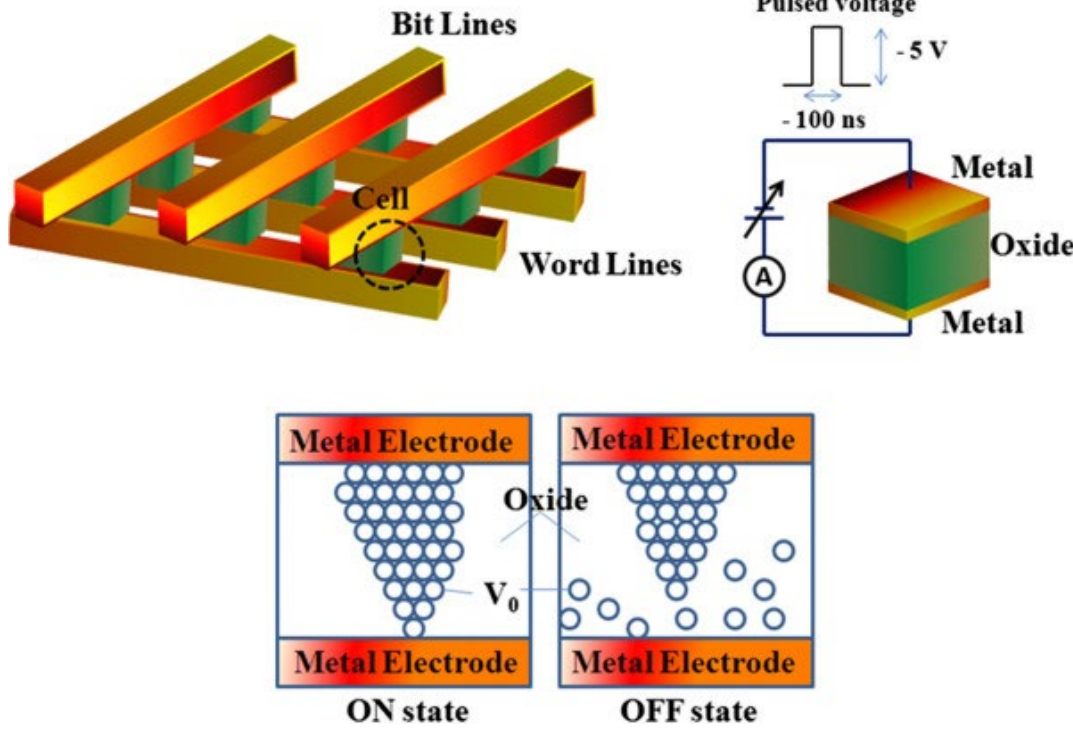


- The floating gate (FG) is interposed between the control gate (CG) and the MOSFET channel. Because the FG is electrically isolated by its insulating layer, electrons placed on it are trapped. When the FG is charged with electrons, this charge screens the electric field from the CG, thus, increasing the threshold voltage of the cell.
- Advantage: high speed erase
- Disadvantage: low endurance



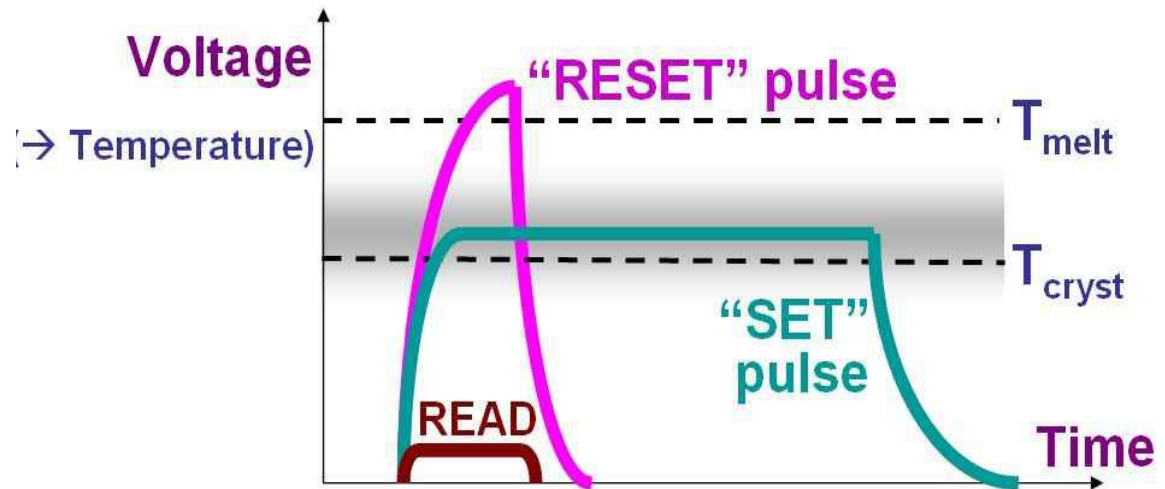
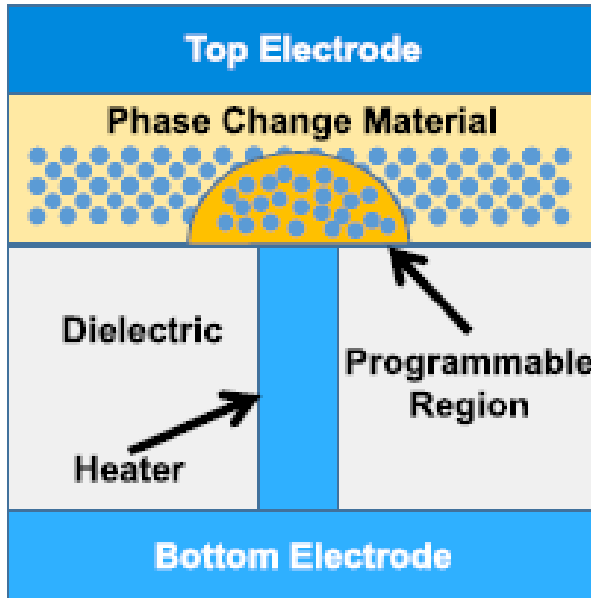
# RRAM

- RRAM is a form of nonvolatile storage that operates by changing the resistance of a specially formulated solid dielectric material



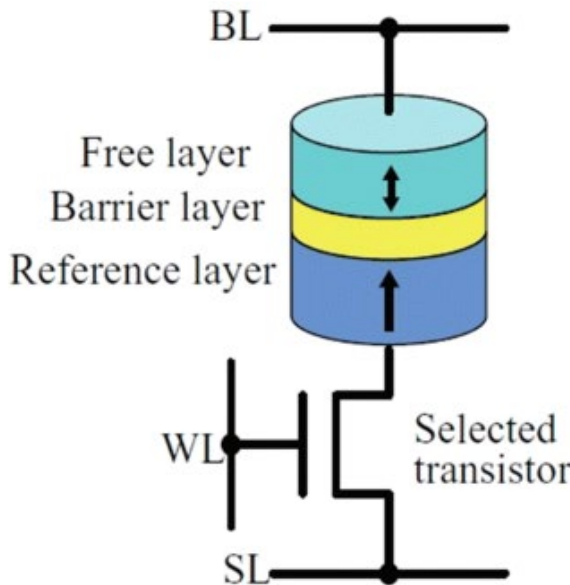
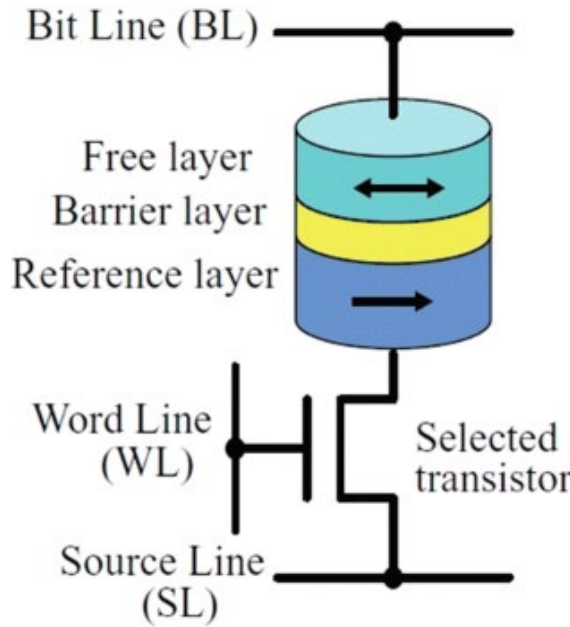
- The basic idea is that a dielectric, which is normally insulating, can be made to conduct through a filament or conduction path formed after application of a sufficiently high voltage.
- Advantage: small cell structure, faster than MRAM and PCRAM
- Disadvantage: limited reliability and uniformity

# PCRAM (Phase change memory)



- To SET the cell into its low-resistance state, an electrical pulse is applied to heat a significant portion of the cell above the crystallization temperature of the phase change material.
- In the RESET operation, a larger electrical current is applied in order to melt the central portion of the cell.
- The read operation is performed by measuring the device resistance at low voltage, so that the device state is not perturbed.

# MRAM



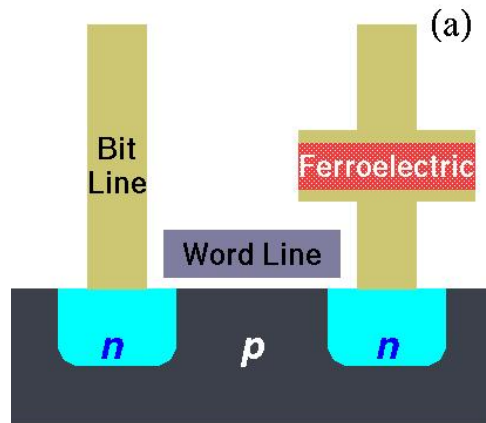
- In MRAM cells, data is stored as low and high resistance states in a magnetic tunnel junction (MTJ).
- MTJ comprises of two nano magnets separated by a thin insulator layer. When the magnetization in the free layer is parallel (or antiparallel) to the magnetization in the reference layer, the MTJ is in low-resistance (high-resistance) state.
- Advantage: high speed
- Limitation: high power consumption

# FRAM

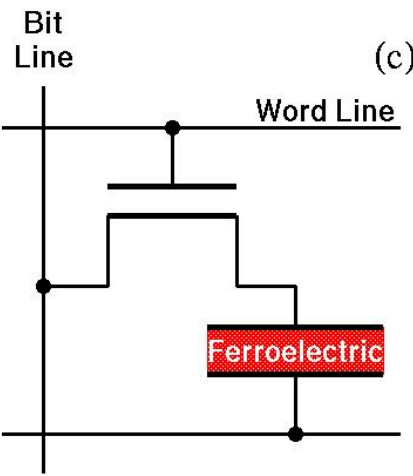
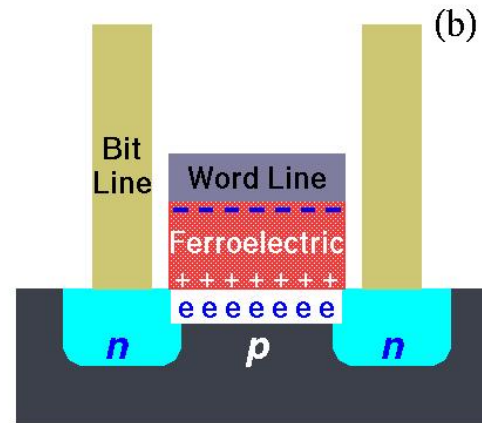
- Ferroelectric RAM (FRAM) is a random-access memory using a ferroelectric layer to achieve non-volatility.
- FRAM has two types:
  - 1T1C: Each storage element, a cell, consists of one capacitor and one transistor
  - 1T: Each storage element consists of one transistor only.

# FRAM types

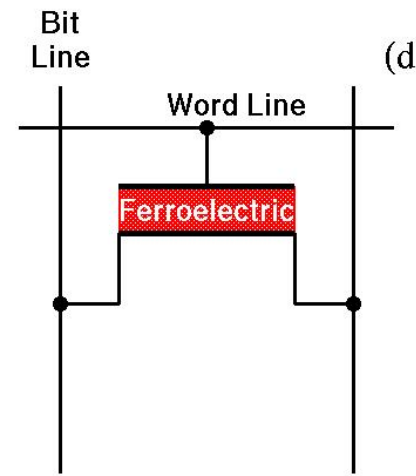
1T1C FRAM



1T FRAM

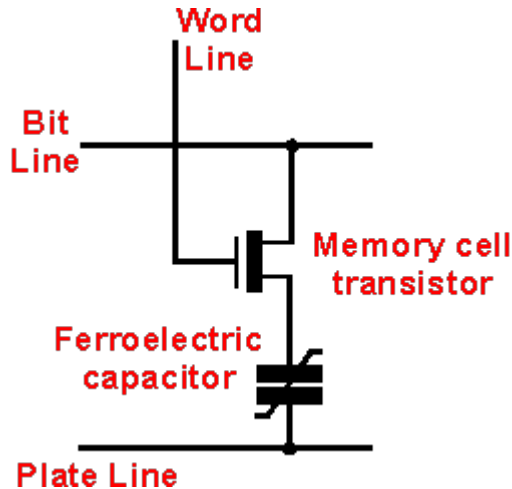


1T1C type



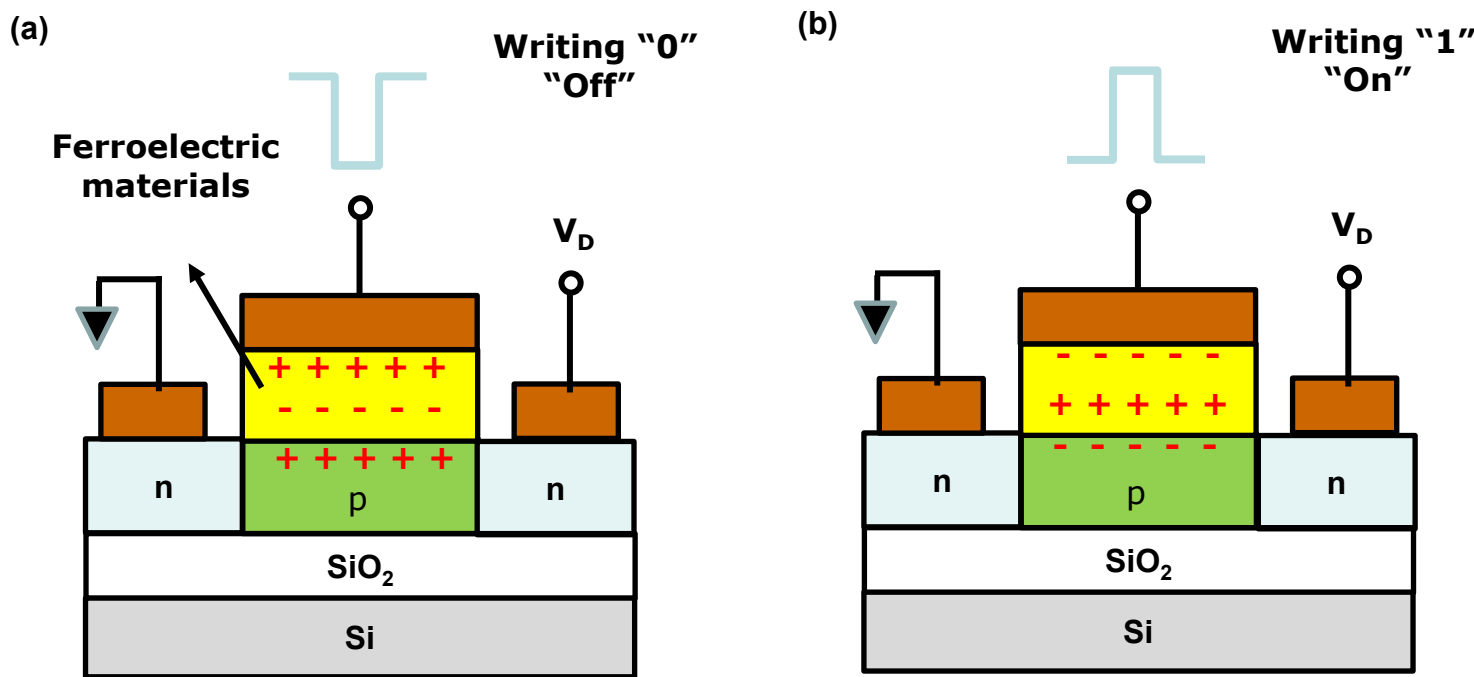
1T type

# 1T1C FRAM Operation



- Writing is accomplished by applying a field across the ferroelectric layer by charging the plates on either side of it, forcing the atoms inside into the "up" or "down" orientation thereby storing a "1" or "0".
- Reading: The transistor forces the cell into a particular state, say "0". If the cell already held a "0", nothing will happen in the output lines. If the cell held a "1", the re-orientation of the atoms in the film will cause a brief pulse of current in the output. The presence of this pulse means the cell held a "1".
- Since this read process overwrites the cell, reading FeRAM is a destructive process, and requires the cell to be re-written if it was changed.

# 1T FRAM Operation

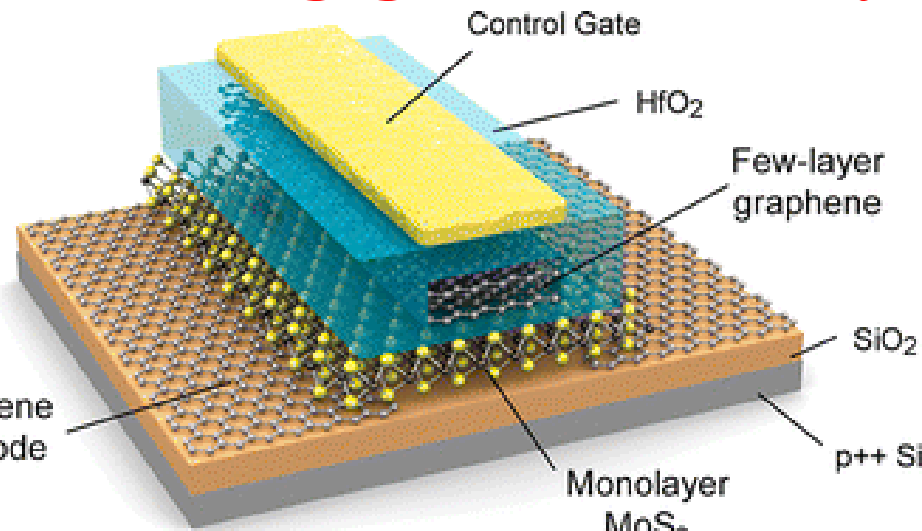


## Operating principle of the 1T FRAM.

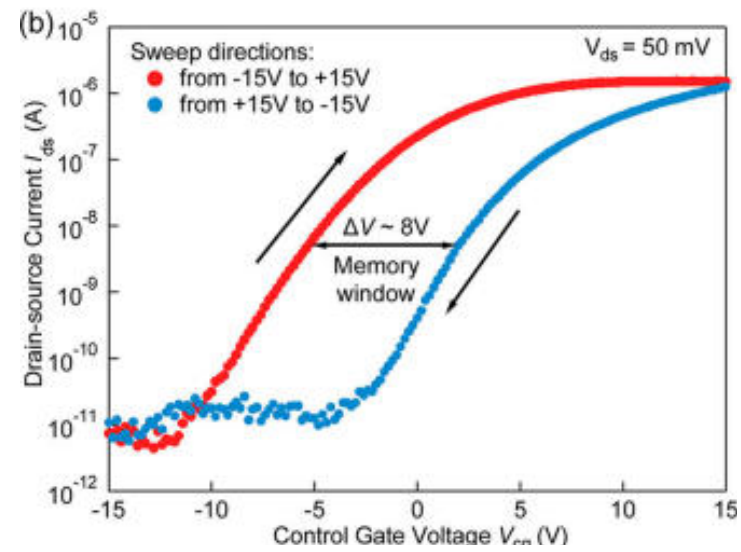
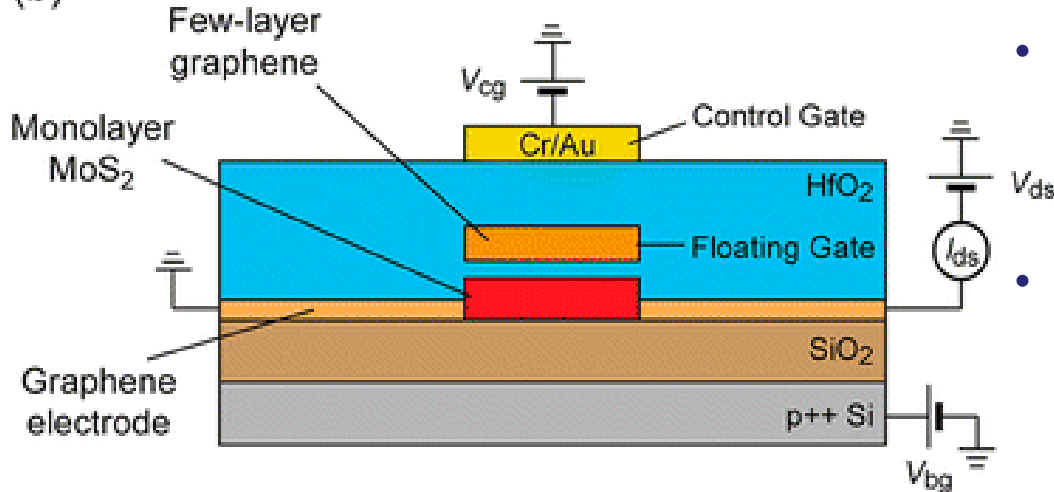
- The application of a negative gate pulse induces a ferroelectric polarization that causes the transistor to be “off” with a zero gate voltage.
- The application of a positive gate pulse induces a ferroelectric polarization that causes the transistor to be “on” with a zero gate voltage.
- The read operation in 1T FRAM is non-destructive, so write-back is not needed.

# Floating gate memory based on graphene

(a)



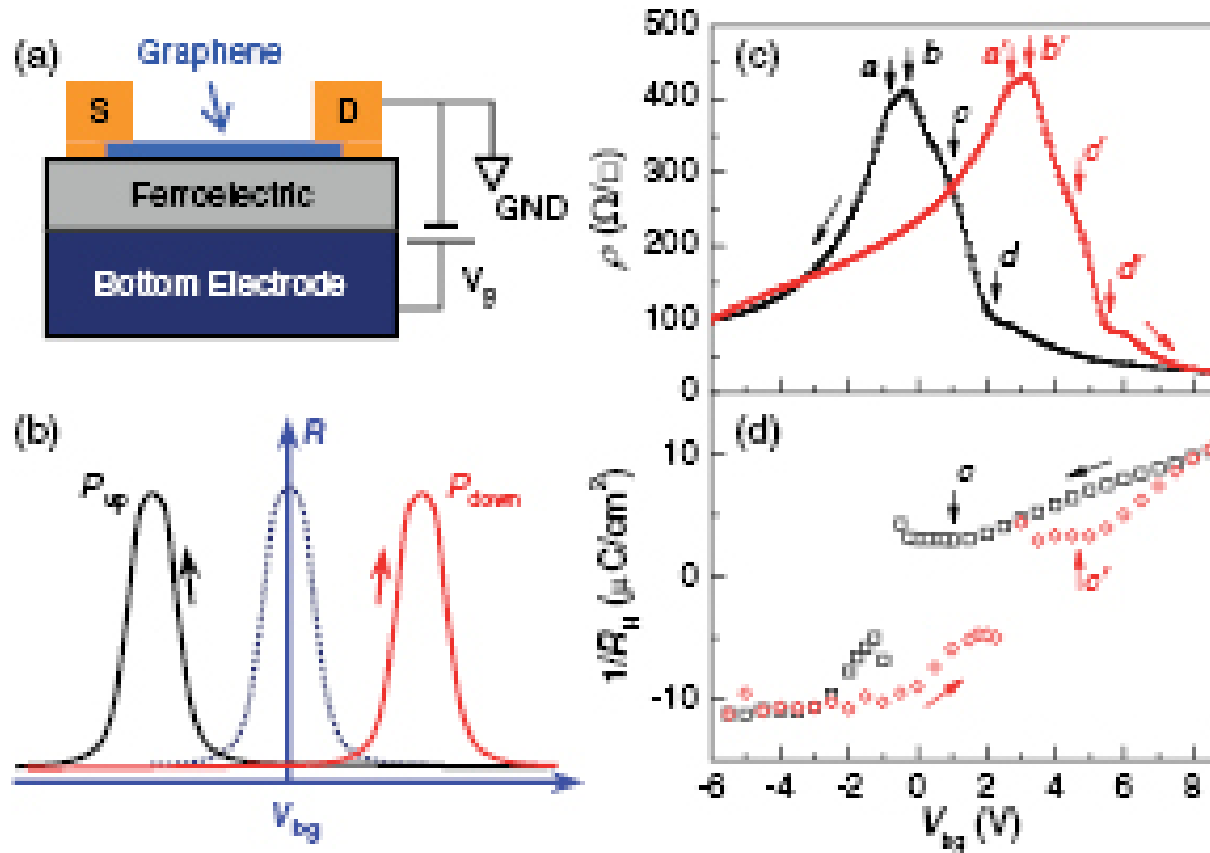
(b)



- A nonvolatile memory cell was built using multiplayer graphene as floating gate or charge trapping layer and MoS<sub>2</sub> as a channel.
- Because of its band gap and 2D nature, monolayer MoS<sub>2</sub> is highly sensitive to the presence of charges in the charge trapping layer, resulting in a factor of  $10^4$  difference between memory program and erase states.

Simone Bertolazzi, Andras Kis, et.al., ACS Nano, 7, 3246, 2013

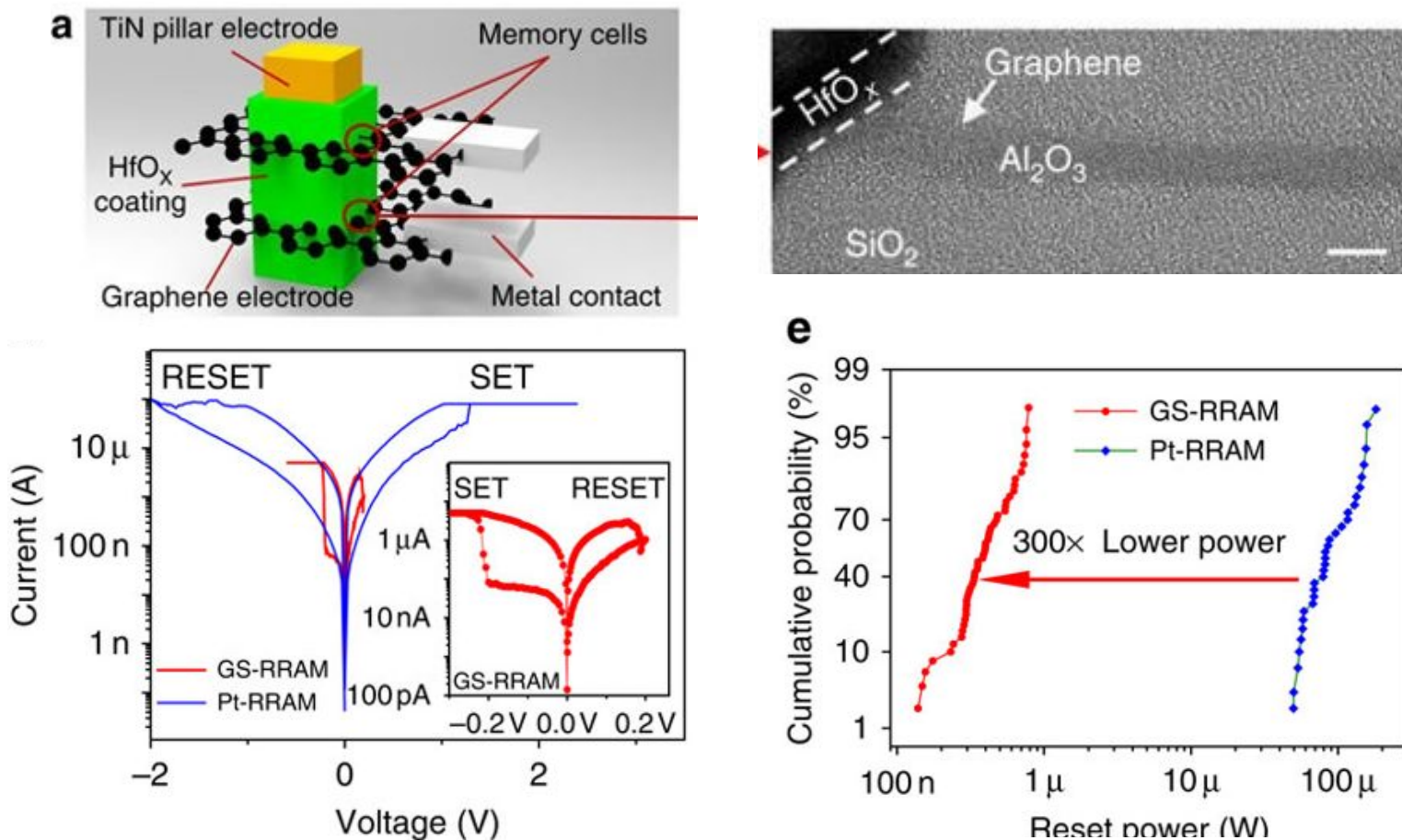
# FRAM based on graphene



- When a ferroelectric is employed as the gate material for graphene FETs, the built-in polarization field  $P$  dopes graphene with a high density of electrons or holes, depending on the polarization direction, which sets an offset to the Dirac point.

A. Rajapitamahuni, X. Hong, Nano Letters, 13, 4374, 2013

# Vertical RRAM based on graphene



The authors use the atomically thin nature of the graphene edge to assemble a resistive memory stacked in a vertical three-dimensional structure. These devices consumes much less power than traditional RRAM based on metal electrodes.

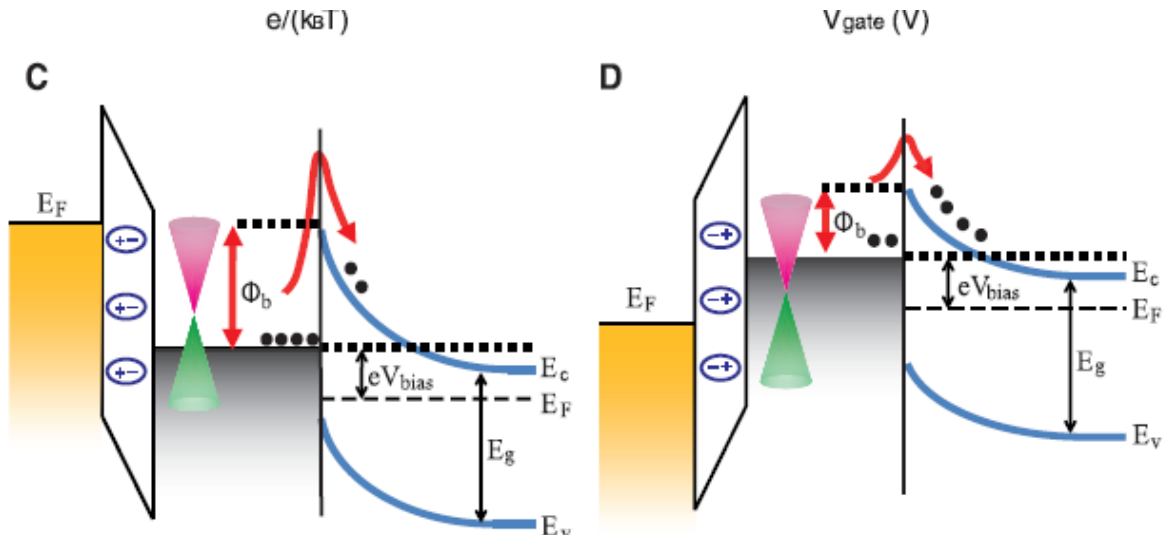
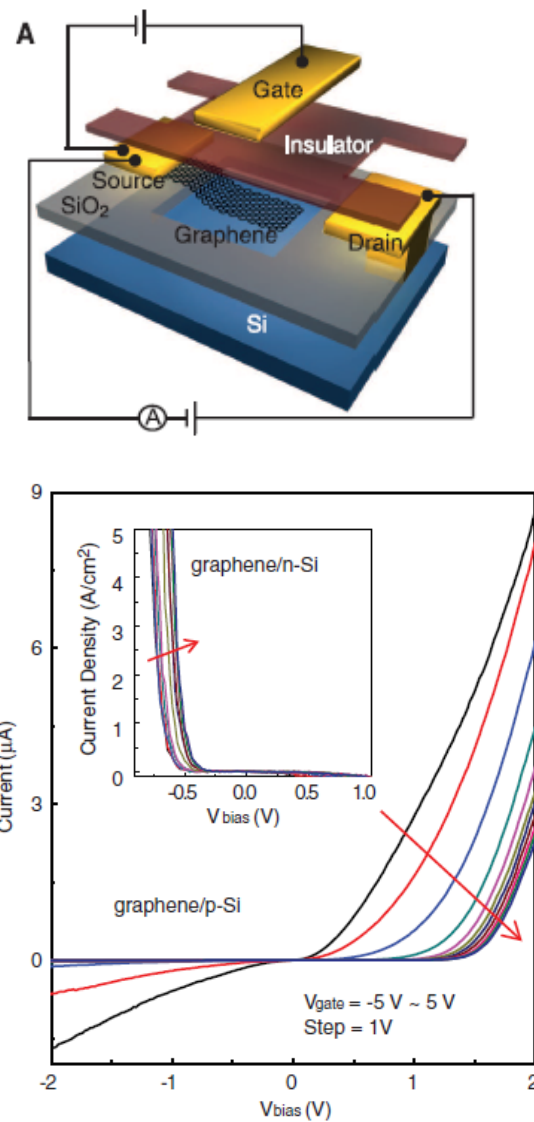
S. Lee, P. Wong, Nature Communications, 9407, 2015

# Outline

- Introduction of graphene
- Synthesis of graphene
- Current transport and electronic devices
  - Current transport
  - Electronic devices
    - Graphene RF devices
    - Graphene tunneling devices
    - Graphene varactor
    - Graphene memory
    - Graphene barrister
- Optical properties and photonic devices
- Bandgap engineering in graphene



# Graphene barristor



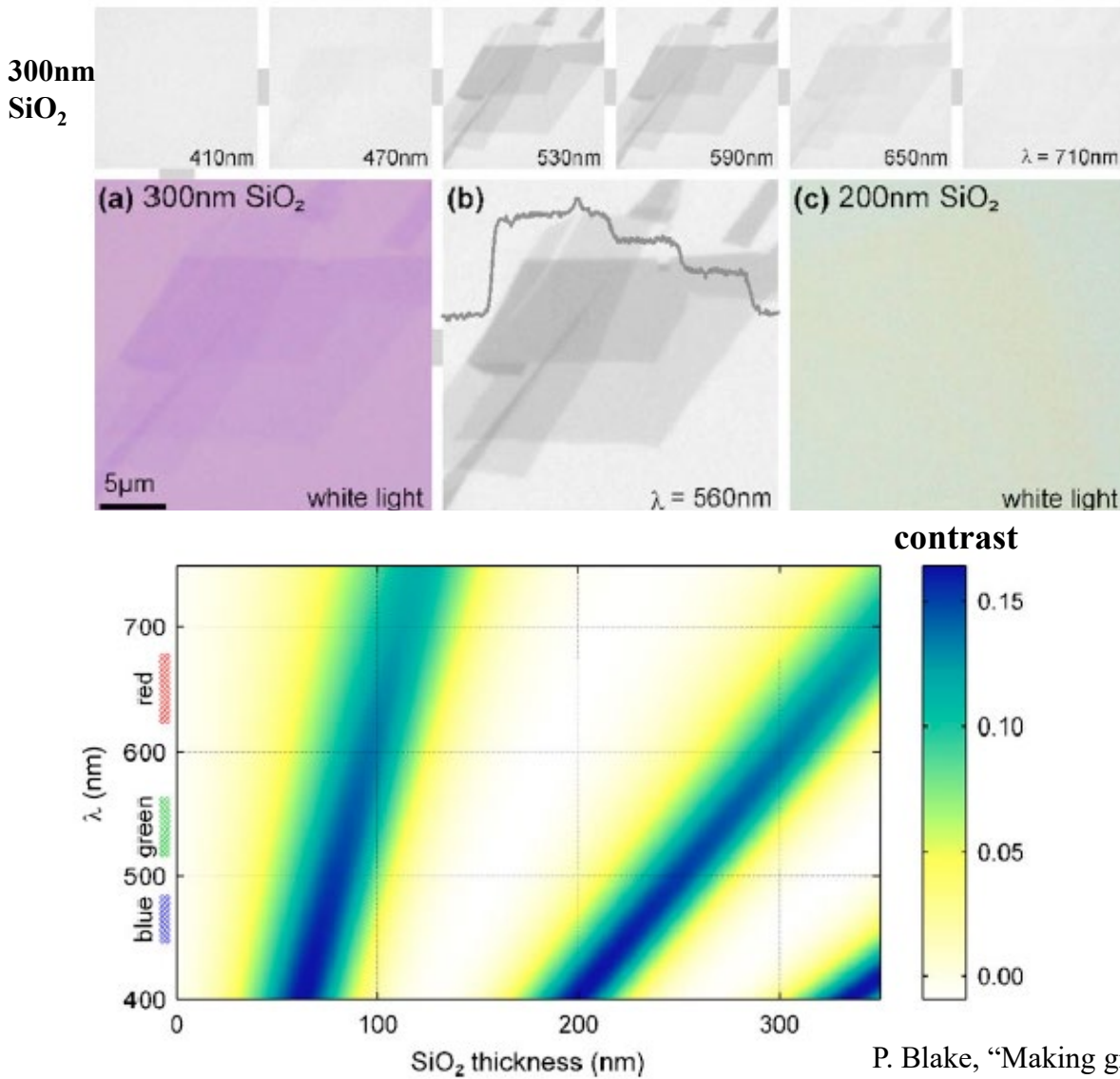
- A graphene variable-barrier “barristor” with large modulation on the device current (on/off ratio of  $10^5$ ) is achieved by adjusting the gate voltage to control the graphene-silicon Schottky barrier.

H. Yang, K. Kim, et.al., Science, 336, 1140, 2012

# Outline

- Introduction of graphene
- Synthesis of graphene
- Current transport and electronic devices
- Optical properties and photonic devices
  - ■ Optical absorption
  - Photodetector
  - Optical modulator
  - Plasmonic device
- Bandgap engineering in graphene

# Making graphene visible



- Graphene's visibility depends strongly on both thickness of  $\text{SiO}_2$  and light wavelength.
- By using monochromatic illumination, graphene can be isolated for any  $\text{SiO}_2$  thickness, albeit 300 nm and 100 nm are most suitable for its visual detection.

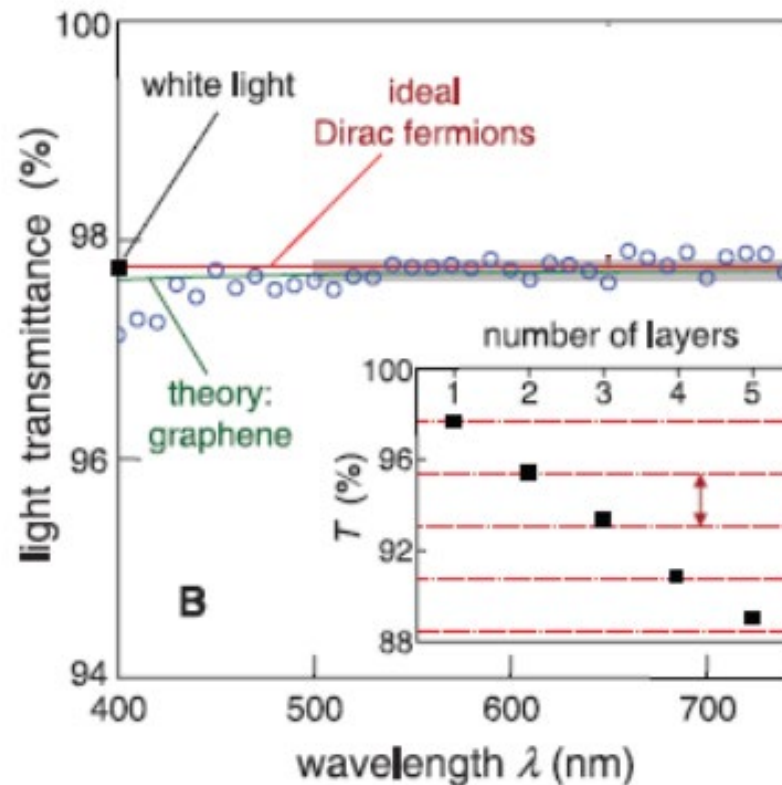
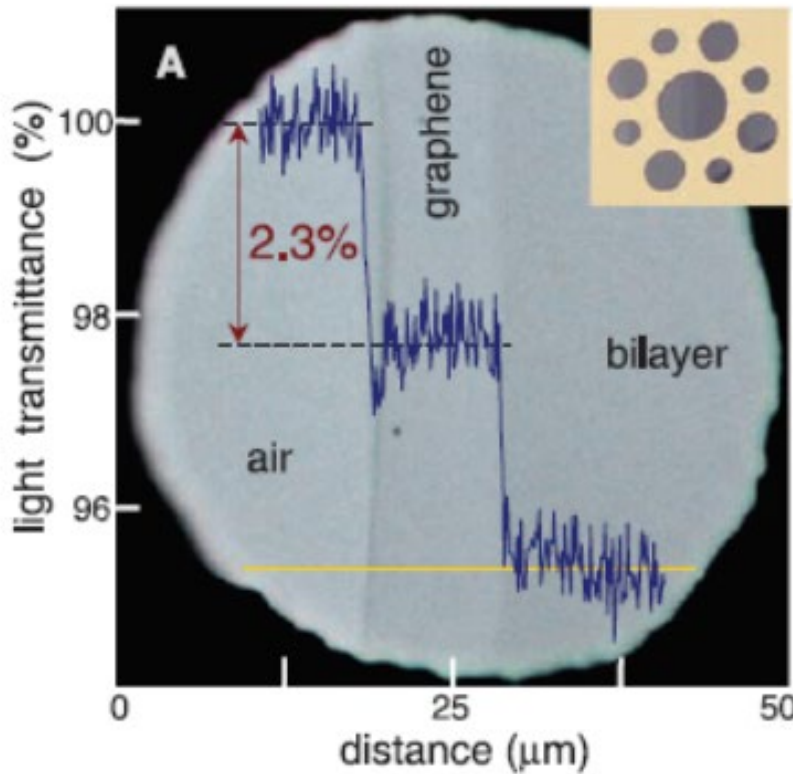
Contrast is defined as

$$C = \frac{I_{\text{sub}} - I_{\text{GR}}}{I_{\text{sub}}}$$

$I_{\text{sub}}$  and  $I_{\text{GR}}$  are reflected light in the presence and absence of graphene

P. Blake, "Making graphene visible", Appl. Phys. Lett. 91, 063124 (2007)

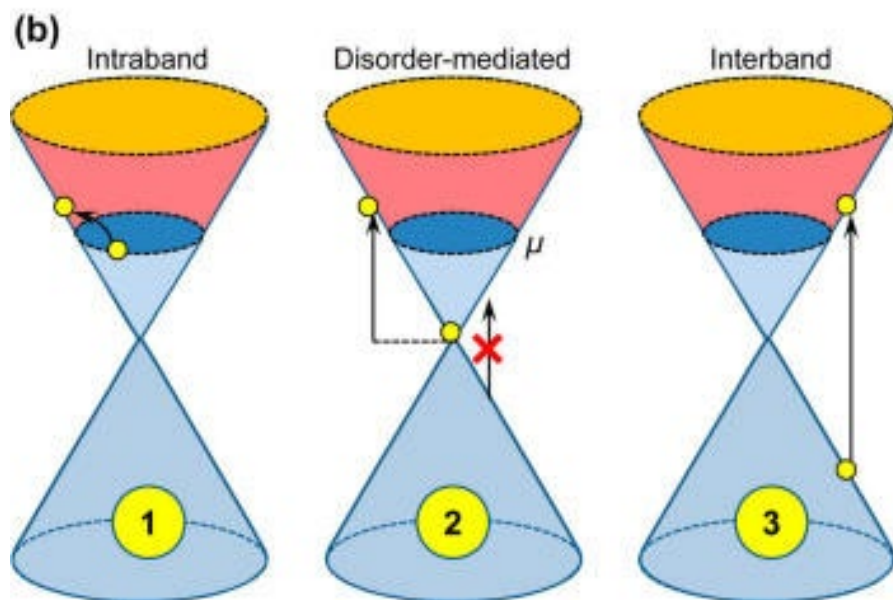
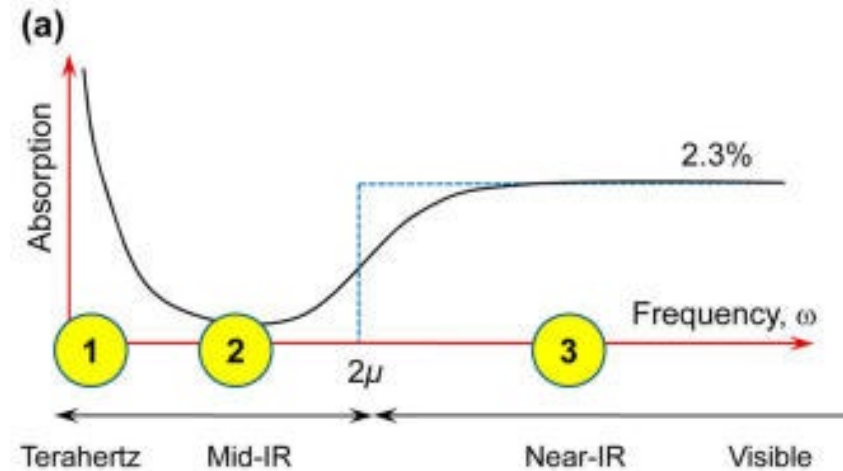
# Transparency and absorbance of graphene



Despite being only one atom thick, graphene is found to absorb a significant (~2.3%) fraction of incident white light.

R. Nair, A. Geim, et.al., Science, 320, 1308, 2008

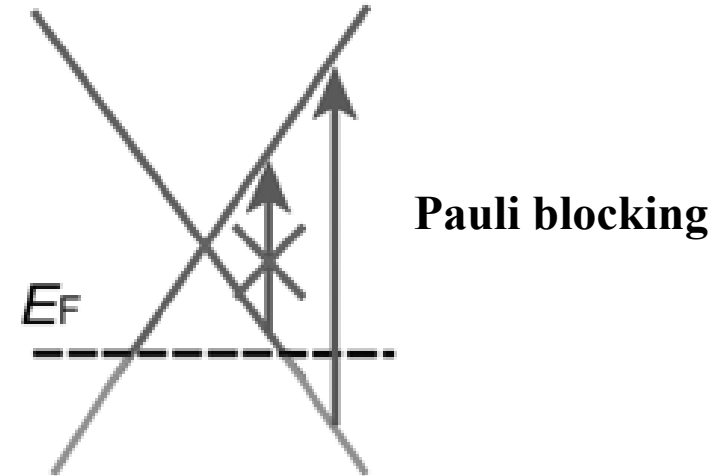
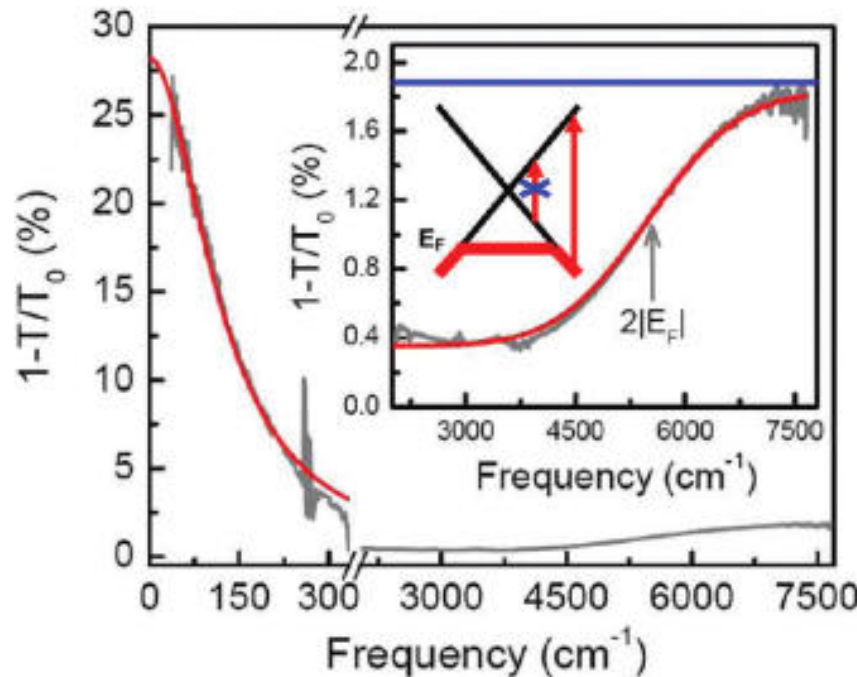
# Graphene absorption spectrum



- At near-infrared to visible frequencies, absorption is due to direct interband transitions.
- In doped graphene at the mid-infrared regime, Pauli-blocking occurs and the optical conductivity is minimal.
- At terahertz frequencies, the absorption is due to intraband free carriers absorption.

Tony Low, ACS Nano, 8, 1086, 2014

# Infrared absorption spectra of CVD graphene



- Due to Pauli blocking, the interband absorption of photons with energy below  $2|E_F|$  is suppressed.
- In the far-IR region, the absorption increases rapidly with decreasing frequency due to free carrier absorption.

H. Yan, Ph. Avouris, et.al., ACS Nano, 5, 9854, 2011

Ph. Avouris, et al. 2D Materials: properties and devices, 2017

# Outline

- Introduction of graphene
- Synthesis of graphene
- Current transport and electronic devices
- Optical properties and photonic devices
  - Optical absorption in graphene
  - Graphene photodetectors
- • Background and motivation
  - Measurement setup
  - Photocurrent Mechanism
  - Enhancement of photocurrent
- Graphene optical modulators
- Graphene plasmonic devices
- Bandgap engineering in graphene

# Recap: photodetector basics

- Photodetector is a device that senses light.
- Photocurrent is the electric current through a photodetector as the result of exposure to light.

$$I_{ph} = I_{light} - I_{dark}$$

- Responsivity

$$R = \frac{I_{ph}}{P_{in}}$$

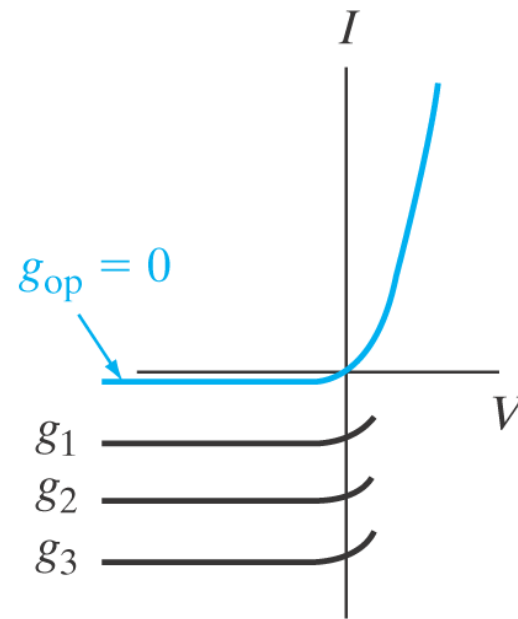
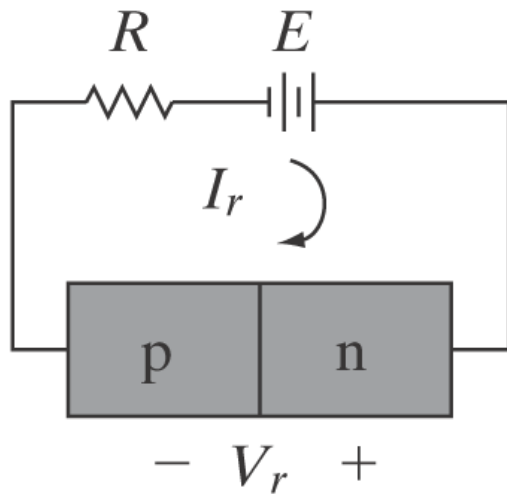
→ Incident light power

- External quantum efficiency

$$\eta_{ext} = \frac{J_{ph}/q}{P_{in}/h\nu}$$

*number of carriers collected*  
*number of incident photons*

# Recap: silicon photodetector



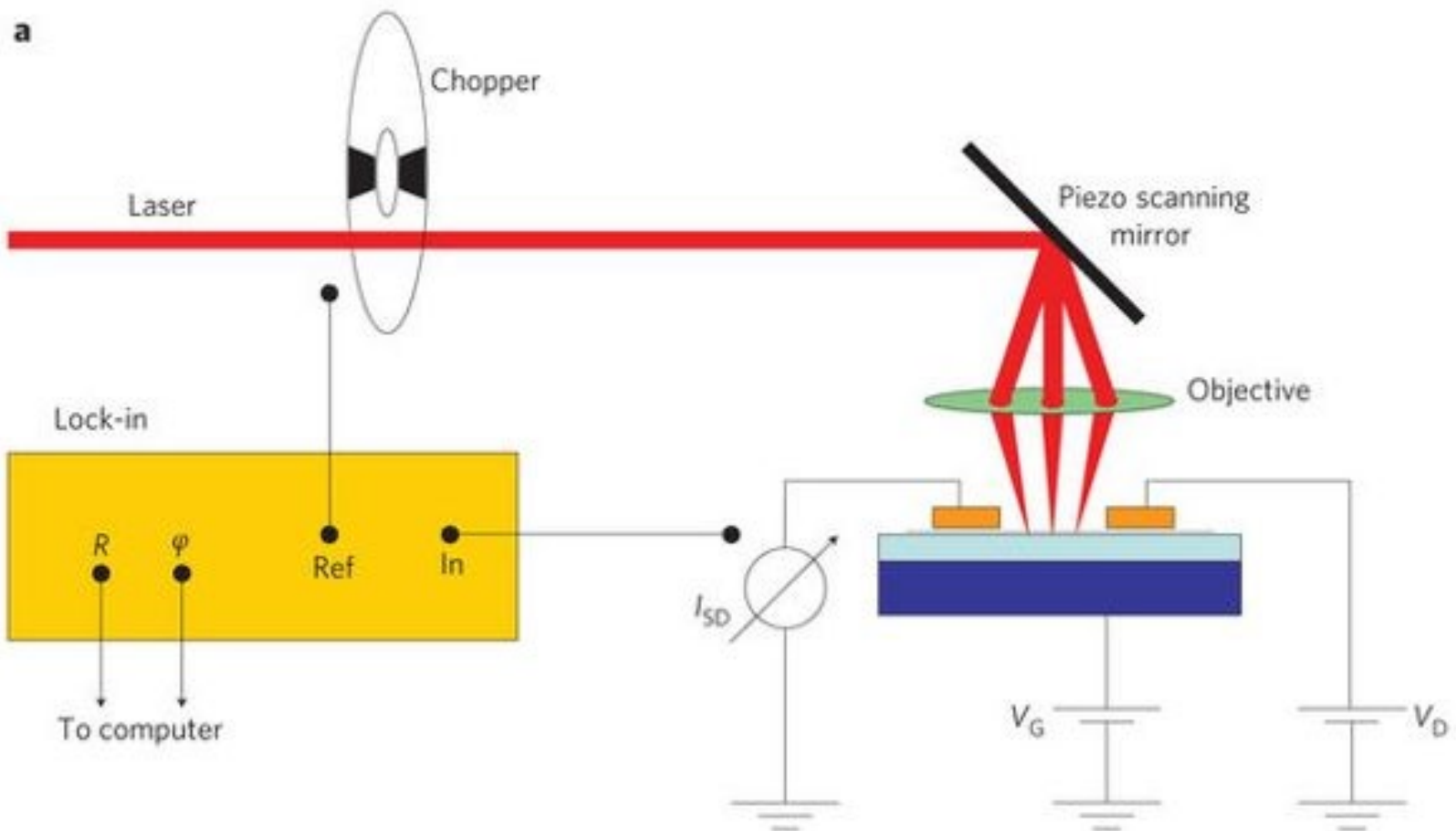
$$g_3 > g_2 > g_1$$

Silicon pn junction can serve as a photodetector. When the photodiode is reverse biased, the current is proportional to the optical generation rate, which can be used to detect the power density of the incident light.

# Why graphene is promising for photodetector application?

- Graphene is gapless. This enables charge carrier generation by light absorption over a very wide energy spectrum including ultraviolet, visible, infrared and terahertz spectral regimes.
- High carrier mobility enables ultrafast conversion of photons or plasmons to electrical currents or voltages.
- Tunable optical properties via electrostatic doping which enables its applications in modulators.
- Graphene is compatible with CMOS, making it a strong contender for low-cost and large-scale optoelectronic systems.
- Graphene is flexible, which can enable flexible photodetectors.

# Typical photocurrent measurement setup



- While a chopped and focused laser beam is scanned over the sample, the a.c. photocurrent amplitude and phase are obtained using a lock-in amplifier referenced to the chopping frequency.

Marcus Freitag, Phaedon Avouris, Nature Photonics, 7, 53, 2013

# Outline

- Introduction of graphene
- Synthesis of graphene
- Current transport and electronic devices
- Optical properties and photonic devices
  - Optical absorption
  - Photodetector
    - Background and motivation
    - Measurement setup
  - • Photocurrent Mechanism
    - Enhancement of photocurrent
  - Optical modulator
  - Plasmonic device
- Bandgap engineering in graphene

# Physical mechanisms enabling photodetection

## Photovoltaic

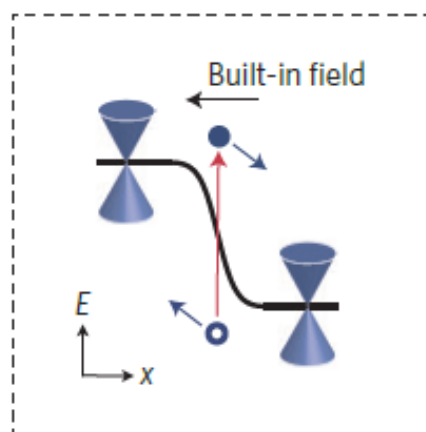
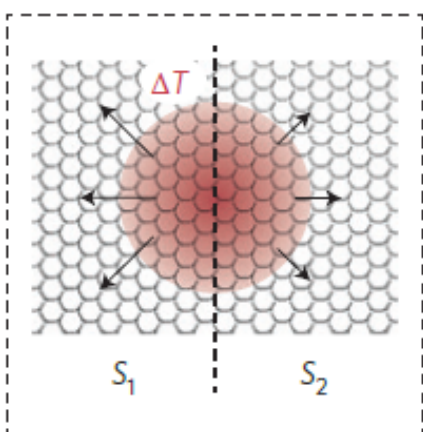
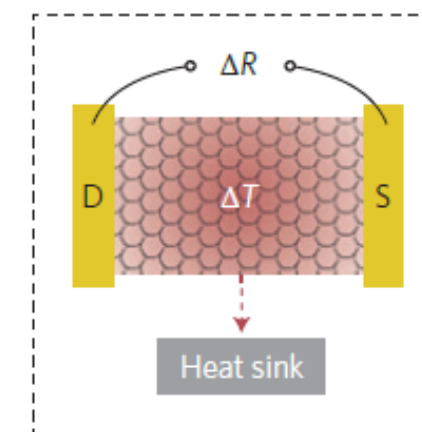


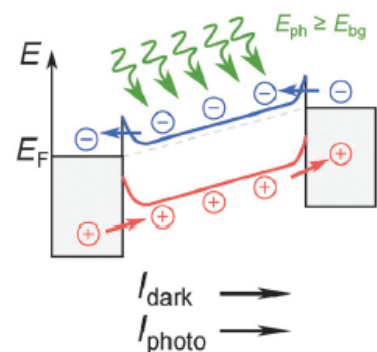
## Photo-thermoelectric



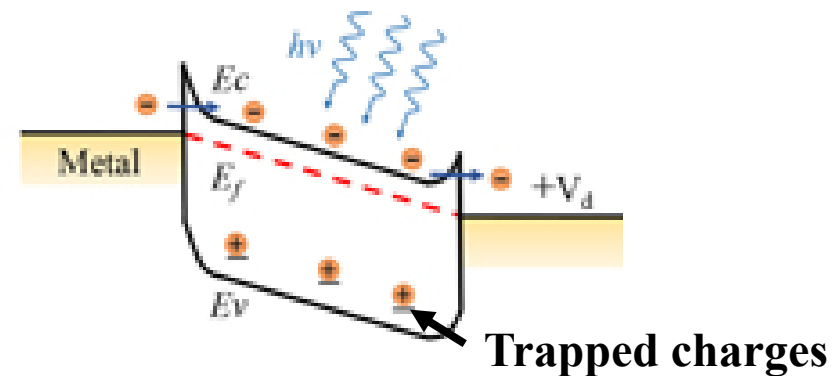
## Bolometric



## Photoconductive



## Photogating

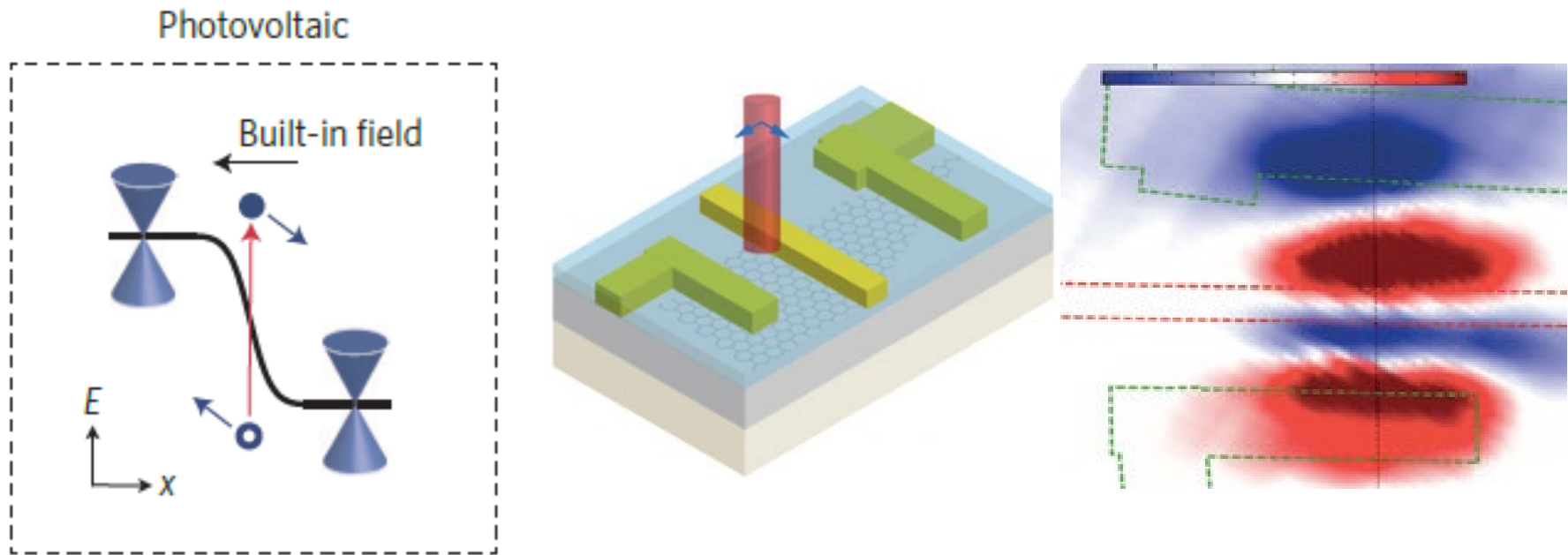


F. Koppens, et al., Nature Nanotechnology, 9, 780, 2014

M. Buscema, et al., Chem. Soc. Rev., 44, 3691, 2015

# Photovoltaic effect

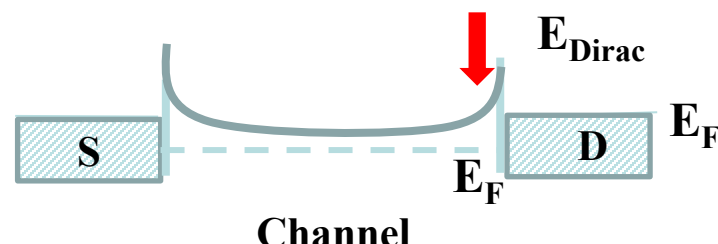
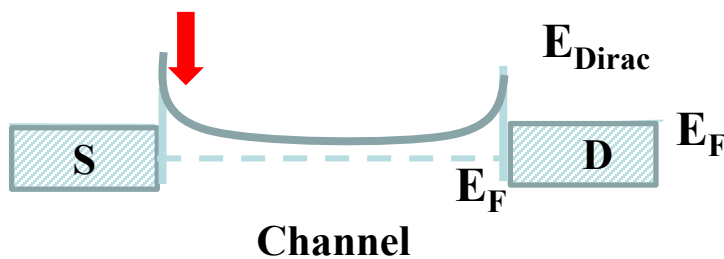
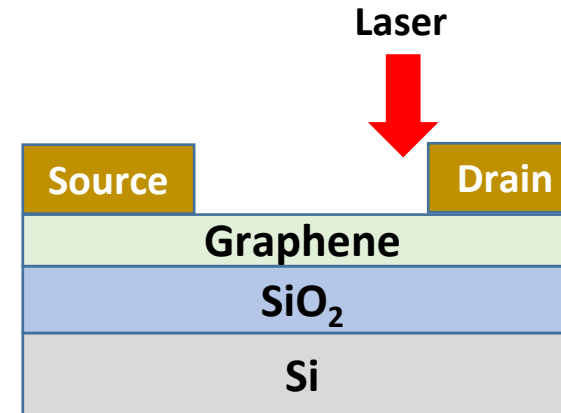
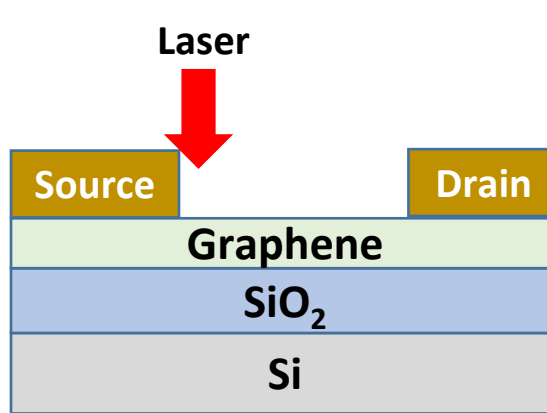
Photovoltaic (PV) photocurrent generation is based on the separation of photo-generated electron–hole (e–h) pairs by built-in electric fields at pn junctions, metal/semiconductor junctions or non-uniformly doped regions.



- The built-in field can be introduced either by local chemical doping, electrostatically by the use of (split) gates, or by taking advantage of the work-function difference between graphene and a contacting metal.

# Question

When we put the laser spot near the source contact, we detected a positive photocurrent at the drain. Assuming photovoltaic effect is the dominant mechanism for the photocurrent in this case, if we move the laser spot to the drain side, will the photocurrent be positive or negative?



$$V_G = 0V \quad V_D = 0V$$

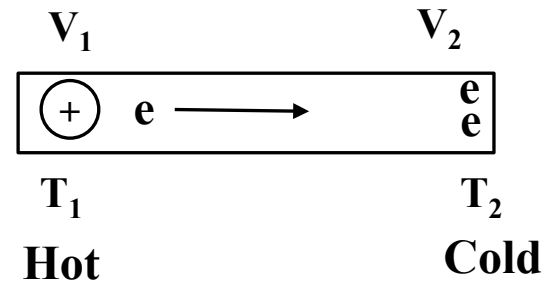
# Thermoelectric effect

- Thermoelectric effect is the direct conversion of temperature differences to electric voltage and vice versa.
- Seebeck effect is the conversion of heat directly into electricity.

Consider a bar of a conductor with a temperature gradient across it. The mobile charge carriers will tend to diffuse away from the hot end. For an isolated bar, though, there can't be any net current, so a voltage gradient develops such that the drift current balances out the diffusion tendency.

## Seebeck coefficient

$$S = -\frac{\Delta V}{\Delta T}$$



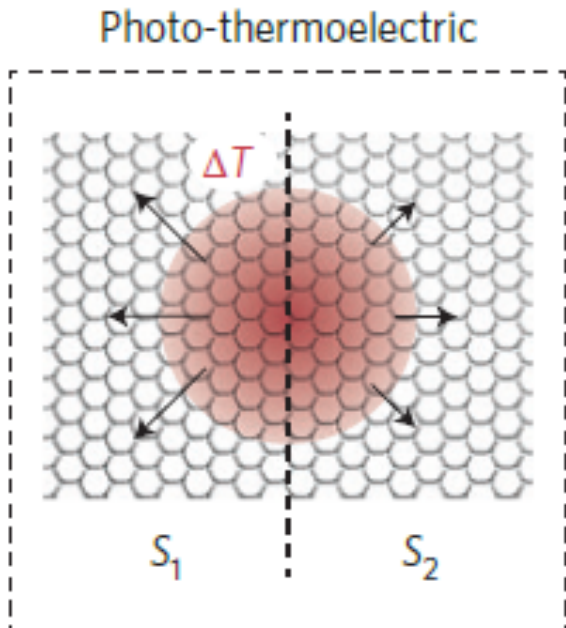
In p-type semiconductors, S is positive. In n-type semiconductors, S is negative.

# Photo-thermoelectric effect

The photogenerated hot electrons can produce a photovoltage by the photo-thermoelectric (PTE) effect (Seebeck effect):

$$V_{PTE} = (S_1 - S_2)\Delta T_e$$

where  $S_1$  and  $S_2$  (in  $\text{V K}^{-1}$ ) is the thermoelectric power (Seebeck coefficient) in the two graphene regions with different dopings, and  $\Delta T_e$  is the electron temperature difference between the regions.

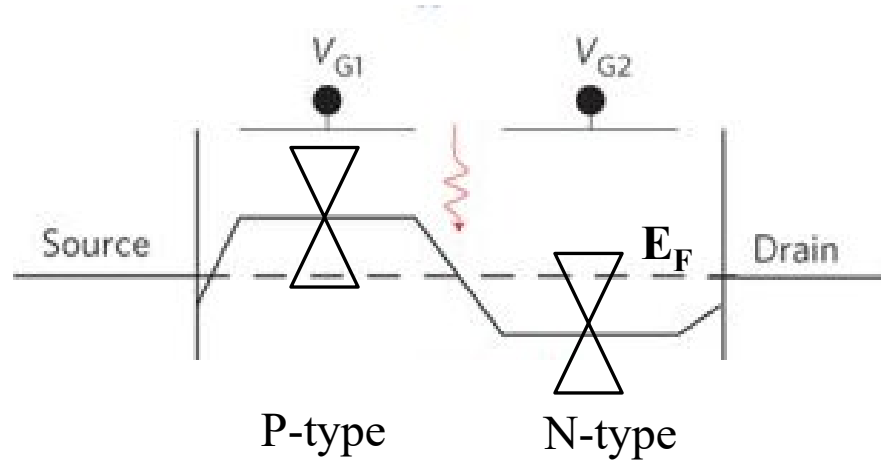


The Seebeck coefficient  $S$  is related to the electrical conductivity  $\sigma$  by the Mott formula:

$$S = -\frac{\pi^2 k_B^2 T_e}{3q} \frac{1}{\sigma} \frac{\partial \sigma}{\partial \varepsilon}$$

# Question

- If we have a graphene pn junction shown below, when we shine light at the junction interface, will the photocurrent due to photo-thermoelectric effect point to the left or the right direction?

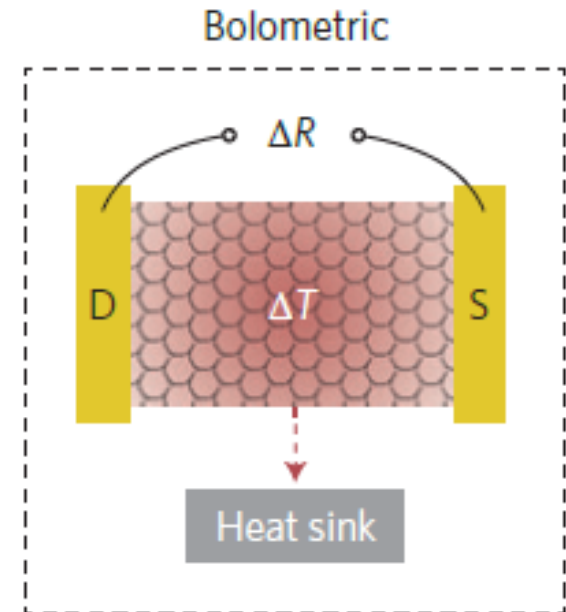


# Bolometric effect

Light absorption creates heat and a temperature change  $\Delta T$ , and thus a resistance change in the channel. The signal is given by

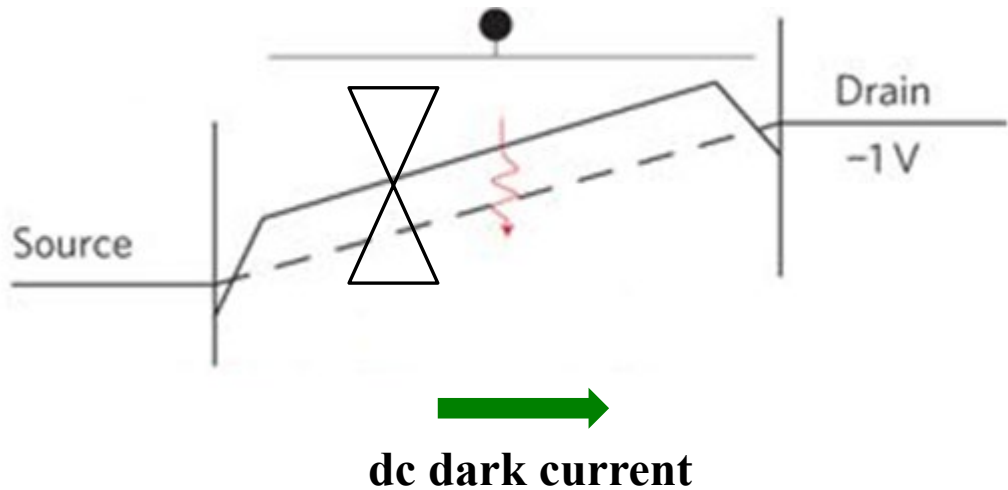
$$\Delta V = I_{dc} \Delta R = I_{dc} \frac{dR}{dT} \Delta T$$

The conductance change induced by the incident light can be due to two mechanisms: (1) a change in carrier mobility due to the associated temperature change; or (2) a change in the number of carriers contributing to the current.



# Question

For a heavily p-type doped graphene transistor, when we apply negative drain bias, the dc current is pointing to the drain. When photons are incident on the graphene channel, is the photocurrent due to bolometric effect pointing to the drain or the source contact? Here assuming the carrier mobility reduces with increasing temperature and the total carrier density is nearly unchanged due to heavy doping.

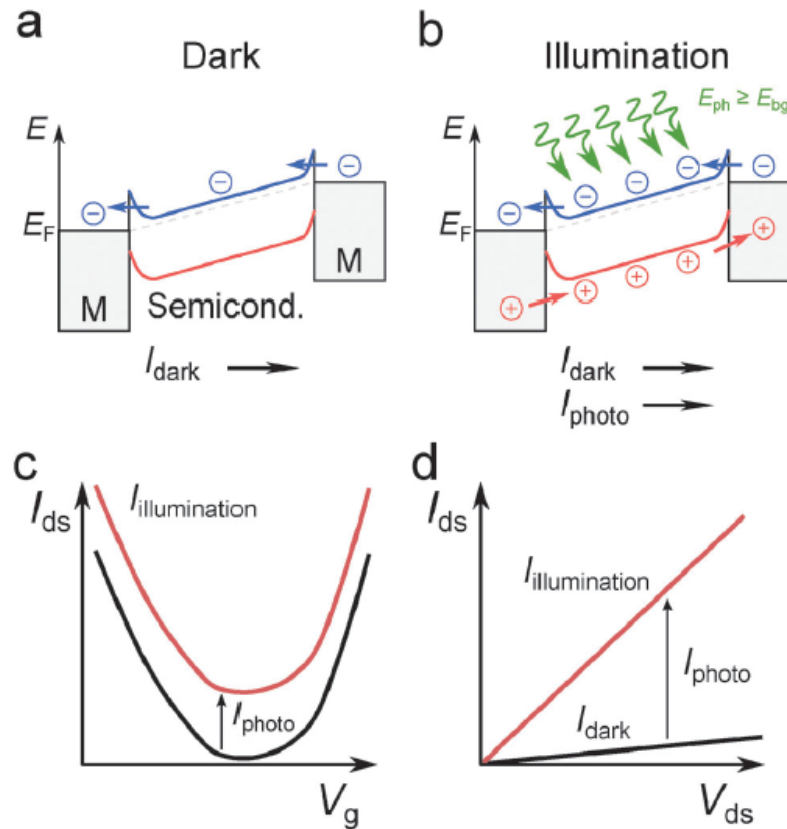


# Photoconductive effect

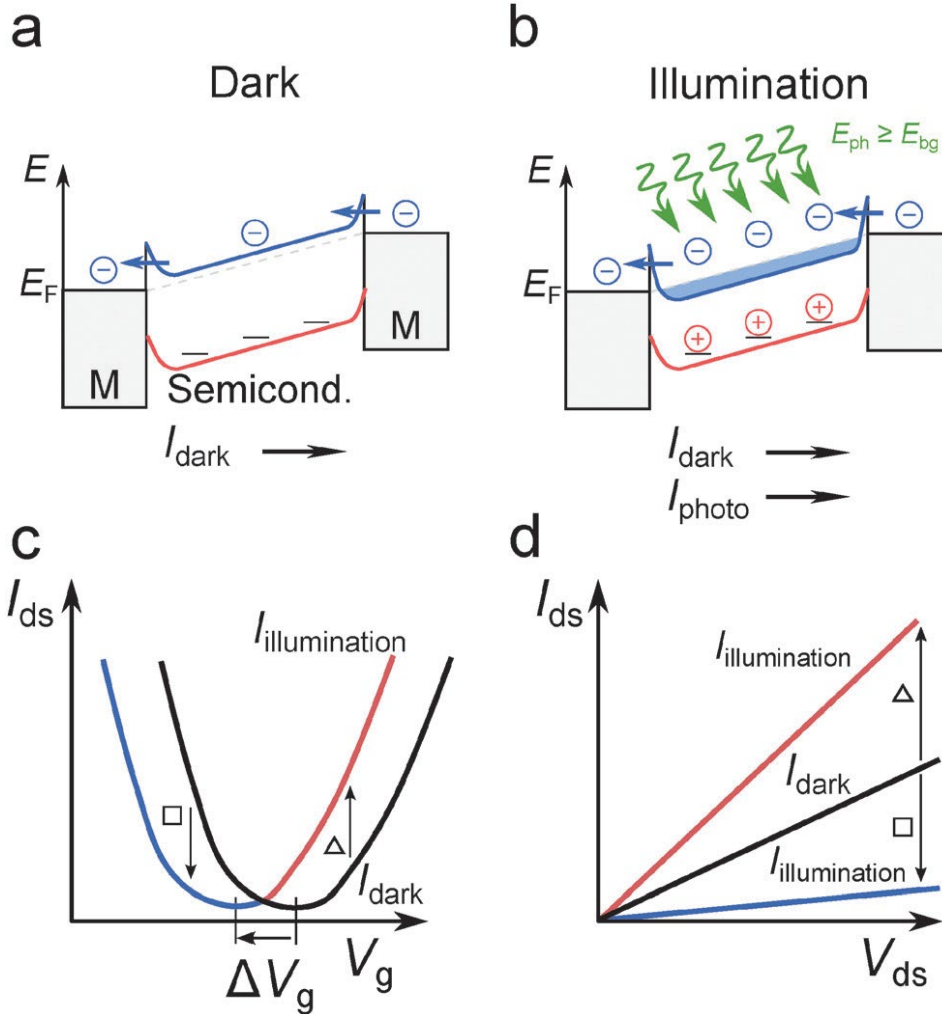
Photons create electron-hole pairs, providing additional conductance carriers in the device. The change in conductance is given by

$$\Delta\sigma = \Delta n e \mu$$

Where  $\Delta n$  is the steady-state photo-excited charge density.

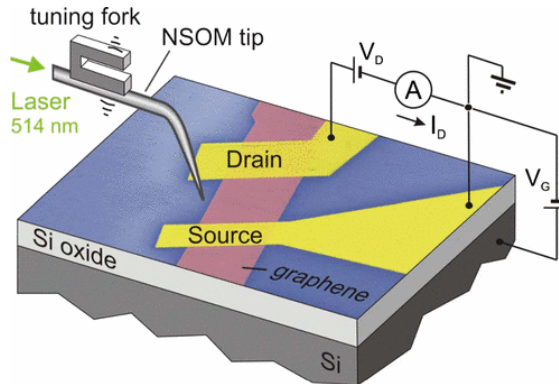


# Photogating effect

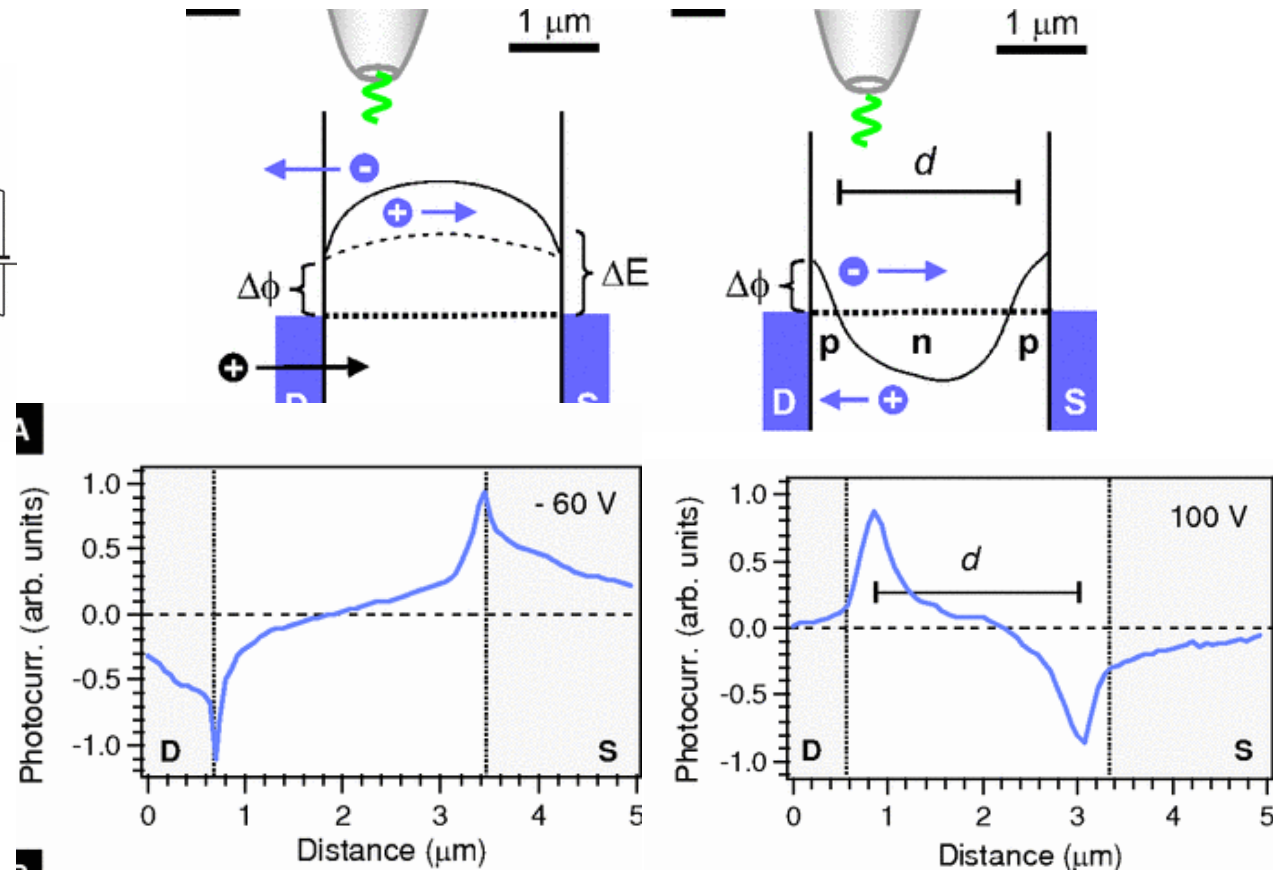


- If photo generated holes/electrons are trapped in oxides or floating gate, they act as a local gate, effectively modulating the resistance of the material.
- These holes/electrons can be either generated in 2D material or generated in nanoparticles, molecules or charge traps in the vicinity of the 2D material.

# Example 1: Role of contacts in graphene transistors



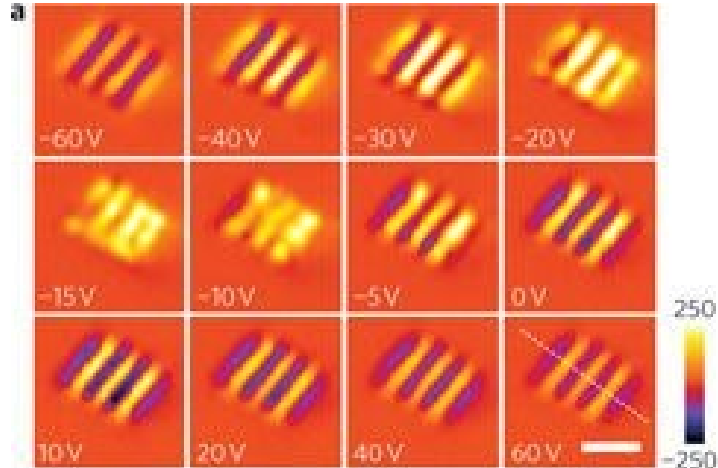
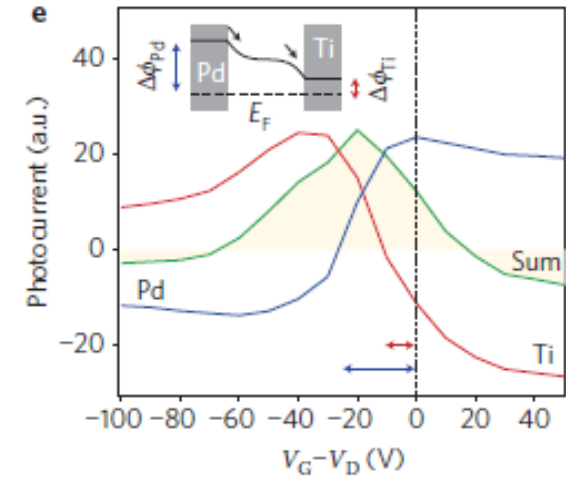
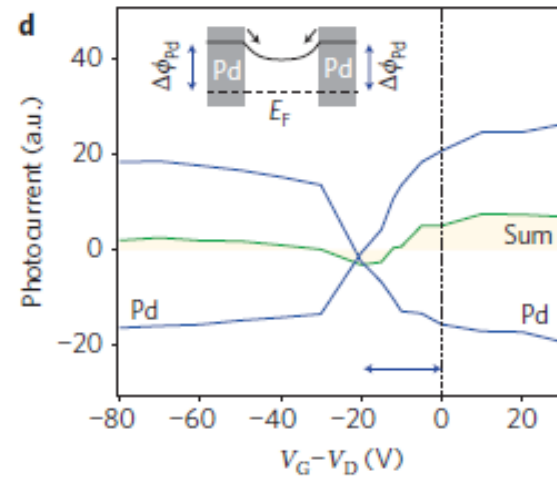
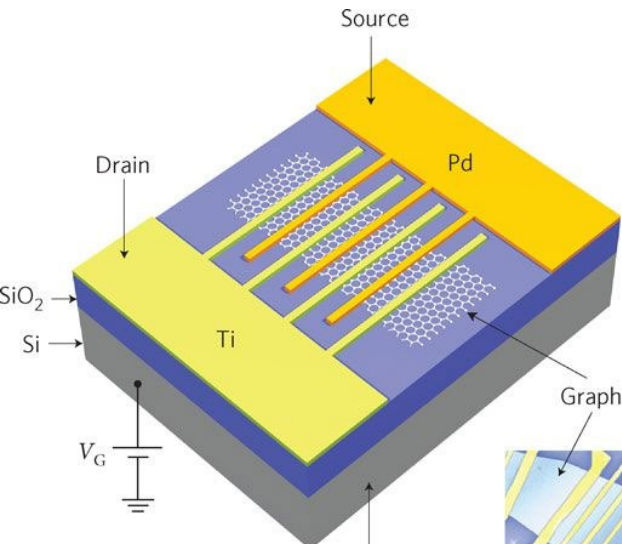
Pd contact introduces p doping of the graphene underneath the electrodes.



- At negative gate biases, the band bending at the contacts becomes steeper and photocurrent becomes stronger than that without bias.
- At positive gate biases, a p-n junction forms close to the contacts, which induce photocurrent in the opposite direction as that in negative bias.

T. Mueller, et al., Physical review B, 79, 245430 2009

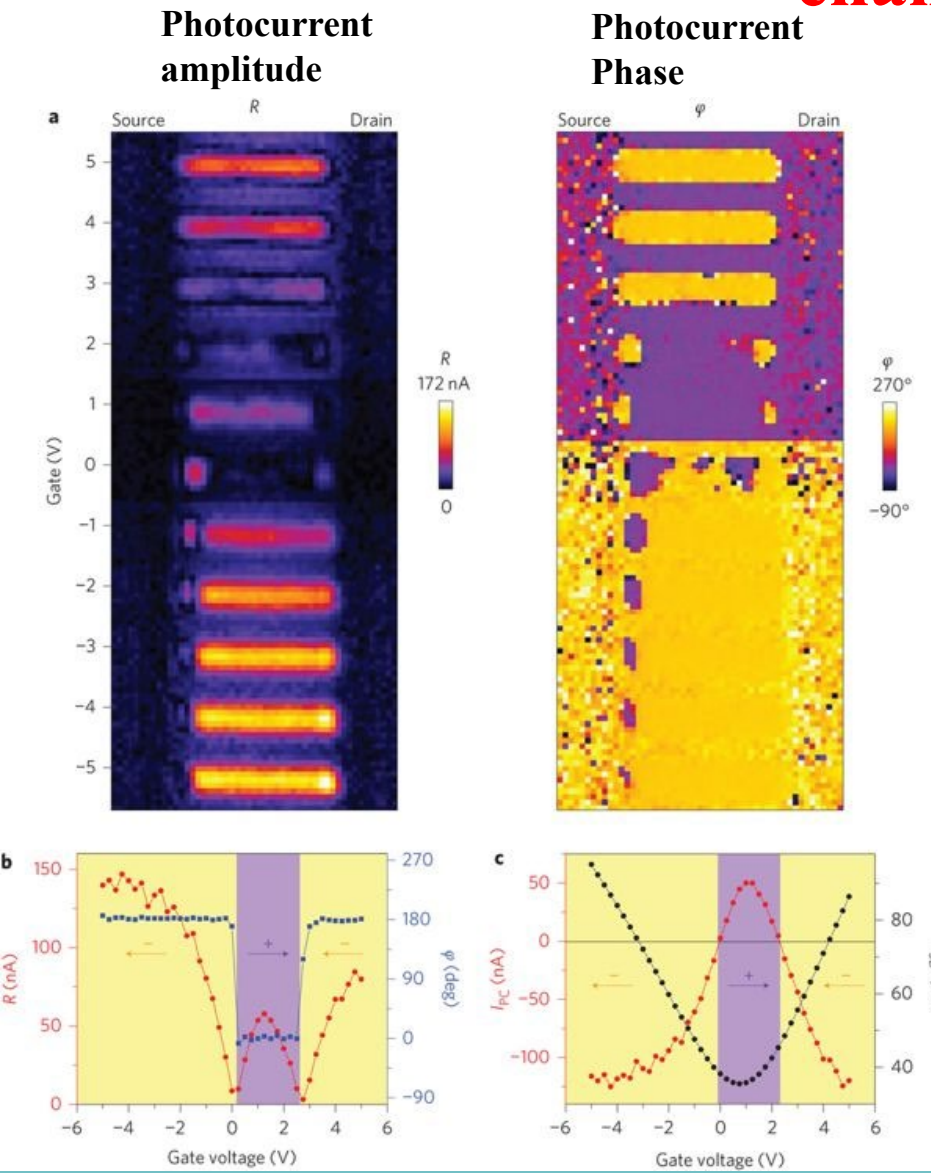
## Example 2: Graphene photodetector with asymmetric contacts



- An asymmetric metallization scheme is adopted to break the mirror symmetry of the internal electric-field profile in conventional graphene field-effect transistor channels, allowing for efficient photodetection.
- External responsivity of 6.1 mA/W at an operating wavelength of 1.55 mm was demonstrated, representing a 15-fold improvement compared with a graphene phototransistor with symmetric contacts.

T. Mueller, Ph. Avouris, et.al., Nature Photonics, 4, 297, 2010

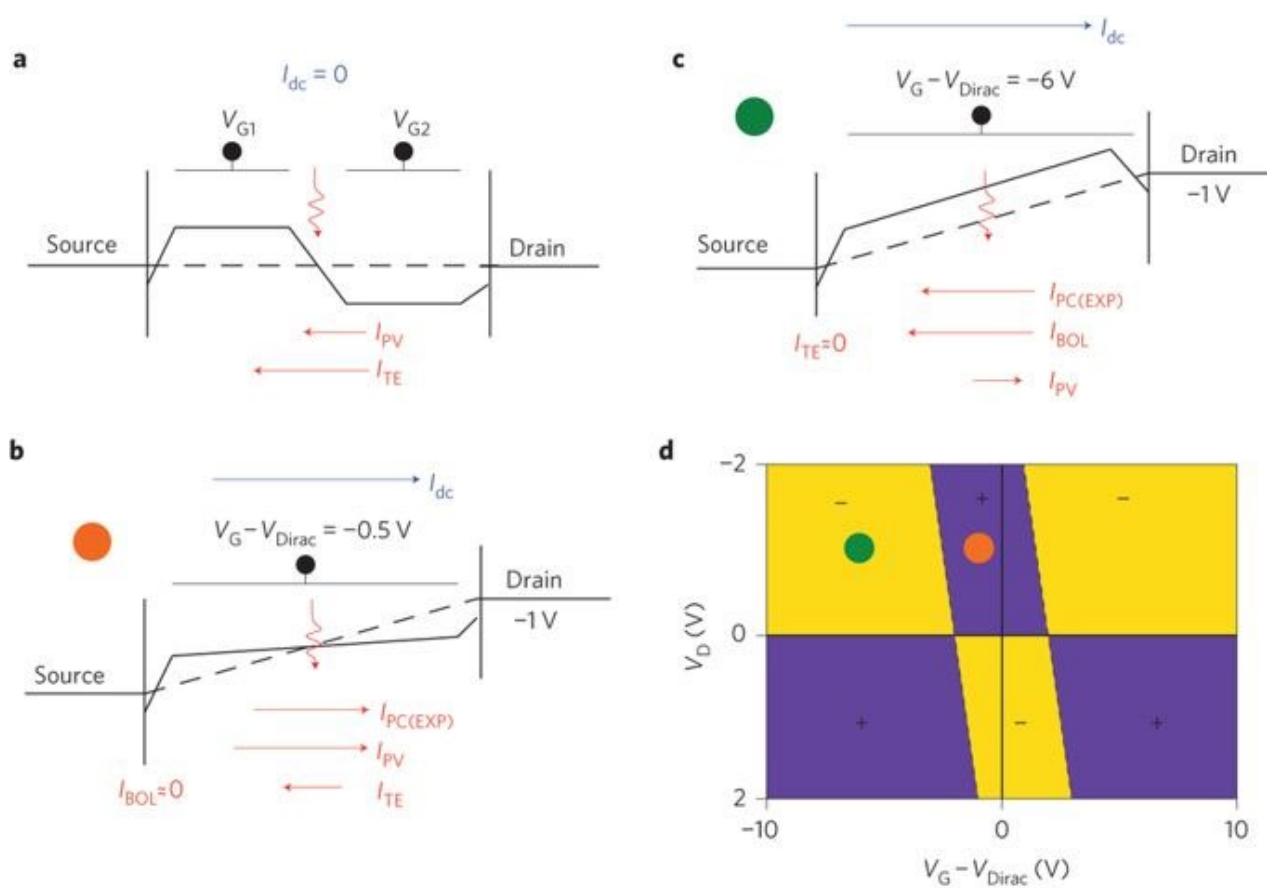
# Example 3: Photoresponse at the center of graphene channel



- When the laser spot is at the center of the graphene channel, the photocurrent switches sign twice as the Fermi level in the device is swept from p-type over intrinsic to n-type.

Marcus Freitag, Phaedon Avouris,  
Nature Photonics, 7, 53, 2013

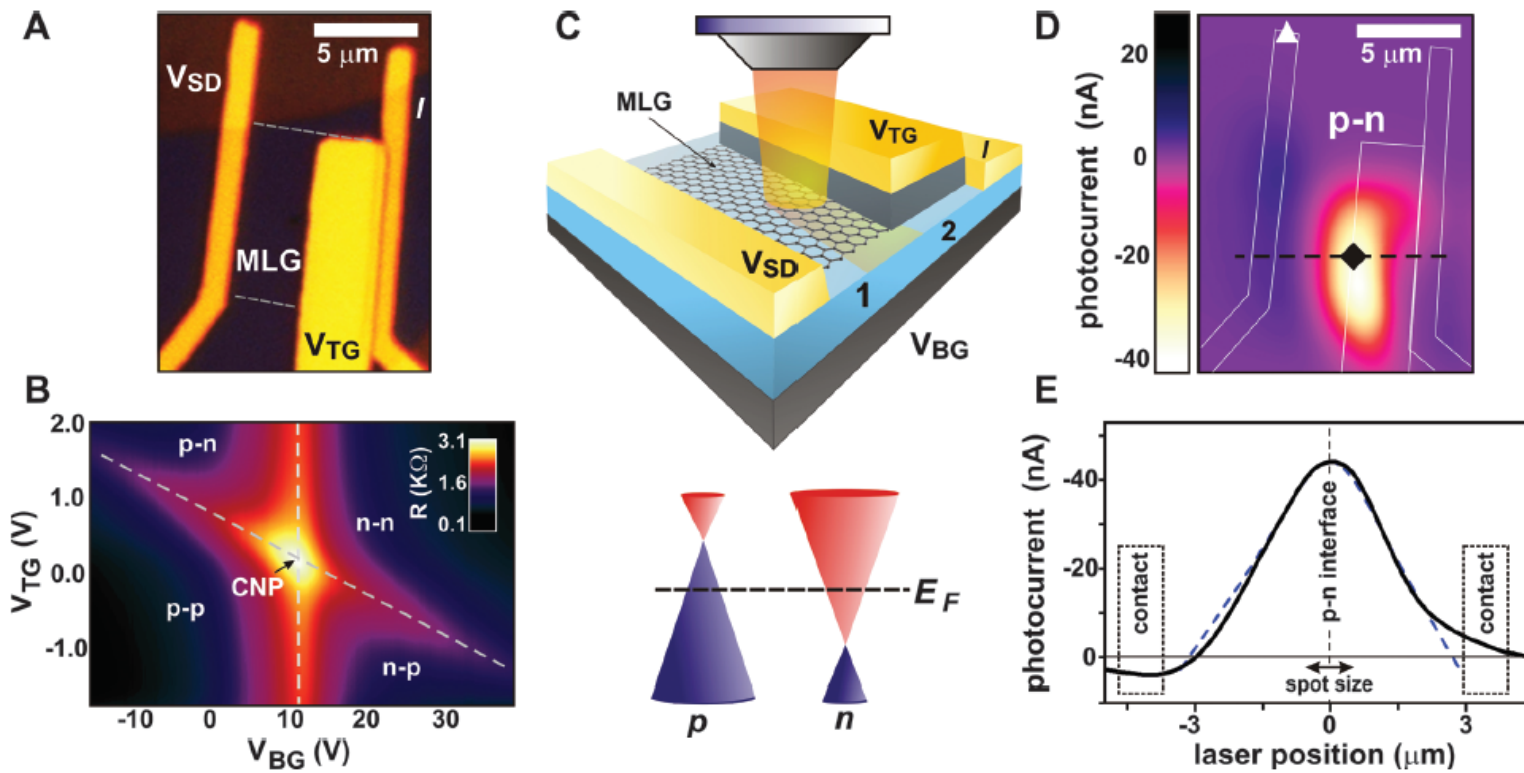
# Example 3: Photoresponse at the center of graphene channel



When the channel doping is high, the photo-thermoelectric effect is negligible. The photovoltaic effect does exist but the bolometric effect is dominant.

When the graphene channel is intrinsic, photovoltaic effect dominates because the increase in carrier temperature leads to extra electrons and holes, while the bolometric effect can be ignored.

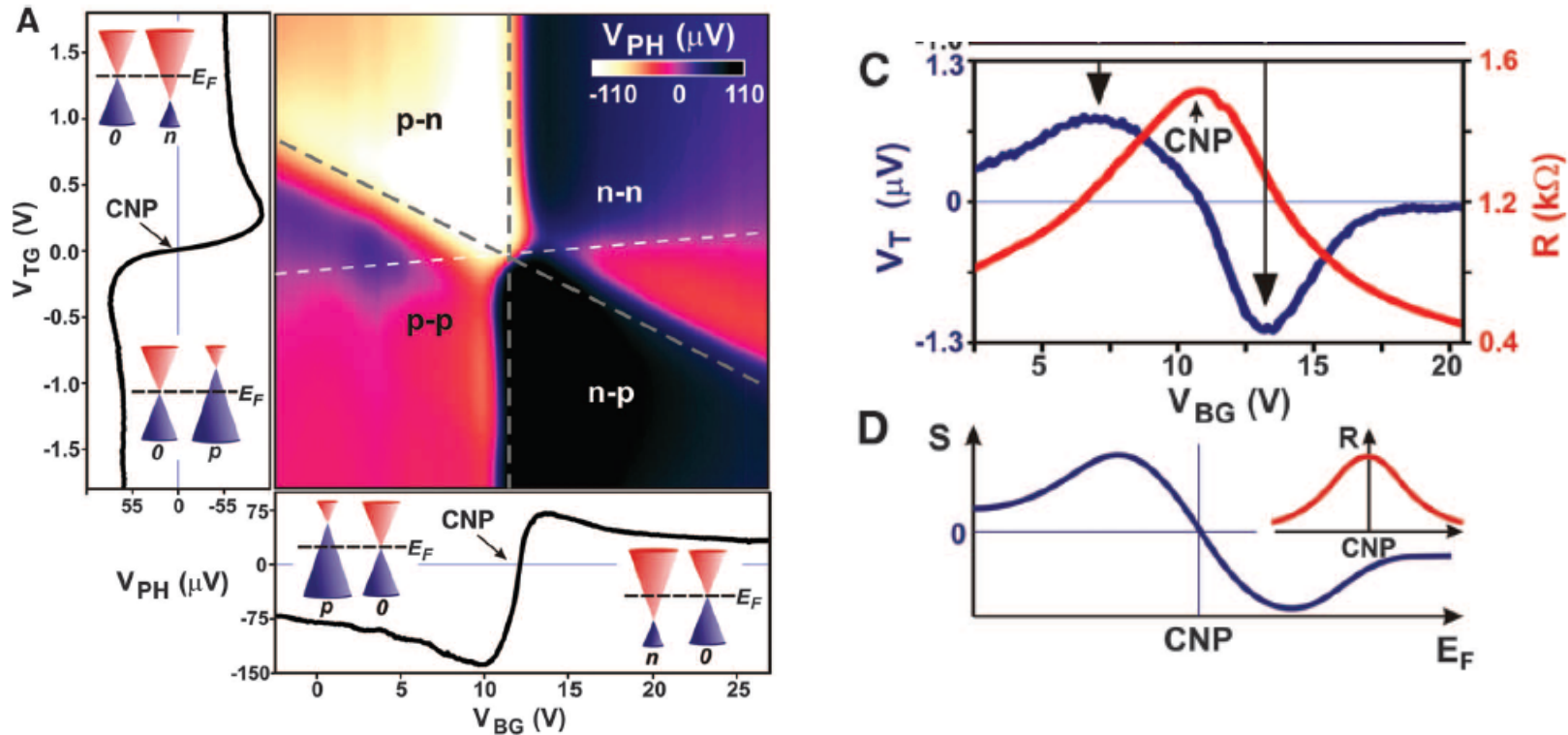
# Example 4: Photoresponse at graphene pn junction



- Optoelectronic measurements were carried out on dual gate voltage–controlled graphene p-n junction devices in the presence of local laser excitation.
- Dual gate control allows one to explore the photoresponse as a function of carrier polarity, varied independently in two adjacent regions.

N. Gabor, Pablo Jarillo-Herrero, Science, 334, 648, 2011

# Example 4: Photo-thermoelectric effect at pn junction



$$\text{Seebeck coefficient } S = - \frac{\pi^2 k_B^2 T_e}{3q} \frac{1}{\sigma} \frac{\partial \sigma}{\partial \varepsilon}$$

- Local laser excitation at the p-n interface leads to striking six-fold photovoltage patterns as a function of bottom- and top-gate voltages.
- Photo-thermoelectric effect dominates the intrinsic photoresponse at graphene pn junction.

N. Gabor, P. Jarillo-Herrero, Science, 334, 648, 2011

# Example 5: Photogating effect in graphene photodetector

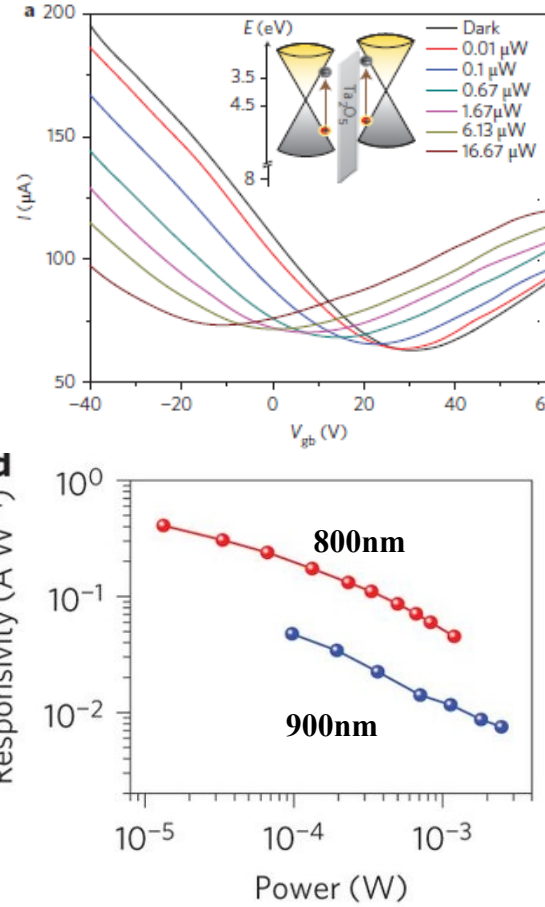
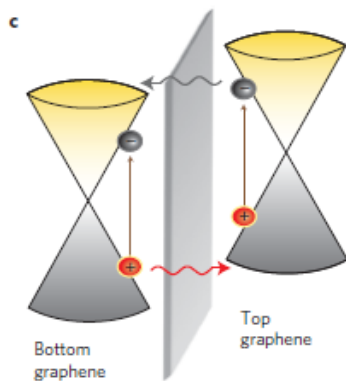
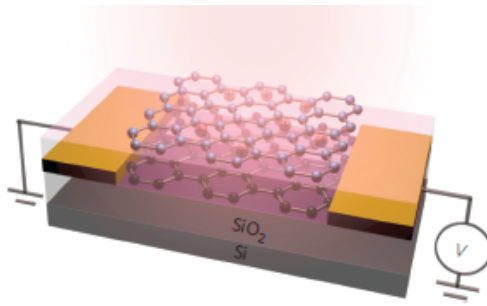
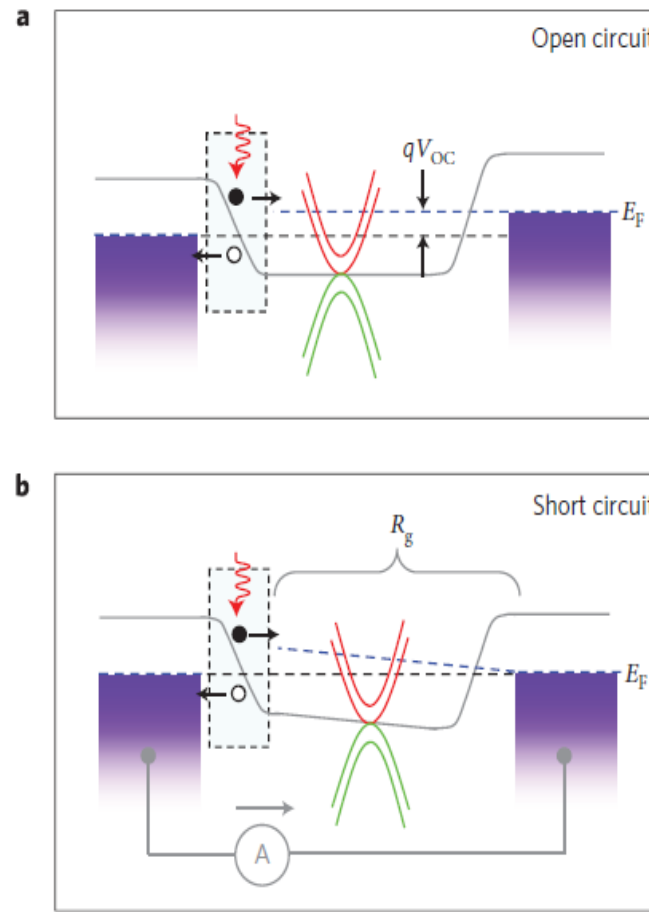
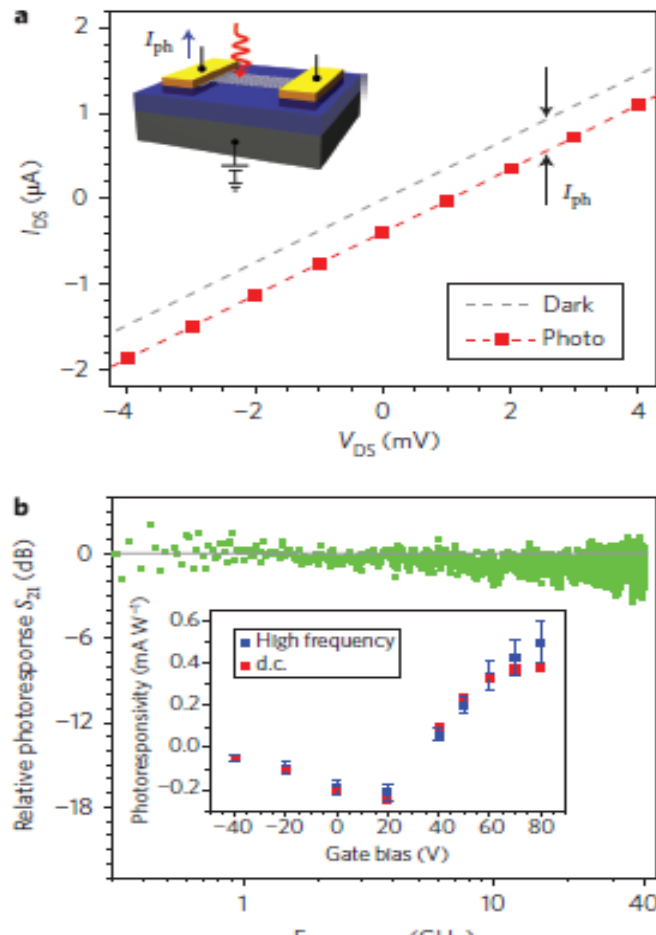


**Photo responsivity  $> 1 A/W$**

- The photodetector consists of a pair of stacked graphene monolayers (top layer, gate; bottom layer, channel) separated by a thin tunnel barrier.
- Under optical illumination, photoexcited hot carriers generated in the top layer tunnel into the bottom layer, leading to a charge build-up on the gate and a strong photogating effect on the channel conductance.

C. Liu, Z. Zhong, et.al., Nature Nanotechnology, 9, 273, 2014

# Example 6: Ultrafast graphene photodetector



- When light is incident in the high E-field region at graphene/metal contact, electron–hole pairs are generated and separated.
- The photoresponse does not degrade for optical intensity modulations up to 40 GHz.

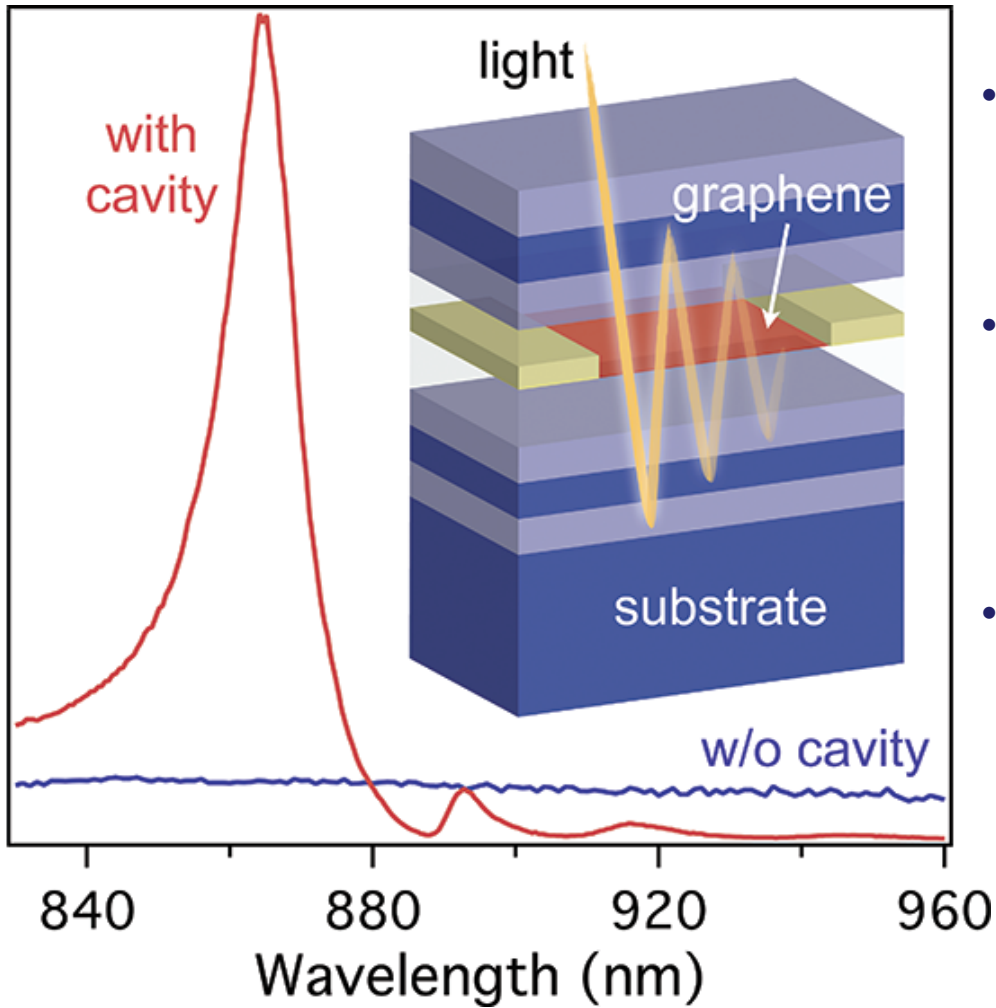
F. Xia, Ph. Avouris, et. al., Nature Nanotechnology, 4, 839, 2009

# Outline

- Introduction of graphene
- Synthesis of graphene
- Current transport and electronic devices
- Optical properties and photonic devices
  - Optical absorption
  - Photodetector
    - Background and motivation
    - Measurement setup
    - Photocurrent Mechanism
  - Enhancement of photocurrent
    - Optical modulator
    - Plasmonic device
- Bandgap engineering in graphene

# Graphene Photodetector with Microcavity

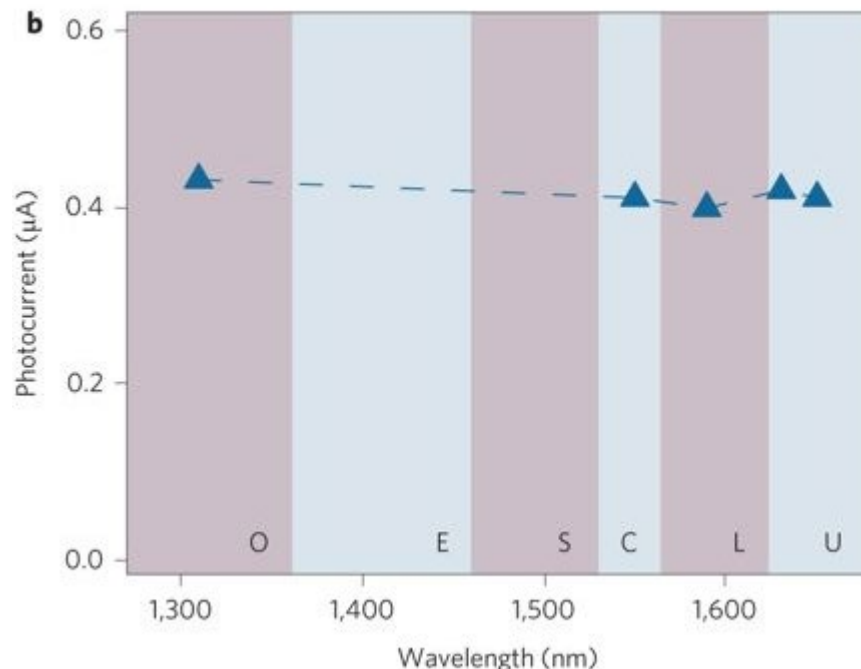
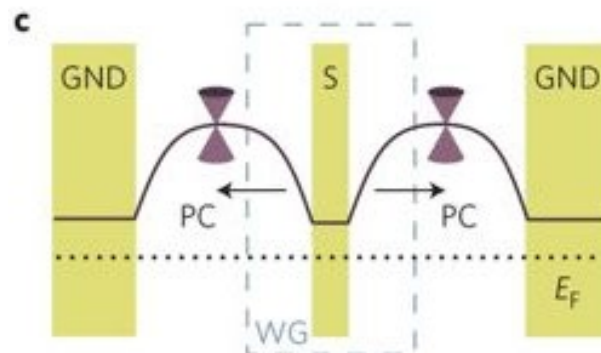
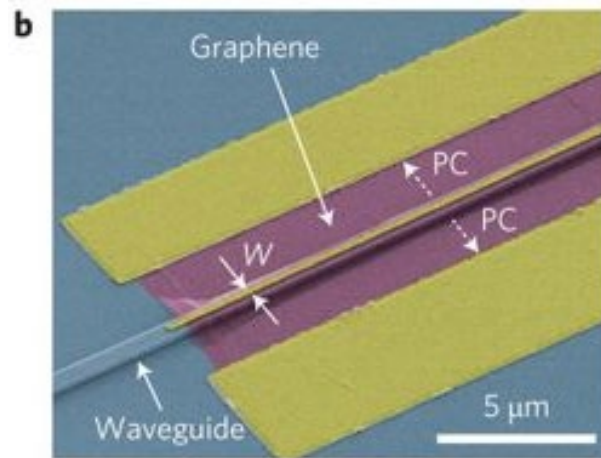
Photocurrent



- One approach to enhance absorption is based on integration into an optical microcavity.
- By monolithically integrating graphene with a microcavity, the optical absorption is 26-fold enhanced, reaching values >60%.
- The graphene-based microcavity photodetector shows responsivity of 21 mA/W.

Marco Furchi, Thomas Mueller, Nano Lett. 12, 2773, 2012

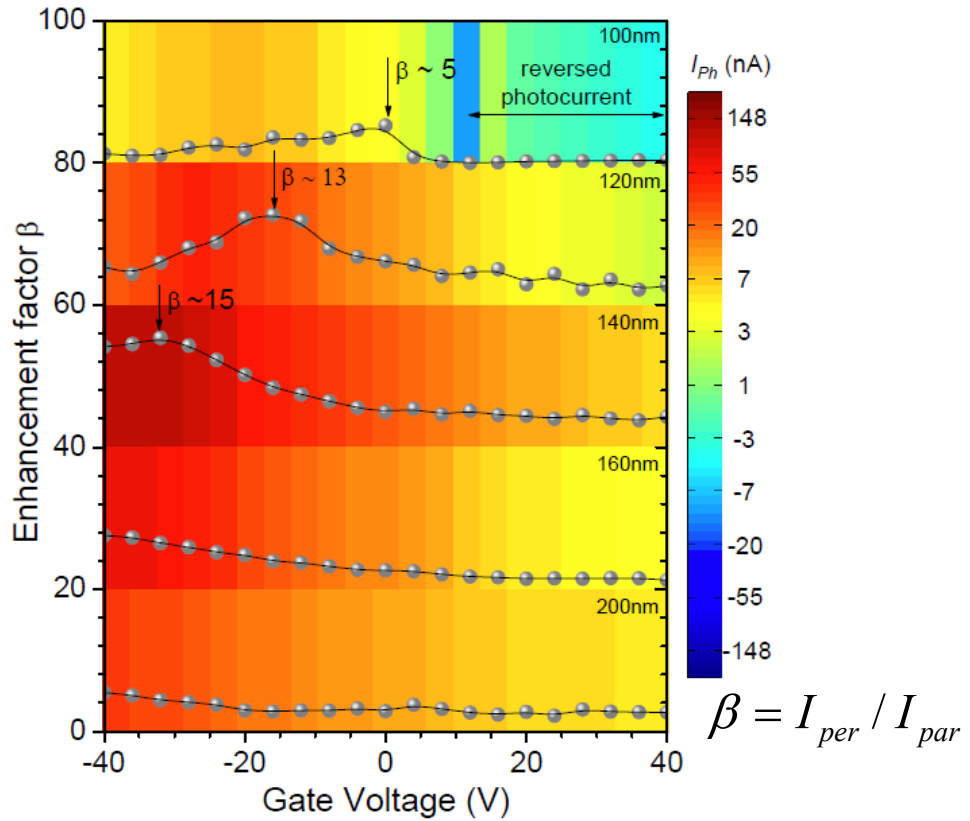
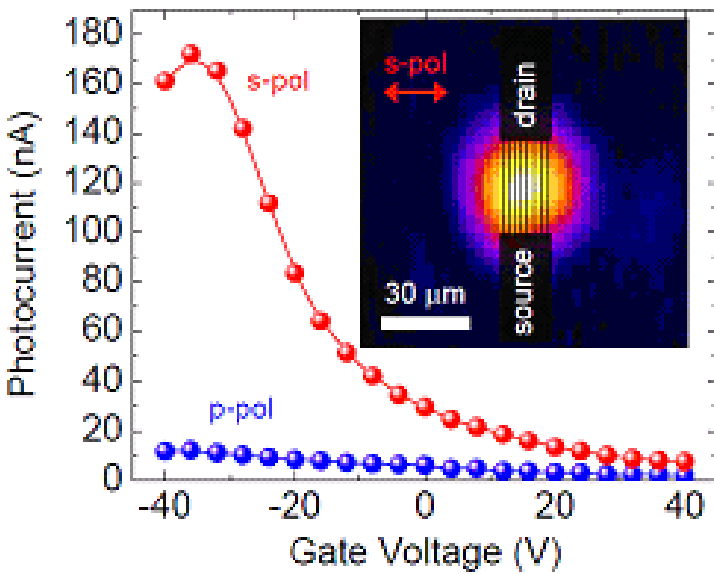
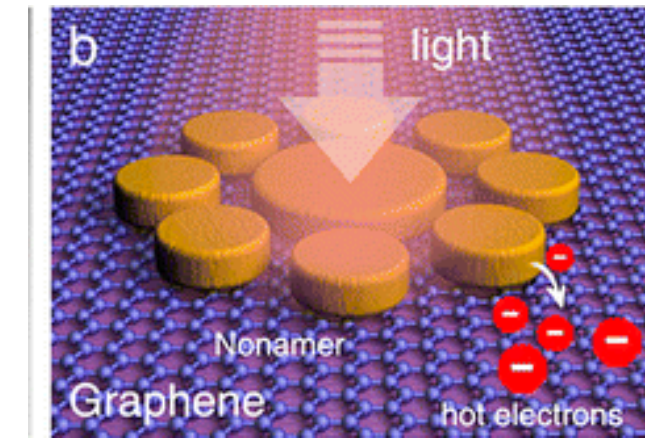
# Graphene Photodetector with Waveguide



- Another approach involves the coplanar integration of graphene with an optical waveguide.
- Optical mode in a silicon-on-insulator waveguide couples to a monolayer graphene deposited on top. An almost flat photoresponse across all-optical telecommunication windows (from O- to U-band) was demonstrated.

A. Pospischil, Nature Photonics, Vol. 7, p892, 2013

# Graphene photo-detectors with plasmonic structures



- A third method to increase the photoresponse involves the use of the field enhancement resulting from the excitation of surface plasmons.
- For a detector consisting of an array of 140 nm graphene nanoribbons, the enhancement is 1,500%

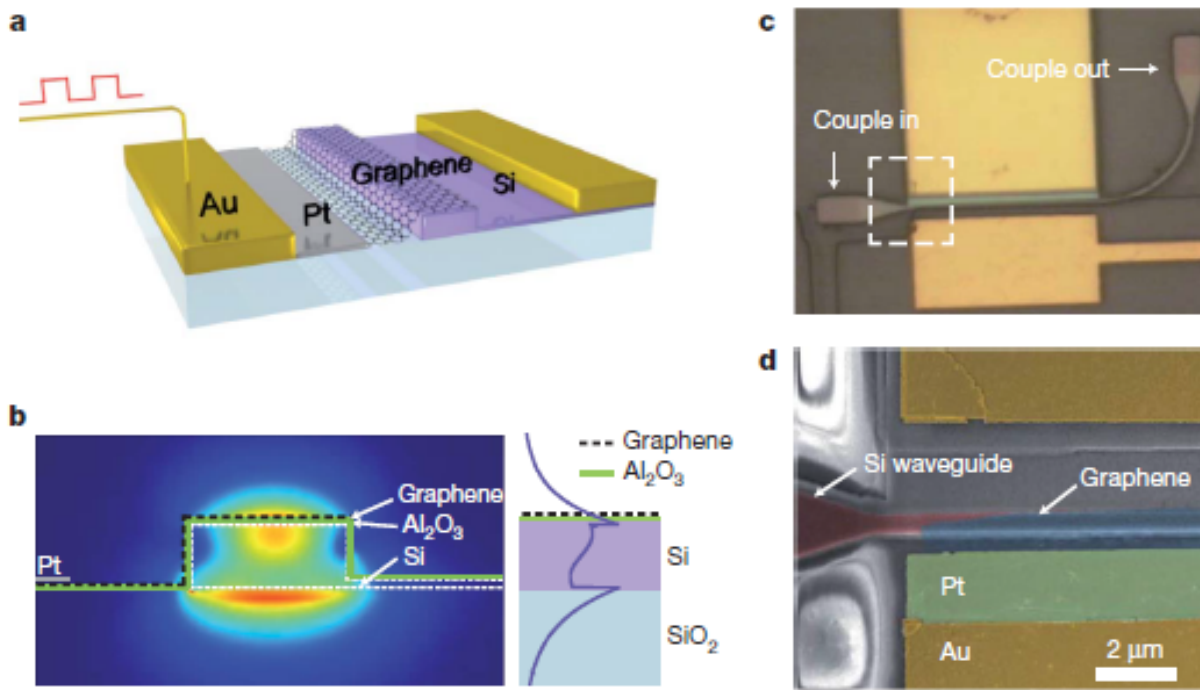
M. Freitag, T. Low, W. Zhu et al., Nature Communications. 2013  
Z. Fang, et al., ACS Nano, 6, 10222, 2012

# Outline

- Introduction of graphene
- Synthesis of graphene
- Current transport and electronic devices
- Optical properties and photonic devices
  - Optical absorption
  - Photodetector
  - Optical modulator
  - Plasmonic device
- Bandgap engineering in graphene



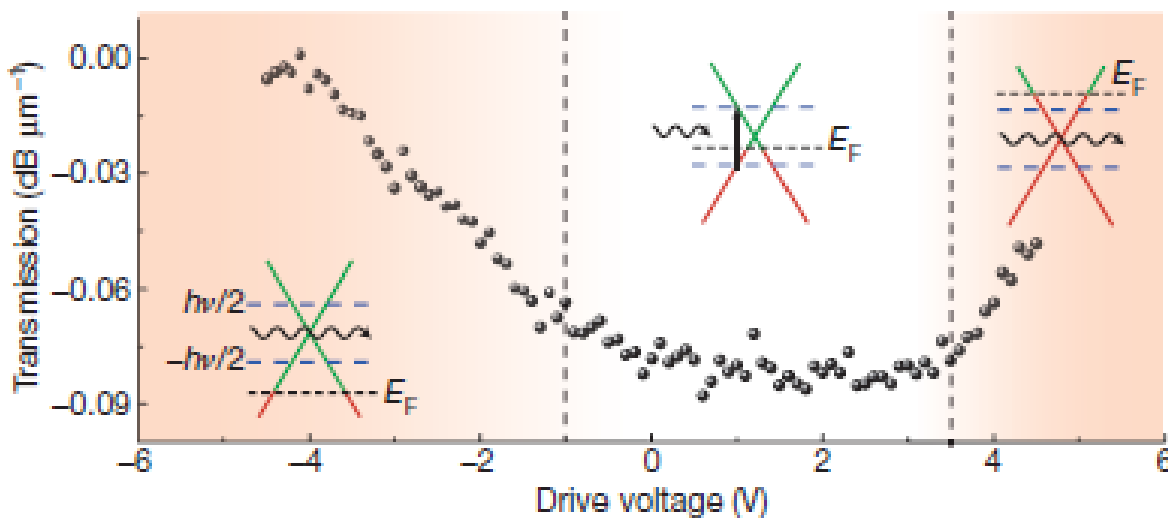
# Graphene optical modulator



- A broadband, high-speed, waveguide integrated modulator based on monolayer graphene was demonstrated.
- By electrically tuning the Fermi level of the graphene sheet, the guided light can be modulated at frequencies over 1GHz, together with a broad operation spectrum that ranges from 1.35 to 1.6 mm under ambient conditions.

Ming Liu, Xiang Zhang, et.al., 474, 64, 2011

# Principle of graphene optical modulator



$$\text{Transmission} = 10 \log_{10} \frac{W_t}{W_i}$$

$W_i$  is the power of incoming wave  
 $W_t$  is the power of transmitted wave

- At low drive voltage, the Fermi level of graphene is close to the Dirac point, and interband transitions occur when electrons are excited by the incoming photons.
- At large negative drive voltage, the Fermi level is lowered below the transition threshold owing to positive charge accumulation. As a result, there are no electrons available for interband transitions, and hence the graphene appears transparent.
- By applying a drive voltage between the graphene and the waveguide, we can tune the Fermi level of the graphene, and therefore modulate the total transmission.

Ming Liu, Xiang Zhang, et.al., 474, 64, 2011

# Outline

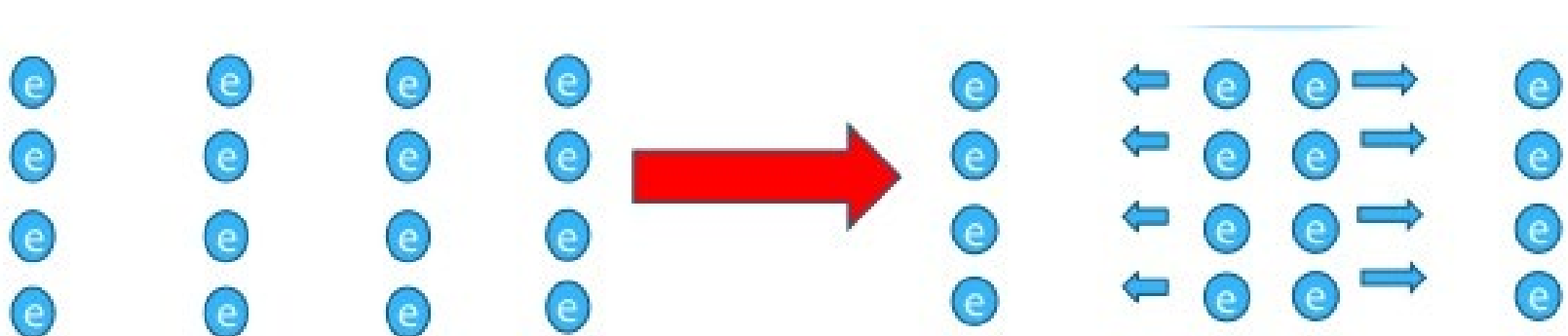
- Introduction of graphene
- Synthesis of graphene
- Current transport and electronic devices
- Optical properties and photonic devices
  - Optical absorption
  - Photodetector
  - Optical modulator
  - Plasmonic device
- Bandgap engineering in graphene

# Definition of plasma and plasmon

**Plasma:** is a medium with equal concentration of positive and negative charges of which at least one charge type is mobile.

**A plasma oscillation in a metal is a collective longitudinal excitation of the conductive electron gas.**

**Plasmon:** is a quantum of a plasma oscillation.



# Plasma phenomena

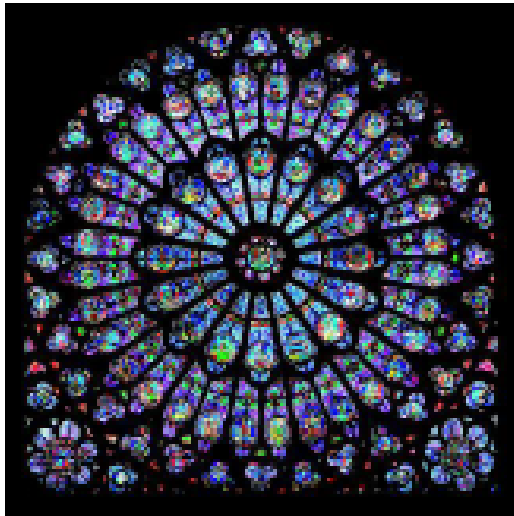
Thunder



Plasma etcher



Stained glass window



Gold nanoparticles



# Plasmon frequency in metal

The dipole moment density  $D = \epsilon_0 E + P = \epsilon \epsilon_0 E$

The motion of a free electron in a electric field:  $m \frac{d^2 x}{dt^2} = -eE$

$$\rightarrow \epsilon = 1 - \frac{ne^2}{\epsilon_0 m \omega^2}$$

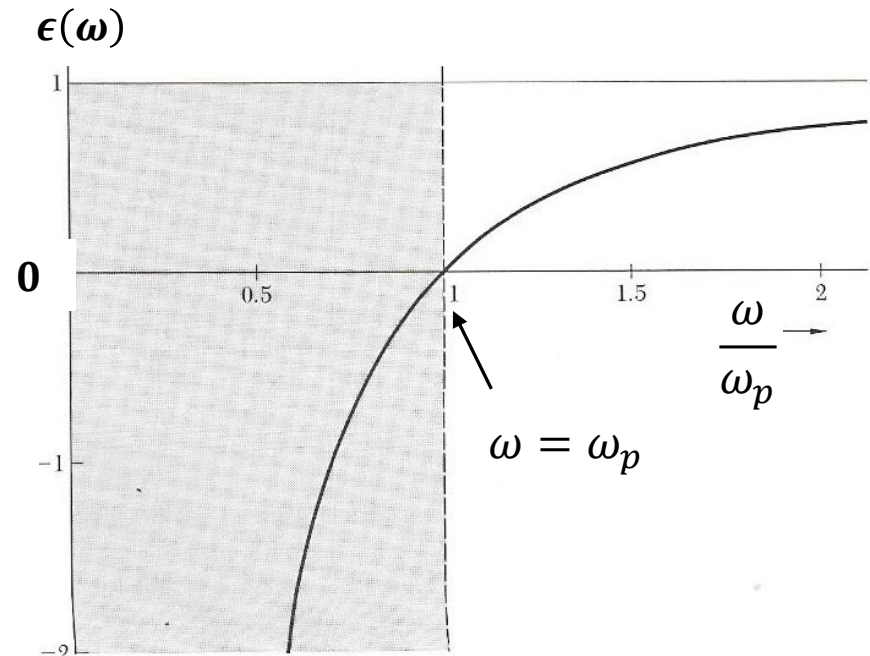
When  $\epsilon = 0$ , the frequency corresponds to plasma frequency

$$\omega_p \equiv \frac{ne^2}{\epsilon_0 m}$$

$$\rightarrow \epsilon(\omega) = 1 - \frac{\omega_p^2}{\omega^2}$$

The dispersion relation is:

$$\omega = \sqrt{\omega_p^2 + c^2 K^2}$$



# Plasmonic effect in graphene

- The plasmon resonant frequency in graphene nanodisk is

$$\omega_p = \sqrt{\frac{3D}{8\epsilon_m\epsilon_0 d}}$$

where D is Drude weight,  $\epsilon_m$  is the media dielectric constant,  $\epsilon_0$  is the vacuum permittivity and d is the diameter of the graphene disks.  $D = (v_F e^2 / \hbar)(\pi |n|)^{1/2}$

- The plasmon dispersion can be written as:

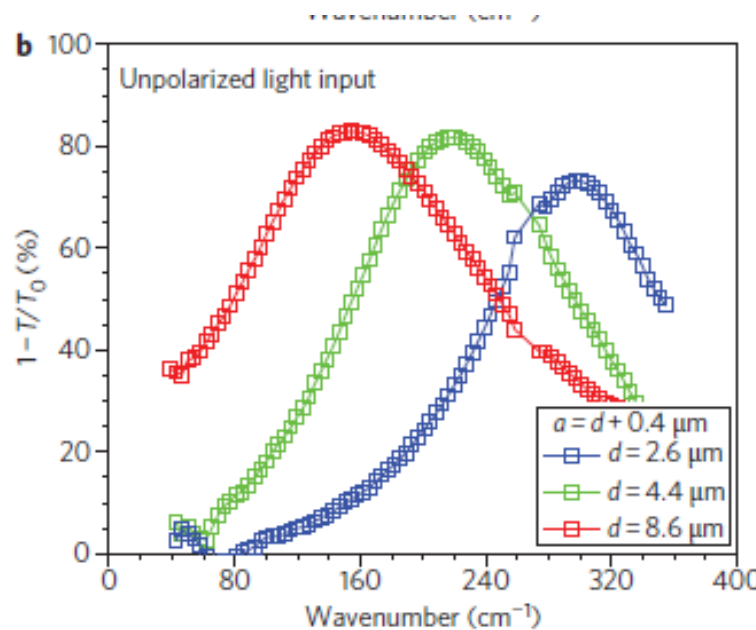
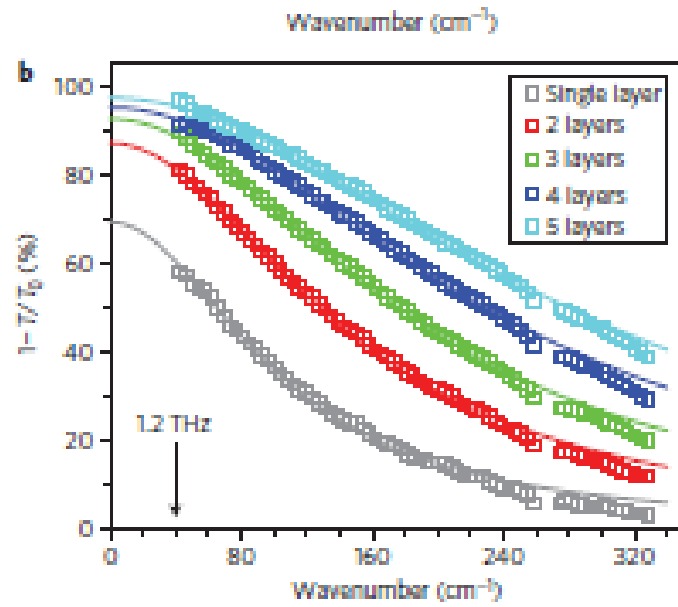
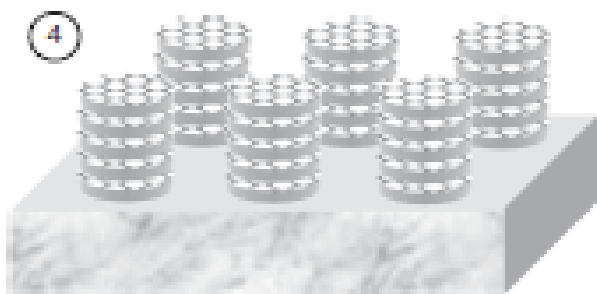
$$\omega_{pl} = \sqrt{\frac{e^2 E_F q}{2\pi\hbar^2 \epsilon_0 \epsilon_r}}$$

Where q is the wave vector,  $\epsilon_r$  is the average dielectric constant of its surrounding medium

H. Yan, F. Xia, et.al., Nature Nanotechnology, 7, 330, 2012

T. Low, ACS Nano, 8, 1086, 2014

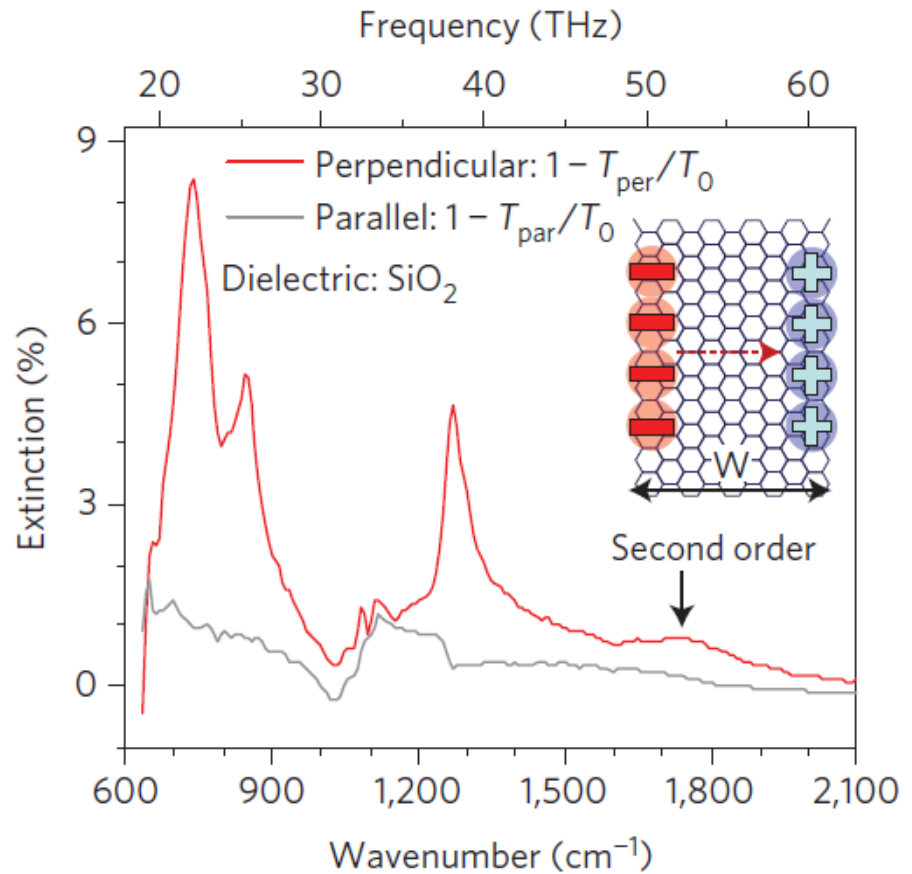
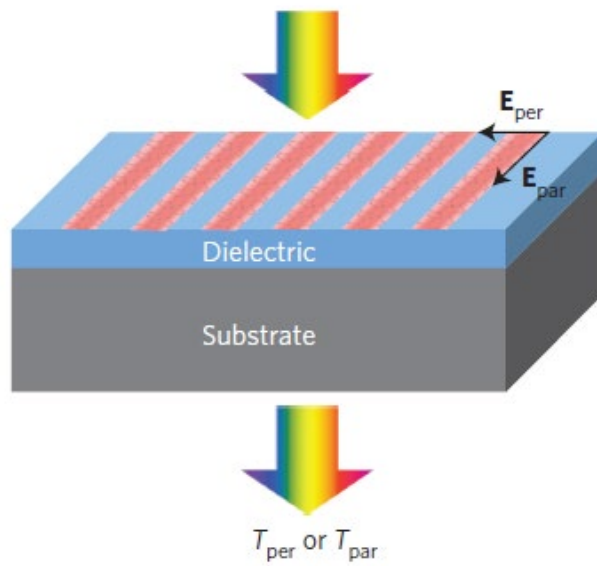
# Plasmonic devices using graphene nanodisks



- Using patterned graphene/insulator stacks, we demonstrate widely tunable far-infrared notch filters with 8.2 dB rejection ratios and terahertz linear polarizers with 9.5 dB extinction ratios.
- An unpatterned stack consisting of five graphene layers shields 97.5% of electromagnetic radiation at frequencies below 1.2 THz.

H. Yan, F. Xia, et.al., Nature Nanotechnology, 7, 330, 2012

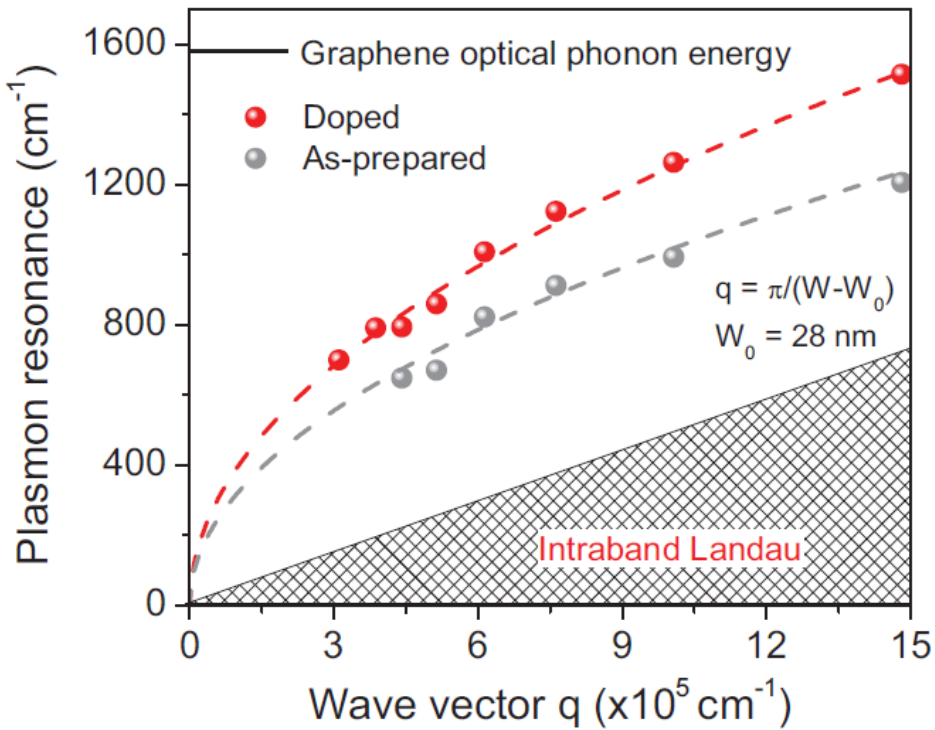
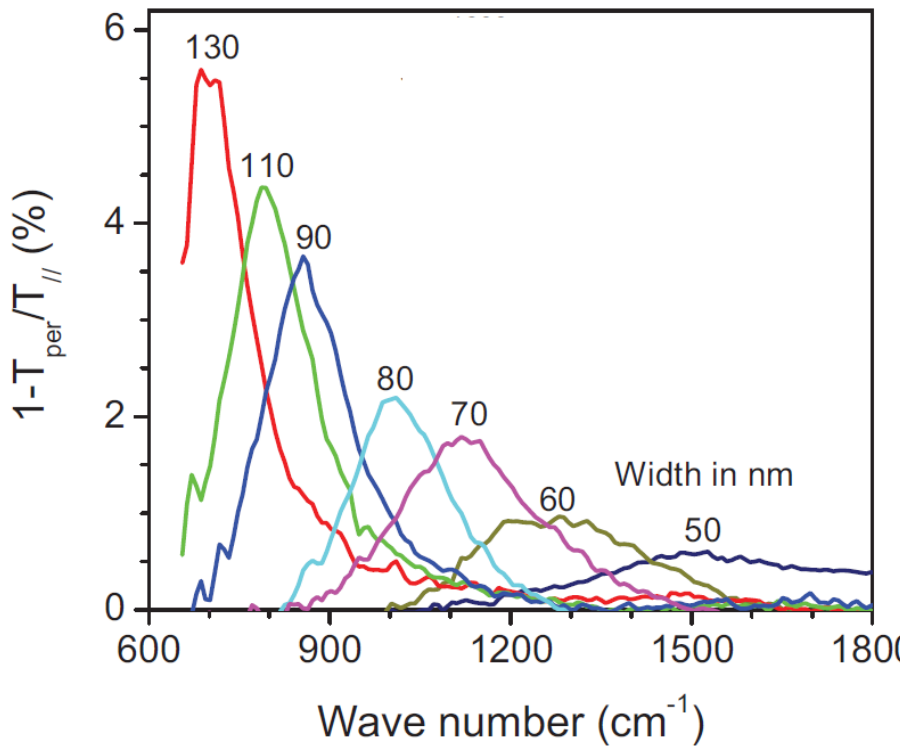
# Graphene nano-ribbons



- The extinction spectrum with perpendicular polarization shows prominent resonance peak, due to excitation of localized plasmons, while the spectrum with parallel polarization has no resonance peaks due to a lack of plasmon excitation.

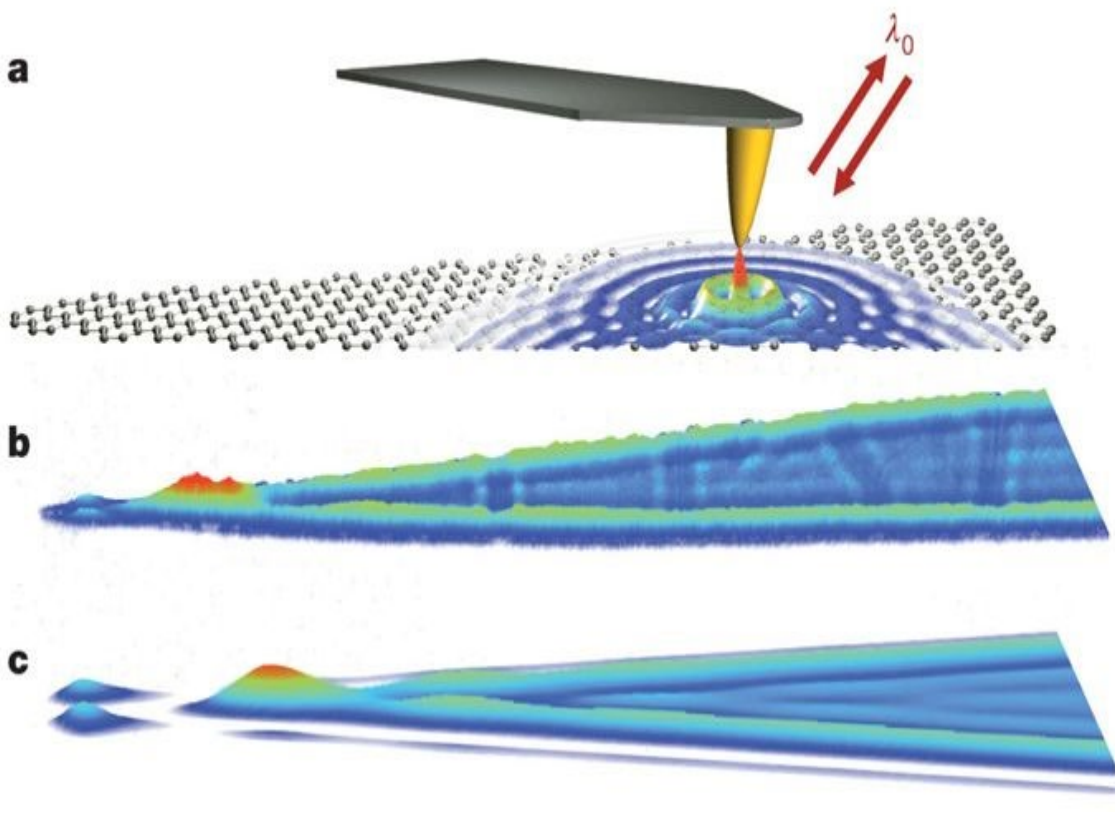
H. Yan, T. Low, W. Zhu, Nature Photonics, 2013

# Graphene nano-ribbons on diamond-like-carbon



- Plasmon resonance frequency follow  $q^{1/2}$  dispersion, where  $q = \pi / W_e$  and  $W_e$  is the effective ribbon width.

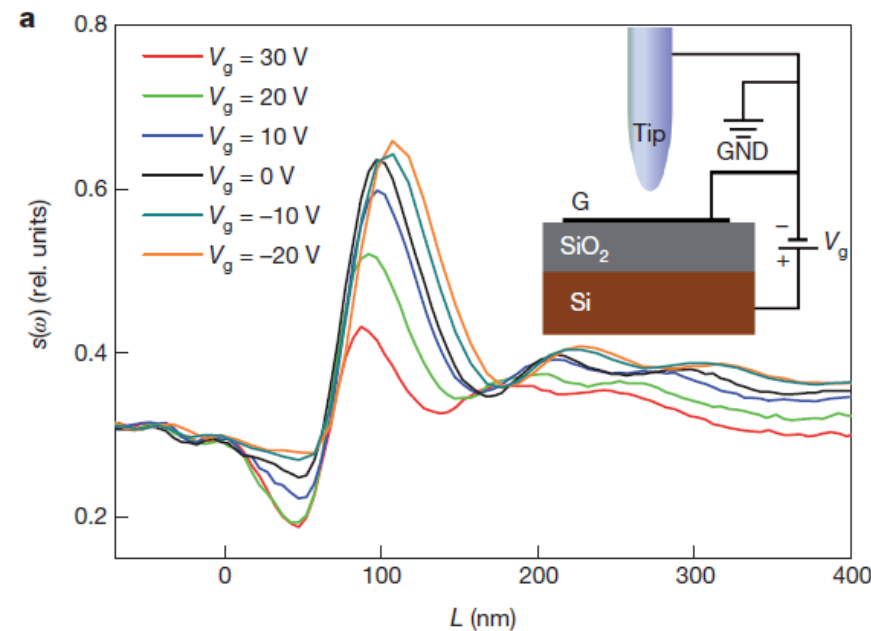
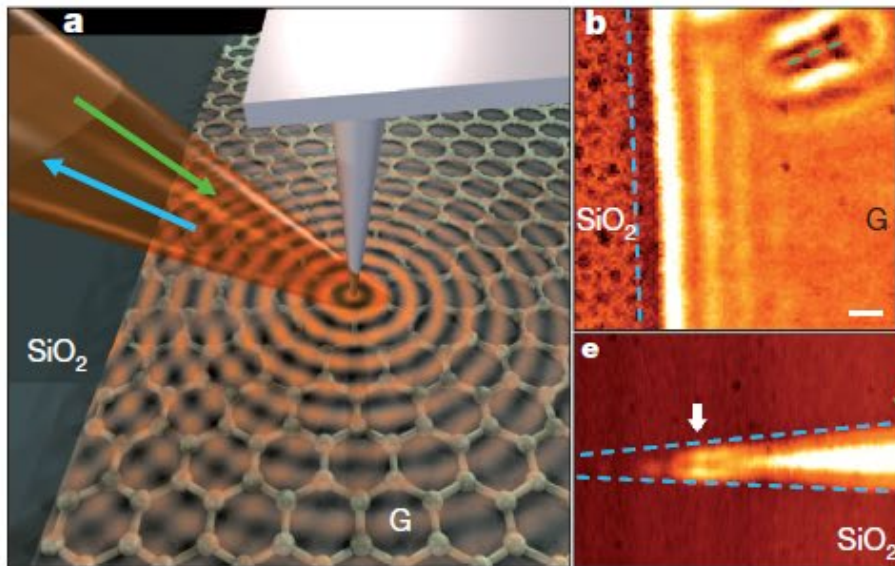
# Nano-imaging of graphene plasmons



- The authors launched and detected propagating optical plasmons in tapered graphene nanostructures using near-field scattering microscopy with infrared excitation light.
- The extracted plasmon wavelength is very short—more than 40 times smaller than the wavelength of illumination
- Graphene nanostructure serves as a tunable resonant plasmonic cavity.

J. Chen, F. Koppens, et.al., Nature, 487, 77, 2012

# Gate-tuning of graphene plasmons revealed by infrared nano-imaging

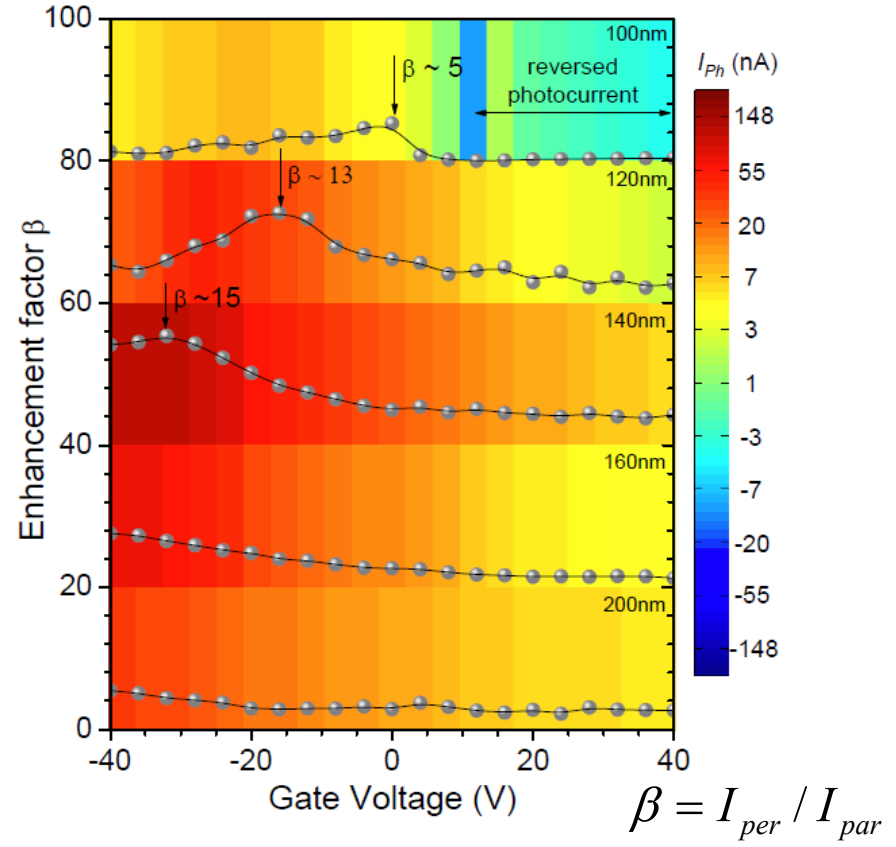
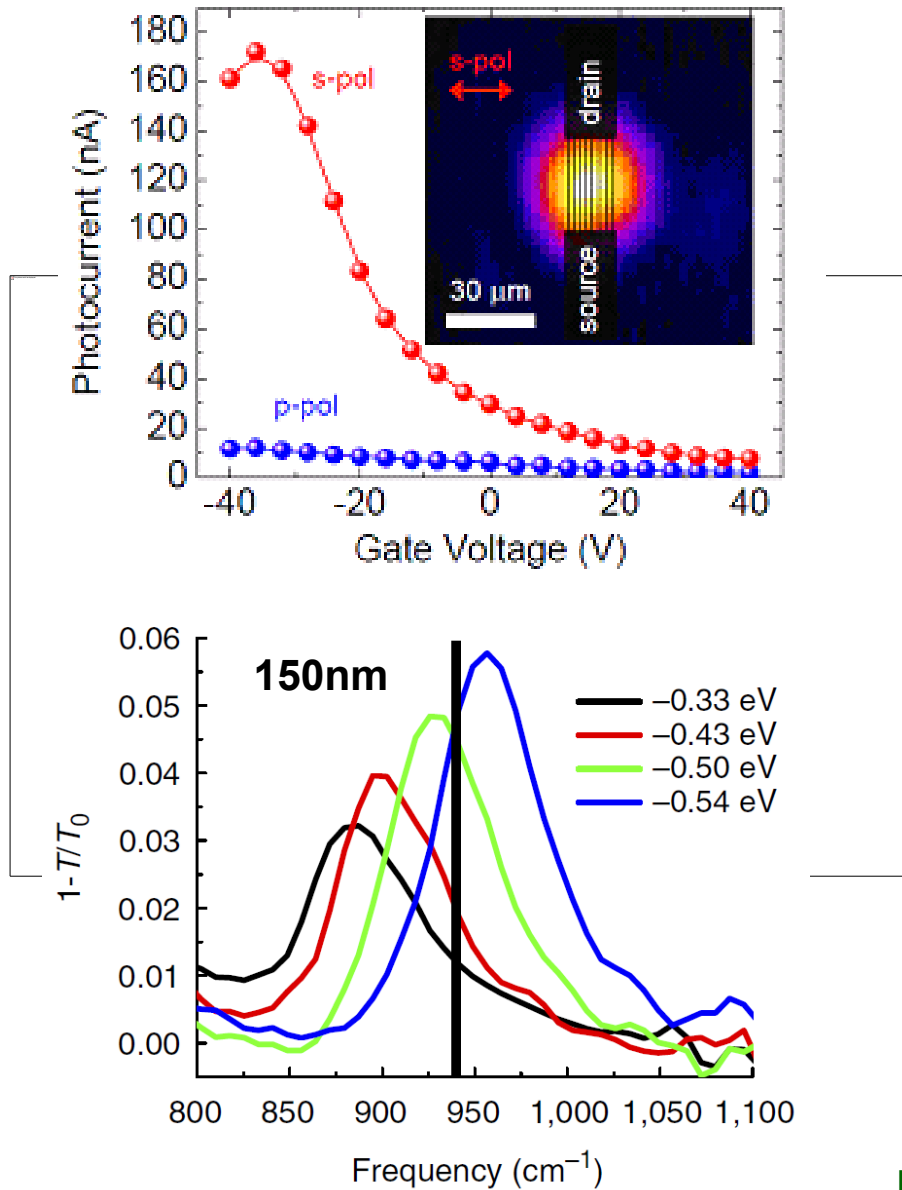


- Using plasmon interferometry, we investigated losses in graphene by exploring real-space profiles of plasmon standing waves formed between the tip of our nano-probe and the edges of the samples.
- The amplitude and the wavelength of these plasmons was altered by varying the gate voltage

$$\lambda_p \propto |n|^{1/2}$$

Z. Fei, D. Basov, et.al., Nature, 487, 82, 2012

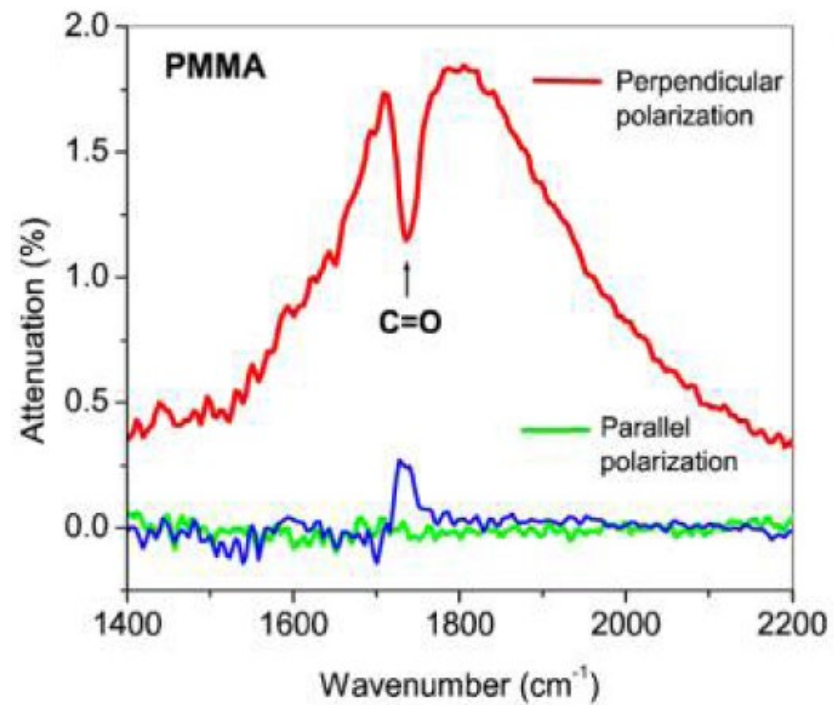
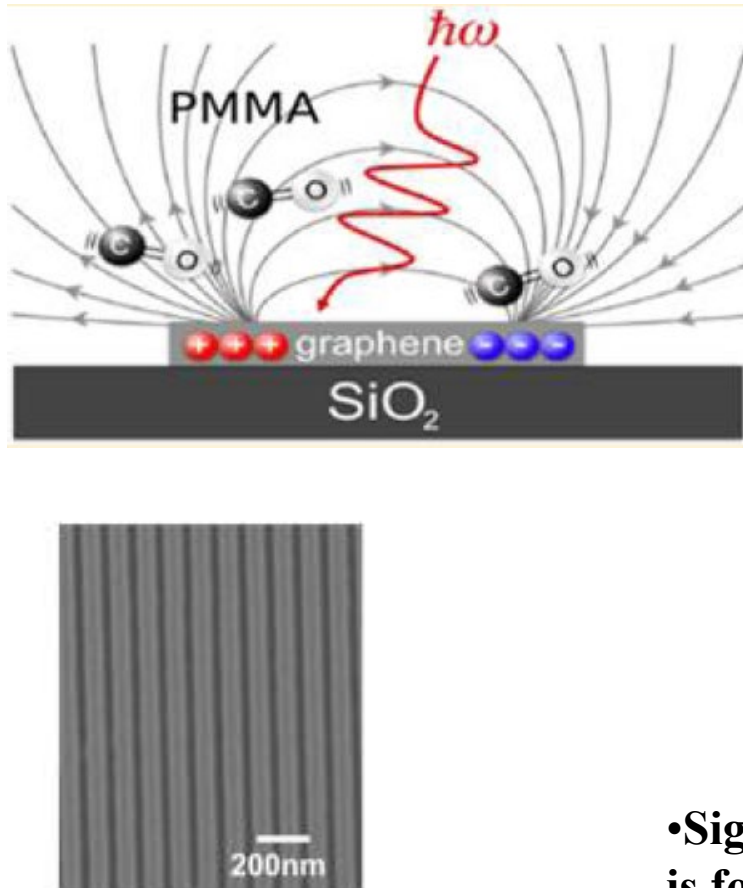
# Graphene plasmonic photo-detectors



• Photocurrent enhancement factors reach a maximum near the gate voltages where the plasmon-phonon resonances coincide with the laser excitation frequency. The enhancement factor can reach as high as 15.

M. Freitag, T. Low, W. Zhu et.al. Nature Commu. 2013

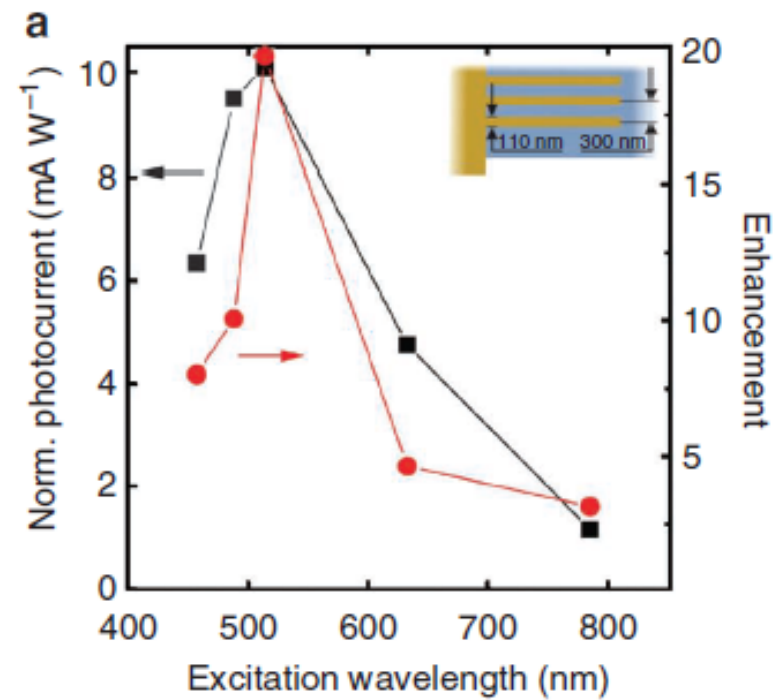
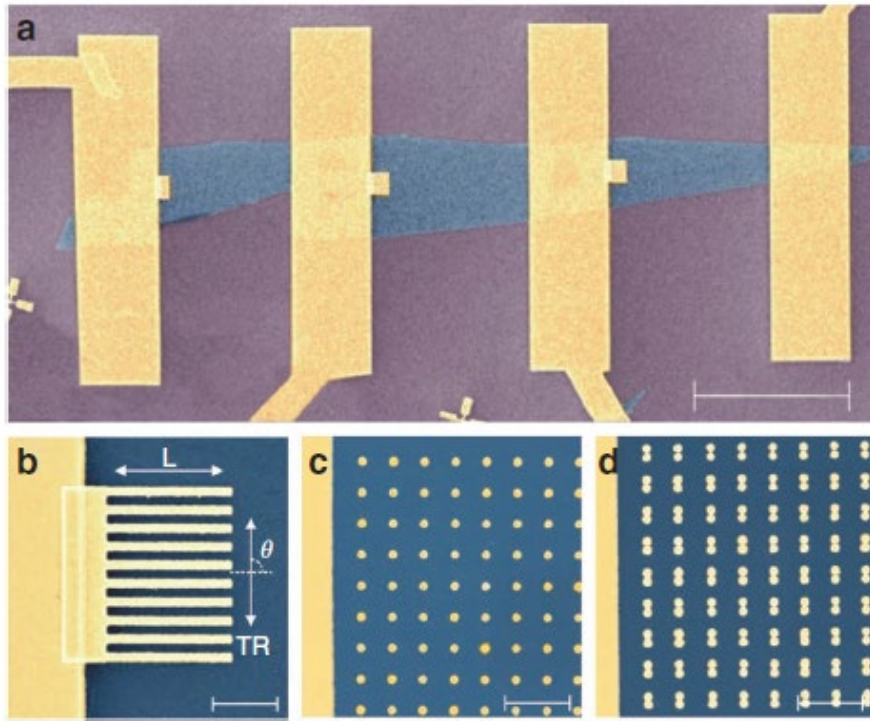
# Graphene plasmon enhanced vibrational sensing of surface-adsorbed layers



- Signal depth of the plasmon-induced transparency is found to be 5 times larger than that of light attenuated by the carbonyl vibration alone

Y. Li, H. Yan, D. Farmer, W.Zhu et al, Nano Letters, 2014

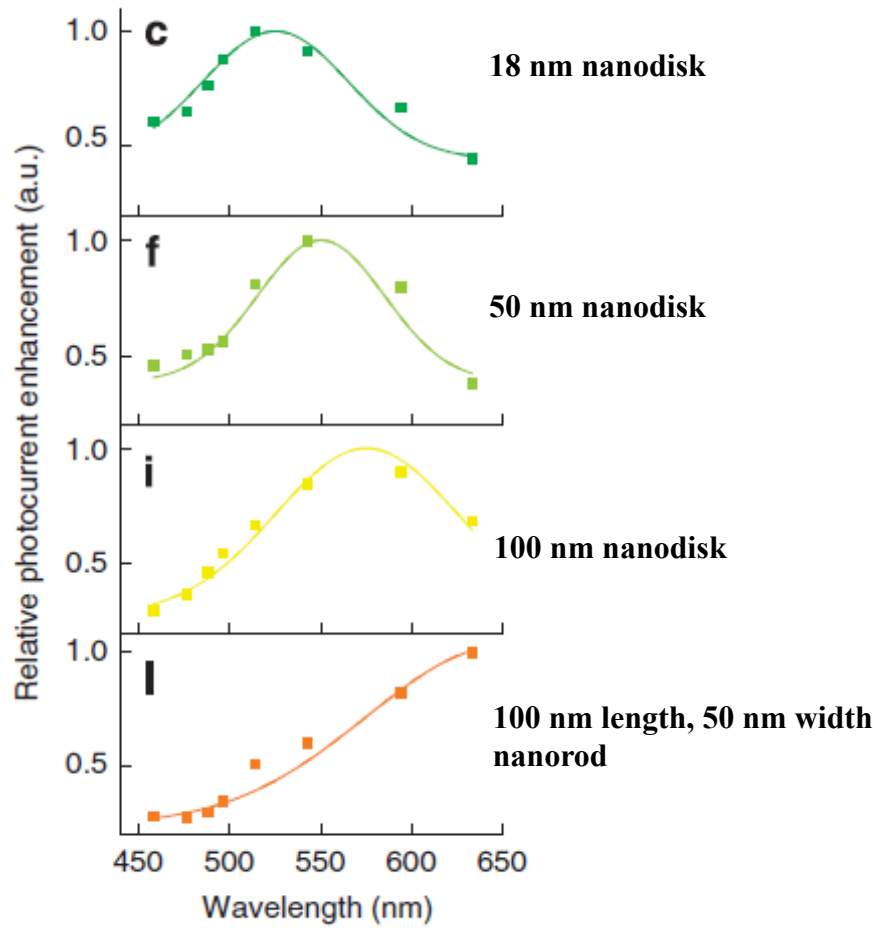
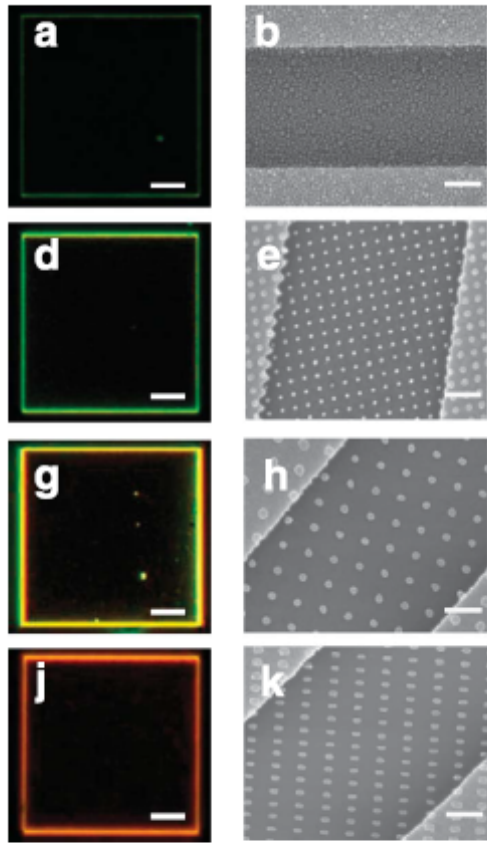
# Plasmonic enhancement of photovoltage in graphene



By combining graphene with plasmonic nanostructures, the efficiency of graphene-based photodetectors can be increased by up to 20 times.

T. Echtermeyer, K. Novoselov, et.al., Nature Communications, article 1464, 2011

# Plasmon resonance enhanced multicolour photodetection



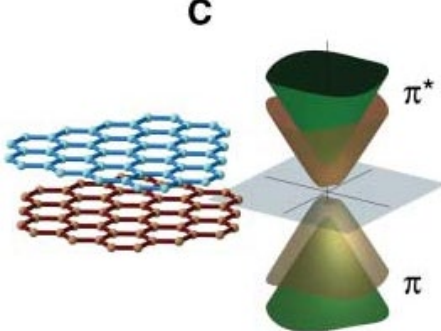
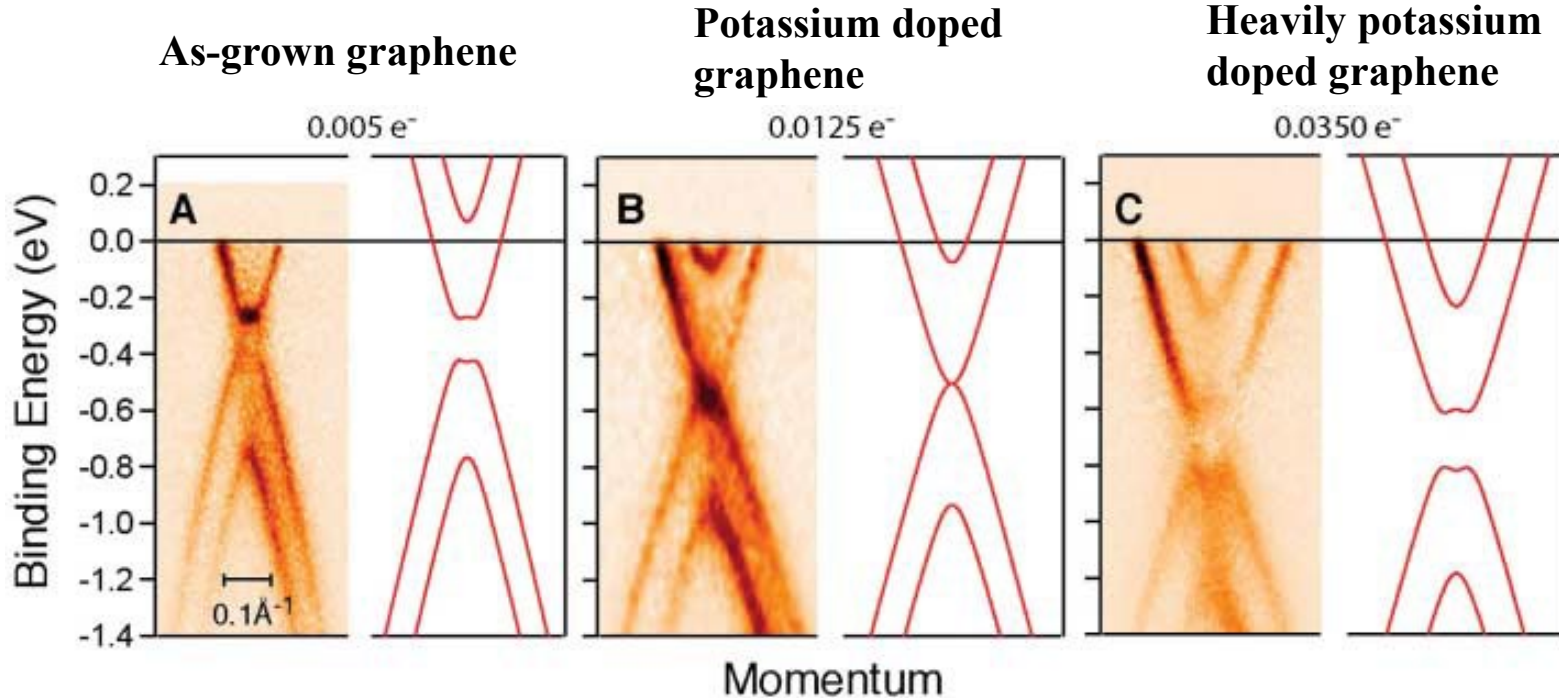
- Plasmonic nanostructures of variable resonance frequencies selectively amplify the photoresponse of graphene to light of different wavelengths, enabling highly specific detection of multicolours

Yuan Liu, Nature Communications volume 2, 579 (2011)

# Outline

- Introduction of graphene
- Synthesis of graphene
- Current transport and electronic devices
- Optical properties and photonic devices
- Bandgap engineering in graphene
  - **Band opening in bilayer graphene**
  - **Band opening in graphene nanoribbon (GNR)**

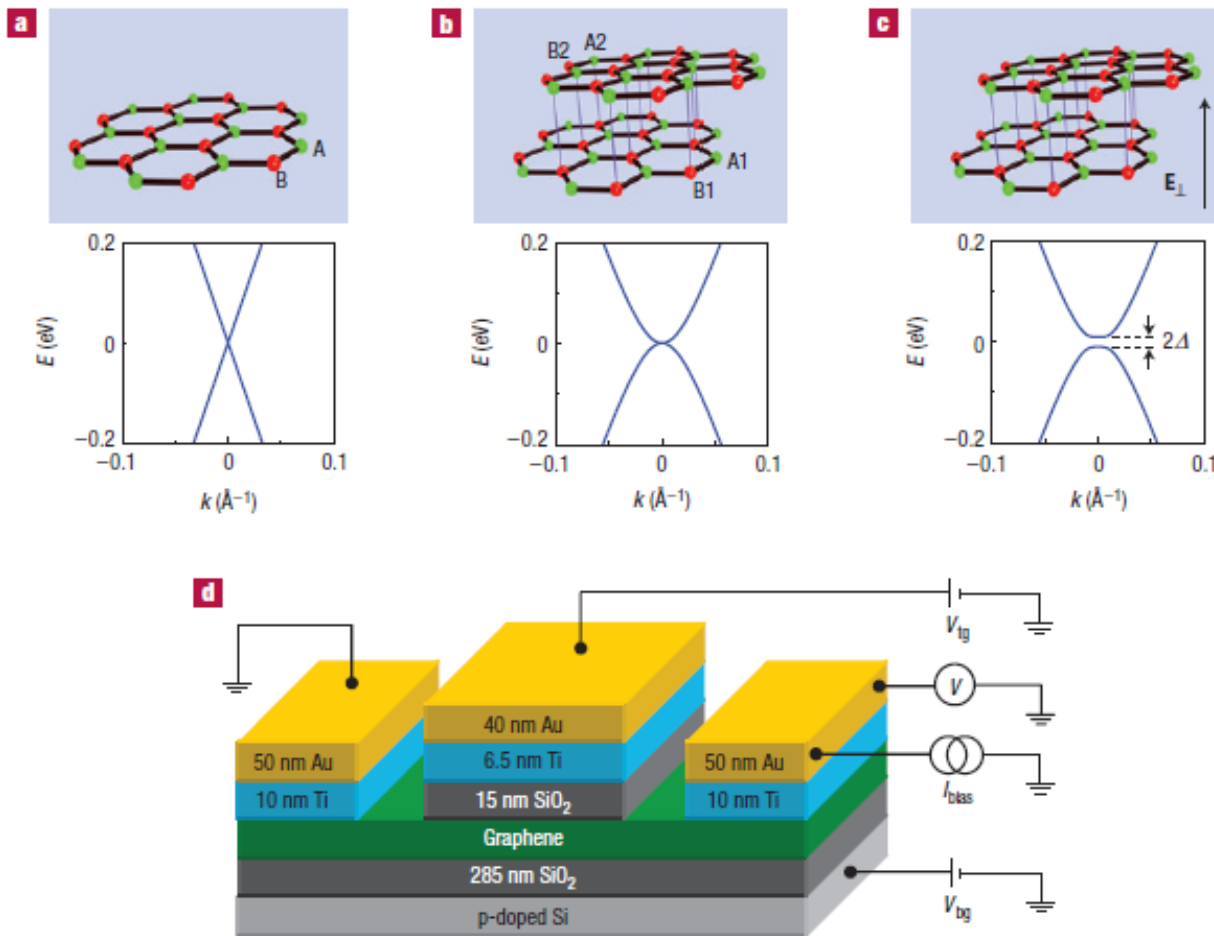
# Band gap opening of bilayer graphene



- The symmetry of the bilayers is broken by the dipole field created between the depletion layer of the SiC and the accumulation of charge on the graphene layer next to the interface, rendering a band gap opening in the as-prepared films.
- Further n-type doping by the deposition of potassium atoms onto the vacuum side forms another dipole. By selectively adjusting the carrier concentration in each layer, the band gap opening can be adjusted.

T. Ohta, E. Rotenberg, et.al, Science 2006, 951

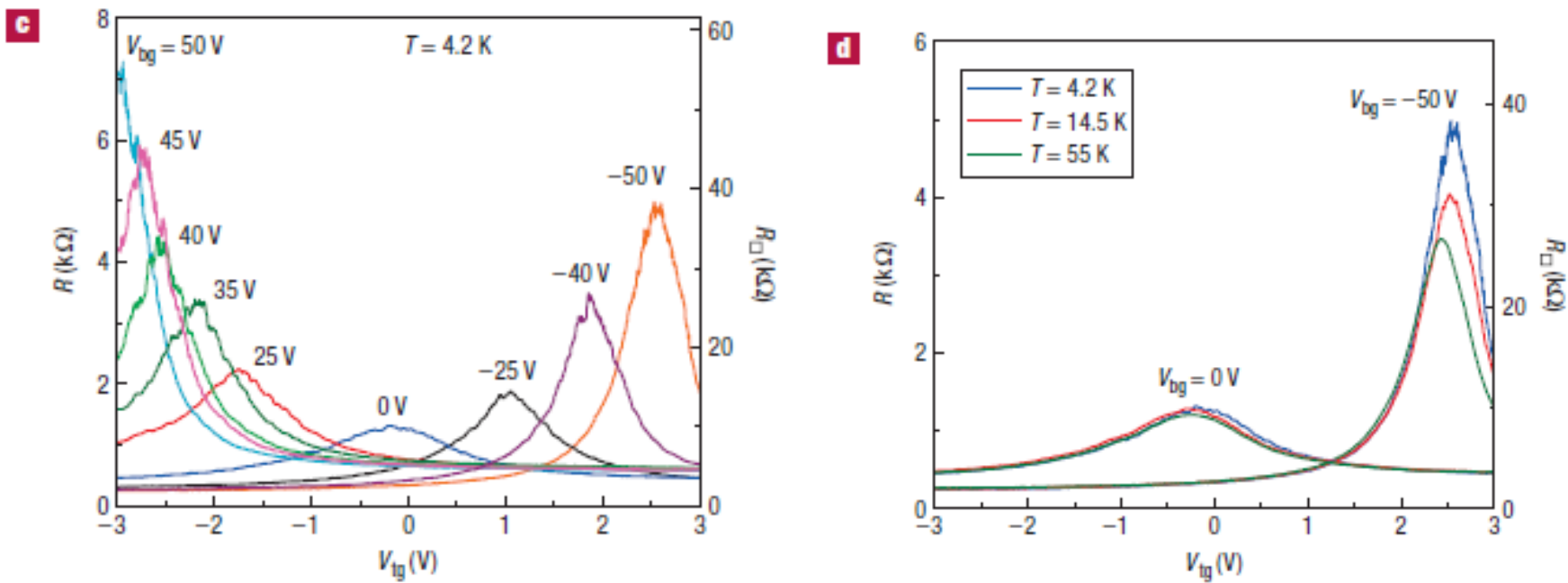
# Band gap opening in bilayer graphene



By using a double-gate device configuration, an electric field can be applied perpendicular to the bilayer graphene plane.

J. Oostinga, L. Vandersypen, et.al., Nature Materials, 7, 152, 2008

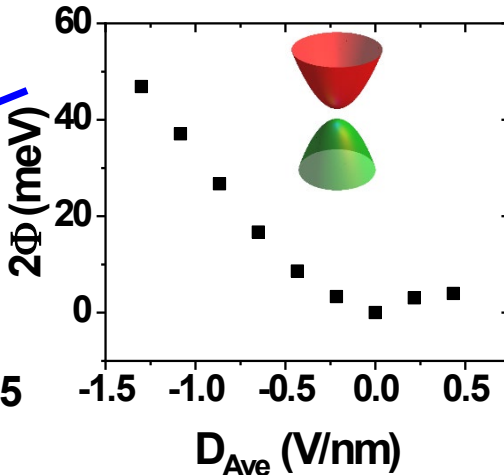
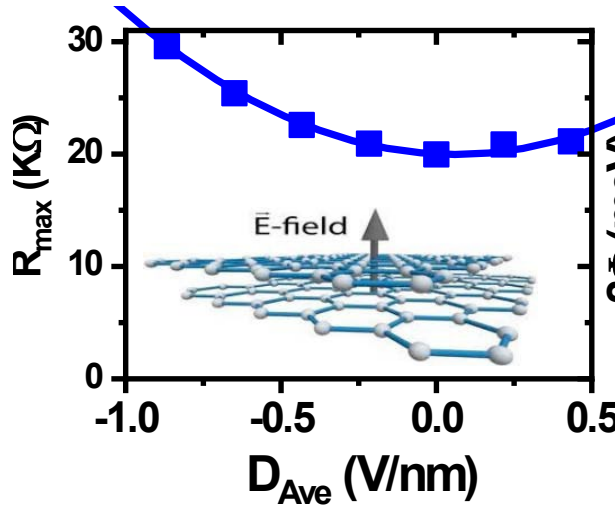
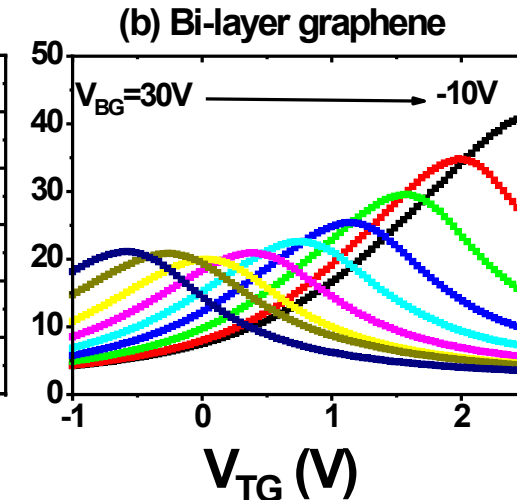
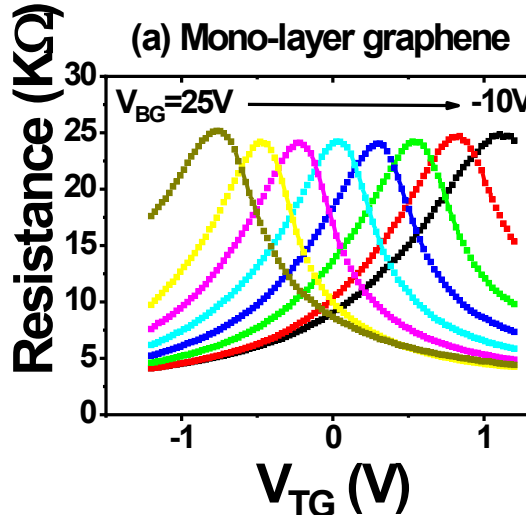
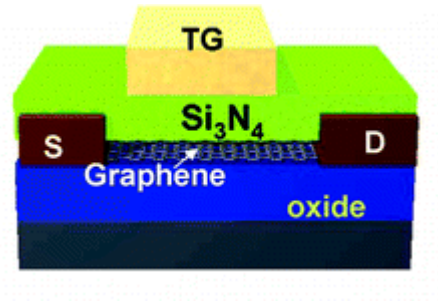
# Band gap opening in bilayer graphene



- The dependence of the resistance on temperature and electric field, strongly suggest that the gate-induced insulating state originates from the opening of a bandgap between valence and conduction bands.

J. Oostinga, L. Vandersypen, et.al., Nature Materials, 7, 152, 2008

# Extract bandgap opening from resistance



Average displacement field:

$$D_{Ave} = \epsilon_b (V_{BG} - V_{BG}^0) / d_b$$

$$\frac{R_{Dirac}^0}{R_{Dirac}} = \frac{\ln(1 + e^{-\Phi/k_B T})}{\ln 2}$$

where  $\Phi$  is half of the bandgap

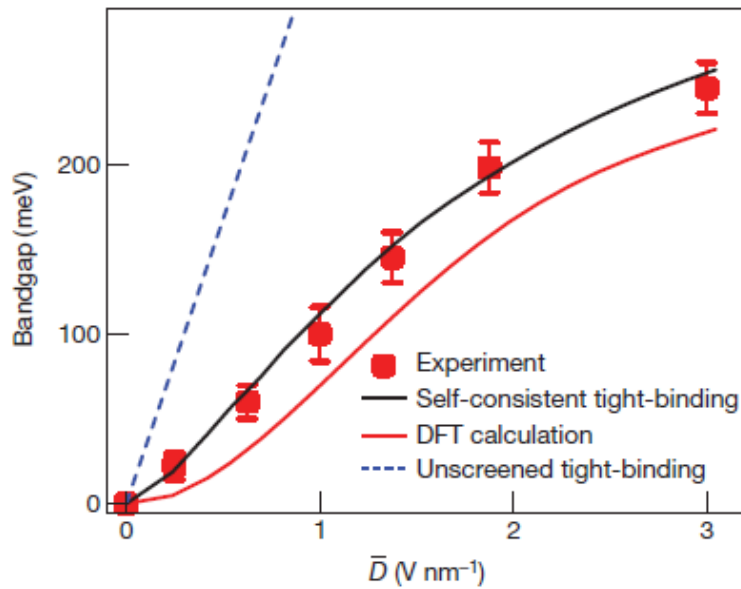
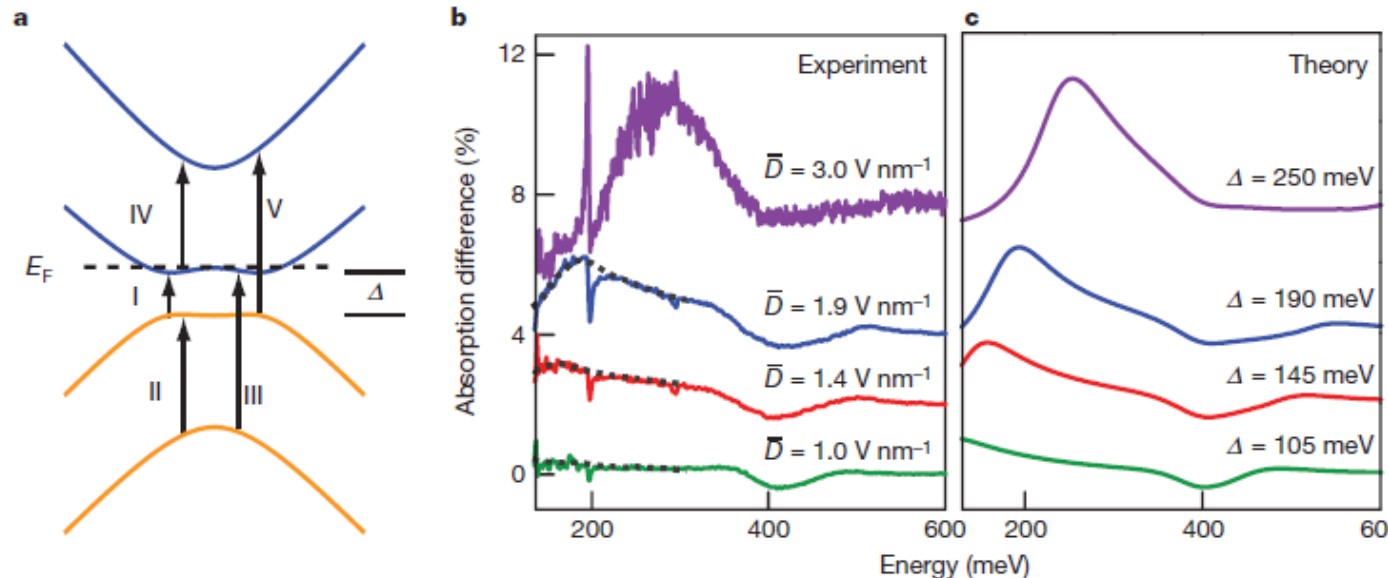
$R_{Dirac}^0$  is Dirac resistance when  $D_{Ave} = 0$

$R_{Dirac}$  is Dirac resistance when  $D_{Ave} \neq 0$

- The bandgap opening in bilayer graphene can be extracted from resistance ratio.

W. Zhu, et.al. Nano Letters, 2010

# Tunable bandgap in bilayer graphene



- Using a dual-gate bilayer graphene field-effect transistor (FET) and infrared microspectroscopy, the authors demonstrated a gate-controlled continuously tunable bandgap of up to 250 meV.

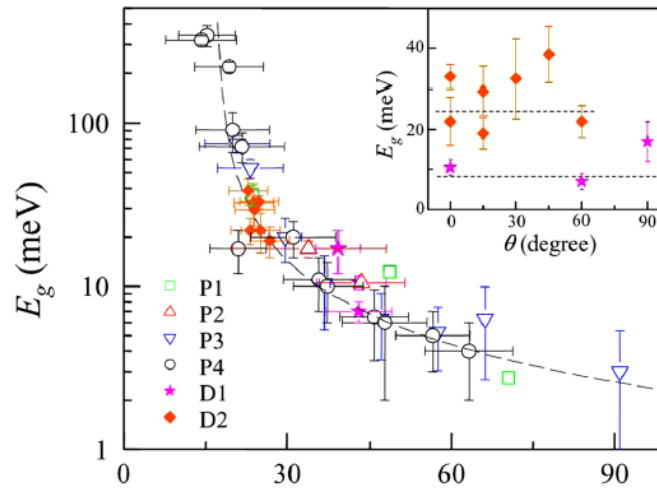
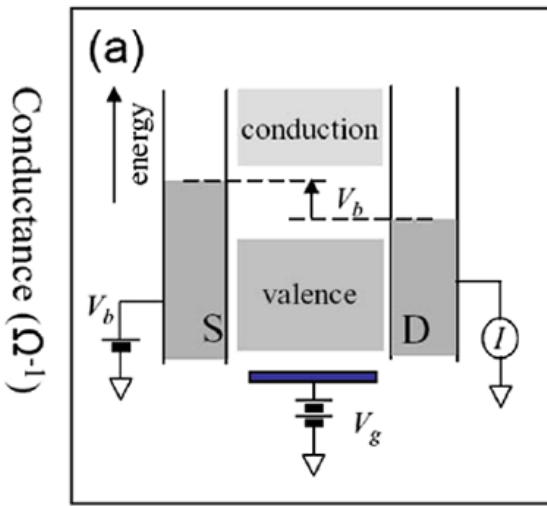
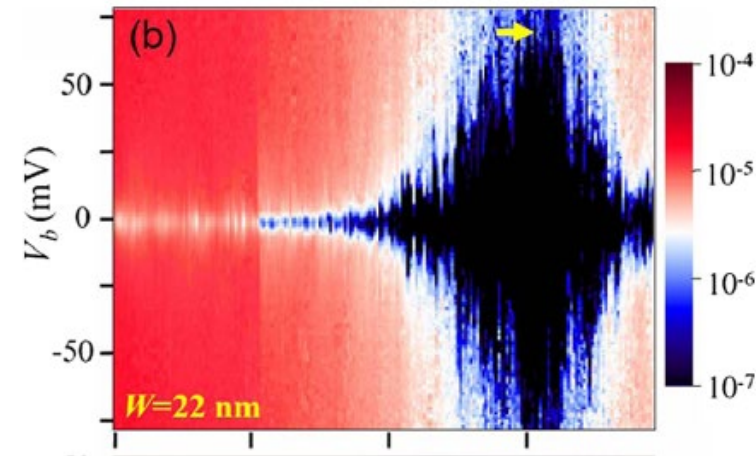
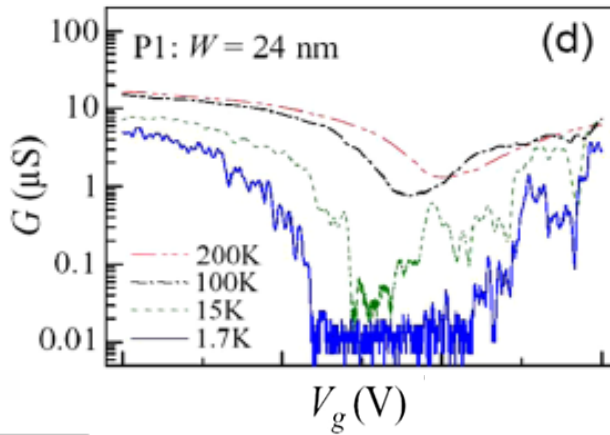
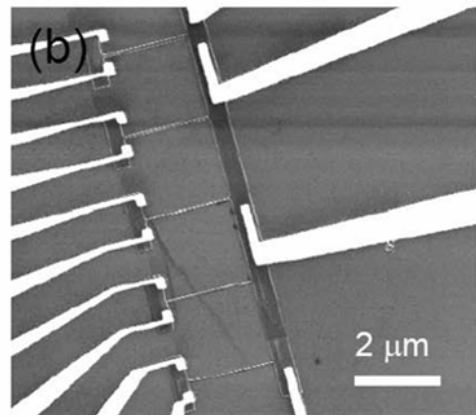
Displacement field:  $\bar{D} = (D_t + D_b)/2$   
Where  $D_b = \epsilon_b (V_b - V_b^0)/2$

Y. Zhang, F. Wang, et.al., Nature, 459, 820, 2009

# Outline

- Introduction of graphene
- Synthesis of graphene
- Current transport and electronic devices
- Optical properties and photonic devices
- Bandgap engineering in graphene
  - **Band opening in bilayer graphene**
  - **Band opening in graphene nanoribbon (GNR)**
    - GNR formed by lithography
    - GNR synthesized via a bottom-up approach
    - GNR grown on SiC steps
    - GNR formed by unzipping carbon nanotube
    - GNR formed by exfoliation

# Form GNR by photolithography

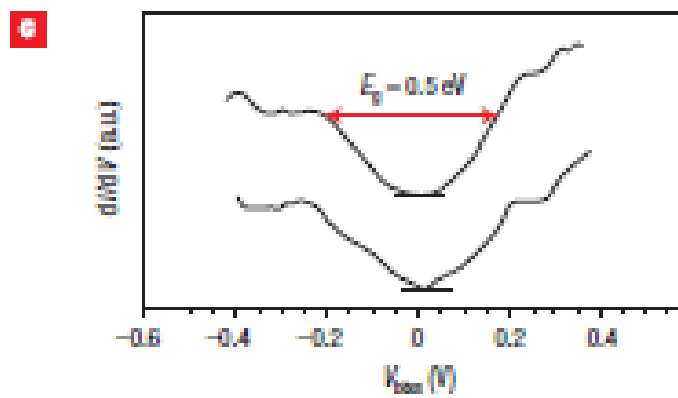
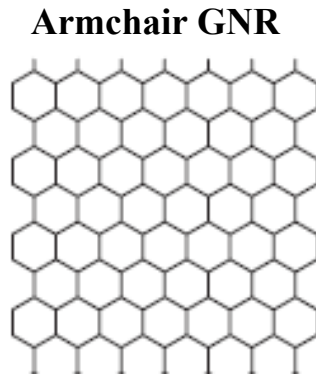
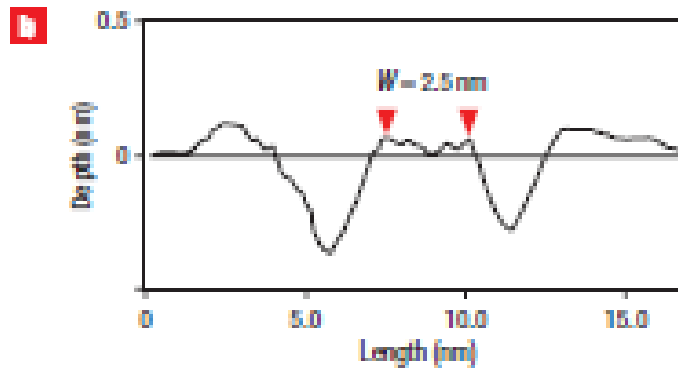
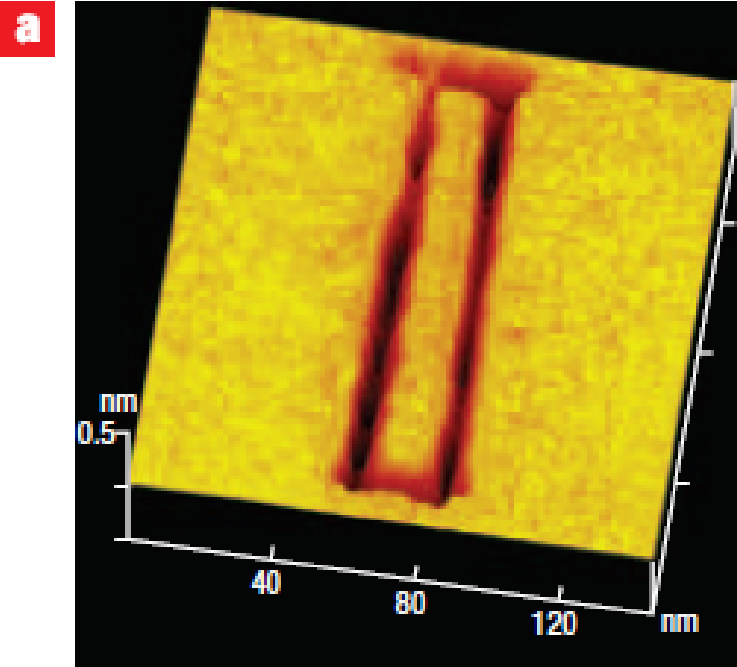


$$E_g = \alpha / (W - W^*)$$

- GNRs were made by photolithography and plasma etching. The sizes of these energy gaps were investigated by measuring the conductance in the nonlinear response regime at low temperatures. The energy gap of GNR scales inversely with the ribbon width.

Melinda Han, Philip Kim, et.al. Physical Review Letters, 98, 206805, 2007

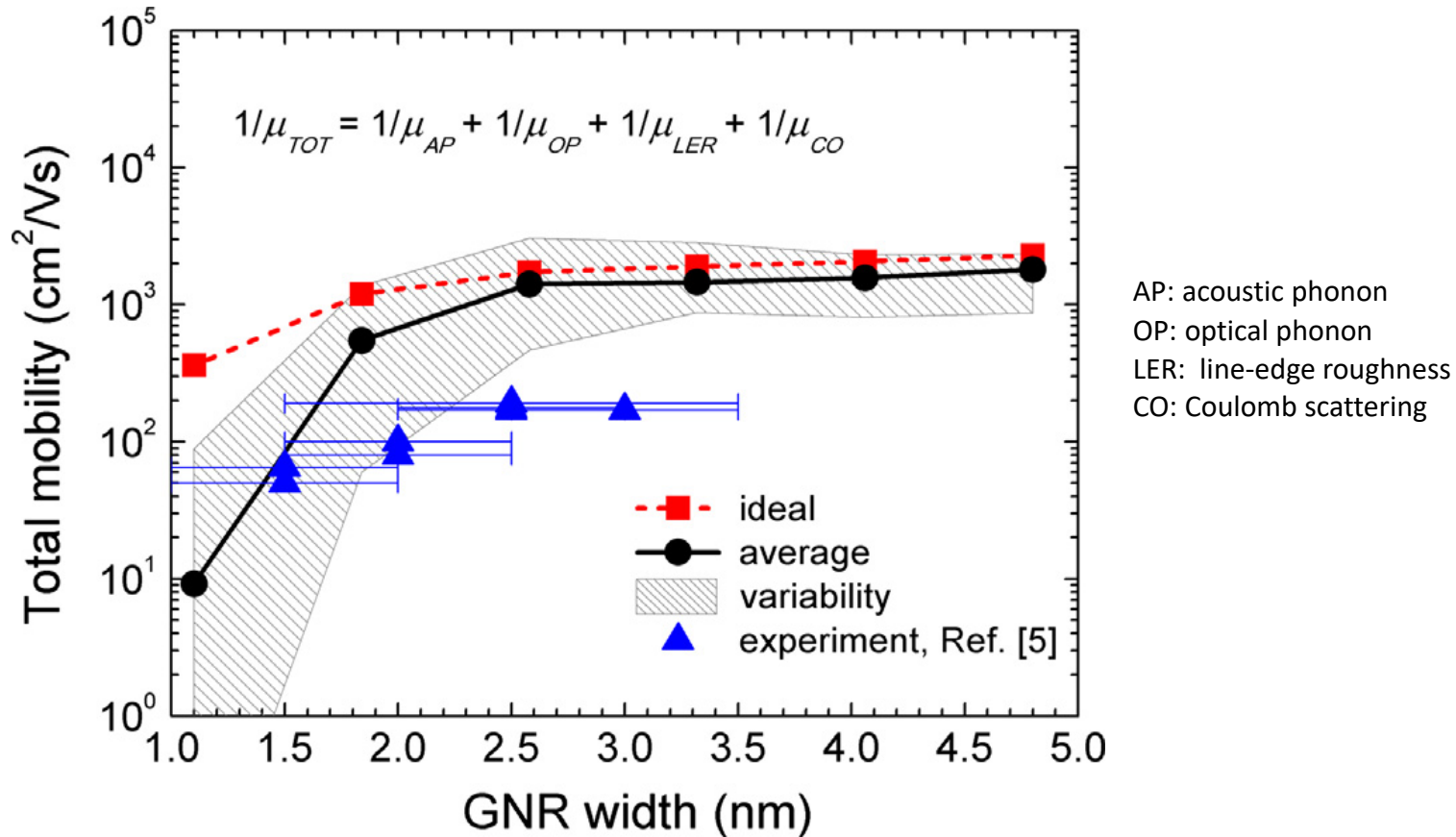
# Graphene nanoribbon



- Patterning of graphene nanoribbons using STM gives well-defined widths and predetermined crystallographic orientations.
- Opening of confinement gaps up to 0.5 eV is demonstrated.

L. Tapaszto, et.al., Nature Nanotechnology, 2008, 3, 397

# Limitation of GNR formed by lithography



- The mobility of GNR decreases monotonically as the width reduces.
- Edge roughness induced by lithography and etching is one of the key factors that degrade the mobility.

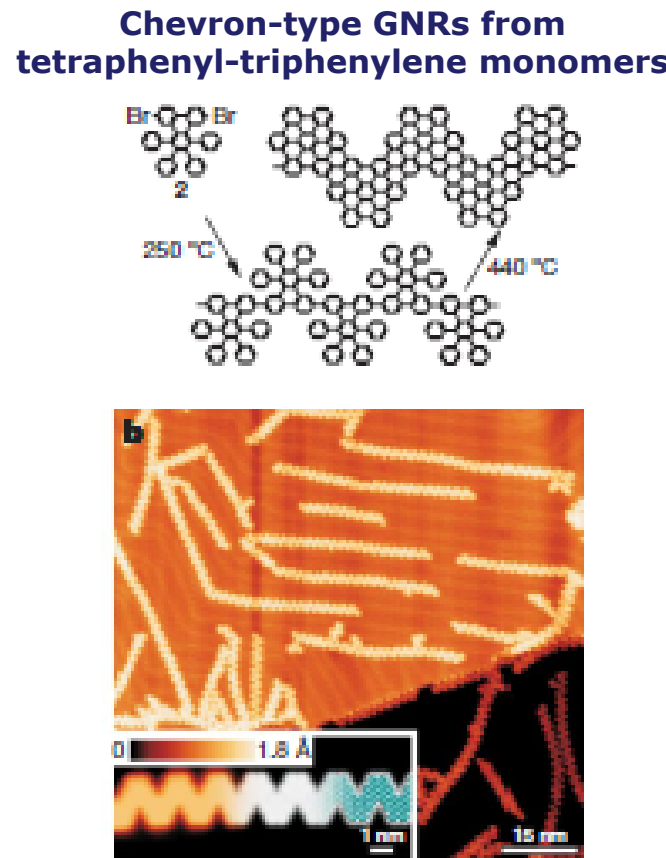
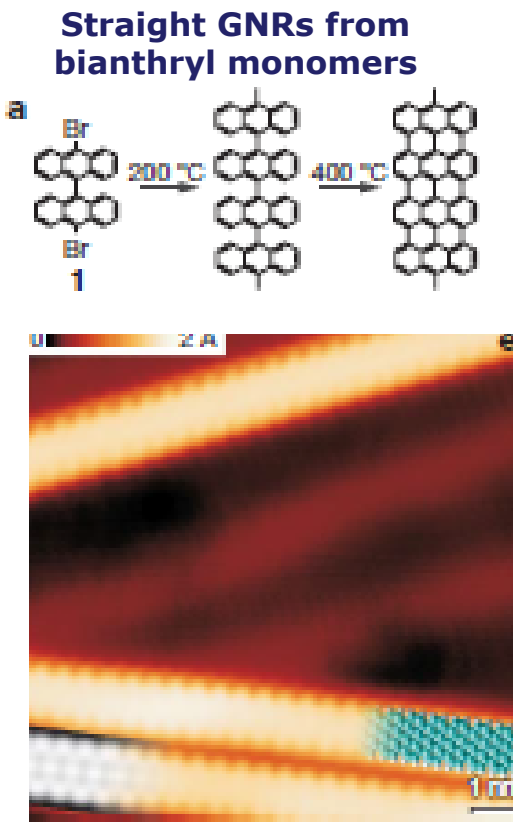
M. Poljak, et al., Solid-State Electronics, 108, 67, 2015

# Outline

- Introduction of graphene
- Synthesis of graphene
- Current transport and electronic devices
- Optical properties and photonic devices
- Bandgap engineering in graphene
  - **Band opening in bilayer graphene**
  - **Band opening in graphene nanoribbon (GNR)**
    - GNR formed by lithography
    - GNR synthesized via a bottom-up approach
    - GNR grown on SiC steps
    - GNR formed by unzipping carbon nanotube
    - GNR formed by exfoliation



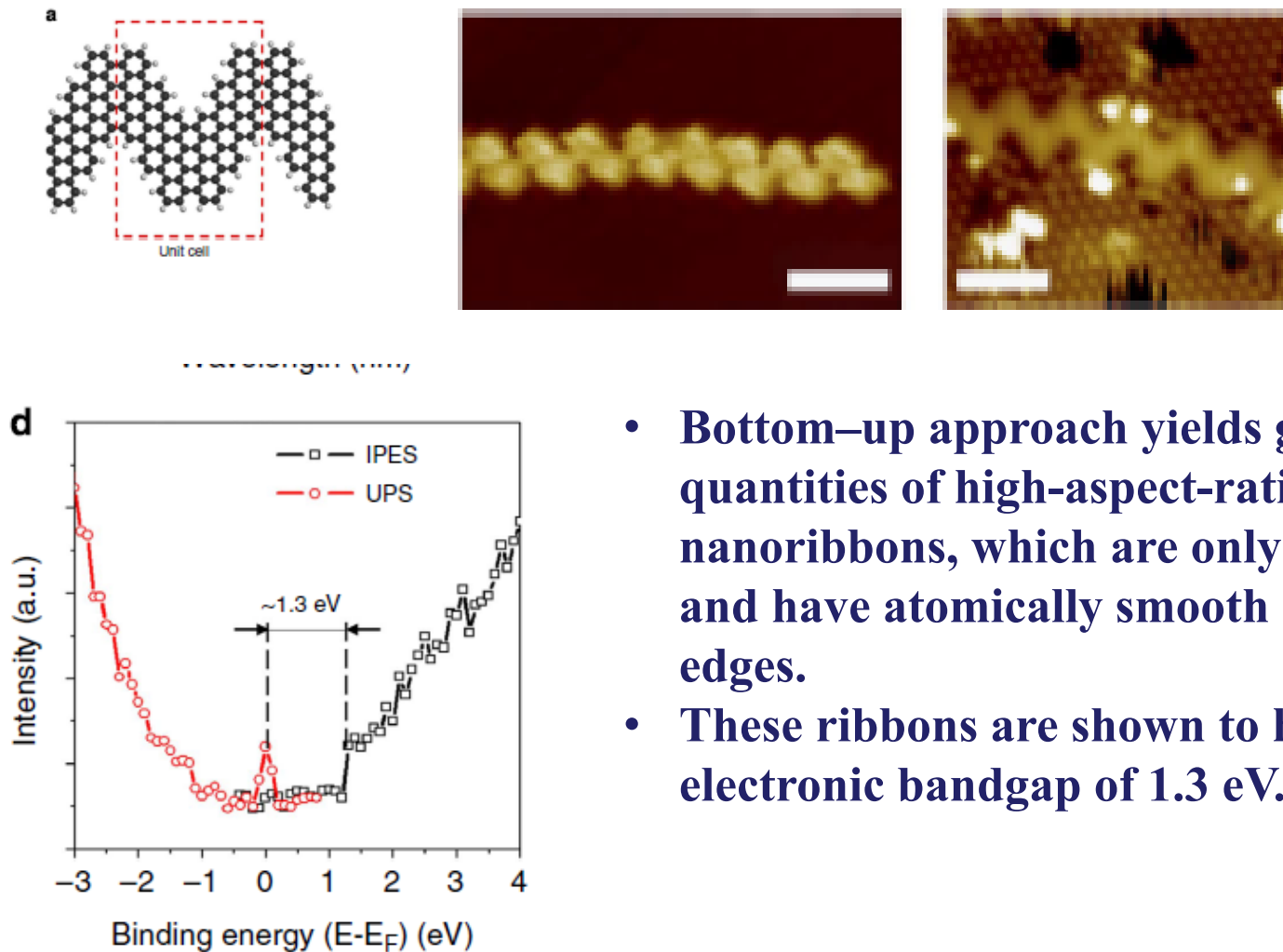
# Bottom-up synthesis of GNR



- GNR was synthesized using a bottom-up approach via thermal sublimation of the monomers.
- The topology, width and edge periphery of the graphene nanoribbon products are defined by the structure of the precursor monomers.

J. Cai, R. Fasel, et.al., 466, 470, 2010

# Solution synthesis of narrow graphene nanoribbons



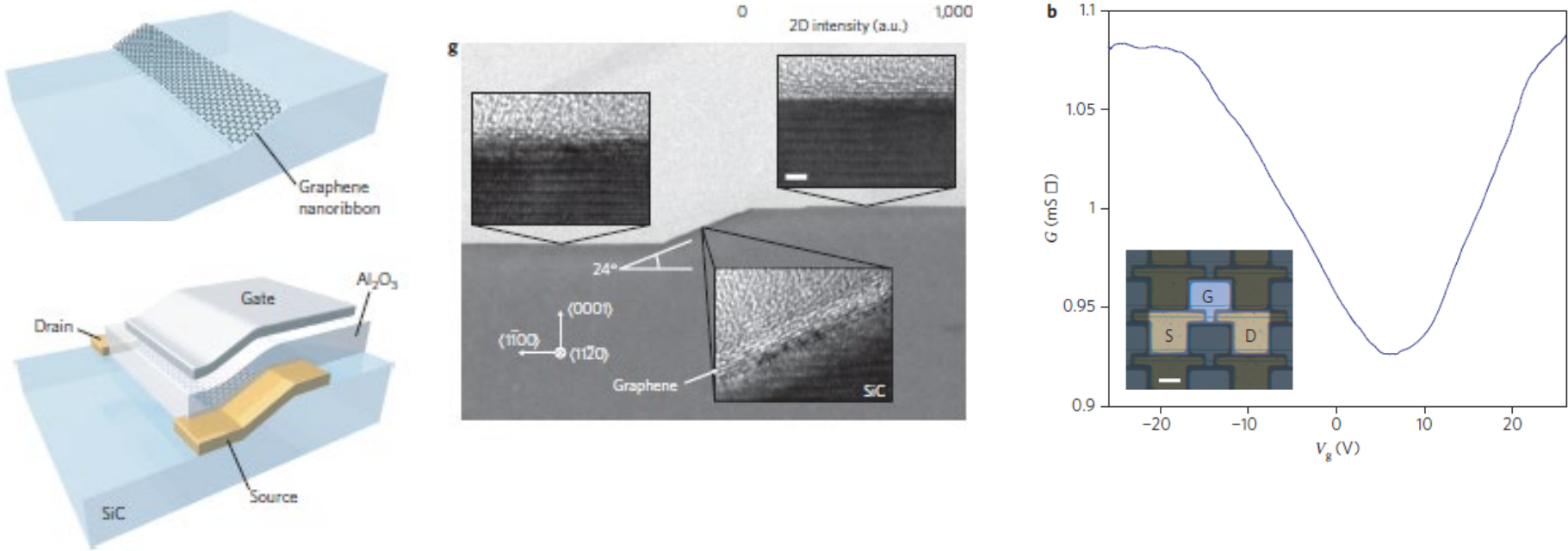
- Bottom-up approach yields gram quantities of high-aspect-ratio graphene nanoribbons, which are only 1 nm wide and have atomically smooth armchair edges.
- These ribbons are shown to have a large electronic bandgap of 1.3 eV.

Timorhy. Vo, Alexander Sinitskii, et.al., Nature Communications, article 4189, 2014

# Outline

- Introduction of graphene
- Synthesis of graphene
- Current transport and electronic devices
- Optical properties and photonic devices
- Bandgap engineering in graphene
  - **Band opening in bilayer graphene**
  - **Band opening in graphene nanoribbon (GNR)**
    - GNR formed by lithography
    - GNR synthesized via a bottom-up approach
  - • GNR grown on SiC steps
  - GNR formed by unzipping carbon nanotube
  - GNR formed by exfoliation

# GNR grown on SiC step facet



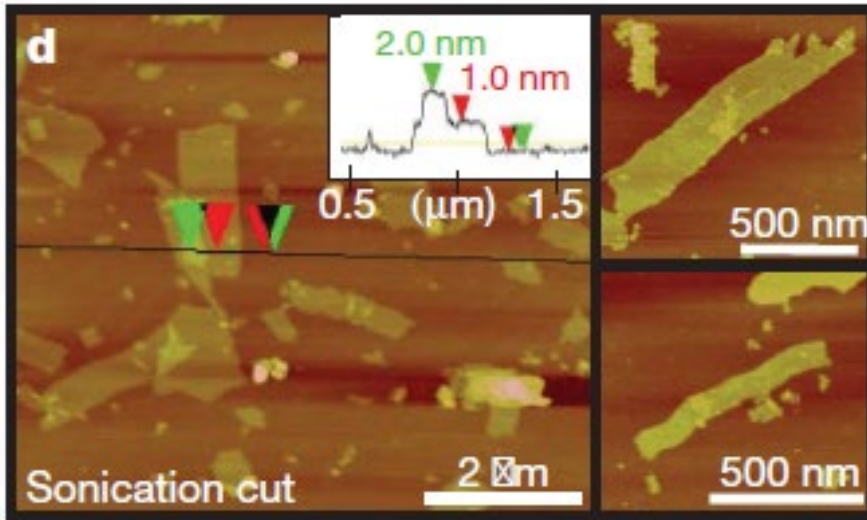
- Graphene nanoribbons were grown on the crystal facet of silicon carbide.
- On-off ratio of 10 and carrier mobilities up to  $2,700 \text{ cm}^2/\text{V}\cdot\text{s}$  at room temperature are observed.

M. Sprinkle, W. De Heer, et.al., Nature Nanotechnology, 5, 727, 2010

# Outline

- Introduction of graphene
- Synthesis of graphene
- Current transport and electronic devices
- Optical properties and photonic devices
- Bandgap engineering in graphene
  - **Band opening in bilayer graphene**
  - **Band opening in graphene nanoribbon (GNR)**
    - GNR formed by lithography
    - GNR synthesized via a bottom-up approach
    - GNR grown on SiC steps
  - • GNR formed by unzipping carbon nanotube
  - GNR formed by exfoliation

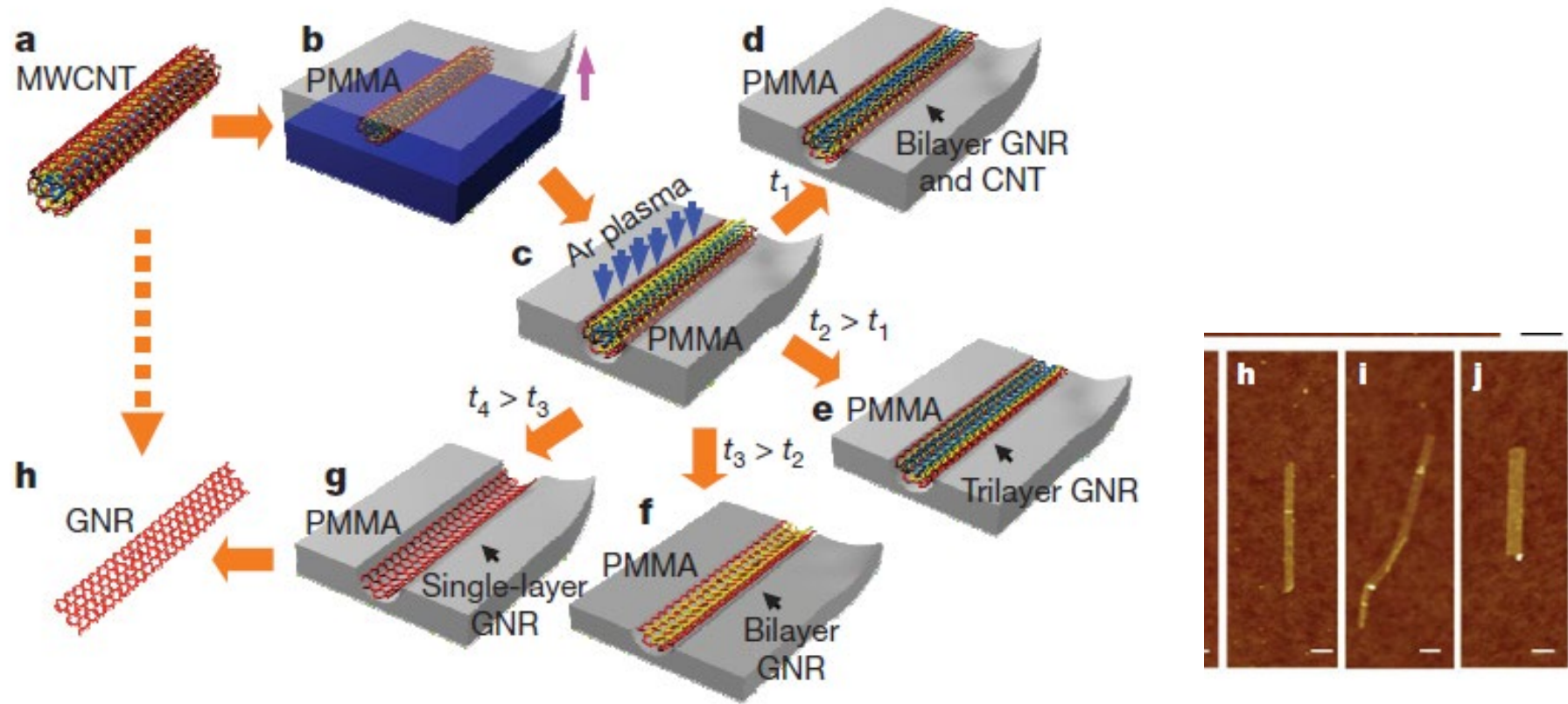
# GNR: unzip carbon nanotube (1)



- Graphene nanoribbons were obtained by suspending multiwall carbon nanotubes (MWCNTs) in concentrated sulphuric acid followed by treatment with  $\text{KMnO}_4$ .
- Ribbon width is  $\sim 100\text{nm}$ .

D. Kosynkin, J. Tour, et.al., Nature, 458, 872, 2009

# GNR: unzip carbon nanotube (2)



- GNRs can also be made by unzipping multiwalled carbon nanotubes using plasma etching of nanotubes partly embedded in a polymer film.
- The GNRs have smooth edges and a narrow width distribution (10–20 nm).

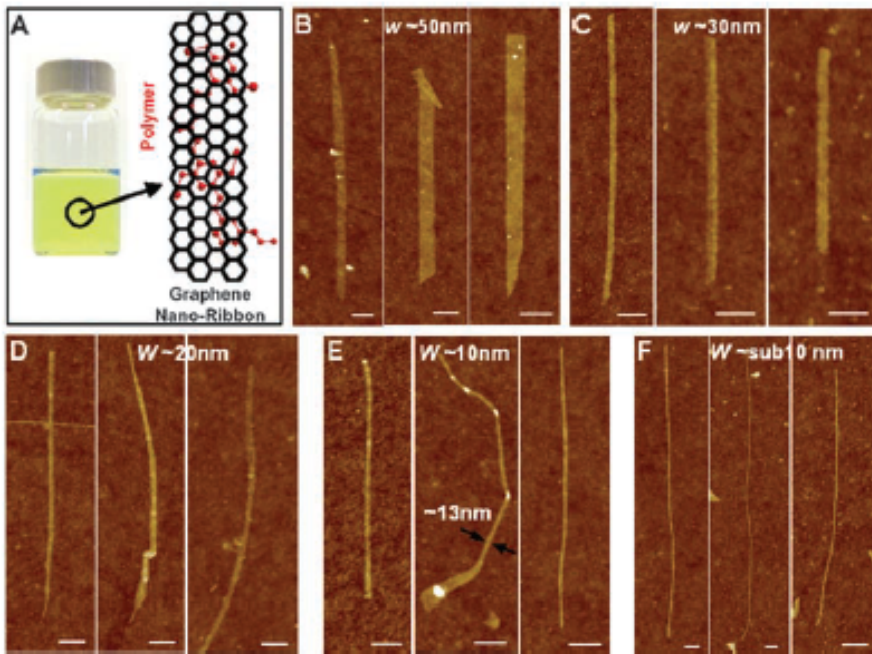
Liying Jiao, et al., Nature, 458, 877, 2009

# Outline

- Introduction of graphene
- Synthesis of graphene
- Current transport and electronic devices
- Optical properties and photonic devices
- Bandgap engineering in graphene
  - **Band opening in bilayer graphene**
  - **Band opening in graphene nanoribbon (GNR)**
    - GNR formed by lithography
    - GNR synthesized via a bottom-up approach
    - GNR grown on SiC steps
    - GNR formed by unzipping carbon nanotube
    - **GNR formed by exfoliation**



# GNR by chemical exfoliation

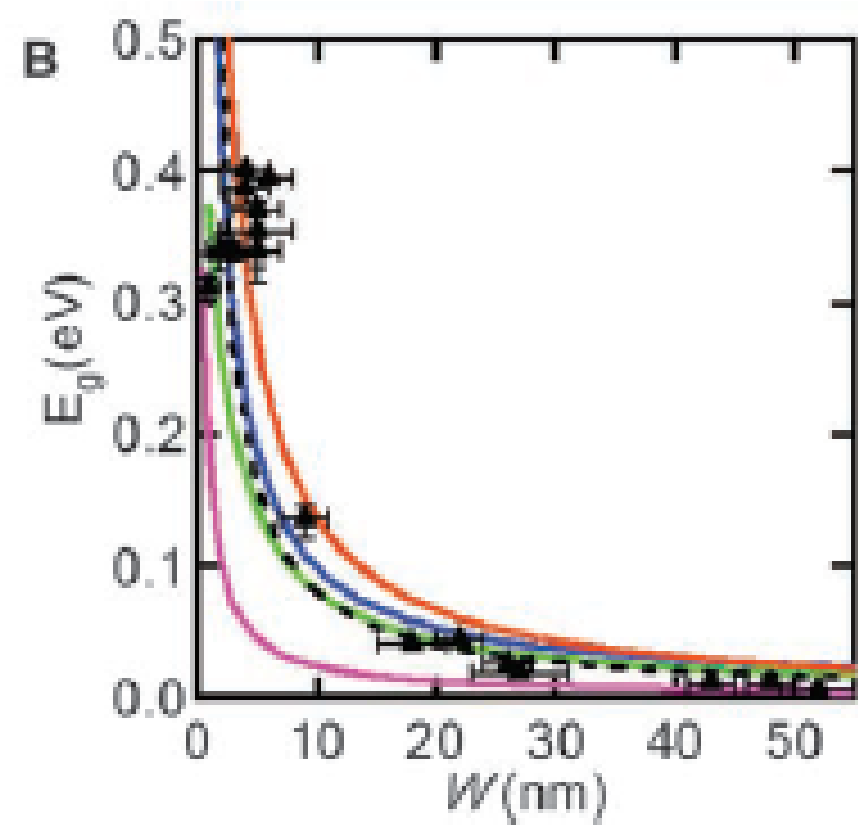
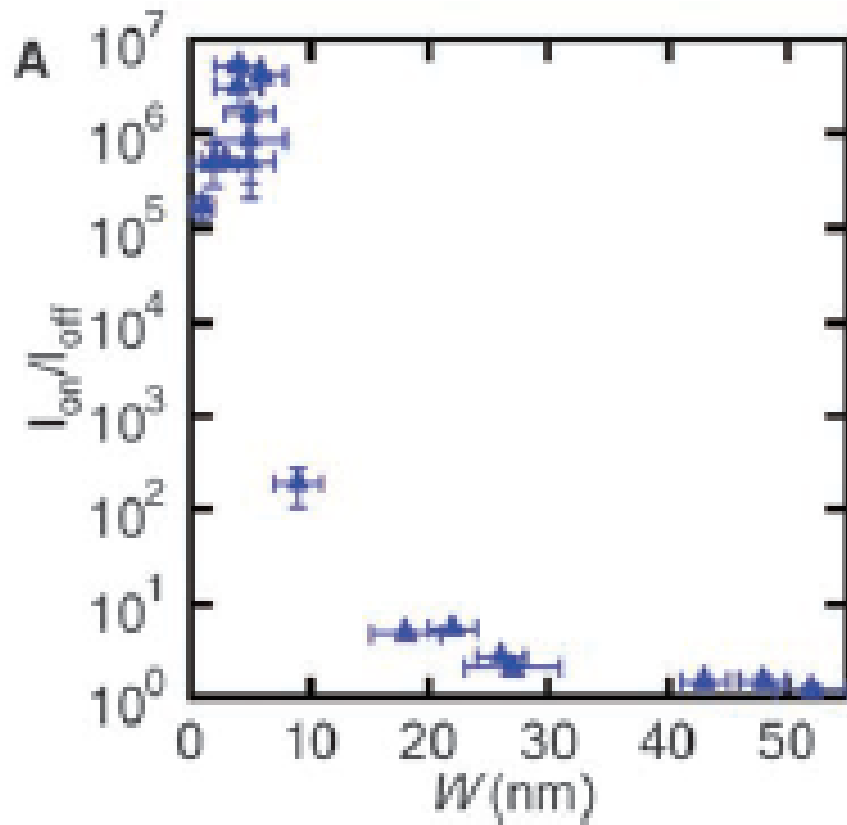


- Graphene nanoribbons (GNR) can be obtained by chemically exfoliation using polymers and sonication.
- GNR down to sub-10-nm width was demonstrated.

Details: Exfoliate commercial expandable graphite by brief (60 s) heating to 1000°C in forming gas (3% hydrogen in argon). The resulting exfoliated graphite was dispersed in a 1,2-dichloroethane (DCE) solution of poly(m-phenylenevinylene-co-2,5-dioctoxy-p-phenylenevinylene) (PmPV) by sonication for 30 min to form a homogeneous suspension. Centrifugation then removed large pieces of materials from the supernatant.

X. Li, H. Dai, et.al., Science, 319, 1229, 2008

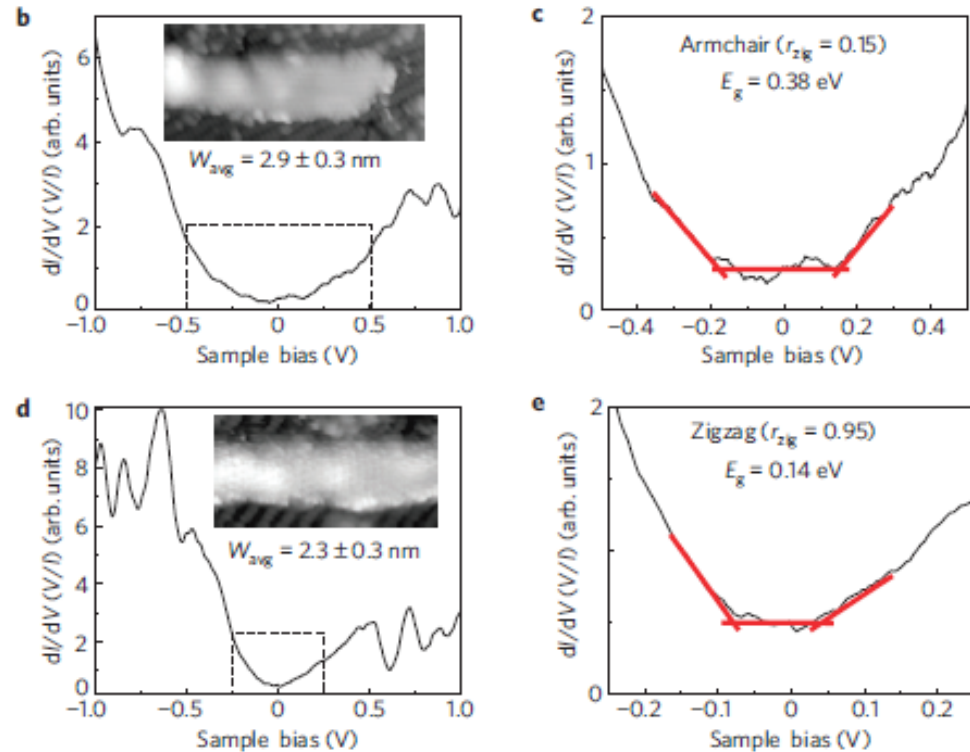
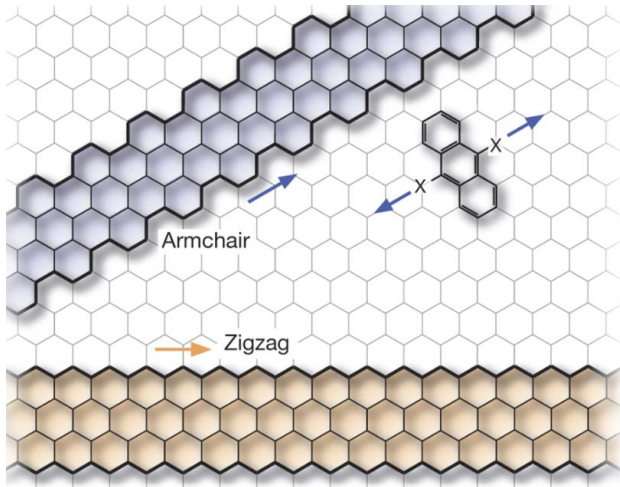
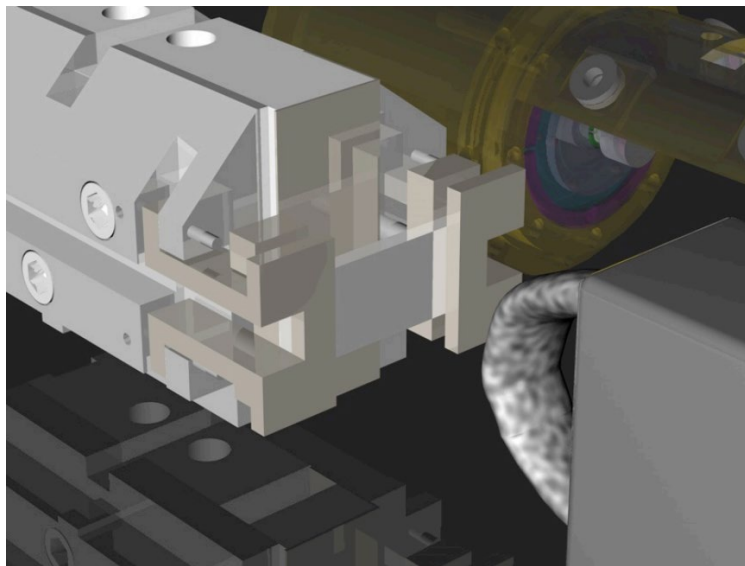
# Band gap opening in graphene nanoribbons



- Sub-10-nm GNRs characterized in the experiments exhibited  $I_{on}/I_{off} > 10^5$
- The bandgap was estimated from the current on/off ratio.

X. Li, H. Dai, et.al., Science, 319, 1229, 2008

# GNR deposited by dry contact transfer (DCT)



GNRs were deposited by dry contact transfer in STM tool. GNRs with a higher fraction of zigzag edges exhibit a smaller energy gap than a predominantly armchair-edge ribbon of similar width.

K. Ritter, J. Lyding, Nature Materials, 8, 235, 2009

# Summary

## Band structure

### Monolayer graphene



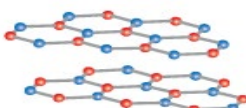
$$D_{Ave} = 0$$



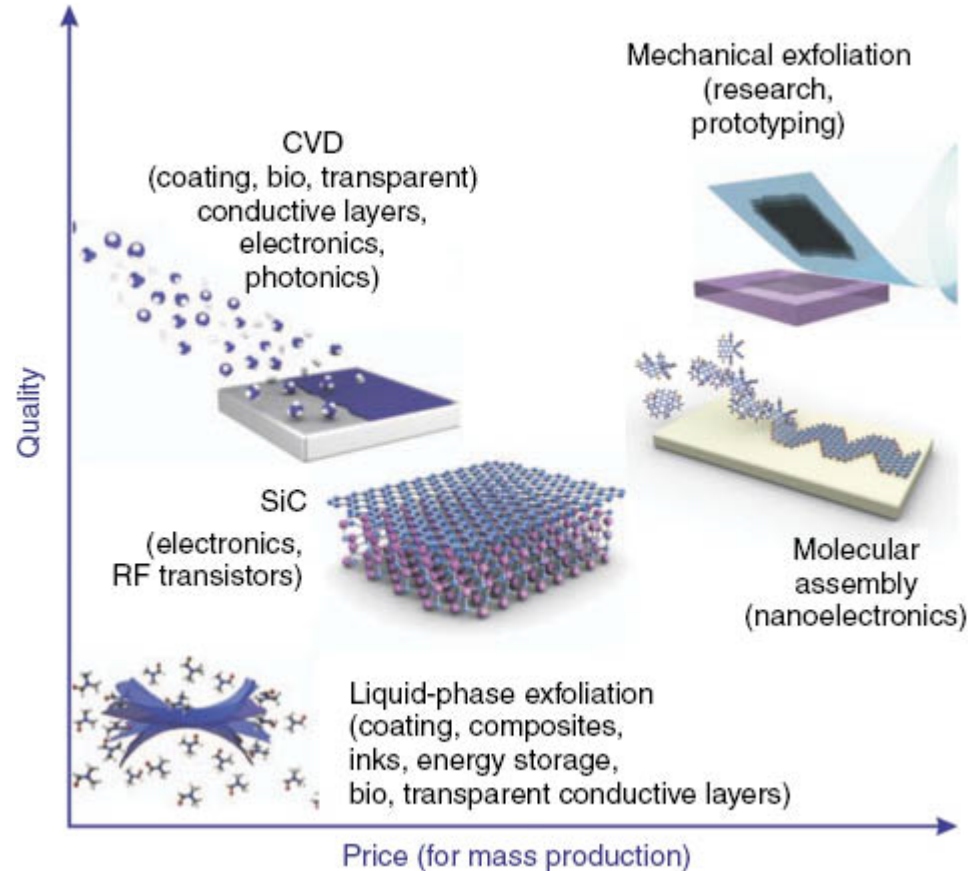
$$D_{Ave} \neq 0$$



### Bilayer graphene

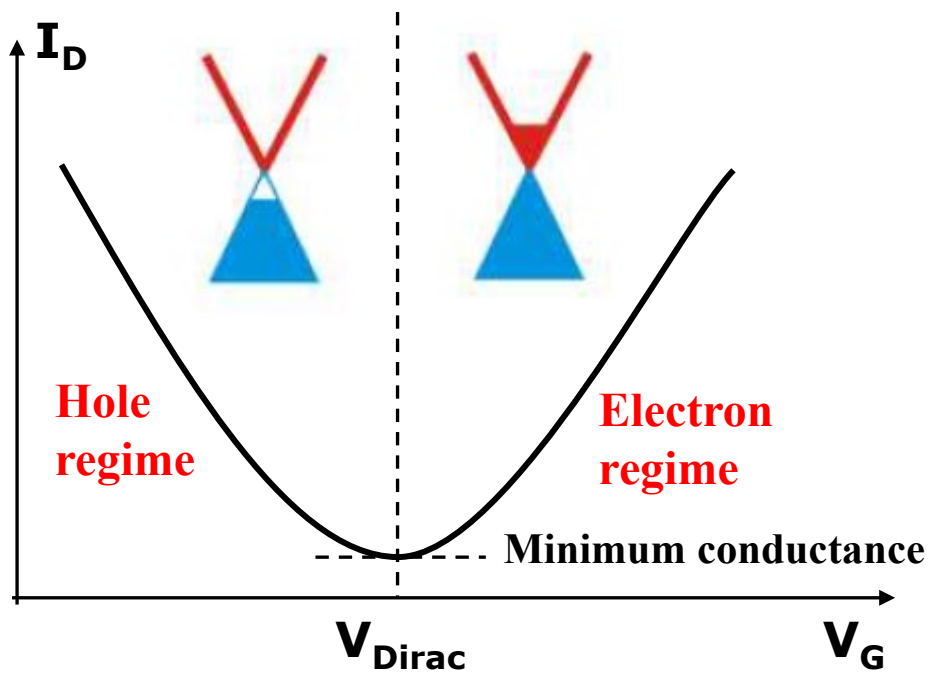


## Synthesis of graphene

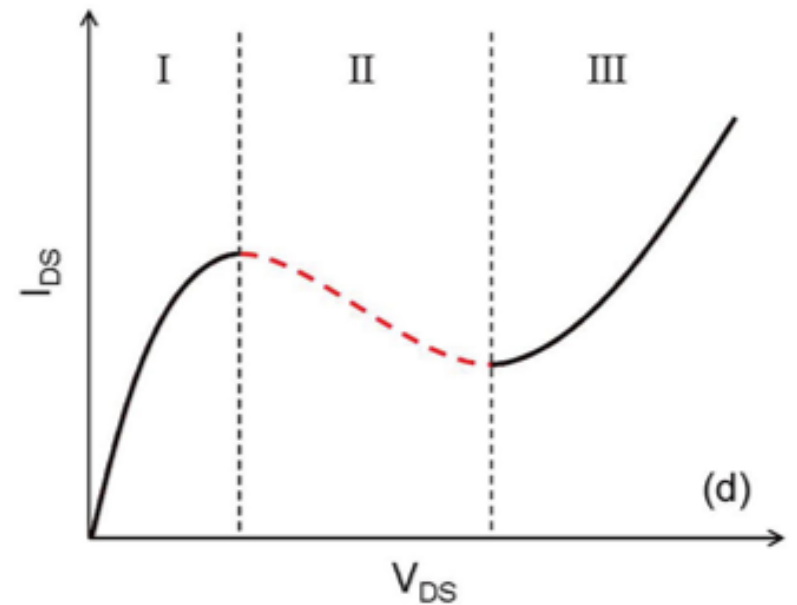


# Current transport in graphene

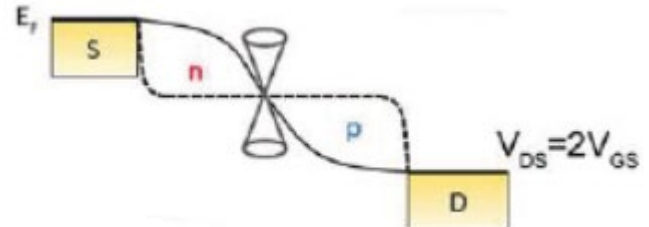
Transfer characteristics



Output characteristics

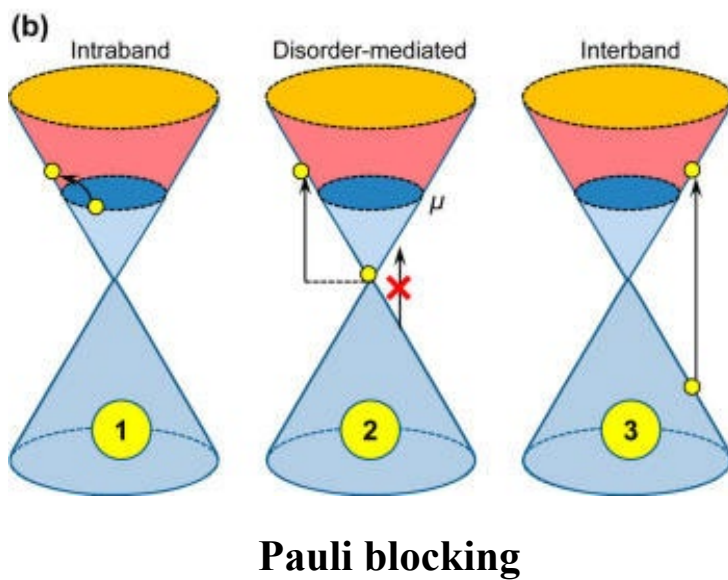
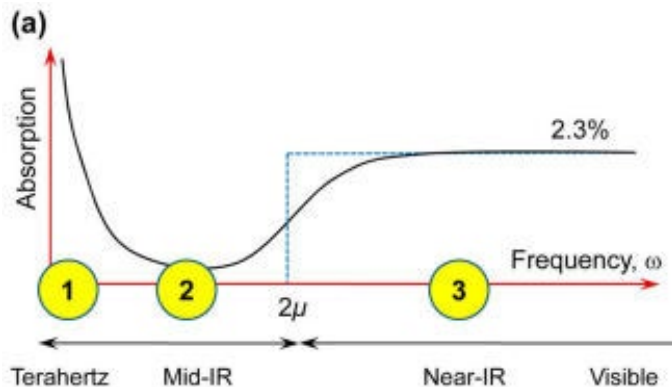


Negative differential resistance (NDR)

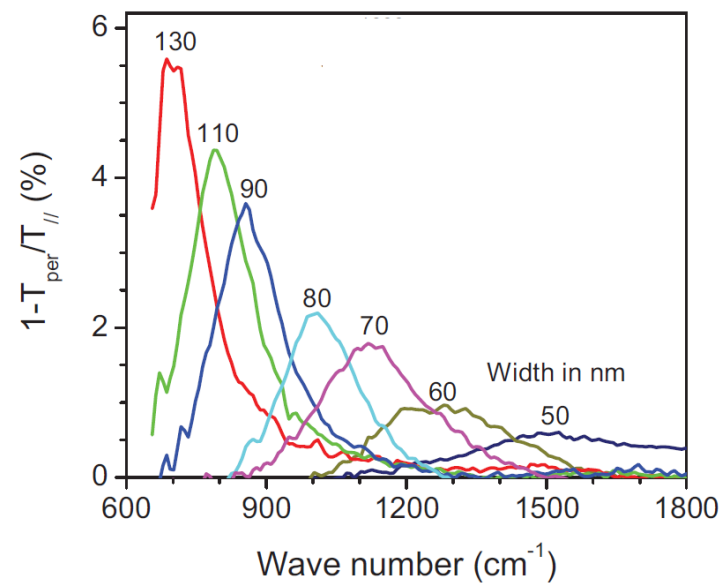
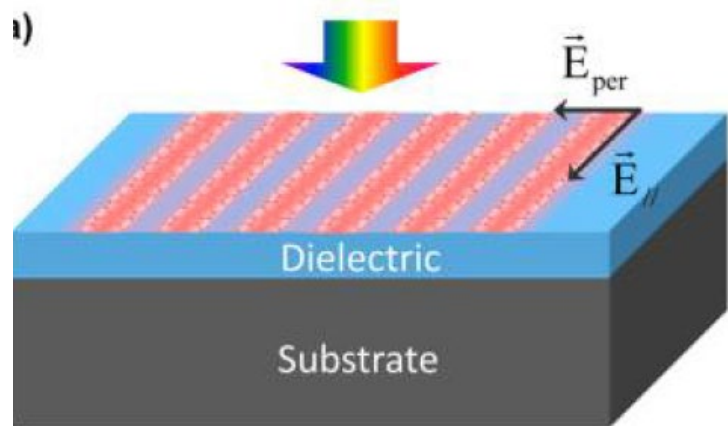


# Optical properties of graphene

## Optical absorption

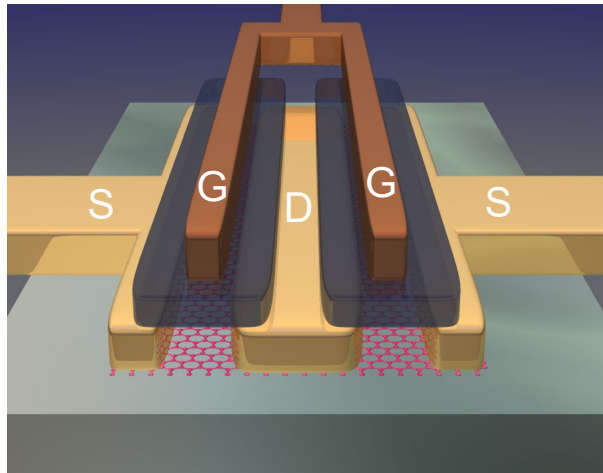


## Graphene plasmonics

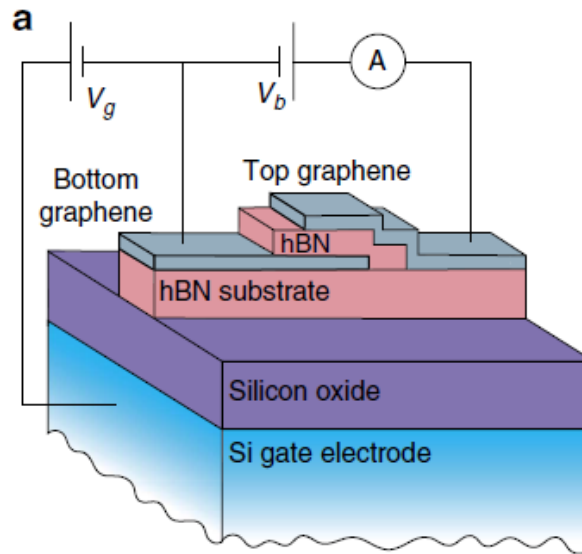


# Electronic devices based on graphene

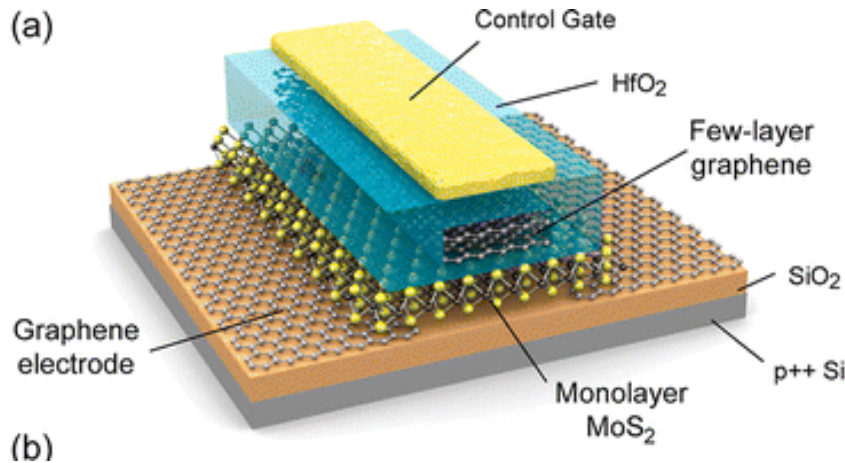
Graphene RF device



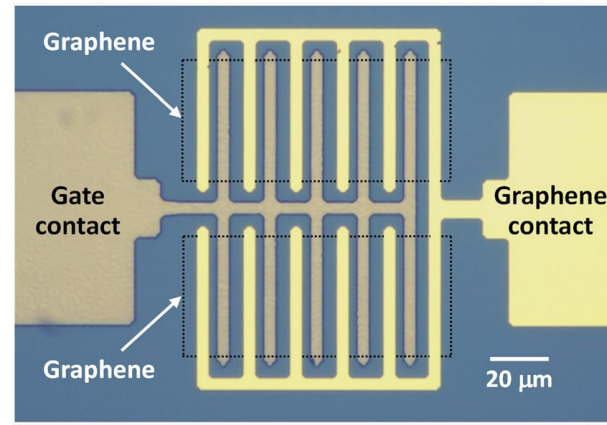
Graphene Resonant tunneling device



Graphene memory

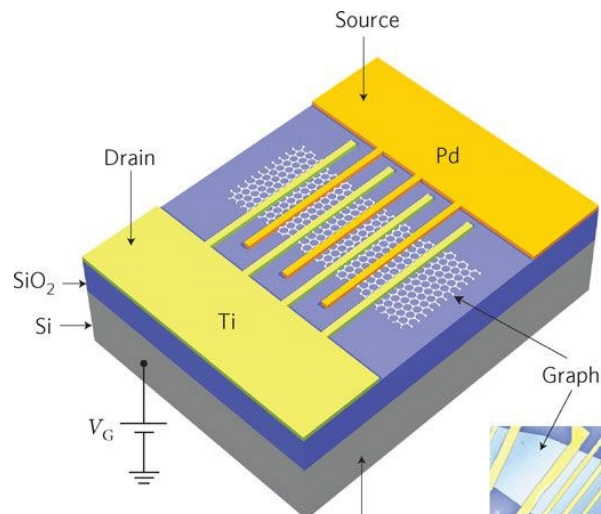


Graphene varactor

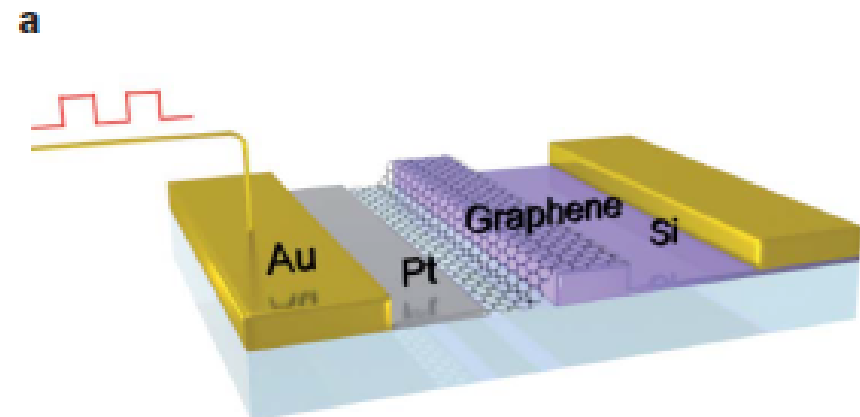


# Photonic devices based on graphene

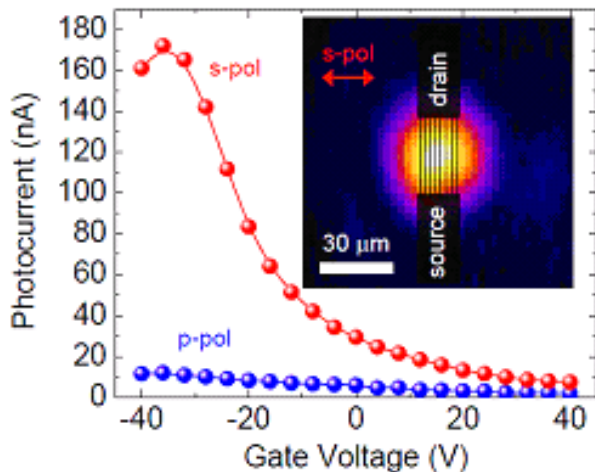
## Graphene photodetector



## Graphene optical modulator



## Graphene plasmonic devices



## Graphene sensors

